HYDROLOGIC ASPECTS OF NORTHERN PIPELINE DEVELOPMENT

HYDROLOGIC ASPECTS

OF

NORTHERN PIPELINE DEVELOPMENT

1974

A series of 12 reports
Based on studies conducted in 1973 by
Glaciology Division
Water Resources Branch
Department of the Environment

for the

Environmental-Social Program
Northern Pipelines

July 1974

Environmental-Social Committee
Northern Pipelines
Task Force on Northern Oil Development
Report No. 74-12

The data for this report were obtained as a result of investigations carried out under the Environmental-Social Program, Northern Pipelines, of the Task Force on Northern Oil Development, Government of Canada. While the studies and investigations were initiated to provide information necessary for the assessment of pipeline proposals, the knowledge gained is equally useful in planning and assessing highways and other development projects.

Résumé en français

Le présent résumé indique le degré d'avancement des études hydrologiques effectuées en 1973 par la Division de la glaciologie de la Direction des ressources en eau, dans le cadre du Programme socio-écologique des pipelines du Nord. Certains des projets mentionnés ont débuté en 1973, tandis que d'autres représentent la poursuite et l'extension du programme de 1972. Seize rapports de recherche contenant les données et les résultats d'étude accumulés jusqu'à la fin de 1972 ont été publiés en un volume dont on peut se procurer un exemplaire à Information Canada.

En 1973, nous avons surtout visé à établir les données hydrologiques qui n'ont pas fait l'objet de nos études de 1972. L'objectif secondaire a été de poursuivre les travaux grâce auxquels de nouvelles données pourraient contribuer à améliorer considérablement la base statistique de certaines conclusions.

Au cours de 1973, nous avons poursuivi les travaux entrepris dans les bassins de recherche du ruisseau Twisty, du ruisseau Boot et du lac Peter, ainsi que les études de la débâcle, de l'embâcle et de l'affouillement par la glace dans le chenal principal du Mackenzie. En collaboration avec le Groupe d'étude écologique de la route du Mackenzie, nous avons recueilli des données sur le débit de 5 petits affluents du Mackenzie, afin de vérifier l'exactitude des critères de calcul des buses de la route. Dans le delta du Mackenzie, nous nous sommes attachés à déterminer les taux de sédimentation au moyen de techniques dendrochronologiques, les taux d'érosion des berges des chenaux et la répartition saisonnière du débit entre les chenaux du delta. A l'ouest du delta, nous avons entrepris dans les monts Richardson, l'examen des caractéristiques physiques des bancs de neige semi-permanents.

En plus des recherches _in situ_, nous avons continué l'étude des caractéristiques géomorphologiques et hydrologiques des bassins versants des affluents du Mackenzie. Parmi les travaux en cours, le rapport mentionne pour la première fois, les expériences en laboratoire relatives à la pollution par le pétrole des rivières englacées. Au cours de l'année, nous avons terminé une nouvelle étude globale concernant la simulation des effets résultant de la modification du mollisol dans les régions de pergélisol du Nord canadien.

Contents

Summary Report

On 1973

Hydrologic Studies Relevant To Pipelines

By

D. K. Mackay

Glaciology Division

Water Resources Branch

Department of the Environment

under the

Environmental-Social Program

Northern Pipelines

TABLE OF CONTENTS

SUMMARY REPORT ON 1973 HYDROLOGIC STUDIES

RELEVANT TO NORTHERN PIPELINES

BY

D. K. MACKAY

Introduction

This report summarizes the progress of hydrology studies carried
out in 1973 by Glaciology Division, Water Resources Branch, within the
Environmental-Social Program, Northern Pipelines. Some of the research
projects discussed began in 1973, while others reflect the continuation
and extension of the 1972 program. Sixteen research reports containing data
and results of studies to the end of 1972 have been published in one volume
available through Information Canada (9).

Our principal objective in 1973 was to provide information on hydro-
logical concerns not actively studied or covered by our 1972 studies. A
secondary objective was to continue those projects in which the statistical
foundation of some conclusions would be markedly improved by additions to the
data base.

During 1973 projects in Twisty Creek, Boot Creek and Peter Lake
research basins were continued as were break-up, ice jamming and ice scour
studies on the Mackenzie main stem. In cooperation with the Mackenzie Highway
Environmental Working Group, discharge data were collected on 5 small Mackenzie
tributaries to check on the adequacy of highway culvert design criteria. In
the Mackenzie Delta, emphasis was placed on determination of sedimentation
rates using dendrochronology techniques, on erosion rates of channel banks,

and on the seasonal flow distribution among delta channels. To the west

of the Delta in the Richardson Mountains, an examination of the physical

characteristics of semi-permanent snow banks was undertaken.

In addition to field research, analyses of both geomorphic and

hydrologic characteristics of Mackenzie tributary basins were extended.

Another continuing project, involving laboratory experiments into oil

pollution of ice covered rivers, is reported herein for the first time.

A broad, new study concerning simulation of active layer modification effects

in permafrost regions of Northern Canada was completed during the year.

Work Carried Out

1.   Mackenzie River and Tributaries

1.1 Break-up, ice jams and river scour.

Reconnaissance of Mackenzie break-up continued with special attention

being paid to logging ice jam locations and to the fluviogeomorphic effects of

ice action (8). The 1973 break-up was relatively placid with numerous minor

or partial ice jams occurring in the main stem down to Arctic Red River. A

fairly large jam below the Arctic Red River junction was observed blocking the

channel for some time.

Inclement weather over some reaches of river during break-up affected

the river scour project. Sections of interest to the river scour study were not

photographed at the time appropriate for comparison purposes, thereby limiting

the success of the project. Our intention is to continue the study into the

1974 break-up period.

1.2 Oil in ice-covered rivers.

Studies of oil pollution in ice covered rivers continued with
present work concentrated on a literature search and on laboratory experiments
(7). Hot crude oil released in a 1.5 m. diameter ice-covered basin was monitored
to determine spreading rate and related behavioural characteristics of the oil
over varying periods of time.

1.3 Discharge and fish passage through culverts.

A project was carried out in co-operation with the Mackenzie Highway
Environmental Working Group to assess design criteria of 7-day delay discharges
at culvert sites (12). Surveys of 5 small basins with culvert sites on the high-
way route south of Norman Wells, indicated that icings on stream beds and flood
plains are regular features of their hydrologic regimes.

1.4 Morphometric analyses

Work involving morphometric data collection in tributary basins,
especially on the eastern side of the Mackenzie River, was continued (13).
Flood characteristics of a number of basins were estimated using the relation-
ships established in an earlier report (9). Among the larger basins investigated
on the eastern side, 100-year floods for the Blackwater River at the Mackenzie
(drainage area 3157 (sq. miles) as well as the rivers Ochre (drainage area 445 sq.miles)
and Donnelly (drainage area 614 sq. miles) were estimated at 10.37, 12.24 and 14.82
cfs/sq. mile respectively. Among basins on the western side, 100-year floods for
the Ramparts River at the Mackenzie (drainage area 2908 sq. miles) and the Hume
(drainage area 1754 sq. miles) and the Little Bear rivers at the Mackenzie
(drainage area 877 sq. miles) were estimated at 12.71, 17.44 and 11.93 cfs/sq.
mile respectively.

1.5 Research basins

Data collection continued on water budget elements in 3 small
research basins. For the first time spring snowmelt runoff was measured
in Boot Creek; and in Peter Lake basin, the amount of water withdrawn for
use in drilling operations was monitored (1). In addition, an experiment
was commenced at Peter Lake to study the undercatch of precipitation which
is attributable to rain gauge design. In the subarctic alpine basin of
Twisty Creek, work on water budget components was expanded and new rainfall/
runoff peaks were recorded (6).

2.   Mackenzie Delta

2.1 Seasonal flow distribution

Miscellaneous discharge measurements were made over the 1973
summer season but not in sufficient quantity to describe the delta flow
distribution. Beginning in the summer of 1974 the Water Survey of Canada
will install gauges in a number of delta channels to monitor sediment and
discharge on a continuous basis in conjunction with Beaufort Sea studies.

Mackenzie Delta discharge and ice thicknesses were measured in
March and miscellaneous hydrometric measurements were taken during the open
water season (2). March 1974 flow distribution in the outer delta differed
from that of March 1972 and 1973. The delta ice cover was generally thinner
in 1973 than in the other 2 years.

2.2 Channel bank erosion

Channel banks in the south end of the Mackenzie Delta were surveyed
to estimate erosion rates of a variety of bank types (10). The significant
factors involved in bank recession were analyzed and discussed for this portion
of the delta.

The results of the study suggest it should be expanded over the delta to improve the data base and to determine its utility in other areas.

2.3 Sedimentation

Sampling of trees in the Mackenzie Delta continued with a view to establishing sedimentation rates by analyses of adventitious root growth (4). In addition, an enquiry into 3 pingo-like humps on the Peel River flood plain began with flood level surveys, determination of active layer depths and establishment of vegetational zoning. A detailed study of the features including microtopography, active layer thickness, ground ice content and plant communities is contemplated in 1974.

3.   Hydroclimatology-permafrost relations

3.1 Uses of dendrochronology

The uses of dendrochronology in permafrost environments are discussed by Henoch (5). Some of the clues to past climate rendered by dendrochronologic techniques are important in the analyses of geomorphic processes and forms.

3.2 Active layer simulation

The relations between active layer thickness and regional climate were assessed using computer simulation techniques (3). The effects of surface melting and drying as well as destruction or removal of the organic surface mat on active layer thickness were also investigated by computer simulation. The results are presented in the form of isoline maps showing the geographical distribution of active layer thickness and the degree to which it is changed by surface modification.

3.3 Semi-permanent snowbeds

Snowbeds in the northern Richardson Mountains and adjacent foothills were examined to associate their distribution and physical characteristics with

localized slope stability and biological activity (11). These features, which may exist for more than one year, provide a moisture supply in summer affecting active layer development, erosion and mass wasting of slopes.

4.   Projects not reported.

Other projects which are still in progress such as lake temperature regimes, Mackenzie river heat budget and some snow-cover/ground temperature relations will be reported on at a later date.

Significant Results

The general conclusion is that the most favourable Mackenzie pipeline route from a hydrological point of view remains as in 1972 (Figure 1).

1.   Ice Jams - Partial ice jamming in the main Mackenzie may be as significant from a river scour point of view as complete cross-sectional jamming. When a partial ice jam develops, such as occurred directly below Fort Simpson in May 1973, the channelling of flow can cause considerable scour (8). This has been indicated by sediment-laden plumes observed streaming below ice-constricted channels.

2.   Mackenzie Delta Flow - Three year's of March discharge measurements show that more than 80 per cent of total Delta inflow is carried by Middle Channel north into the central part of the Delta (Station 18). Farther downstream the pattern of flow dispersion is unstable from year to year as is indicated by the range in discharge from 57 to 91 per cent in Middle Channel (Station 20) opposite Reindeer Station (2). This indicates that water supply in outer distributary channels could be a critical factor in winter oil drilling operations.

3.   Ice Covered Rivers and Oil - In ice covered rivers the release of crude oil
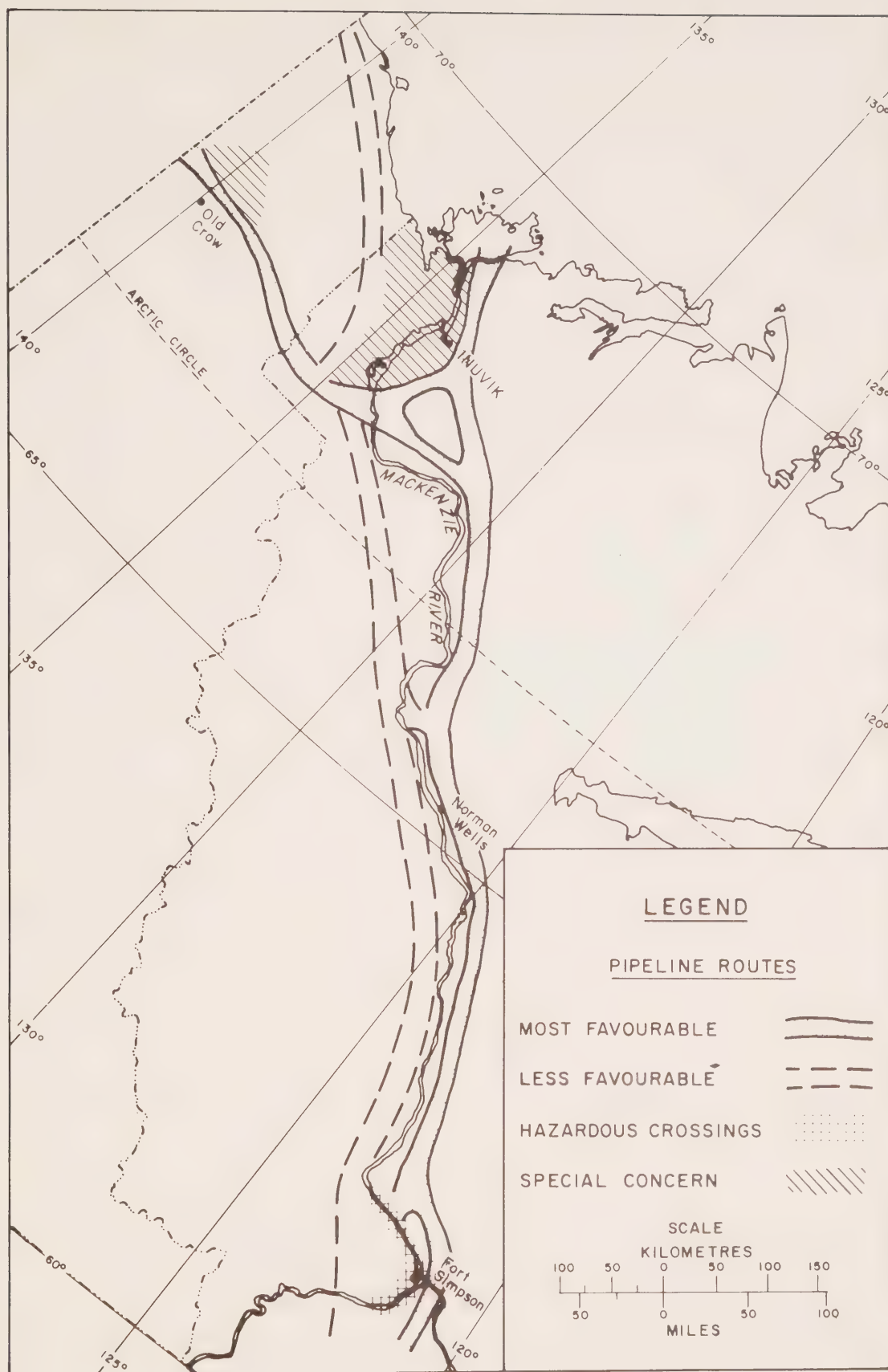
Figure 1.   Mackenzie pipeline routes from a hydrological point of view.

can cause severe environmental problems. Our laboratory experiments indicate that hot crude oil released under an ice cover separates into small globules or particles 0.1 to 2 cm in diameter. These particles form an oil layer about 1 cm thick under smooth fresh water ice. The particles do not adhere to the ice under-surface but become sandwiched if the ice is thickening. A period of 1 to 3 days is needed for the oil to become sandwiched; variations are dependent on ice growth rates and current velocities (7).

4. Delta Bank Recession - An examination of bank erosion rates in the Mackenzie Delta shows that these rates may vary from negligible ones to 30 metres per year or more depending on shape (10). Before structures or other facilities are located adjacent to banks, an examination of bank shape and erosion rate should be made and Outhet's study (10) should be taken into account.

5. Design Floods - New flood peaks which should be considered in establishing regional design criteria for stream crossings by pipeline and highways were measured in our research basins. In Boot Creek, draining a 31 km^2 area of the Caribou Hills, a snowmelt runoff peak of 0.22 m^3/ sec/km^2 was reached on May 27, 1973 (1); and in Twisty Creek, a small basin on the north slope of the Mackenzie Mountains, a new summer rainstorm flood peak of 2.45 m^3/sec/km^2 was established on July 6, 1973 (6). Estimation of 100-year floods using Thakur's model based on morphometric parameters has been improved thereby enhancing its predictive value (13).

6. Use of Dendrochronology - The integrity of an oil or gas pipeline in a permafrost region may depend on the evolution of landforms by active geomorphic processes. Some insight into the age and development of particular forms and processes can be gained by use of dendrochronologic methods (5).

7.   Semi-Permanent Snow Beds - Where proposed routing of pipelines is adjacent to semi-permanent snow beds, care should be taken not to affect the soil environment. Soils in areas around the beds often approach an unstable condition due to snowbed runoff. Moreover, mass wasting may readily occur when summer rainfall events are prolonged and/or intensive (11).

8.   Active Layer Simulation - A simple site energy balance climatic simulation model may be used to estimate changes in active layer development and thickness (3). Such changes are caused by inadvertent or planned surface modification on highway and pipeline routes and may be foreseen for relatively little cost by use of this simple computer model.

From the hydrological point of view, there should be further work on comparative studies of small coastal basins as an adjunct to the Beaufort Sea Program, there should be extensions of the semi-permanent snow-bed and the delta bank erosion projects, and there should be further examination of lakes and bogs which could be affected by the construction and operation of oil and gas plants and pipelines. In our view a greater understanding of northern hydrology and maximum protection for the environment are concomitant goals.

REFERENCES

1. Anderson, J.C. and D.K. MacKay

    1974: Progress of hydrologic studies at Boot Creek and
    Peter Lake watersheds, N.W.T. during 1973. Report 17 to
    Glaciology Division, Water Resources Branch, DOE, 12 p.

2. Anderson, J.C. and R.J. Anderson

    1974: Progress report on winter distribution of flow in the
    Mackenzie Delta, N.W.T. Report 18 to Glaciology Division,
    Water Resources Branch, DOE 17 p.

3. Goodwin, Cecil W. and Sam I. Outcalt

    1974: The simulation of the geographic sensitivity of active
    layer modification effects in Northern Canada. Report 19 to
    Glaciology Division, Water Resources Branch, DOE, 20 p.

4. Henoch, W.E.S.

    1974: Geomorphic and climatic studies in the Mackenzie
    Delta area aided by dendochronology - a progress report.
    Report 20 to Glaciology Division, Water Resources Branch
    DOE, 2 p.

5. Henoch, W.E.S.

    1974: Application of dendrochonology to some hydrological
    aspects of permafrost. Report 21 to Glaciology Division,
    Water Resources Branch, DOE, 15 p.

6. Jasper, J.

    1974: Hydrologic Studies at "Twisty Creek" in the Mackenzie
    Mountains, N.W.T. - 1973 Progress Report. Report 26 to
    Glaciology Division, Water Resources Branch, DOE, 11 p.

7. Keevil, Benjamin E. and Rene O. Ramseier.

    1974: Oil pollution in ice covered rivers. Report 22
    to Glaciology Division, Water Resources Branch, DOE, 10 p.

8. MacKay, D.K., Sherstone, D. and K.C. Arnold

    1974: Channel ice effects and surface water velocities from
    aerial photography of Mackenzie River break-up. Report 23
    to Glaciology Division, Water Resources Branch, DOE, 12 p.

9. MacKay, D.K. et. al.

    1973: Hydrologic aspects of northern pipeline development
    (series of 16 reports to Glaciology Division, DOE)
    Information Canada Cat. No. R27-172, 664 p.

10. Outhet, David

      1974: Determination of bank erosion rates in the Mackenzie
Delta, N.W.T. Report 24 to Glaciology Division, Water
Resources Branch, DOE, 26 p.

11. Peterson, N.J.K.

      1974: Physical characteristics of snowbeds in the Richardson
Mountains, Northwest Territories. Report 25 to Glaciology
Division, Water Resources Branch, DOE, 97 p.

12. Sellars, C.D.

      1974: Fish passage in culverts on the Mackenzie Highway:
the hydrologic problem. Report to Mackenzie Highway
Environmental Working Group (unpublished) 26 p.

13. Thakur, T. and A.G.F. Lindeijer

      1974: Regional geomorphic and hydrologic studies of 27
Mackenzie River Tributary basins. Report to Glaciology
Division, Water Resources Branch, DOE, 30 p.

THE SIMULATION OF THE GEOGRAPHIC SENSITIVITY

OF ACTIVE LAYER MODIFICATION EFFECTS

IN NORTHERN CANADA

by

Cecil W. Goodwin and Sam I. Outcalt

Department of Geography
University of Michigan
Ann Arbor, 48104

TABLE OF CONTENTS

ABSTRACT

The effect of organic layer removal and drying of
the soil surface on active layer depths was investigated
by computer simulation. Simulations were performed with
a standard set of site conditions for 51 locations in the
permafrost region of Canada, using monthly mean 1971 wea-
ther data. Contour maps prepared from the simulation re-
sults illustrate the relationship between regional climate
and the magnitude of active layer depth change due to sur-
face modification. The effect of a surface wetness change
is seen to vary with the climate of a region to a larger
extent than does the effect of organic layer removal, due
to the relatively high sensitivity of the surface energy
balance to the wetness parameter change. The experiments
illustrate the utility of one dimensional geographic point
simulators in the consideration of spatial problems.

I. Introduction. In cold regions, soil can exist in a frozen state from year to year. This condition is called permafrost, and its existence is defined precisely by the absence of soil temperatures of 0° Centigrade or higher throughout the year. Permafrost is widespread in northern regions, and, with the current interest in northern development, studies of the climatological, geomorphic and biological processes operative in permafrost regions are of increasing importance. The possibility of resource extraction on a large scale has focused attention on human perturbations in local and regional ecosystems. In addition to ecosystem effects, construction associated with resource extraction is susceptible to damaging feedback from the disturbed systems. It is important that the nature of the interaction between climate, site, and ecosystem be documented before decisions are made which produce irreversible long term environmental effects and/or expensive engineering failures.

One phenomenon of importance to local and regional ecosystems and to construction activities in permafrost areas is the annual evolution of the active layer, a thin surface layer which melts in response to energy input by solar radiation during the northern summer. Energy absorbed at the ground surface is dissipated into the atmosphere via conduction and evaporation, and infrared re-radiation. A small heat flux into the soil is generated

by conduction and water transport in vapor and fluid forms. The amount of energy available to the soil and the annual regime determine the depth to which the active layer extends for a given soil. The available soil heat is in turn dependent on the surface energy balance in toto; and that energy balance is a complex function of the location's climate and site conditions (e.g. soil thermal properties, vegetative characteristics such as albedo and thickness of the organic mat), and their evolutionary histories.

Construction related activities may alter the surface energy balance, changing the course of active layer melting. For example, removal of an insulative layer of surface vegetation may increase summer soil melting, releasing soil water with subsequent thermal erosion (thermokarst) producing differential settling. Brown et al. (1969) reported doubling of active layer depths due to removal of the surface organic layer. The reader is referred to Gold and Lachenbruch (1973) for a review of the literature on thermal conditions in permafrost. These authors have pointed out the lack of quantitative knowledge both of actual temperature structures in permafrost regions and of the influence of climatic and site conditions in determining those structures. The importance of theoretical knowledge of the operation of natural systems has been stressed by Khilmi (1968).

Most studies of physical-environmental effects on

active layers have been restricted to a limited number of
sites, with restricted temporal climatic data. Most pre-
vious modeling efforts have been of limited scope, due to
the complexity of the processes modeled, the expense of
modeling, and data processing and availability constraints.
Models typically require time series data for several cli-
matic variables, and the specification of dozens of site
parameters (Goodwin and Outcalt, 1974; Nakano and Brown,
1973). Sensitivity testing over such a multivariate space
is quite expensive even when the voluminous observational
data is available. When data requirements are reduced by
structural changes within the model, "accuracy" generally
suffers (Outcalt et al., 1974). In addition, lack of an
adequate soil temperature observation net, particularly
with uniform site conditions, makes model verification ex-
tremely difficult.

It was with the realization of these pragmatic con-
straints that Goodwin (1972) developed a simple model of
active layer formation which, although it is not capable
of precise prediction, nevertheless embodies sufficient
deterministic theory to allow reasonable estimation of the
effect of climate and site perturbations on active layer
formation over regions of interest. This paper reports
the application of that model to the question of regional
variance of process sensitivity to site parameter change.
The work is essentially geographic and exploratory of a

technique. It by no means sweeps the whole space of climate and site parameter variation. The study is limited to two site parameter changes and a temporal scope of one year. Nevertheless, it is felt that an experiment in geographic climatonomy will demonstrate the potential power of that methodology.

II. Methodology. It is not the purpose of this study to predict precisely active layer depths at specific sites, but rather to assess in a semi-quantitative manner the spatial variability of the effects of selected surface modifications on active layer melting. In order to do this, surface parameter values which represent reasonable end-point values of the natural continuous range of the parameters were used for simulation.

Two site parameters were selected for testing: surface organic layer thickness and summer surface wetness. Of the many parameters that could have been selected for study, active layer evolution was previously demonstrated to be highly sensitive to these, and it is anticipated that they are significantly susceptible to modification by human activities.

Four simulations were performed for each of 51 sites over the continuous and discontinuous permafrost region of Canada. The following parameter values were chosen for the simulations: organic layer thickness -- 30 cm and 0 cm,

summer surface wetness -- 1. and .5 (referred to a totally
wet, freely evaporating surface with wetness = 1.). Contour
maps of maximum active layer depth are presented in a later
section for each parameter value combination. In addition,
contour maps are presented which illustrate the effects of
the parameter changes in terms of absolute depth differences.
(Absolute depth differences are mapped since it is probable
that the deleterious effects of increasing active-layer melt-
ing increase in proportion to actual depth increase, rather
than percentage increase.)

Simulations were performed using climatic data for
1971 only, with all site parameters except wetness and
organic layer thickness held constant over the area. The
latter constraint isolates the effects under examination
and simplifies analysis; the former is necessary for prac-
tical reasons. Both constraints give rise to problems of
interpretation of the simulation results.

Since initial soil temperature profiles are not avail-
able, the soil is isolated from its history. In particular,
all sites are assumed frozen for 2 meters depth from the
beginning of the run until soil thaw begins, a condition
which is not, in general, true at the southern limits of the
study. In addition, the constant parameter set chosen will
not be valid at every point over the area.

These facts constrain interpretation of the results,
and it must be emphasized that the values presented on the

maps apply only for sites where the above conditions are realized. The representativeness of the results will increase with the extent to which the specified site parameter set is representative of the area to which it is applied, which will, in general, increase with latitude. The problem of "representativeness" is little understood and is a fertile area for future geographic research.

III. The Model. The computer simulation model used in the present study is an extension of a diurnal digital computer model developed by Outcalt (1972), which was inspired by the analog computer modeling experiments of Myrup (1969). Both models are based on the existence of an equilibrium surface temperature (discussed at length by Outcalt, 1973), which brings the summation of all surface energy transfer components (radiation, soil, sensible and latent heat fluxes) to zero, as required by the principle of energy conservation.

The relationships which estimate the surface energy fluxes are non-linear and involve climatic variables, site parameters, and surface temperature. With all variables and parameters supplied or computed for a given time step, in part conditioned by information from the preceding time step, the equilibrium surface temperature is determined iteratively, thus providing estimates of the mean surface energy fluxes over the time interval. During soil thaw/

refreezing, the value of soil heat flux is partitioned into components of heat content change and phase change of soil water (ice), from which active layer melting is computed. A detailed description of the model, with FORTRAN code, is found in Goodwin (1972).

The model requires mean monthly values over the model year of the climatic variables listed in Table I. Curves are interpolated to these variables by the Fourier synthesis of monthly data points and sampled at 5 day intervals, the basic time step of the model. (January through December values are input, but the November and December values are used to precondition the soil temperature vector and to attenuate the edge effects of Fourier synthesis. The model thus operates from 1 November.) With the site parameters listed in Table II specified initially, simulations are performed for each combination of values of the parameters selected for testing.

The primary advantage of the present model is its low operating cost, approximately 40 cents per year per simulation on the Michigan Terminal System. In addition, climatic data requirements are minimal. These properties enable extensive simulation to be performed over a large area. The inclusion in the model of the set of site parameters important to physical processes allows extensive sensitivity testing on the effects of parameter change. The use of the equilibrium temperature strategy avoids the limiting require-

ment of either collecting surface temperatures or assuming temperature curves, as did Gold et al. (1972). It must be realized that surface temperature is a product of site property variation and thus surface modification effects cannot be explored reliably with air temperature as the site forcing function. The temperature of the surface is part of the answer, not part of the question!

The above results are achieved with obvious sacrifice. Some processes of undoubted importance are not modeled. In particular, snow melt is assumed instantaneous when modeled snow surface temperature exceeds zero degrees Centigrade. Previous work (Goodwin and Outcalt, 1974) has shown, however, that the timing of snow melt has little impact on ultimate active layer depths for small (<50 cm) initial snow depths. It is only when a snow cover extends far into the summer that it affects appreciably the total quantity of heat available for soil thaw.

In addition to model specification errors, the use of long term mean values of meteorological variables introduces uncertainty in the estimate of atmospheric fluxes, due to the non-linear nature of the flux equations and the frequency dependence of energy transfer in a turbulent medium.

Figure 1 compares modeled active layer melting with real depths computed from temperature observations reported by Weller (1973) for a site at Barrow, Alaska. The model underestimates freeze-back from the base of the active layer,

although the course of thaw and the maximum depth attained
are reasonably close. These effects are more accurately
mimicked by more detailed simulators at the expense of at
least a two order of magnitude increase of input information
and simulation time (Outcalt and Goodwin, 1974).

IV. <u>Data</u>. Climatic data for 51 stations over the permafrost
area of Canada was obtained from the Atmospheric Environment
Service, Canada. Monthly radiation data for 1971 was available
for 14 of these stations. These 14 stations will be called
primary stations, and the remaining 37, secondary stations.

Radiation values for all stations were computed by
polynomial regression equations derived from the primary set
for each month. These equations involved the first three
powers of latitude and longitude. Table III compares monthly
values computed by the interpolation equations with avail-
able values for two secondary sites.

For the sake of consistency, all simulations reported
were performed using the computed radiation values. As a
check, simulations were run for the primary stations using
original data. These revealed no significant difference in
maximum active layer depth due to the use of computed radia-
tion values at those sites. Since the primary sites are
well distributed over the entire region, it is expected that
error due to this method of interpolation will be of impor-
tance only at particular sites and will not appreciably al-

ter the final maps.

V. The Maps. It is apparent from Figure 2 that active layer melting over the permafrost region of Canada is closely related to the pattern of regional climate, which is greatly affected by regional air mass climatology as influenced by topography and the annual circulation regime.

Of particular interest is the northerly shift of the contour lines in the area of the proposed Mackenzie Valley Pipeline Corridor. This shift is probably due to a combination of factors such as the large quantity of heat transferred northward by the Mackenzie River, the location of weather stations close to the river (although most stations across the map are located quite close to either lakes or rivers), the continentality of the region, and the movement of tropical maritime air. For comparison, consider Hay's (1971) map of mean monthly precipitable water for July.

Active layer melting maintains the pattern of Figure 2 upon either removal of the organic mat or drying of the surface (Figures 3 and 4). Both changes operating together amplify the pattern (Figure 5). When the active layer depth maps are subtracted one from the other, spatial variation of process sensitivity to parameter change is clearly seen.

In Figure 6, the effect of organic layer removal is isolated, and it is seen to be relatively independent of spatial position. Over the entire area south of the 30 cm

contour line there is little systematic variation. Only south of 65° N latitude is a small latitudinal dependence found.

A more pronounced spatial dependence is seen in Figure 7, which isolates the effect of lowering summer surface wetness. The effect of the two parameters operating in tandem is depicted in Figure 8.

These results are quite understandable. Both parameter changes are effective primarily in the summer. Soil surface wetness is important only when the soil is snowfree. The organic layer acts as a barrier or low frequency by-pass filter to the flow of heat from the soil surface. Removal of the layer allows more of the summer heat pulse to penetrate the deep soil, whereas in winter the effect on energy transfer is masked by the presence of the snow blanket.

Soil heat flux is a relatively small component in the summer surface energy balance, and removal of the organic layer, maintaining the soil in a wet condition, has little effect on the surface equilibrium temperature. Thus, an increase in active layer depth due to organic layer removal is tied relatively weakly to the climatic determinants of the surface energy balance.

Changing surface wetness, on the other hand, affects active layer melting by changing the rate of evaporation, and therefore the surface equilibrium temperature. There is then, through the linking mechanism of the surface energy

balance, interaction between a change of surface wetness and such climatic elements as relative humidity and wind speed. Since these elements have spatial variance, and since the interaction between them and surface wetness is non-linear, the effect of a surface wetness change is non-linear as well, and exhibits strong spatial variation.

Table IV displays the results of the simulations along a line from Inuvik in the Mackenzie Delta area to Ft. Simpson. It is apparent that artificial drainage of areas of peaty soils along the line would have a considerable effect on active layer melting, although the effect of drainage on the thermal properties of the peat layer might lessen the total depth increase. (This relationship is not modeled presently but will be explored in future work with a simulator containing a more refined treatment of soil thermal properties.) Complete removal of the organic mat produces an equivalent active layer depth increase, and both removal and drainage (a probable result of pipeline construction) nearly doubles the maximum depth of the active layer.

VI. Summary and Conclusions. In summary, the research reported in this paper has demonstrated the feasibility of employing a simple site energy balance climatic simulator to a spatial problem. The effects on active layer melting depth of surface modification have been determined quantitatively for a region where the active layer is an important factor

in human settlement and resource extraction.

The simulations have shown that stripping the organic layer from mineral soil produces an appreciable increase in the depth of active layer melting, and that this increase is little affected by regional variation in climate. Change in surface wetness, on the other hand, produces an effect which is sensitive to regional climatic variations.

Interpretation of these results is necessarily con-strained by the theoretical nature of the work. In parti-cular, the problem of "representativeness" must be kept in mind.

We have in effect constrained several axes of a multi-dimensional variate space in order to isolate the effect of a few parameters. This methodology is by no means novel, and is in fact the classical method of sensitivity testing. The importance of the work stems from the fact that the study has been conducted at relatively low cost by the use of a simple computer model and readily available weather data. Much future work on permafrost and its interaction with site and climate will no doubt involve more sophisti-cated models, and these will require extensive data collec-tion. The climate and site-parameter space will be investi-gated by many workers in great detail and over large time spans. This will be an expensive and difficult undertaking, and it is important that preliminary work be done with simple models and available data, so as to approach the multi-

variate problem with an abstract knowledge of basic system sensitivities. It is felt that the methodology reported here, and similar modeling activities, will be of some assistance to that end.

Planned future work at the University of Michigan will address the problem of temporal variance of the spatial pattern of active layer response to surface modification. It is hoped that this effort will lead to a better understanding of both the effect of past climate on present conditions and the temporal decay of the effects of various surface modifications. In addition a model is being developed which will produce time-distance maps of surface modification effects for any given pipeline route. This model may be useful in pipeline routing decisions.

The authors wish at this point to stress the need for the establishment of a net of soil temperature observation sites over the permafrost areas of North America. Soil temperatures and active layer depths should be monitored at each location at sites with soil and surface conditions comparable over the net. These observations would be of great value in model building, and are necessary for verification of the theoretical work in progress.

The authors wish to thank Mr. D. K. MacKay and Mr. A. C. D. Terroux for their invaluable assistance in the procurement of data and computer resources, and Dr. Waldo Tobler of the University of Michigan for his assistance with the mapping. Climatic data was assembled by personnel of the Atmospheric Environment Service under Project No. 04473.

Bibliography

Brown, J., W. Richard, and D. Victor. 1969. The effect of
　　disturbance on permafrost terrain. SR 138, U.S. Corps
　　Engineers, Cold Regions Research and Eng. Laboratory,
　　Hanover, New Hampshire.

Gold, L.W., G.H. Johnston, W.A. Slusarchuk and L.E. Goodrich.
　　1972. Thermal effects in permafrost. In Proceedings
　　of Canadian Northern Pipeline Research Conference,
　　Ottawa, 2-4 February, 1972. Associate Committee on
　　Geotechnical Research, National Research Council of
　　Canada, Technical Memorandum 104, Ottawa.

Gold, L.W. and A.H. Lachenbruch. 1973. Thermal conditions
　　in permafrost -- a review of North American literature.
　　In Permafrost: The North American Contribution to the
　　Second International Conference, ISBN 0-309-02115-4,
　　National Academy of Sciences, Washington, D.C.

Goodwin, C.W. 1972. An annual active-layer simulator for
　　permafrost regions. Unpublished M.S. thesis, The
　　University of Michigan, Ann Arbor.

Goodwin, C.W. and S.I. Outcalt. 1974. The development of a
　　computer model of the annual snow-soil thermal regime
　　in arctic tundra terrain. In Climate of the Arctic,
　　(in press), University of Alaska Press, Fairbanks.

Hay, J.E. 1971. Precipitable water over Canada: II distribu-
　　tion. Atmosphere, Vol. 9, No. 4, 101-111.

Khilmi, G.F. 1968. Philosophical aspects of the problem of
　　transformation of nature. In The Interaction of
　　Sciences in the Study of the Earth, translated by
　　Vladimir Talmy, Progress Press, Moscow.

Myrup, L. 1969. A numerical model of the urban heat island.
　　Jour. Appl. Meteor., Vol. 8, 908-918.

Nakano, Y. and J. Brown. 1972. Mathematical modeling and
　　validation of the thermal regimes in tundra soils,
　　Barrow, Alaska. Arctic and Alpine Research, Vol. 4,
　　No. 1, 19-38.

Outcalt, S.I. 1972. The development and application of a
　　simple digital surface-climate simulator. Jour. Appl.
　　Meteor., Vol. 11, 629-636.

_____. 1973. A brief introduction to synthetic climatology and deterministic modeling strategy. Climatological Bulletin No. 14, McGill University, Montreal.

Outcalt, S.I., C. Goodwin, G. Weller and J. Brown. 1974. Modeling interactive annual snow mass balance and snow-soil thermal evolution at Barrow, Alaska. Unpublished manuscript USACRREL.

Weller, G. and B. Holmgren. 1973. Daily micrometeorological data for summer 1971, site 2, Barrow, Alaska. U.S. Tundra Biome Data Report:73-29.

TABLE I

INPUT DATA: CLIMATIC VARIABLES
(12 Monthly Mean Values: Jan - Dec)

Total Solar Radiation
Air Temperature at Instrument Height
Wind Velocity at Instrument Height
Barometric Pressure
Relative Humidity
Cloud Cover Fraction

TABLE II

INPUT DATA: SITE PARAMETERS

PARAMETER	VALUE

Thermal Properties (From Nakano and Brown (1972))

Material	Conductivity (cal/cm sec °C)	Diffusivity (cm^2/sec)
Snow	0.00020	0.00120
Frozen Organic Layer	0.00028	0.00046
Thawed Organic Layer	0.00067	0.00070
Frozen Mineral Soil	0.00220	0.00420
Thawed Mineral Soil	0.00206	0.00370

Other Parameters

Organic Layer Porosity	0.50
Mineral Layer Porosity	0.42
Snow Depth	1 Jan to melt : 40 cm
	Surface refreeze to 1 Jan : 0 to 40 cm (linear increase)
Snow Surface Wetness	1.0
Instrument Height	150 cm
Snow albedo	0.80
Summer Surface Albedo	0.17
Snow Surface Roughness Length	0.01 cm
Summer Surface Roughness Length	2.00 cm
Organic Layer Thickness	30 or 0 cm
Summer Surface Wetness	1.0 or 0.5

TABLE III

MONTHLY MEAN TOTAL SOLAR RADIATION:

COMPARISON OF INTERPOLATED VALUES WITH OBSERVATION

(Observation source: DOEAES - Monthly Record)

LY/DAY

MONTH	FT. NELSON A, B.C.	EUREKA, N.W.T.
	( ) = Observation value	
Apr	....	282 (267)
May	510 (500)	527 (540)
Jun	469 (451)	562 (581)
Jul	482 (481)	425 (449)
Aug	372 (412)	222 (211)
Sep	201 (225)	105 (92)
Oct	114 (141)	8 (11)
Nov	47 (48)	5 (0)
Dec	31 (28)	....

TABLE IV

RANGE OF ACTIVE LAYER DEPTH AND INCREASE
ALONG A LINE FROM INUVIK TO FT. SIMPSON

ACTIVE LAYER DEPTH (cm)

		Summer Surface Wetness	
		1.0	0.5
Organic Layer	30 cm	71 - 113	105 - 146
Thickness	0 cm	107 - 147	143 - 181

ACTIVE LAYER INCREASE (cm and %)

CAUSE	ABSOLUTE INCREASE	% INCREASE
Organic layer removal	34 - 36	30 - 51
Decreasing Surface wetness	31 - 35	29 - 48
Both	67 - 72	60 - 101
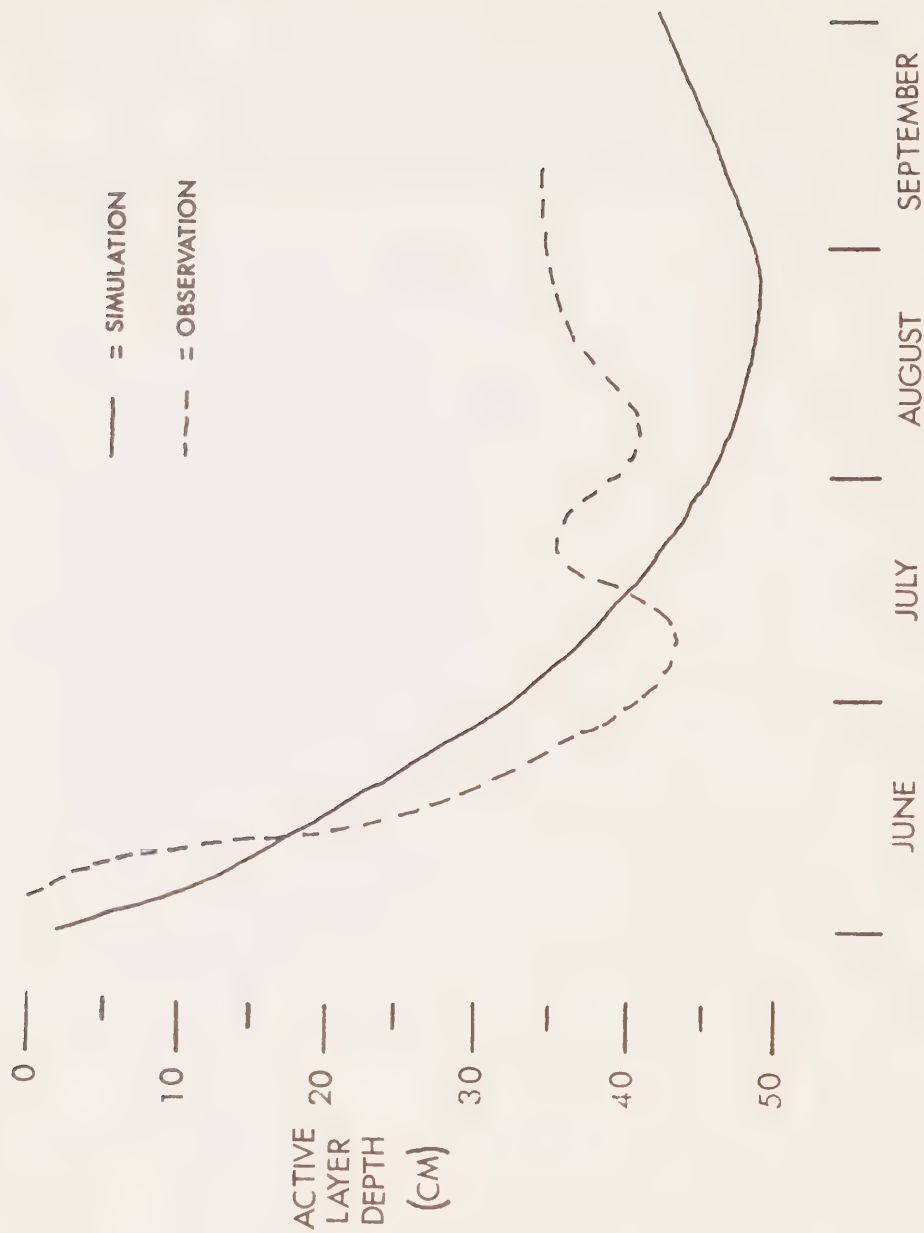
FIGURE 1. 1971 Active Layer Melting for a site near Barrow, Alaska. Observations computed from soil temperature data reported in Weller and Holmgren (1973).
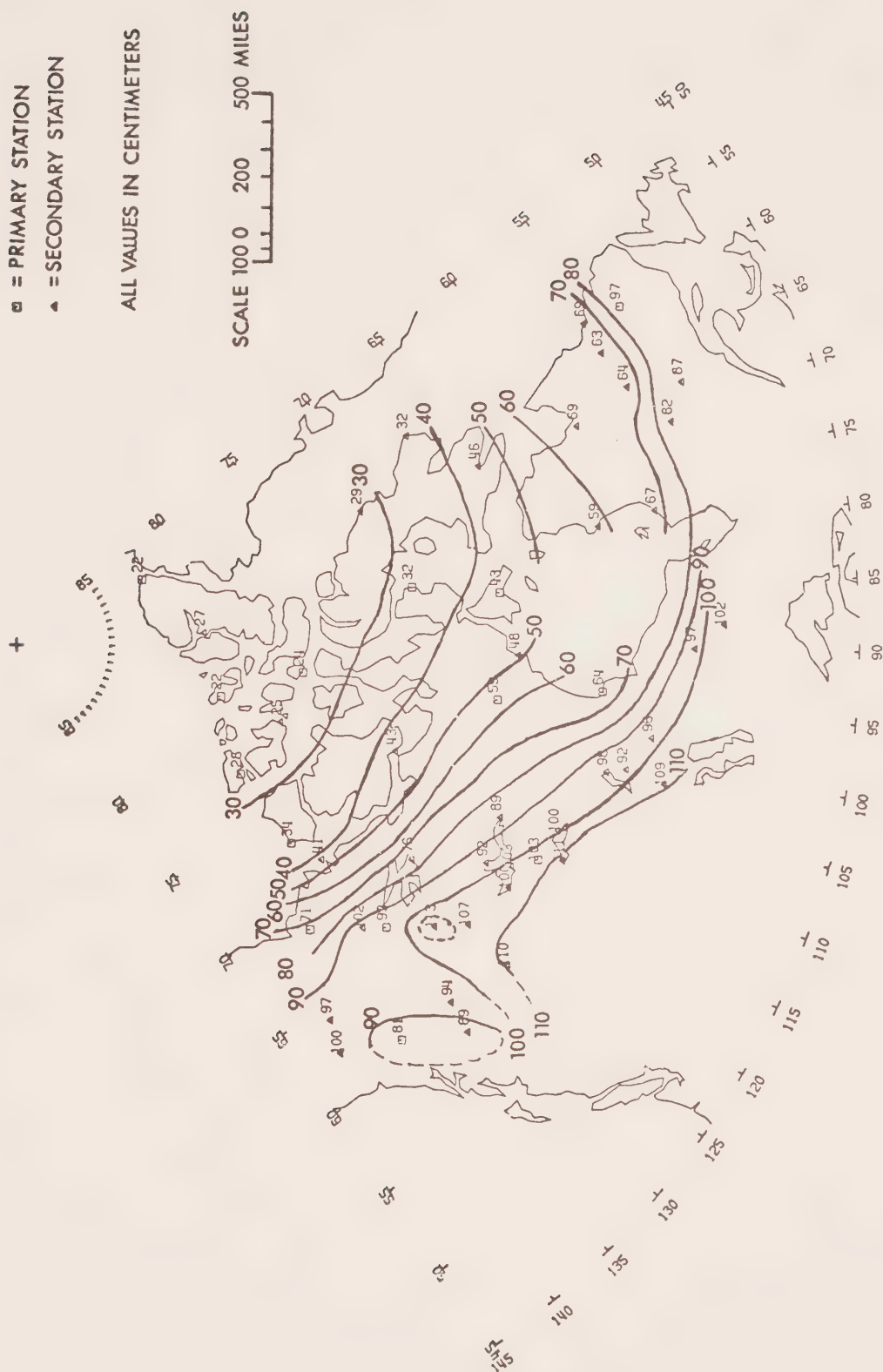
FIGURE 2. Theoretical active layer depths for sites having a 30 cm organic layer depth and a summer surface wetness of 1.0.

FIGURE 3. Theoretical active layer depths for sites having no organic layer and a summer surface wetness of 1.0.

- 44 -

FIGURE 4. Theoretical active layer depths for sites having a 30 cm organic layer depth and a summer surface wetness of 0.5.
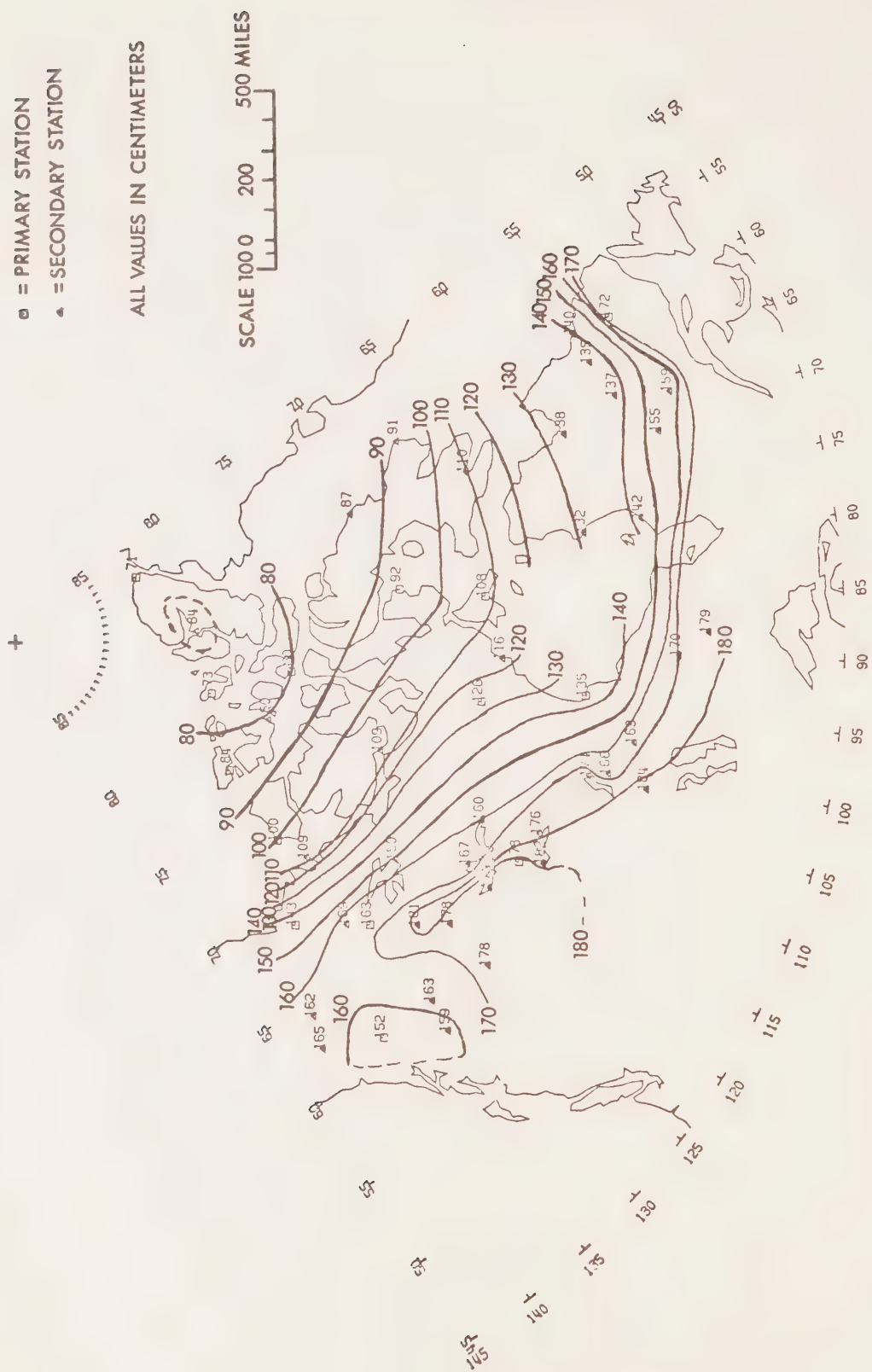
FIGURE 5. Theoretical active layer depths for sites having no organic layer and a summer surface wetness of 0.5.

FIGURE 6. Active layer depth increase due to removal of a 30 cm organic layer with summer surface wetness maintained at 1.0. (Figure 3 minus Figure 2).

- 47 -

FIGURE 7. Active layer depth increase due to a decrease in summer surface wetness from 1.0 to 0.5 for sites having a 30 cm organic layer. (Figure 4 minus Figure 2).

FIGURE 8. Active layer depth increase due to removal of a 30 cm organic layer and a decrease in summer surface wetness from 1.0 to 0.5. (Figure 5 minus Figure 2).

Application of Dendrochronology to some

Hydrological Aspects of Permafrost

by

W.E.S. Henoch

Table of Contents

Abstract

Applications of dendrochronology are discussed with reference to dating geomorphic events which are caused or accelerated by ice in permafrost and to reconstructing the past climate and predicting future climatic trends. It is suggested that the reconstruction of climatic variations calculated from ground temperature profiles can be corroborated by interpretation of temperature anomalies calculated from tree-ring data.

1. Introduction

With the accelerated rate of development in permafrost regions and the anticipated construction of pipelines there is a growing need for thorough knowledge of permafrost. This cannot be achieved by one discipline, but by a concerted effort of multidisciplinary research including dendrochronology, dendro-climatology, and dendrohydrology.

Considerable progress has been achieved in many fields of permafrost research in the last decade but there are several where knowledge is inadequate. Two are: dating of geomorphic processes in permafrost (Brown and Péwé, 1973) including cryogenic processes which control hydrology and create landforms characteristic of permafrost regions; and studies of past climate which can be used to predict the trend of future climate. In both these fields, which are of primary interest to pipeline construction, dendrochronology can make a significant contribution.

Recent new techniques in using a computerized system produce a variety of tree-ring data with speed and accuracy which could not be attained some years ago. In Canada, tree-ring research is carried out at the Western Forest Products Laboratory, Vancouver, B.C.(Parker, 1972; Parker and Jozsa, 1973) and at Brock University, St. Catherines, Ontario (McNeely et al., 1973).

The Glaciology Division of the Inland Waters Directorate applied dendrochronological data to the study of floods and ice jamming on Liard and South Nahanni Rivers and part of the Mackenzie River (Henoch, 1973; Parker and Jozsa, 1973). In this report application of tree-ring data to permafrost studies is discussed.

2.   The Influence of Vegetation on Permafrost and of
        Permafrost on Vegetation

        The mutual relation of vegetation and permafrost is complex. Briefly, it can be said that vegetation protects permafrost from thawing and that permafrost inhibits the growth of vegetation although examples of many exceptions are quoted by Brown (1963) and Péwé (1966).

        Low temperature and the permafrost's impermeability retard the growth of the root system and force roots to grow laterally. Benninghoff (1952) observed that the side of the root in touch with permafrost has restricted growth and that this is reflected in ovoid shape of the cross-profile of the root.

        If, however, trees and brush are removed, causing a disturbance to the surrounding moss and peat, degradation of the underlying permafrost follows. These changes may have significant local effects on the hydrology of the region and thus on the proposed construction of pipelines.

Study of anomalies of tree-ring growth in permafrost
can be a sensitive method of determining the past climate of the
area as any interference with growth of the tree can usually be
dated by analysis of its growth rings. Tree stems and root
samples have been collected in the Mackenzie Delta to determine
whether X-ray of the samples can provide information on the
influence of permafrost on tree growth. Preliminary results
(Parker et al., 1973) show a reduction of growth in tree-rings
of roots of an excavated tree stump, probably owing to the rising
level of permafrost. As the influence of other factors has to
be taken into consideration further studies are needed.

3.   Geomorphic Processes Caused or Accelerated by the
          Presence of Ice in Permafrost

Dendrochronology is well suited for dating landforms
and events originating from geomorphic processes in permafrost.
The application of some of the techniques used in the field
has been described by Henoch (1973) and Parker and Jozsa (1973).

3.1   Cryogenic processes

Cryogenic processes may lead to an increase or
decrease of volume of ground ice. As the result of direct or
indirect action of these processes, trees growing on permafrost
landforms may be injured, destroyed, or have growth aberrations

that can be used for dating and other studies based on tree-ring
chronologies.

3.1.1 Cryogenic processes leading to the increase of ground ice volume

3.1.1.1 Pingos

Pingos overgrown with coniferous trees are found at
the foot of Black Mountain (Aklavik Range, Richardson Mountains).
Some aspects of their formation could be documented and interpreted
by the systematic study of the annual growth of tree-rings.
Homes et al., (1968), for example, estimated the age of the
youngest pingos in Alaska using the age of trees and changes in
the tree communities.

3.1.1.2 Ice wedges

The age and the formation of ice wedges can be
determined if they are found to have affected the trees. A
buried tree, split by an ice wedge, was found near Point Separation
in the Mackenzie Delta in 1973. After the determination of the
age of this tree by tree-ring and radiocarbon dating the minimum
age of the ice wedges can be established.

3.1.1.3 Aggradational ice

Aggradational ice forms when the upper permafrost
surface gradually rises over a period of years and thereby
incorporates the ice lenses formed at the base of the active
layer (Mackay, 1972). Its origin depends on type of soil,

moisture content, vegetal cover, and temperature profile of the active layer.

It is suggested here, that the age and the rate of growth of this type of ice can be studied, in some cases, by dendrochronological methods. Two examples where tree-ring studies can contribute to understanding of the formation of aggradational ice are:

3.1.1.3.1 *Mounds of aggradational ice* - Ice lenses of perennially frozen ground in Mount McKinley, National Park in Alaska, studied by Viereck (1965) appear to be lenses of aggradational ice. They are mounds on which white spruce grow. Viereck suggests that two factors contribute to aggradation of ice under the trees: deep frost penetration, through comparatively thin snow cover under the canopies of trees; inhibition of heat exchange during the summer by a thick mat of moss on the mounds. The growth and collapse of the mounds causes trees to lean and topple over. These events could be dated by tree-ring analysis.

3.1.1.3.2 *Humps of aggradational ice* - Humped topography has been observed in the Mackenzie River Delta, on the terrace of Peel River near Indian Village. Preliminary survey of these humps, which have the appearance of incipient pingos, or palsas has been carried out during the summer of 1973 (Henoch, Parker, and Outhet, in preparation).

The humps are oval but irregular in shape. Their

- 59 -

diameters are 40m, 45m, and 80m, respectively. The largest one is
4m high above summer river level. They are skirted by a drained
lake and flood channels. The southern side of humps is undercut by
the Peel River. A cut-bank of the Peel River exposes the cross
profile of the humps displaying fine silts with high ice content,
horizontally stratified under the channel. However, the stratifi-
cation under the humps appears to have been dislodged from its
horizontal position and assumes an anticlinal structure under each
hump.

The origin of these humps is not certain. It is
believed that aggradation of ground ice governed by the interplay
of flooding and zonal distribution of vegetation are important
factors in their formation.

Intensive sampling of trees growing on the humps was
carried out for statistical analysis of tree-ring data, to
determine the influence of the climate, depth of active layer,
and flooding on the rate of growth of these trees.

Further research should be directed toward investigation
of:

(1) Aggradation of permafrost due to insulating and moisture
     retaining influence of caribou moss.
(2) Ground ice under the humps, its growth and heaving
     effect.

3.1.1.4   Palsa and string bogs

Palsa and string bogs occur in the southern fringe of permafrost and trees seldom grow on them. Palsa, in many ways similar to pingos, are low knolls of frozen peat usually no more than 2m high. They are formed by combined action of peat accumulation and ice segregation in the underlying mineral soil (Brown, 1970).

String bogs are strips of vegetation in shallow depressions generally filled with water. Their origin is not certain but most researchers think that cryogenic processes play an important part in their formation.

Dendrochronological methods have been applied to study the formation of string bogs in Finland (Yli-Vakkuri, 1960; Eurola, 1962). Aartolahti (1965) studied leaning trees growing on string bogs and determined annual growth of tree diameter and its eccentricity as a proportion of radial growth in the direction of lean. As the lean of trees was against the prevailing winds it was apparent that the tilting of the trees was caused by heaving of the ground and the heaving was caused by ice pressure.

These data were thought to represent changes in the intensity of cryogenic processes. An attempt to correlate the data with climate was unsuccessful partly due to the paucity of information.

3.1.2   Cryogenic processes leading to the decrease of ground ice

         volume.

         Examples of landforms originating due to cryogenic

processes and leading to a decrease of the volume of ground ice

are thermokarst and mass movement. Both can be studied by

dendrochronological methods.

3.1.2.1   Thermokarst

         This topography owes its name to its similarity to karst

topography. Melting of ground ice causes land subsidence and

produces hummocky terrain with generally level surface and steep-

sided depressions which are filled with silt and meltwater. Lakes

and ponds, with some dead trees in the water and some living trees

leaning toward the water, are found frequently in the forested

regions of permafrost. The trees indicate the recession of the

shores of thermokarst ponds and can be used to determine the rate

of recession of the shores. For example, Wallace (1948) has

applied dendrochronological methods to study the formation of

thermokarst lakes (cave-in lakes) in Alaska.

3.1.2.2   Mass movement

         Mass movement in permafrost regions manifested by

rotational slips, slides, slumps and solifluction is often caused

or accelerated by thawing of ground ice. A number of landslides

in the permafrost region of the Mackenzie and Liard River valleys

have been studied by using dendrochronological methods. The

results have shown the usefulness of these methods in studying
(1) the minimum age of the landslides; (2) periodicity of poly-
genetic causes of movement; (3) synchronous occurrence of many
of these movements in various landslides (Parker, Jozsa, 1973).

Determination of the age of the landslides provides
information on how long the landslides induced by activities of
man would likely be active. As a significant number of land-
slides has been reactivated synchronously in different localities,
it may be possible to correlate landslide occurrence with climate.
More data, however, are needed.

4.   Dendroclimatology and Permafrost

Rings of trees can provide a unique source of information
on past climate as far back in time as tree-ring chronologies can
be established. Although old trees near the northern tree line
are rare, nevertheless the author has found trees over 500 years
old in the Mackenzie Delta. Giddings (1962) has reported trees
about 1000 years old growing above the Arctic Circle.

Tree-ring width patterns over large regions can be
calibrated with the climatic data and the established relationship
can be used to extrapolate back into the climatic past (Fritts et
al., 1971). The studies have demonstrated that tree ring data
can be used to reconstruct past surface pressure anomalies, storm

tracks, temperature, precipitation or any other climatically related data that are available for calibration with tree-ring data. Fritts (1973) carries out investigation to reconstruct yearly seasonal anomaly patterns of climate (including temperature) and tree ring indices back to 1500 A.D.

Besides the variations in width of tree rings, the density of dated tree-ring series can also be used to obtain past climatic records (Parker, Henoch, 1971). For the climate studies of permafrost regions the variations in tree-ring density might prove to be a more sensitive parameter than the tree-ring width.

While in the arid zone precipitation is the main factor affecting the growth of a tree and the temperature plays a secondary role, in the Subarctic the effect of temperature is more significant than that of precipitation.

It is known, from the studies of ground temperature, that any change of temperature at ground surface is propagated downwards. Cermak (1971) has shown that a detailed record of ground temperature for varying depth can be used to reconstruct past climatic history.

The anomalies of ground temperature profiles could be correlated with temperature fluctuations as derived from dendroclimatic studies. To achieve this, however, the temperature profiles from deep drillings and more good tree-ring chronologies from the permafrost area or vicinity are needed.

5. Conclusions

The review of literature and the author's experience indicate that application of dendrochronological methods to the study of landforms, hydrology, and climate can contribute to solving various problems arising during the planning of pipeline construction and maintenance.

A systematic effort should be made to collect tree-ring samples along the northern tree line to build dendrochronologies which will provide the basis for dendroclimatic studies of permafrost regions. The progress made in the last decade in the development of new techniques to obtain tree-ring data and methods to interpret them justify a wider application of dendrochronology to studies of permafrost.

6. References

Aartolahti, T. 1965. Oberflächenformen von Hochmooren und ihre
     Entwicklung in Südwest-Hame und Nord-Satakunto. Fennia,
     93 (1), 1-268.

Benninghoff, N.W. 1952. Interaction of vegetation and soil frost
     phenomena. Arctic, 5 (1), 34-43.

Brown, R.J.E. 1963. Relation between mean annual air and ground
     temperatures in the permafrost region of Canada. Proceedings,
     Permafrost International Conference, November 1963, 241-46.

Brown, R.J.E. 1970. Permafrost in Canada. Its influence on
    Northern Development. University of Toronto Press, Toronto,
    Ont., 234 p.

Brown, R.J.E., Pévé, T.L. 1973. Distribution of permafrost in
    North America and its relationship to the environment: a
    review, 1963-1973. North American Contribution, Permafrost,
    Second International Conference, 13-28 July, 1973, Yakutsk,
    U.S.S.R., Publ. by National Academy of Sciences, Washington,
    D.C.

Cermak, V. 1971. Underground temperature and inferred climatic
    temperature of the past millenium. Palaeogeography,
    Palaeoclimatology, Palaeoecology, 10, 1-19.

Eurola, S. 1962. Über die regionale Einteilung der südfinnischen
    Moore. Annales Botanici Societatis Zoologicae. Botanicae
    Fennicae "Vanamo", 33 (2), 1-243.

Fritts, H.C. 1973. Tree-ring analysis of environmental variability:
    an extended basis for evaluating inadvertent and natural
    climatic change. Laboratory of Tree-Ring Research, University
    of Arizona, Tucson, Arizona.

Fritts, H.C., Blasing, T.J., Hayden, B.P. and Kutzback, J.E.
    1971. Multivariate Techniques for specifying tree-growth and
    climate relationships and for reconstructing anomalies in
    paleoclimate. J. Applied Meteorology, 10 (5), 845-64.

Giddings, J.L., Jr., 1962. Development of tree ring dating as an
    archeological aid. In: Tree Growth (T.T. Kozlowski, Ed.),
    119-32. The Ronald Press Co., New York, N.Y.

Henoch, W.E.S. 1973. Data (1971) on height, frequency of floods,
    ice jamming and tree-ring studies. Techn. Report No. 5,
    Glaciology Division, Inland Waters Directorate, Department of
    the Environment. In "Hydrologic Aspects of Northern Pipeline
    Development". Publ. by Environmental-Social-Committee,
    Northern Pipelines, Task Force on Northern Oil Development,
    Report No. 73-3, 153-190.

Henoch, W.E.S., Parker, M.L., Outhet, D. (in preparation).
    Vegetation, permafrost, and tree-ring transect across an
    area of ice-heaved topography in the Mackenzie Delta.

Holmes, G.W., Hopkins, D.M. and Foster, H.L. 1968. Pingos in
    Central Alaska. U.S.A. Geological Survey Bulletin 1241-H.

Mackay, J.R. 1972. The world of underground ice. Annals of the
    Association of American Geographers, 62 (1), 1-22.

McNeely, R., Neale, J., Benkel, M., Rustenburg, J., and
    Terasmae, J. 1973. Studies in dendrochronology, No. 1.
    Application of X-ray densitometry in dendrochronology.
    Research Report Series, No. 16, Brock University, Department
    of Geological Sciences, St. Catharines, Ontario, 30 pp.

Parker, M. 1972. Techniques in X-ray densitometry of tree-ring
    samples. Western Forest Products Laboratory, Faculty of

Forestry, University of British Columbia, Vancouver, British
Columbia, 11 pp.

Parker, M.L. and Henoch, W.E.S. 1971. The use of Engelmann spruce
latewood density for dendrochronological purposes. Canadian
J. Forest Research, 1 (2) 90-98.

Parker, M.L. and Jozsa, L.A. 1973. Dendrochronological investi-
gations along the Mackenzie, Liard and South Nahanni Rivers,
N.W.T. Part 1: Using tree damage to date landslides, ice
jamming and flooding. Techn. Report No. 10, Glaciology
Division, Inland Waters Directorate, Department of the
Environment. In: "Hydrologic Aspects of Northern Pipeline
Development" Publ. by Environmental-Social Committee,
Northern Pipelines, Task Force on Northern Oil Development,
Report No. 73-3, p. 313-464.

Parker, M.L., Jozsa, L.A. and Bruce, R.D. 1973. Dendrochronological
investigations along the Mackenzie, Liard and South Nahanni
Rivers, Northwest Territories. Part II: Using tree-ring
analysis to reconstruct geomorphic and climatic history.
Western Forest Products Laboratory, University of British
Columbia, Vancouver 8, B.C. Technical Report to Glaciology
Division, Inland Waters Directorate, Department of the
Environment, Ottawa, Ontario.

Péwé, T.L. 1966. Permafrost and its effect on life in the North.
Corvalis: Oregon State University Press, 40 pp.

Viereck, L.A. 1965. Ground, Mount McKinley, National Park,
     Alaska. Arctic, 18 (4), 262-67.

Wallace, A.R. 1948. Cave-in lakes in the Nabesna, Chisana and
     Tanana river valleys, eastern Alaska. American J. Geology,
     56 171-81.

Yli-Vakkuri, P. 1960. Metsiköiden routa-ja lumisuhteista. (Snow
     and frozen soil in the forest). Acta Forestalia Fennica,
     71 (5), 48 p.

Channel Ice Effects And Surface Water
Velocities From Aerial Photography
Of Mackenzie River Break-up

by

D. K. MacKay, D. A. Sherstone and K. C. Arnold

Glaciology Division,
Water Resources Branch,
Inland Waters Directorate,
Department of the Environment

Under the

Environmental – Social Program,
Northern Pipelines

Table of Contents

ABSTRACT

Aerial surveillance and photography during the 1972 and 1973 Mackenzie River break-up periods were carried out to monitor channel ice effects and to map water surface velocities. Some visible effects of ice action are discussed and illustrated with reference to the problems of navigation, highway and pipeline crossings, and settlement location. Surface water velocities are mapped for some sections to illustrate the possibilities of the method and its relevance to river scour, to the movement of spilled oil and to general hydrographic work.

Channel ice effects and surface water

velocities from aerial photography of

Mackenzie River break-up

by

D.K. MacKay, D.A. Sherstone and K.C. Arnold

Introduction

Aerial photographs of Mackenzie River spring break-up were
taken in 1972 and in 1973 to expand the information base available on
northern river ice disintegration processes and to test methods of mapping
surface current velocities. Previous to 1972, only scattered air and ground
observations were made with consequent limitations on the interpretation
of ice break-up.

A continued examination of Mackenzie break-up (see selected
reference list) is warran ed for a number of reasons. From the economic
point of view, the river forms a vital transportation link between north
and south. Its use as a waterway, however, is severely limited by the
shortness of the open season. More information on break-up could conceivably
improve its utilization b; etailing progress of break-up and by revealing
changes in the deep water ι annel caused by ice movement.

The economic argument may become very important in the near future
if northern oil and gas exploration activities are successful and production
decisions are reached. Pipelines may then be built with consequent heavy
demands on river cargo space that could tax the capacities of freight
handling facilities on the Mackenzie. A complicating factor is the
possible increase in movement of road-building equipment and supplies for
construction of the Dempster and Mackenzie Highways. Eventually, these
roads will provide all-weather, year-round alternatives to shipping via

water during the short season on the Mackenzie but, in the interim, it
seems clear that full use of the river is important for northern economic
development.

In an engineering sense, break-up surveillance is important
for the information it provides for highway and pipeline planning,
construction, and maintenance. Bank erosion and bed scour caused by
ice movement and ice jamming can affect location and design of pipeline
and highway river crossings as well as river docking facilities. Ice
jams can cause localized high water on the main Mackenzie and backwater on
its tributaries. This, in turn, may induce washouts at pipeline or road
crossings of rivers and streams. It seems, therefore, that for both
economic and engineering reasons, continued scrutiny of break-up processes
on the Mackenzie River is warranted.

The general pattern of Mackenzie River break-up is well known
(17, 15, 12). In summary, radiational melting of snow begins along banks
and on slopes in early April causing a rise in river stage and development
of shore leads. As runoff from tributaries flowing into the Mackenzie
main stem increases, transverse leads open across the full width of the
river (Figure 1). A further development of this stage is the intermittent
downstream movement of sections of the main ice cover. The movement of the
main ice cover is partly dependent on break-up of the Liard River, the
major Mackenzie tributary.

When Liard ice moves, in April or early May , its streamflow can
exceed the Mackenzie's which it joins directly above Fort Simpson.
Normally the rising Liard flow pushes ice wreckage (Figure 2) high
onto channel banks with remnant ice entering the Mackenzie and stopping in
the river stretch opposite Fort Simpson and below. If the stage continues

to rise, ice in the Mackenzie moves downstream leaving the river open at the settlement. Often the Mackenzie ice cover above the Liard junction (Figure 3) remains intact for some days thereafter.

During the 1972 break-up and through the early summer season, extremely high water conditions were experienced on the Mackenzie River and in its Delta. With these high water levels, a few large ice jams developed, two of which were of some consequence. One jam, below Fort Simpson, caused flooding in part of the settlement; and the other jam, at Fort Norman was sufficiently high to push or spill ice into the lower rim of the village. In the Delta, masses of ice were deposited on levees and some central-outer portions below Reindeer Station were covered by floodwaters.

In contrast to 1972 conditions, water levels in 1973 were reasonably normal with many small or partial jams developing (Figures 4 and 5). Only one fairly large size jam occurred, that being near the proposed Canadian Arctic Gas Pipeline crossing above Point Separation. In other respects, the progress of break-up was normal.

Channel Ice Effects

Ice moving in a river during break-up erodes channel islands, beds, and banks. Many of the erosional effects on these features can be documented, at least in part, by aerial surveillance.

The heads of many channel islands are subject to strong ice push (Figure 6) and those of alluvial origin are probably subject to annual modification in shape. Others of bedrock or till are less affected, the latter by forming a protective boulder veneer on their upstream ends.

Channel beds are open to abrasion or corrasion by the tumbling action of ice wreckage and by ice grounding in shallows. Along some river stretches, the

planing action of ice has formed boulder pavements (Figure 7) visible at low
water. Above the pavements and along the banks of many river reaches, there is
evidence of gouging and redistribution of bank materials by ice shove action.
Often, banks are topped by ice shove ridges. Such features are generally
developed by initial onshore ice movement. Any subsequent ice shove or pressure
is attenuated by the facade of stranded ice as implied in Figures 8 and 9.
Some of these features may not be detectable on aerial photos but their information
can be insinuated at locations where ice stranding or jamming is observed.

The most important of channel erosion effects are due to ice jamming.
Ice jams affect channel morphology in a number of ways. The increase in head
with flow moving under the jam can cause appreciable bed scour. In some instances,
a jam in the navigation channel will direct flow into an ancillary channel,
deepening it and changing the distribution of flow, (Figure 10). The redistribution
of flow may be accentuated by jamming in subsequent years until the ancillary
becomes the main channel.

Partial jams can also cause marked changes in channel cross-sections
through flow redirection, erosion and deposition. During partial ice jamming,
flow is concentrated in a particular part of the cross-section. This flow con-
centration could cause more scour than expected by normal evaluation methods.
If this occurred at underwater pipeline crossings or bridge locations, both
piers and pipeline could be undermined or exposed.

Backwater on the Mackenzie's tributaries and the main stem caused by
ice jamming is a factor in the planning of highway and pipeline routes. Moreover,
it is of practical importance in settlement location and in design of water
supply and sewage systems. Aerial photography is certainly the best method of
documenting the effects of backwater including the flooding of settlements. The

settlements of Fort Simpson, Fort Norman, old Fort Good Hope and Aklavik on the Mackenzie have all been subject to floods in which ice played an important role (9, 13). Aerial photography following the 1972 flood recession is available for Fort Simpson. At Fort Norman, there are photographs of both the early and late stages of the 1972 ice jam in which some ice entered the lower village.

Surface Current Velocities

The analysis of surface flow over a period of time may aid in distinguishing scour and fill in critical river sections of interest to pipelines and highways. The reasons for this possibility are that changes in channel roughness, shape and gradient should affect water surface velocities and, secondly, these velocities can be mapped from air photos. Two ways of estimating surface current velocities from air photos are examined and discussed in this report.

In the first instance, discrete blocks in moving ice wreckage are located with respect to channel shore control points on consecutive air photos. If the aircraft speed and the interval between exposures is known, then the velocity of ice movement can be calculated as illustrated in Figure 11. One of the limitations of this method is the large number of plotted movements that must be measured to produce flow lines (Figure 13) over a given stretch of river.

An alternative method is to contour the apparent stereo parallax (Figure 12) that results from water surface movement over the interval between photo exposures. The important criteria, as indicated in previous studies (4,5,6,7,19), are as follows:

1) Visible foaming, sedimentation or artificially introduced discrete control points in the water to permit measurement of the moving surface water;

2) Shore control points to permit " tying in " of water data to a rigidly controlled shore datum;

3) Rigid control and recording of the interval between photographic exposures to permit precise determination of displacement.

In the Mackenzie study, ice wreckage combined with substantial volumes of sediment and flood debris satisfied the first criterion. Adequate shore and water control, however, was often lacking due to the mismatch of flight line direction with river orientation. Moreover, excessive pitch and yaw was often discernible when photo transparencies were examined in a precision stereo plotter. This was particularly evident on photos taken during times when the aircraft was following bends in the river. The initial 1972 study, therefore, was restricted to two test sites near a possible pipeline river crossing and where, fortunately, high quality photography was available. The river at these sites also contained a considerable amount of suspended sediment, discrete ice blocks, and some foam from turbulent flow.

Contour plots of two 1972 test sites, located at miles 607 and 612, approximately 20 miles above the Sans Sault Rapids, are shown in Figures 14 and 15. These two sites represented the first experimental tests to determine the usefulness of this technique and were the only test sites which could be completed in the plotting time available. A visual comparison of the contour and discrete ice block measurement plots shows a reasonably good correlation between the two techniques. A further comparison with Canadian Hydrographic Service Chart 6420 suggests close agreement of the high flow velocity paths with the two alternate navigation channels.

In view of the encouraging results obtained with the samples tested in 1972 it was decided to examine further 1972 aerial photography in this manner and to then examine these same areas during similar 1973 break-up stages. Photography of the 1973 break-up is limited as ice clearance in the upper reaches of the river (upstream of Wrigley) occurred prior to the arrival of the photo aircraft.

Imagery of moving ice debris in the areas of miles 607 and 612 was again obtained, but the relatively low concentrations of moving ice and lack of turbidity prevented continuous contouring of the surface (Figure 16). The area in which contouring was completed proved too fragmentary to permit a full comparison of 1972 and 1973 data. Values derived from discrete ice block measurements indicate that velocities were generally similar in both years; the average derived flow velocities using this method were 4.07 and 3.45 m.p.h. for the 1972 and 1973 tests respectively. These values may be suspect due to a decreased density of ice " wreckage " in 1973, but the stage-discharge throughout the 1972 break-up season exceeded that in 1973 which tends to support the reported velocities.

In order to provide sites for future comparison of surface velocity patterns, additional 1972 photography was examined and stretches were selected near Wrigley (2 sites) and Camsell Bend. These stretches (Figures 17, 18 and 19) provide ideal test sites for contouring since the river is both narrow and straight for a distance of roughly 20 miles. Of the Wrigley sites the southern stretch (Figure 17) is the most interesting since it covers an uninterrupted distance of ten miles and includes a channeling of the flow due to the occurrence of fast ice (Mile 364) and a resultant " compression " of contour spacing. This indicates a rapid rate of velocity change due to channel constrictions (this effect also occurs at Mile 370). The section covered by the test plot also includes a zone of back eddies (indicated by the " negative " or " depression " contours) and a large area of significant surface shear in the Y plotting direction, which causes increased residual parallax and the resultant loss of a contourable surface.

Over the 10-mile Wrigley stretch (Figure 16), ice wreckage is evenly distributed with block sizes grading from large at the down-stream end to small

at the upstream one. The only area of open water is just below the constriction

at Mile 364 which poses some difficulty in carrying out the contouring. The

Canadian Hydrographic Service Chart 6414 covering the plotted section shows sand

deposits and shoals at the ice covered constrictions. These are normally exposed

during periods of low summer flow. Maximum surface flow velocities at Miles 364 and

370 (Figure 18) coincide with the deep water navigation channels shown on the

hydrographic charts.

The contour velocity values in the 1973 test sites were derived from

the discrete ice block measurement system (4,5,6,7). In 1972 the calculation of

velocity contour values was initially made using a similar triangle solution and

the discrete ice block measurement system as a check.

The results to date indicate the following:

1) Maximum ice wreckage concentrations occur in the areas of maximum velocity.

Examination of this data using a Spatial Data color display densitometer lends

credence to this evidence (20).

2) It is possible to contour the velocities of a complete water surface using

photogrammetry. This suggests the possibility of relating changes in surface

patterns to changes in bed conditions.

3) Surface water velocity plots could be a significant tool in assessing

distribution and movement of oil following spills, and

4) Such plots may be beneficial in staging hydrographic work on rivers by

indicating changes in the navigation channel.

In summary the use of aerial photography during particular stages

of spring break-up can provide useful data on changes in channel morphology

caused by ice action and on the opening of sections of the river for navigation

purposes. Possibly, of greater importance is the application of such photography

to oil spill, bed scour and other hydrographic problems through the provision of

a graphic portrayal of surface water conditions.

ACKNOWLEDGMENTS

SELECTED REFERENCES

1.   ALLEN, W.T.R. and CUDBIRD, B.S.V. 1971. Freeze-up and break-up dates of water bodies in Canada. Can., Ministry of Trans., Can. Met. Serv., CLI-1-71, 144 pp.

2.   BURDYKINA, APP. 1968. On the conjugation of the break-up processes of the Yenesei and Mackenzie Rivers. Trudy Glavnoi Geofizicheskoi Observatorii, 227, pp. 38-41.

3.   BROWN, R.J.E. 1957. Observation on break-up in the Mackenzie River and its delta in 1954. J. Glaciol, 3, No. 22, pp. 133-142.

4.   CAMERON, H.L. 1952. The Measurements of Water Current Velocities by Parallax Methods. "Photogrammetric Engineering", Vol. 18, No. 1 pp. 99-104.

5.   CAMERON, H.L. 1962. Water Current and Movement Measurement by Time Lapse Air Photography. An Evaluation. "Photogrammetric Engineering", Vol. 28, No. 1, pp. 158-163.

6.   FORRESTER, W.D. 1960. Plotting of Water Current Patterns by Photogrammetry. "Photogrammetric Engineering", Vol. 26, No. 5, pp. 726-736.

7.   KELLER, M. 1963. Tidal Current Surveys by Photogrammetric Methods. "Photogrammetric Engineering", Vol. 29, No. 5, pp. 824-832.

8.   KINDLE, E.M. 1920. Arrival and departure of winter conditions in the Mackenzie River Basin. Geog. Rev., 10, pp. 388-399.

9.   MACKAY, D.K. 1965. Break-up on the Mackenzie River and its delta, 1964. Geog. Bull. (Ottawa), 7, pp. 117-128.

10. _____ 1966. Mackenzie River and Delta ice survey, 1965. Geog. Bull. (Ottawa), 8, pp. 270-278.

11. _____ 1969. The ice regime of the Mackenzie Delta, N.W.T. IASH Symposium on the Hydrology of Deltas, Bucharest, May, 1969, pp. 356-362.

12. MACKAY, D.K. and J.R. MACKAY. 1972. Break-up and ice jamming of the Mackenzie River, Northwest Territories, In: Mackenzie Delta Area Monograph, Ed. D.E. Kerfoot, Brock University, pp. 87-93.

13. _____ 1973. Locations of spring ice jamming on the Mackenzie River, N.W.T. In: Hydrologic Aspects of Northern Pipeline Development, Information Canada Cat. No. R27-72, pp 233-257.

14. MACKAY, J.R. 1960. Freeze-up and break-up prediction of the Mackenzie River, N.W.T. NAS-NRC Symposium on Quantitative Methods in Geography sponsored by ONR, Chicago, May 5-6, 43 pp.

15. MACKAY, J.R. 1960. Freeze-up and break-up of the lower Mackenzie
     River, Northwest Territories. In: Geology of the Arctic -
     Vol. 2. (Edited by) G.O. Raasch, Univ. of Toronto Press,
     Toronto, pp. 1119-1134.

16. _____ 1961. A study of freeze-up and break-up at Fort
     Good Hope, N.W.T. In: Thought, Publ., W. J. Gage, Toronto,
     Ontario, p. 65-71.

17. _____ 1963. Progress of break-up and freeze-up along the
     Mackenzie River. Geog. Bull. (Ottawa), No. 19, pp. 103-116.

18. _____ 1963. The Mackenzie Delta area, N.W.T. Geogr.
     Branch, Mines and Tech. Surv., Memoir 8, Ottawa, 202 p.

19. OROS, C.N. 1952. River Current Data from Aerial Photography,
     "Photogrammetric Engineering" Vol. 18, No. 1, pp. 96-99.

20. SHERSTONE, D.A. 1973. Remote Sensing Techniques applied to
     Current Velocity Measurement and River Ice Jamming. In:
     Fluvial Processes and Sedimentation, Proceedings of
     Hydrology Symposium, University of Alberta, Edmonton,
     pp 403-419.

21. WILLIAMS, G.P. and D.K. MACKAY, 1973. Characteristics of
     Ice Jams. In: Seminar on Ice Jams in Canada, NRC Tech.
     Memo No. 107, Ottawa, pp 17-35.

Figure 1
Mackenzie River at Wrigley showing transverse cracks
across the river at Hodson Creek and Wrigley River.

Figure 2
Liard River ferry crossing site on the Fort Simpson side,
May 5, 1973. Note the ice wreckage stacked approximately
10 metres above the river level.

Figure 3
Junction of the Liard and Mackenzie Rivers on May 6, 1973.
The ice cover on the Mackenzie above the junction is still
intact. In the foreground, silt-covered ice wreckage from
the Liard litters the water approaches to Fort Simpson.

Figure 4
Minor ice jamming adjacent to Normal Wells settlement
on May 13, 1973.

Figure 5
Ice concentration in the deep water channel below
Fort Simpson, May 7, 1973. The dark sediment-laden
ice is from the Liard River.

Figure 6
Ice push on the head of an island in the Mackenzie
near Mile 225. In the background, an ice ridge may
be seen traversing the main channel.

Figure 7
Boulder paving on the Mackenzie River. The planing action
of moving ice during break-up is partly responsible for
development of these forms.

Figure 8
At Fort Simpson (May 6, 1973) stranded shore ice acts as a
buffer limiting erosion by the mass of ice wreckage moving
downriver. The dark area of jumbled ice, encompassed by
shear lines, is from the Liard River entering the Mackenzie
from the right background.

Figure 9
Shear lines caused by moving ice near the cliffs of
The Ramparts, May 16, 1973.

Figure 10
Ice jamming the navigation channel at Mile 470 causes
some deflection of flow to the left around the islands.

SIMILAR TRIANGLE SOLUTION FOR
ICE BLOCK VELOCITY CALCULATION

$$\frac{AA'}{EF} = \frac{BC}{BC'}$$

$$\frac{AA'}{D\,(t_1 t_2)} = \frac{\text{APPARENT VERT. DIS}}{\text{FLYING HEIGHT} + \text{AV}}$$

AA' REPRESENTS ACTUAL
MEASURED DISPLACEMENT
OF ICE BLOCK

APPARENT POSITION
OF ICE BLOCK
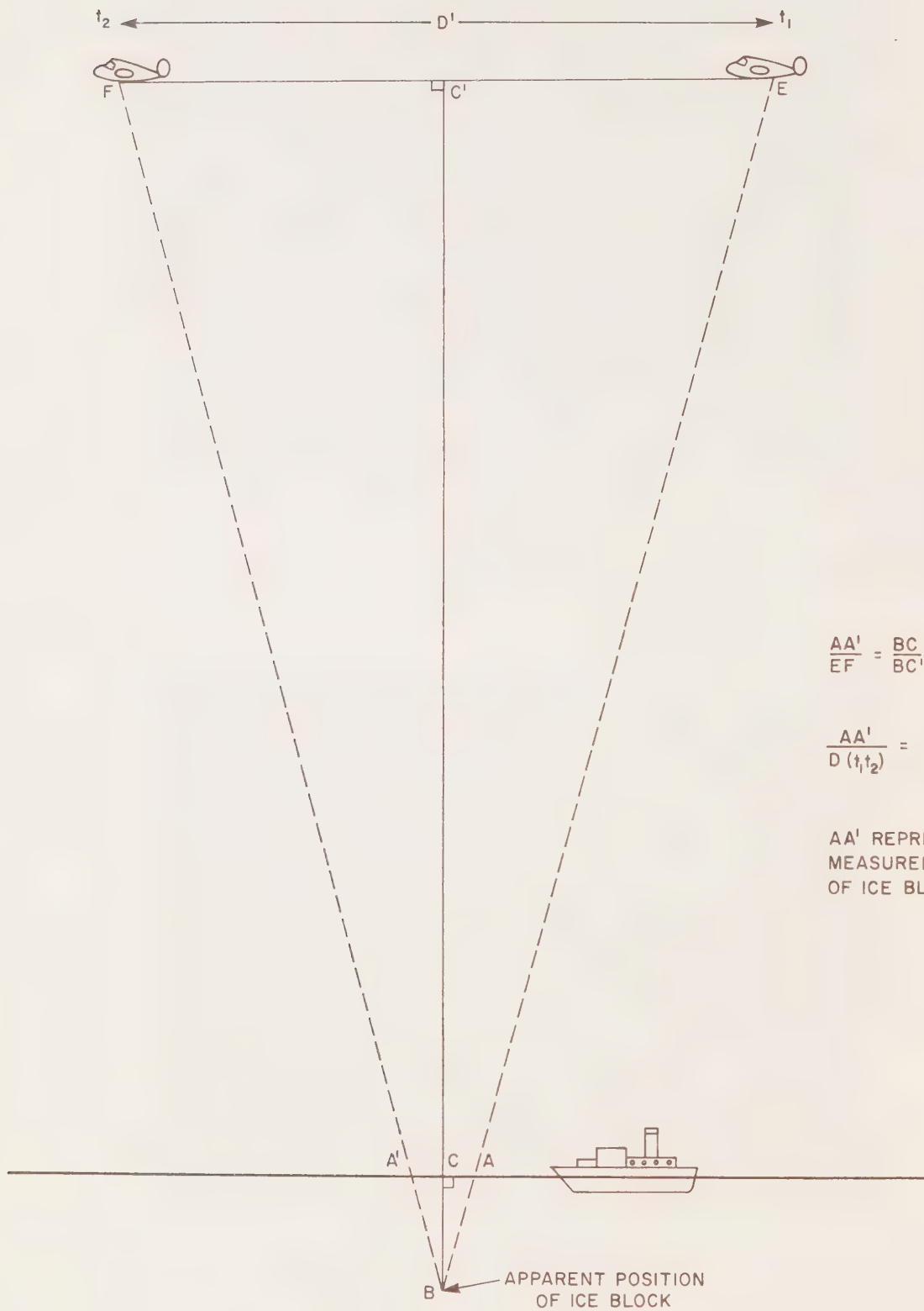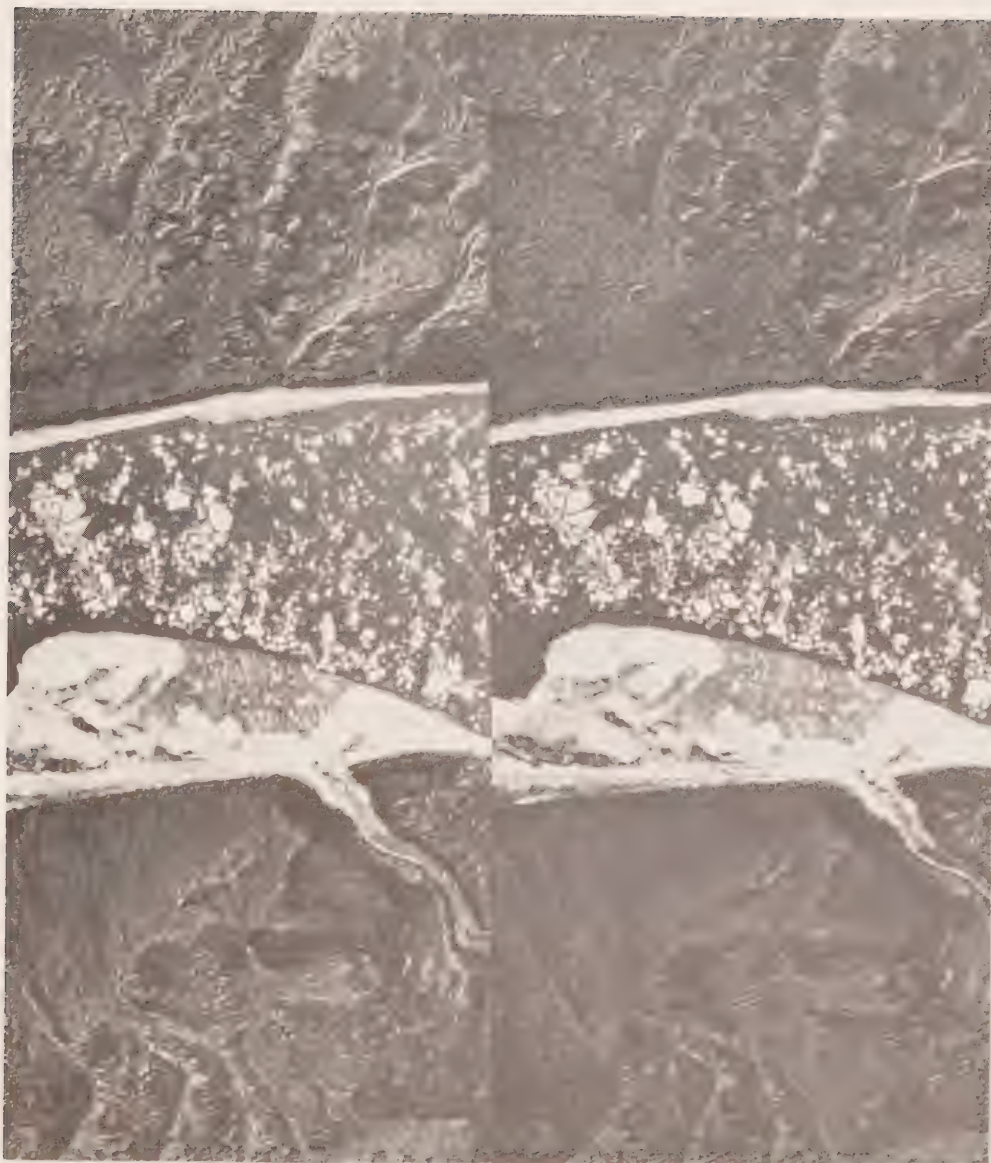
Figure 11

Figure 12
Stereo pair illustrating false parallax caused by ice
movement, Mile 610, Mackenzie River, May 19, 1972.
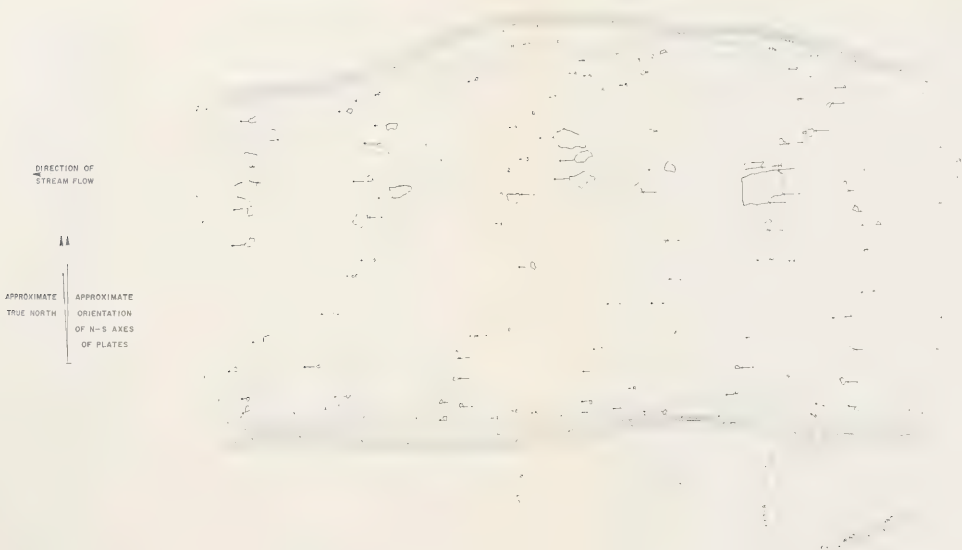
Figure 13

Discrete ice block movement test plot, Mile 612,
Sans Sault area (1972 photography). Vector arrows
indicate downstream movement of each block between
photo exposures.

DIRECTION OF
STREAM FLOW

APPROXIMATE
TRUE NORTH

APPROXIMATE
ORIENTATION
OF N-S AXES
OF PLATES

MACKENZIE RIVER A-7 TEST SITE #158

MILE 612 (CARCAJOU RIDGE AREA)

HORIZONTAL SCALE: APPROX. 1:8,850

VERTICAL SCALE: APPROX. 1:8,333

CONTOUR INTERVAL: REAL: 1.0 mm
APPARENT: 65 FT.
PHOTO INTERVAL: 23 SEC.

DASHED 'CONTOUR' LINES INDICATE AREAS IN
WHICH RESIDUAL PARALLAX REMAINS AFTER
CLEARING REMAINDER OF MODEL

HORIZONTAL SCALE: 8,850
FEET 500   0   500   1000   1500   2000 FEET
METRES 100   0   100   200   300   400   500   600 METRES

VERTICAL SCALE 1:8,333
FEET 500   0   500   1000   1500   2000 FEET
METRES 100   0   100   200   300   400   500   600 METRES
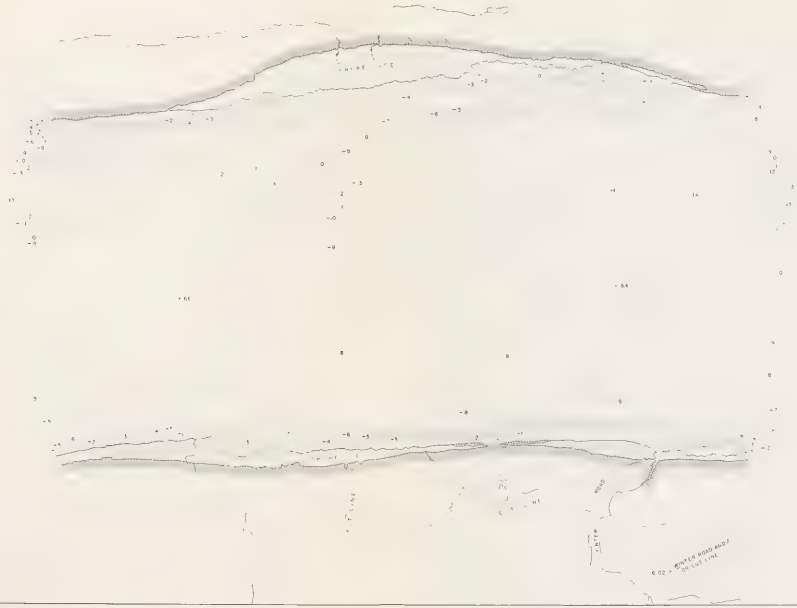
Figure 14

Surface contouring, Mile 607 Sans Sault area, 1972
photography. Values shown for each contour level
are machine intervals and not velocity values.
Velocity values derived as described in text. Dashed
lines indicate area of slight plotting difficulty due
to small amounts of residual parallax.

MACKENZIE RIVER A-7 TEST SITE #158

MILE 612 (CARCAJOU RIDGE AREA)

HORIZONTAL SCALE: APPROX. 1:8,850

VERTICAL SCALE: APPROX. 1:8,333

CONTOUR INTERVAL: REAL: 1.0 mm
APPARENT: 65 FT.
PHOTO INTERVAL: 23 SEC.

DASHED 'CONTOUR' LINES INDICATE AREAS IN
WHICH RESIDUAL PARALLAX REMAINS AFTER
CLEARING REMAINDER OF MODEL

Figure 15

Mile 606, Sans Sault area, 1972 photography. The
first test site attempted using photogrammetric method
of stream velocity contouring. Excessive parallax and
stereo gaps prevented further work at this location.
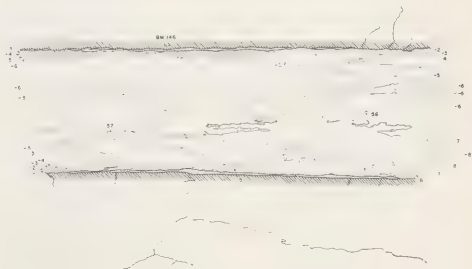
MACKENZIE RIVER A-7 TEST SITE #15B

MILE 606 (CARCAJOU RIDGE AREA)

HORIZONTAL SCALE: APPROX. 1:31,200

VERTICAL SCALE: APPROX. 1:8,333

CONTOUR INTERVAL; REAL, 1.0 mm.
                 APPARENT: APPROX. 65 FT.
PHOTO INTERVAL; 23 SEC.

WATER DATA AND SHORE DATA ARE NOT RIGIDLY
TIED VERTICALLY DUE TO EXCESSIVE RESIDUAL
PARALLAX ALONG RIGHT EDGE OF MODEL, SHORE
CONTROL POINTS FOR LEVELING ARE NOT READABLE
IN BOTH SET-UPS

Figure 16

Surface contouring, Miles 608-610, 1973 photography, Sans Sault area. Contouring is fragmentary due to lack of turbidity. Photography of this stretch of the river was acquired later in the break-up than previous years' photography. Contour values are shown in m/sec.

CONSTRUCTION CUT LINES

CLEARING (C)

GROUNDED SHORE ICE

LAKE

MACKENZIE RIVER A-7 TEST SITE 73-3

MILES 608-610 (CARCAJOU RIDGE AREA)

CONTOUR INTERVAL: APPROX. 0.13 m/sec (0.29 mph)

HORIZONTAL SCALE APPROX. 1:13,133

FEET 2000   1000   0   2000   4000 FEET
METRES 500   250   0   500   1000 METRES

'BOXED' AREA INDICATES
STUDY SITE FOR 1972
BREAK-UP

SEISMIC CUT LINES

MACKENZIE HIGHWAY CONSTRUCTION ROADS

Figure 17
Surface contouring, Mile 375, Wrigley area (northern
site), 1973 photography.

MACKENZIE RIVER A-7 TEST SITE 73-1

MILE 375 (OCHRE RIVER AREA)

CONTOUR INTERVAL APPROX

NOTE 'DASHED' CONTOUR LINES INDICATE AREAS
OF SLIGHT RESIDUAL PARALLAX PREVENTING
COMPLETE CERTAINTY IN LOCATING CONTOURS

Figure 18

Surface contouring, Mile 360-370, Wrigley area (southern site) 1973 photography.
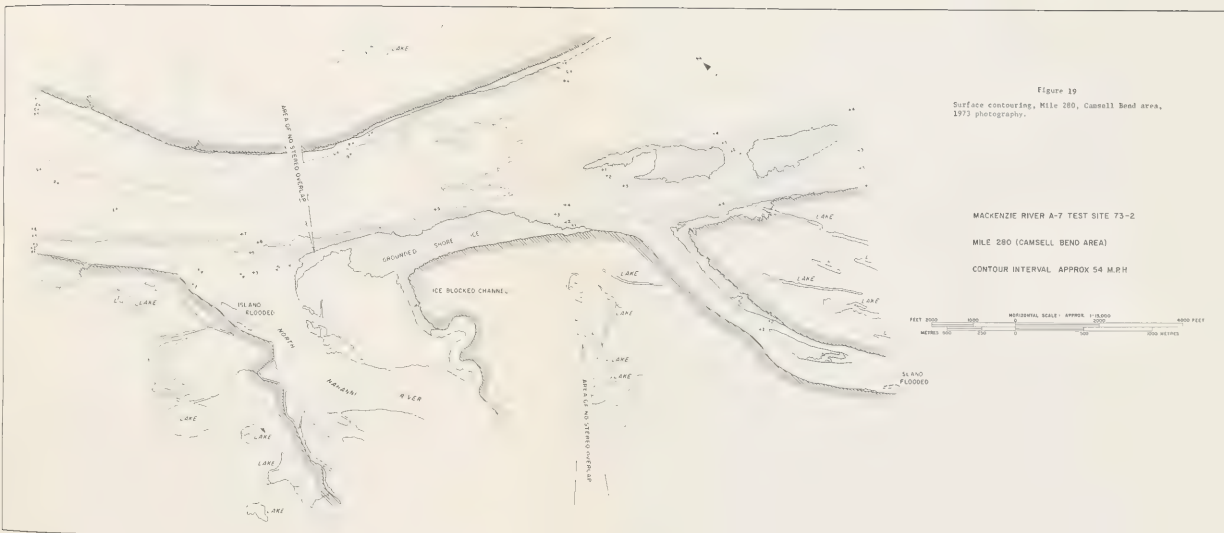
N

APPROXIMATE LIMITS
OF SHORE BOUND ICE

APPROXIMATE LIMITS
OF FAST SHORE ICE

SETTLEMENT OF
WRIGLEY (OLD)

MACKENZIE RIVER TEST SITE 73-4

MILE 360-370 (SETTLEMENT OF WRIGLEY (OLD) AREA)

CONTOUR INTERVAL APPROX 25 m.p.h (calculated)

velocities fall between +/< 25 m.p.h. and +28+6.90 m.p.h.

Figure 19

Surface contouring, Mile 280, Camsell Bend area,
1973 photography.

MACKENZIE RIVER A-7 TEST SITE 73-2

MILE 280 (CAMSELL BEND AREA)

CONTOUR INTERVAL APPROX 54 M.P.H.

PHYSICAL CHARACTERISTICS OF SNOWBEDS
IN THE RICHARDSON MOUNTAINS,
NORTHWEST TERRITORIES

BY

N.J.K. PETERSON

REPORT 25 TO

GLACIOLOGY DIVISION
WATER RESOURCES BRANCH
DEPARTMENT OF THE ENVIRONMENT

under the
Environmental-Social Program
Northern Pipelines

TABLE OF CONTENTS

LIST OF FIGURES

ABSTRACT

Physical characteristics of snowbeds in the Richardson Mountains
are investigated. The study conducted in the vicinity of Canoe
Lake (23 miles west of Aklavik) was carried out in the field
season lasting from May 14 – August 20, 1973. It examines the
impact of late snowbeds upon biological elements and other
physical processes in and adjacent to snowbeds. Role of other
factors affecting active layer development, ground temperature
regime and slope stability, in association with snowbeds is
discussed.

Introduction

This study was undertaken to examine the physical characteristics of snowbeds in the northern Richardson Mountains, Northwest Territories, Canada (Map A). Though snowbeds do vary in size, in most cases snow at the beginning of the melt season ranges from one to six meters in depth. The last of the snow melts sometime in the latter part of July or in August, or during colder summers, can last for more than one year. For the most part, though, snowbeds in the northern Richardson Mountains are annual or biennial features. This study was conducted in the vicinity of Canoe Lake, N.W.T. (68°,04'N,135°,30'W),23 air miles west of Aklavik, N.W.T. One snowbed, referred to as Snowbed *1, was studied intensively during a field season lasting from May 14 to August 20, 1973. Several other snowbeds in the immediate area were kept under observation throughout the summer, and, as time and access permitted, surveys of major snowbeds in the region were carried out over a period of four months.

Work performed during the 1973 season was the continuation of a three year project on the impact of late snowbeds upon associated biological elements and upon physical processes in and adjacent to the snowbeds. Other than their importance in the life cycles of many small mammal species and insects in the mountains, as well as containing a very specialized flora, snowbeds can be important as a source of water during the summer for smaller streams in the Richardson Mountains. Moisture from melting snow can also have a profound effect on the stability and active layer development of slopes under and near the deeper snow accumulations.

Materials and Methods

During the fall of 1972, wooden poles 270 cm long and 2.5 cm in diameter were placed around three snowbeds in order to mark the borders of the snowbeds and to determine snow depth the following spring. Snow depth throughout the 1973 season was determined by measurement along these poles or by probing with a 3/8 inch diameter, 2 meter sectioned, aluminum pole. Snow melt was determined by either the drop in actual snow

MAP A - CANOE LAKE AREA (from 'Aklavik 107B sheet, Scale 1:250,000)
KEY

FA - - - location of photographs

depth as measured by probing or by melt along one inch diameter, white wooden poles placed at 5 or 10 meter intervals in three profile lines perpendicular to the length of the snowbed. Due to some difficulties with thick ice layers within the snowpack, (snow depth and melt), were also checked by digging snow pits, generally to ground level. Profiles of snow type, such as location of ice layers, were measured in these snow pits and the density of the snow in each major snow or ice layer was determined using aluminum cylinders 20 and 48 cm long and 4.7 cm wide. A beam balance was used to weigh the samples on location. Densities of the surface layer of snow were also measured throughout the summer. The melt rate of Point CD75, at the center of the snowbed, was used as the standard rate, as CD75 represented both average conditions on the snowbed and the longest readings for snow melt. To record horizontal retreat of the snow, the snow border was marked with coloured flagging tape at 3 to 7 day intervals.

Albedo and incoming shortwave radiation were measured along the three profile lines with a portable MK6 Sol-A-Meter, produced by Matrix, Inc., Phoenix, Arizona. This meter, with a spectral response between 0.35 and 1.15 microns, measures incident solar energy in BTU per hour per square foot, with a ±5% accuracy, and albedo, in percentage of incident radiation, with a ±2% accuracy. All values were taken perpendicular to the immediate slope, and those of incident solar radiation converted to calories per cm^2 per minute. Incoming shortwave radiation was also measured with a recording bimetallic actinograph, made by C.F. Casella & Co., Ltd., London. The actinograph was placed at the upper edge of Snowbed *1 (location point CD 20), on the same SE facing slope as Snowbed *1. Values, taken at 15 minute intervals, were converted to $cal/cm^2/15$ minutes or 24 hours, by a computer program written by M. Smith, Geography Department, Carleton University, Ottawa.

Wind profiles throughout the summer for Snowbed *1 were measured with a hand-held anemometer, made by C.F. Casella & Co., London, model 204026, in meters per second or kilometers per hour. Measurements were taken at 1 meter above the ground and averaged over 2 minutes. Wind direction was determined with a compass. Total wind runs, in kilometers
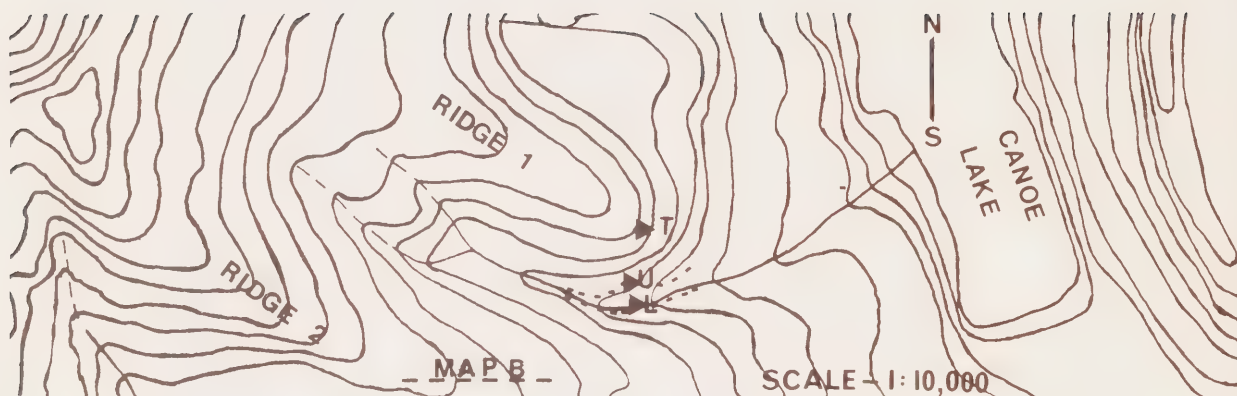
LOCATION OF INSTRUMENTS

◀ T   - anemometer at the top of Ridge 1

◀ U   - upper anemometer, upper rain gauge, actinograph,
         hygrothermograph

◀ L   - lower anemometer, lower rain gauge

---   - approximate May 15, 1973 snowborder, snowbed 1

over recorded time periods, were measured with three cup counter anemometers placed at 1.5 meters above the ground. The anemometers, model W5002 made by Casella & Co., had an accuracy of ± 1.6 kilometers per hour. The three anemometers were located on a transect down Ridge 1 (see Map B), with the anemometer on the top of Ridge 1 at 1550 feet elevation, the upper anemometer at 1350 feet (just before the top edge of the gulley containing the main part of Snowbed *1), and the lower anemometer at 1300 feet (in the band of lower shrub willows, but not sheltered by adjacent willows during winds from a northerly direction).

Local air temperature and relative humidity were determined with a recording hygrothermograph, model E9389, produced by R. Fuess, Berlin, placed on a stand 30 cm above the ground, on the upper edge of the snowbed. For determination of daily averages, chart values were taken every half hour.

Precipitation was collected in two standard 5 inch diameter rain gauges, model W5002, Casella & Co., Ltd., London, set at 30 cm above the ground to avoid splash-up from surrounding vegetation. A standard snow gauge was installed in September, 1972, but unfortunately, it was knocked over by a snowmobile during the winter and no record obtained.

Readings for total wind, precipitation, snow melt and snow depths were taken as early as possible in the morning. Values for daily average temperature and relative humidity, maximum and minimum temperature and relative humidity, and total shortwave radiation were taken from midnight to midnight. Profiles of albedo, incoming shortwave radiation, wind and snow density were taken as close as possible to solar noon. These profiles were run along three lines, perpendicular to the length of the snowbed, about 40 meters apart, starting with the upper May 15, 1972 and 1973, snow border as the zero point. The East Doweling (ED), Central Doweling (CD), and West Doweling (WD) lines were respectively on the east end, central portion, and west end of the snowbed. All distances along these lines were measured with a 30 meter metal tape.

Soil temperatures beneath the snow bed were sampled by 66 thermistors with a direct temperature read-out, non-recording meter built by the

Carleton University Science Workshop. The thermistors had been
installed in August, 1972, at depths of 0, 5, 10, 15, 30, or 50 cm
in the ground. Those at "0" cm were placed either next to the soil surface
under the immediate vegetation cover over the ground, or under the
first leaves of the litter layer. Those thermistors at lower depths
were inserted into the ground with a $\frac{1}{4}$ inch aluminum probe, thereby
minimizing disturbance of the ground. At the end of September, 1972, the
thermistor wires were elevated on poles 1.5 to 2 meters above the
ground. Temperature readings taken in November were done for those
thermistors which could be located on their poles, and, in the 1973
season, readings started once the wires and tops of the poles had
melted out or were dug out. Unfortunately, the weight of the winter
snow broke some of the poles, so that the wires became deeply buried.
Readings, in these cases, were not obtainable until much later in
the season. For most of the thermistors, though, temperature values with
a snow cover still present were recorded. Other gaps in the readings
occurred when the author was in other field locations. During the
1973 season, readings were usually taken in the morning, at noon,
and as late as possible in the evening (generally about 6 pm). At
the end of the summer, the thermistors were recalibrated in an ice
bath.

Active layer depths throughout the summer were measured with a
$\frac{1}{4}$ inch solid aluminum probe along profile lines, or by the actual depth
of soil pits. The presence of large chunks of rock or of bedrock in
areas adjacent to the snowbed made active layer determination difficult
there.

RESULTS

Distribution of Snowbeds

As seen by Pictures FA1 and FA2 in the Appendix, snowbeds are
by no means unusual features in the northern Richardson Mountains.
Though many slopes are snow-covered at the beginning of the melt season,
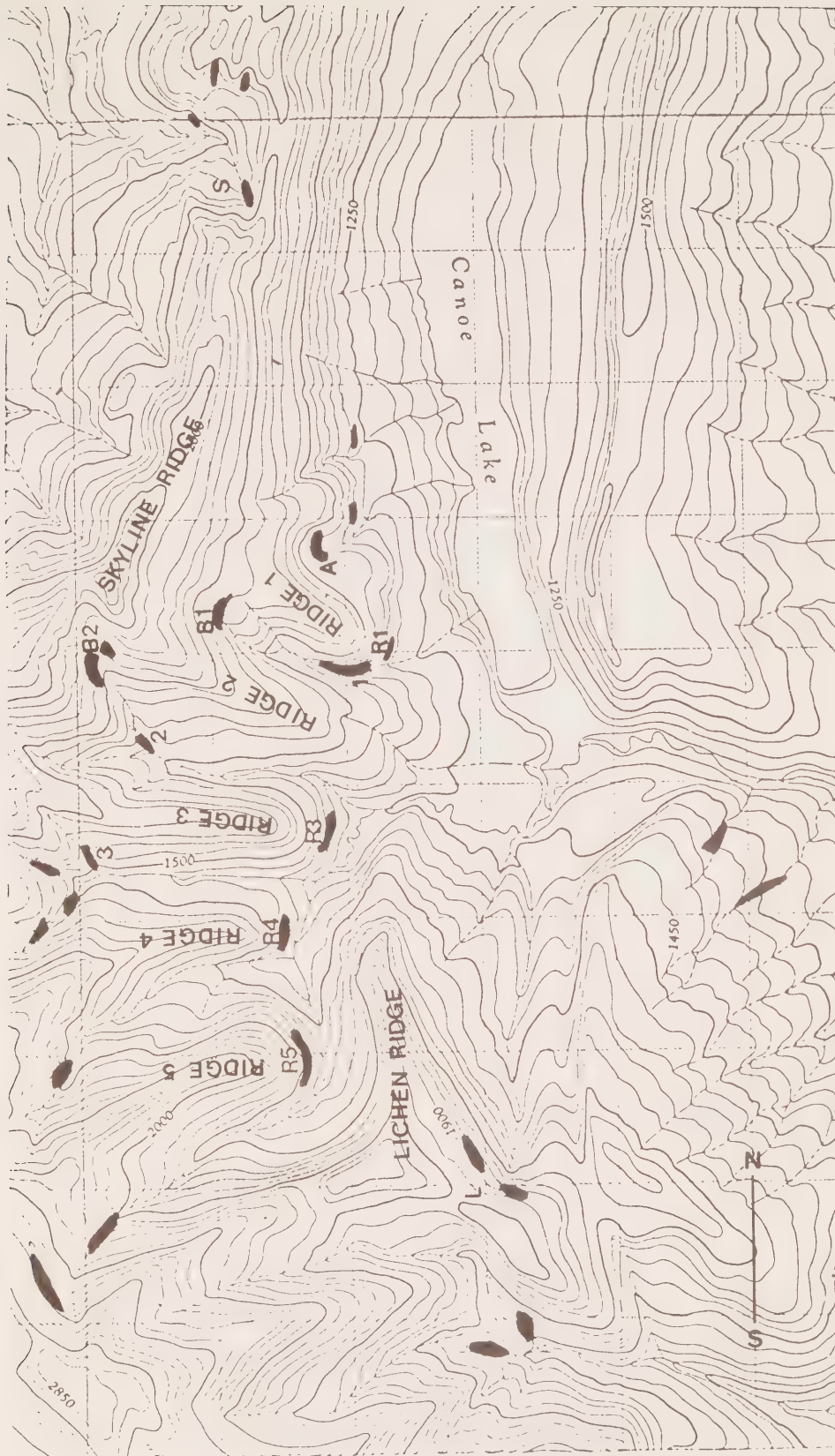
MAP C - SNOWBED LOCATION
KEY
●   - location of snowbed, July 1, 1973
XO   - name of snowbed

- 121 -

this snow cover is not long lasting, melting by the beginning to
middle of June. The deeper accumulations of snow are found in
depressions greater than one meter, in creek gulleys of any orien-
tation (though the drifts are deeper on southerly facing banks, or,
in the case of wide stream valleys, are confined along southerly to
easterly facing banks), and on southerly to easterly (usually SE)
facing slopes. Map C shows location of snowbeds, chiefly those that
were watched more closely over the summer. All those labelled on
Map C still had snow left in the second week in July, but only Snowbed
A had snow left at the end of the summer season. The melt of the
majority of Canoe Lake snowbeds in 1973 was three to four weeks ahead
of the melt in 1971 and 1972.

Snowbeds are not features unique to the Richardson Mountains
but are found throughout the western Arctic. As Pictures F1 to F4
show, the Shingle Point, Yukon region has many such larger snowbeds.
During the middle of July, 1973, these snowbeds were much larger and
thicker than those of the Canoe Lake area. Some, such as in Picture F3,
had as much as one meter of ice on the bottom, suggesting that these
accumulations of snow had lasted longer than one year. In an aerial
survey over Shingle Point on September 1, there still were large patches
of snow along the coast and creek valleys. Location of some snowbeds in the
Shingle Point area is indicated in Map D.

Profile Lines and Areas

Pictures A1 to A4 show the snowbed most intensively studied
during the summer. Though three profile lines, used for various data
determinations, were run across the snowbed perpendicular to the length
of the snowbed and the contours of the slope, data used in this report
have come mainly from the center line (CD line - see Picture A3), which
ran in a straight line, heading 32° west of true north, from the May 15,
1972 and 1973 snowborder (Point CD0) to the easterly gentle slope of the
next ridge. The following outline gives CD points, taken at 5 meter
intervals along the slopes, giving slope angle, area location, and major

MAP D - SHINGLE POINT AREA (from Blow River 117A sheet, Scale 1:250,000)

KEY

    F - location of photographs

type of vegetation. Plant specimens were identified by the author
and verified by Dr. J. Lambert, Biology Department, Carleton University,
and by Bill Cody, Plant Research Institute, Ottawa. Some of the plant
communities have been previously described by Lambert (1968). For
correct plant names, see Table 7. (Appendix)

CD -20 to 0   -   Picture A2

-   slope angle 5 to 10°, direction South

-   above the May 15, 1972 and 1973 snow border,
    on Ridge 1 (see Map C). Winter snow cover
    0 to 5 cm over tops of solifluction features,
    up to 60 cm in depressions. Most areas without
    winter snow cover.

-   landscape dominated by elongated solifluction
    features (lobes), lichen-moss communities inter-
    spaced with bare mud and rock patches, and
    hollows with 10 to 30 cm high shrubs and a cover
    of moss. Soil very rocky. Average growth height
    on lobe tops 1 to 5 cm.

CD 0   -   Picture A2

-   slope angle 5°, slope direction S

-   May 15, 1972 and 1973 snowborder. 50 cm drop
    in elevation from the slope above.

CD 0 - 35   -   Picture A2

-   slope angle 0 to 10°, slope direction S

-   early melt area (May 17-27, 1973). Snowpatch
    with 5 to 35 cm of snow. Always covered with
    shallow snow in the winter, but the snow is early in
    melting. Moderately drained - no standing water.

-   dominated by wet mossy hollows, patches of lichen
    (Cladonia sp.), scattered 10 to 30 cm high birch
    (Betula glandulosa) and willow shrub (Salix pulchra),
    occasional tussocks of cotton grass (Eriophorum
    vaginatum L.), patches of Cassiope tetragona and
    other heath plants (Empetrum nigrum, Vaccinium
    uliginosum, Vaccinium vitis-idaea, and Ledum
    palustre), plus other assorted vasculars including
    Arctostaphylos alpina, Carex sp., Petasites frigidus,
    Equisetum arvense, and Arctagrostis latifolia.
    Average growth height 10 to 20 cm.

CD 25 - 30 -   location of actinograph, upper anemometer, upper
    rain gauge, and hygrothermograph

CD 40 - 45 -   Picture A1

-   slope angle 10 to 15°, slope direction SE

-   melt area May 30 - June 6, 1973. Start of snow
    over one meter in depth. Upper edge of Snowbed *1.

- Drop in elevation of at least one meter
  from CD 35. Well drained.

- band of 50 to 100 cm high shrub willows
  (<u>Salix pulchra</u>) of almost continuous cover.
  Leaf litter over 80% of the ground surface in
  this band.

CD 45   - Picture Al

            - slope angle 10°,slope direction SE

            - melt area June 6, 1973. Well drained.

            - edge of upper willows and upper meadow (see CD 50)

CD 50 - 55   - Pictures Al and A3

            - slope angle 20°, slope direction SE

            - melt area June 17-27, 1973. Soil with only
  scattered large rocks. Locally, the slope up
  to 45°. Well drained.

            - upper meadow vegetation generally 20 to 40 cm
  high, though in patches up to 80 cm in height.
  Usually an 80 to 100% cover of moss (especially
  <u>Polytrichum</u> sp.) with a lush, thick growth of
  grasses, sedges, horsetail and flowering herbaceous
  species. Some areas with almost a 100% cover of
  ground willow (<u>Salix</u> <u>Chamissonis</u>) 2 to 5 cm in
  height. Meadow species including <u>Petasites</u>
  <u>frigidus</u>, <u>Arctagrostis</u> <u>latifolia</u>, <u>Equisetum</u> <u>arvense</u>,
  <u>Saxifraga</u> <u>punctata</u>, <u>Carex</u> <u>podocarpa</u>, <u>Artemesia</u>
  <u>arctica</u>, <u>Artemesia</u> <u>Tilesii</u>, <u>Arnica</u> <u>lessingii</u>,
  <u>Antennaria</u> <u>monocephala</u>, <u>Achillea</u> <u>borealis</u> and
  <u>Polygonum</u> <u>bistorta</u> in this area.

CD 60   - Pictures Al and A3

            - slope angle 10°, slope direction SE

            - melt area June 27 - July 2, 1973. Well drained.

            - 40 to 70% cover of moss (especially <u>Polytrichum</u> sp.).
  Vegetation 20 to 30 cm in height, not as thick as CD
  45-55, with 30% cover provided by the ground willow,
  <u>Salix</u> <u>polaris</u> <u>subsp.</u> <u>pseudopolaris</u>, 1 to 2 cm in height.
  Other vascular plants in this area including <u>Carex</u>
  <u>podocarpa</u> (30% cover), <u>Saxifraga</u> <u>punctata</u>,
  <u>Arctagrostis</u> <u>latifolia</u>, <u>Equisetum</u> <u>arvense</u>, <u>Oxyria</u>
  <u>digyna</u>, and <u>Myosotis</u> <u>alpestris</u>.

CD 65   - Pictures Al and A3

            - slope angle 12°, slope direction SE

            - melt area July 5-8, 1973 (late melt area). Well
  drained.

- 30 to 80% of the area bare mud and rock. Vegetation sparse, low growth (average 5 to 10 cm), but species composition like CD 60.

CD 70
- Pictures A1 and A3
- slope angle 15°, slope direction SE
- melt area July 8-12, 1973 (late melt area). Well drained. Bottom edge of SE facing slope from CD 40 to CD 70.
- 10% bare mud and rock with a 40 to 70% cover of moss (especially Bryum sp. and Drepanocladus sp.). Vascular plants sparse, with Oxyria digyna (very common), Poa arctica, Equisetum arvense, and Ranunculus pygmaeus.

CD 75
- Pictures A1 and A3
- slope angle 2°, slope direction S
- melt area July 12, 1973 (late melt area). Moderately drained. Flat bottom area of snowbed.
- patches of bare mud and rock over 30% of the area. Moss cover (especially Drepanocladus sp.) over 70% of the area. Plants 2 to 20 cm in height, with such species as Arctagrostis latifolia, Poa arctica, Carex Lachenali, Eriophorum Scheuchzeri, Ranunculus pygmaeus, Saxifraga punctata, and Salix polaris subsp. pseudopolaris.

CD 80
- Pictures A1 and A3
- slope angle 5°, slope direction S
- melt area July 8, 1973 (late melt area). Locally well drained.
- 100% cover of moss (especially Drepanocladus sp.) with ground willow (Salix polaris subsp. pseudopolaris), Poa arctica, Oxyria digyna, Arctagrostis latifolia, Ranunculus pygmaeus, Petasites frigidus, Saxifraga punctata, and Equisetum arvense. Growth 2 to 20 cm in height.

CD 85
- Pictures A1 and A3
- slope angle 7°, slope direction S
- melt area July 5 - 8, 1973 (late melt area). Poorly drained.
- lower wet meadow with 100% moss cover (especially Drepanocladus sp. and Bryum sp.). Vascular plants including Ranunculus nivalis, Carex Lachenali,

Saxifraga punctata, Arctagrostis latifolia, Equisetum arvense, Salix polaris subsp. pseudopolaris, and Oxyria digyna. Growth generally 10 to 20 cm high. Occasional dead shrub willows (Salix pulchra).

CD 90   - Pictures A1 and A3

             - slope angle 2°, slope direction S

             - melt area June 27-July 2, 1973. Poorly drained.

             - lower wet meadow. Vegetation 20 to 50 cm high (see CD 85). Scattered dead Salix pulchra bushes.

CD 95   - Pictures A1 and A4

             - slope angle 8°, slope direction S

             - melt area June 14, 1973. Poorly drained - ground very soggy.

             - lower wet meadow. Vegetation 10 to 20 cm high (see CD 85). Scattered live 10 to 20 cm high young Salix pulchra.

CD 100   - Pictures A1 and A4

             - slope angle 0°

             - melt area June 10-June 14, 1973. Poorly drained.

             - main band of lower willows (Salix pulchra)- average height one meter, though up to two meters in height. 100% moss cover (especially Drepanocladus sp.) with scattered elongated vasculars, including Equisetum arevense, Artemesia Tilesii, Polemonium acutiflorum, Carex Lachenali, Arctagrostis latifolia, and occasionally Salix Chamissonis.

CD 102   - location of lower anemometer and lower rain gauge

             - in a patch of open meadow in the lower willow band

CD 105   - Pictures A1 and A4

             - slope angle 0°

             - melt area June 10-June 14, 1973. Poorly drained.

             - lower willows (50 to 80 cm high) mixed with a lush meadow growth (20 to 35 cm high) composed of Artemesia Tilesii, Poa arctica, Epilobium angustifolium, Saxifraga punctata, Equisetum arvense, and occasional Salix Chamissonis.

- 127 -

CD 105-110   -   Ground collapsed this spring between CD105
and CD110 due to the underground flow of water
during spring runoff (see diagram).

CD 105   CD 110   CD 115   2m   NW FACING SLOPE   CREEK

CD 110   -   Pictures A1 and A4

         -   slope angle 0°

         -   melt area June 17, 1973. Well drained.

         -   lush, 40 to 60 cm high Calamagrostis canadensis,
meadow with scattered plants of Carex podocarpa,
Polemonium acutiflorum, Equisetum arvense, Salix
Chamissonis, and Viola epipsila.

CD 115   -   Pictures A1 and A4

         -   slope angle 0°

         -   bottom of creek bed at base of NW facing slope.
Large pieces of rock over most of the area, in
places bedrock (sandstone) exposed at the surface.
Active layer "depths" taken on adjacent bank.

CD 120   -   Pictures A1 and A4

         -   slope angle 45°, slope direction 12° west of
true north (NW).

         -   melt area June 10-June 14, 1973. Well drained.
Five meters above the creek on the NW facing slope.

         -   Vegetation mainly shrub growth with Salix pulchra
(50 to 70 cm high), birch (Betula glandulosa, 20 cm high)
and Vaccinium uliginosum (20 cm high).

CD 125   - Pictures A1 and A4

             - slope angle 45°, slope direction NW

             - melt area May 27, 1973. Well drained.

             - 100% moss cover (especially Polytrichum sp.,
               Dicranum sp., and the lichen, Peltigera sp.).
               Vegetation damp, but well drained, 10 to 15 cm
               high with heath type species and shrub willow
               and birch.

CD 133   - Pictures A1 and A4

             - slope angle 40°, slope direction NW

             - May 17, 1973 snow border (winter maximum snow
               border)

CD 125-140   - Pictures A1 and A4

             - slope angle 40 to 45°, slope direction NW

             - well drained, vegetation 1 to 10 cm high,
               mostly lichen, moss and woody tundra species.

CD 140   - top of NW facing slope. Ridge 2.

             - area of scattered mud patches. Vegetation lichen
               dominated.

CD 140-160   - Pictures A1 and A4

             - slope angle 2 to 5°, slope direction NNE to NNW

             - on slope of next ridge (Ridge 2 - see Map C).
               Main ridge slopes eastward, though these points
               locally slope gently in a northerly direction.
               Well drained, though hollows damp.

             - area of Eriophorum vaginatum L. tussocks and
               hummocks dominated by sedges and grasses. 80 to
               100% ground cover of moss and lichen, though some
               patches of bare mud on hummock tops. Hollows
               between hummocks 10 to 50 cm deep with a 100%
               cover of moss and with 10 to 20 cm high birch
               (Betula glandulosa) and willow (Salix pulchra)
               shrubs.

The snowbed was further divided into representative areas, chosen
on the basis of vegetation type, date of exposure, depth of snow,
drainage, and location in the snowbed. Some of these factors are outlined
in Tables 3A and 3B. The rest will be described here. Albedo values are
usually the average of 22 area values, taken over snow-free ground in August.

- 129 -

Upper Lobe   -   Picture Al

             -   slope angle 0 to 2°, slope direction S

             -   10 to 30 meters above the May 15, 1972 and 1973 snowborder. Snow largely confined to hollows 5 to 30 cm (maximum 50 cm) deep, though snow cover over the tops of raised solifluction features can be up to 15 cm during some parts of the winter. Most lobe tops bare of snow throughout the year, though. Well drained on the tops of lobes, hollows of variable drainage (the vegetation in hollows is usually wet, with the surface 1 to 3 cm dry occasionally). Albedo of lobe tops ranges from 21.5 to 23%, with an average of 22%. The albedo of hollows ranges between 21 and 23%, with an average of 21.9%.

             -   landscape dominated by flat, elongated solifluction features running downslope in a northern to southern orientation. Vegetation on lobe tops generally lichen dominated (Cladonia sp.,40 to 60% cover), with a 10 to 20% moss cover (especially Dicranum and Polytrichum sp.) and woody vascular plants such as Vaccinium uliginosum, Ledum palustre and Salix artica Pall. subsp. artica. Other less common vasculars include Arctostaphylos alpina, Pedicularis Kanei, Anemone narcissiflora, Lupinus arcticus and Vaccinium vitis-idaea. Vegetation usually dry and well drained.

             -   most hollows have a 100% moss cover (especially Dicranum sp. and Drepanocladus sp.). Wide variation in shading is proportional to the amount of shrubby plants in the hollow, such as Betula glandulosa and Salix pulchra. Some hollows deep, with 70 to 90% shrub cover over moss (shrub cover including Betula glandulosa, Salix pulchra, Vaccinium vitis-idaea, Ledum palustre, and Vaccinium uliginosum). Other hollows 5 to 10 cm deep, vegetated mainly by moss and Vaccinium uliginosum. Plants tend to reach the tops of hollows or extend to a maximum of 10 cm above the level of the hollow (see diagram).

Upper Birch - Picture A1

- slope angle 10 to 20°, slope direction 32° east of south

- from above the winter snow border in some years (1972 covered, 1973 exposed) to a melt area of May 26, 1973. Starting where the slope of Ridge 1 suddenly drops in elevation into the gulley containing Snowbed *1. Well drained. Albedo from 11 to 23%, depending on the ground cover underneath the shrub layer. Average albedo 18.6%. Temperature of the ground under the shrub layer is dependent upon the depth of leaf litter, amount of moss cover, and amount of overhead shading by the birch.

- intermittent border 3 to 5 meters thich of shrub birch (Betula glandulosa) along the upper edge of Snowbed *1. Birch height 10 to 70 cm, average 41.5 cm. Birch cover usually complete, with a ground cover of dry, loosely packed moss and dead leaves, with scattered plants such as Vaccinium vitis-idaea (in some areas up to 80% ground cover), Vaccinium uliginosum, Empetrum nigrum, Pyrola grandiflora Radius, and occasional grass and sedge leaves.

Upper Willows- Pictures A1 and A3

- slope angle 15°, slope direction SE to ESE

- melt area May 27 to June 7, 1973. Can be with or without a birch shrub border immediately above. Well drained. Albedo from 12 to 23%, depending on the ground cover under the shrub layer. Average albedo 18.8%. Temperature of surface proportional to exposure (nearness to border of the willows), type of ground cover and amount of overhead shading.

- band 3 to 5 meters wide of shrub willows (Salix pulchra) along the upper edge of the snowbed (level with CD 40-45). Willow height from 30 to 150 cm, average 79 cm. Willows not continuous-broken by open patches with meadow or heath vegetation. Under the willows proper, loosely packed leaf litter is common, with much dead wood and large, live, horizontally lying stems and trunks. Patches of loosely packed moss (especially Drepanocladus) also common. Undergrowth, for the most part, is sparse and spindly, with such species as Arctagrostis

latifolia, _Artemesia arctica_, _Stellaria longipes_, _Vaccinium uliginosum_, _Poa artica_, _Petasites frigidus_, _Viola epipsila_ and _Achillea borealis_.

Upper Meadow   -   Pictures A1, A3 and A4

- slope angle 20°, slope direction SE to locally E or S facing

- melt area June 7-June 27, 1973. Well drained once the snow border passed the area. Albedo from 24 to 35%, with an average of 26.9%.

- lush, mostly herbaceous flowering plant growth. On level with CD 45-60. 0 to 15 meters from the upper willow band. Most values used for this report were recorded at the level of CD52, 9 meters from the upper willows, in a melt area of June 10 - June 17, 1973. The vegetation here is dominated by _Salix Chamissonis_ (up to 90% cover), which has an overall height of 2 to 10 cm Other meadow areas, with overall growth heights of 5 to 30 cm contain variable amounts of _Salix Chamissonis_ along with the more common herbaceous species of _Achillea borealis_, _Dodocatheon frigidus_, _Equisetum arvense_, _Carex podocarpa_, _Artemesia arctica_,_Aconitum delphinifolium_, _Arnica lessingii_, _Anemone Richardsonii_, _Anemone narcissiflora_, _Polygonum bistorta_, _Polygonum viviparum_, _Arctagrostis latifolia_, _Castilleja Raupii_, and _Pedicularis sudetica_. The amount of moss cover is variable, with pockets of 70 to 100% cover (especially _Polytrichum_ sp. and _Drepanocladus_ sp.) over about 50% of the meadow area.

Upper Late Melt   -   Pictures A1, A3 and A4

- slope angle 15°, slope direction SE to S

- melt area June 27-July 11, 1973. Level with CD 65-70. Well drained once the snow border has retreated past this point. Local drainage pathways usually filled with flowing water, though. Most areas with a hard, tannish surface mud, wet below 2 to 5 cm. Albedo from 17.5 to 24% with an average of 20.4%.

- band of sparsely vegetated mud and rock 20 meters from the upper willows. 40 to 100% of the surface hard mud, pebbles, and/or sandstone boulders up to 50 cm by 30 cm by 20 cm in volume. Vegetation present (growth from 2 to 4 cm, maximum 20 cm) includes clumps of moss (especially _Drepanocladus_ sp.

and _Bryum_ sp.), and scattered plants of
Arctagrostis latifolia, _Ranunculus nivalis_,
Carex podocarpa, _Arnica lessingii_, _Oxyria
digyna_, _Ranunculus pygmaeus_, _Equisetum arvense_,
and _Saxifraga punctata_. Most growth is below
10 cm in height and scattered between the rock
and mud patches.

Lower Late Melt   — Pictures A1, A3 and A4

                  — slope angle 0 to 2°, slope direction S

                  — melt area July 5 to last melt in July, 1973.
                     Poorly drained, ground usually saturated to the
                     surface. Flowing water in 1 to 3 cm deep drainage
                     pathways. Debris from melted snow common on the
                     surface of the exposed ground.

                  — lower flat slope of the snowbed. Next to and
                     extending 10 meters south from the SE facing upper
                     slope. On level with CD 75-80. Patches of bare
                     mud and rock over 30 to 100% of the surface in
                     areas. Moss cover important - usually 70% cover
                     (especially _Drepanocladus_). Plants 2 to 20 cm
                     high. Sparse. Common species include _Oxyria
                     digyna_, _Ranunculus pygmaeus_, _Carex Lachenalii_, _Poa
                     arctica_, _Equisetum arvense_, _Arctagrostis latifolia_,
                     Salix polaris subsp. _pseudopolaris_, _Petasites
                     frigidus_, _Saxifraga punctata_, and occasionally
                     Eriophorum scheuchzeri.

Lower Meadow   — Pictures A1, A3 and A4

                  — slope angle 0 to 2°, slope direction S

                  — melt area June 7–June 30, 1973. Poorly drained,
                     ground usually saturated to within a few cm of
                     the surface. Standing water in places. Albedo
                     from 21 to 29%, with an average of 26.8%.

                  — wet meadow on the lower side of the snowbed. 0 to
                     8 meters from the lower willow band. Vegetation
                     not high, 5 to 20 cm, with a 100% ground cover of
                     moss (especially _Drepanocladus_ sp. and _Bryum_ sp).
                     Common vascular plants include _Carex podocarpa_,
                     Carex lachenali, _Carex aquilinus_, _Arctagrostis
                     latifolia_, _Salix polaris_ subsp. _pseudopolaris_,
                     Equisetum arvense, _Petasites frigidus_, _Saxifraga
                     punctata_, _Ranunculus pygmaeus_, and _Poa arctica_.
                     Sedges (_Carex_ sp.) usually form the largest
                     proportion of the plant cover.

Lower <u>Salix</u> <u>Cham.</u> – Pictures A1 and A 3

- slope angle 2$^{\mathrm{o}}$, slope direction S

- melt area June 14, 1973. Locally better drained than most of the lower snowbed. Saturated during times of high runoff from the snowbed or slopes above. No standing water. Albedo 27 to 29.5%, average 28.3%.

- on the lower side of the snowbed; better drained area with a 60 to 80% ground cover of the ground willow, <u>Salix Chamissonis</u>, common also in upper meadow areas. Height usually 5 cm. Scattered individuals of the same vascular plants as the lower meadow (growth up to 30 cm) mixed through the <u>Salix Chamissonis</u>, with occasional young shrub willow stems 10 cm high (<u>Salix pulchra</u>), plus <u>Vaccinium uliginosum</u> (5 cm), <u>Artemesia Tilesii</u> (10 cm), and <u>Pedicularis sudetica</u> leaves (3 cm).

Lower Willows – Pictures A1, A3 and A4

- slope angle 0 to 2$^{\mathrm{o}}$, slope direction S

- melt area June 7–14, 1973, though as late as June 30 in localized, sheltered patches. Ground usually saturated within 10 to 20 cm of the surface, and often saturated within 1 to 5 cm of the surface. Albedo from 10 to 19%, average 15.1%. Light reaching the ground cover under the willows patchy due to shading by the willows.

- band 10 to 20 meters thick of 1 to 2 meter high shrub willow (<u>Salix pulchra</u>). Located south and below the SE facing, steep slope of the snowbed and the lower wet meadow, but north of the creek at the bottom of the snowbed and the steep, NW facing creek bank. Includes CD 100–105. Ground cover, under the almost continuous canopy of willows, generally 100% cover of moss (especially <u>Drepanocladus</u> sp.), with elongated vegetative shoots of such green vascular plants as <u>Viola epipsila</u>, <u>Arctagrostis latifolia</u>, <u>Petasites frigidus</u>, <u>Equisetum arvense</u>, <u>Artemesia Tilesii</u>, and <u>Polemonium acuteflorum</u>. Leaf litter is sparse.

<u>Formation and Ablation of Snowbeds</u>

<u>Formation</u>

As seen from Tables 3 and 4, (Appendix), the total snow depth in this region over a winter is unevenly distributed, even early in the winter,

due to drifting by the wind. Over the tops of ridges, snow deposition
is minimal, though local depressions can be filled to a depth of one
meter. On the sides of ridges and in flat bottom lands, the snow is
generally 0 to 25 cm deep. Slight depressions or drops in topography,
hollows between solifluction features and vegetation tussocks, and most
mudslide scars have average snow depths of 25 to 70 cm. These patches
of snow are penetrable by light when the snow is dry (Sellers, 1968)
and generally melt early in the season (from the middle of May to the
first week in June). Snowbeds, on the other hand, with depths of snow
in excess of one meter, melt out from the middle of June to the end of
the summer season. The larger snowbeds usually ablate by the end
of August. However, in some years they may not melt completely.
Snowbeds are confined to the deeper depressions, creek gulleys, and
sudden steep drops in topography along southerly facing slopes.
The occurrence of larger drifts on SE facing slopes is an expression of
the prevailing northwest wind in the winter.

Snowbeds in the Richardson Mountains occur year after year in
the same location, as manifested by airphotos (1954, series A14133-93,
Air Photo Division, Department of Energy, Mines, and Resources, Canada),
personal communication with Dr. J. Lambert, who also worked in this area
in the mid-1960's, the author's three summers in the field in the Canoe
Lake area (1971-1973), and the distinct vegetation patterns associated
with the snowbeds. From the author's experience, though, the snowbeds
did vary in depth and in the exact location of the face of the drift
each year, but covered approximately the same area each season, with a similar
proportion of snow distribution throughout the snowbed. Time of snow
disappearance did vary considerably, though, with a three to four week
range over the three summers.

The characteristics of snowbeds are influenced by inter-
relationships among topography, wind and amount of snowfall. Table 2
(Appendix) illustrates the relationship between these variables. The
location of the anemometers in Table 2 is shown on Map B. As seen in
this table, the drop of wind down the slope of Ridge 1 is consistent,
and is especially noticeable during storms from the northwest

or west (such as August 13-the wind varied from 20 km/hr average at the top of the ridge, to 14 km/hr just above the snowbed with a drop of about 45 meters in elevation, to 4 km/hr at the bottom of the snowbed with a drop of about 15 meters in elevation). The August 1 wind profile, Graph 1E, better illustrates this wind drop down the slope. When the wind passes over the sudden drop in topography from CD35 to CD50 (a gradient of 5° at CD35 to a gradient of 45° at CD50, with a change of 2.5 meters in elevation), wind speed decreases drastically, with the effect that, if the wind is carrying snow, much of its load is dropped, and a drift develops downslope from the drop in topography. The wind picks up again along the lower slopes, but is reduced in the bank of one to two meter high willows at the bottom of the snowbed area (CD95 to CD115), again dropping snow. Once going up the northwest facing slope along the 3 to 5° easterly facing slope of the next ridge (CD120-160), the wind rapidly picks up speed, blowing snow away from these areas. This pattern of snow deposition is shown in the snow depth recordings listed for Tables 3 and 4. The snow depths above the snowbed on September 19, 1972, were negligible on the surface of solifluction features, though in the birch filled depressions, snow was up to 60 cm deep. Snow patch areas (such as CD0-35) had an intermittent cover of up to 20 cm. With the sudden drop in topography at the upper willows (CD40-45), the snow depth rose to 120 cm, with a drift extending about five meters into the upper meadow. Below the drift, the snow depth over the upper and lower slopes ranged between 10 and 20 cm, up to the area of the lower willows. Snow depths listed for the lower willows (10 to 20 cm) are misleading, as much of the deposited snow actually rested on the branches of the willows. The northwest facing slope was clear of snow, but hollows in the hummock area above were filled to a depth of 30 cm. By November 24, 1973, the snow deposition pattern had changed. Areas immediately above the snowbed were covered with snow from 0 to 15 cm. Snow in the region of the upper willows had been redeposited further downslope, decreasing the snow depth here from 120 to 75 cm. The main drift of Snowbed *1, now much further extended, covered the upper slopes of the meadow with depths around 140 cm.

Even the lower flat meadow areas had depths from 60 to 160 cm, with the greater depths being recorded in areas where the upper slope ended and the lower flat slope began (160 cm of snow). The lower willows, with a snow ground cover of 75 cm, still had much snow caught up on branches and leaves. As can be seen by these data, the snowbed changed shape from a steep faced drift at the top of the slope in September, to a much flatter, deeper drift by November. By May, 1973, though, as Tables 3 and 4 show, the areas above the snowbed were mostly free of snow, the shallow snow patch areas had snow from 8 to 33 cm, and the snowbed proper had measured depths from 84 to 510 cm. Picture C(Appendix) shows the lip of the drift, which by this time had extended at a 10° angle as far as CD90-95. The actual drift itself had a face 2 to 2½ meters high. Upper willow areas in early May were covered with snow over 2 meters deep. This deep drift, extending out at a 10 to 20° angle from the drop in topography, was deepest in the flat meadow area adjacent to the bottom of the SE facing slope (CD65-75). Once past the face of the drift, the snow covering the lower meadow and lower willows was 150 to 200 cm deep, with a deeper area at CD115 (the location of the creek bed). Snow extended up the northwest facing slope about 10 meters, but had been swept from the upper parts of the hill. Only hollows between hummocks on the slope behind were filled with snow, along with shallow drainage pathways.

Other snowbeds examined in the region also showed this development of drifts along southerly facing slopes, due to sudden drops in topography. The other common mode of snowbed formation was the filling in of local, deep depressions that were narrow enough to be totally covered, such as creek gulleys.

Ablation

The factors affecting melt rates of snowbeds are many and inter-acting. It was found, for the particular snowbed studied, that incoming solar radiation was by far the most important factor determining melt rate. First, though, the other factors affecting ablation will be considered.

Wind

Wind has an input into the melt rate of snow by controlling
the rate of horizontal water vapour transfer in the air above the snow.
Wind moving across snow surfaces will create a water vapour
gradient above the surface proportional to the rate of removal
of saturated air. Sublimation of snow and evaporation of water from
melted snow is faster into air of lower water content.

As seen from Graphs 1A to 1G, the movement of wind across
the snowbed changed considerably through the season as the snow
melted. On May 26 the snow cover was at a slope of 10 to 20°,
compared to a slope of 10° for the area above the snowbed. Snow
melt had only begun, with a drop of about 30 cm since May 14 in
the central portion of the snowbed. Snow cover was continuous,
except for CD30. The face of the main drift forming the snow cover
was at CD90, with CD95 half way down the face of the drift. CD100-
105 were located in the flat creek gulley which was still covered by
115 and 163 cm of snow respectively. CD110 and 115 were unreachable -
spring runoff in the creek had begun the night of May 25 and water
was flowing over the snow in this area. Wind flow, from the WNW,
across the snowbed (Graph 1A) did decrease slightly down the slope
but its effect upon water vapour levels must have been relatively
uniform across the slope and must have been of some significance
since the wind only dropped slightly in speed down the snowbed.
Table 2 (Appendix), also shows this effect; e.g. on May 21, the
daily average wind speed on top of the ridge behind the snowbed was
15 km/hr. At the start of the main part of the snowbed (CD25), it
was 13.8 km/hr, and at the bottom of the slope (CD120), it was 11.5 km/hr.
The decrease in wind velocity was less than a third across the snow-
bed. On May 26, the averages were 9.5, 8.5, and 6.7 km/hr respectively.
This even effect of the wind was noticed also with snow piled up at
the sides of snowpits. This snow soon melted (in less than a week)
to the level of the rest of the snowbed from a height of 40 to 70 cm
above the general surface of the snowpack.

GRAPH 1A

WIND PROFILE
MAY 28, 1973 (A)

DISTANCE ALONG CD TRANSECT (METERS)

GRAPH 1B

WIND PROFILE
JUNE 2, 1973 (B)

DISTANCE ALONG CD TRANSECT (METERS)

GRAPH 1C

WIND PROFILE

JUNE 9, 1972 (C)

GRAPH 1D

WIND PROFILE

JULY 5, 1972 (D)

- 140 -

GRAPH 1E

WIND PROFILE

AUG. 1, 1973. (E)

DISTANCE ALONG CD TRANSECT (METERS)

GRAPH 1F

WIND PROFILE

MAY 26, 1973 (A)
JUNE 2, 1973. (B)
JUNE 9, 1973. (C)
JULY 5. 1973. (D)
AUG. 1, 1973. (E)

DISTANCE ALONG CD TRANSECT (METERS)

GRAPH 1G

SNOWMELT vs WIND SPEED
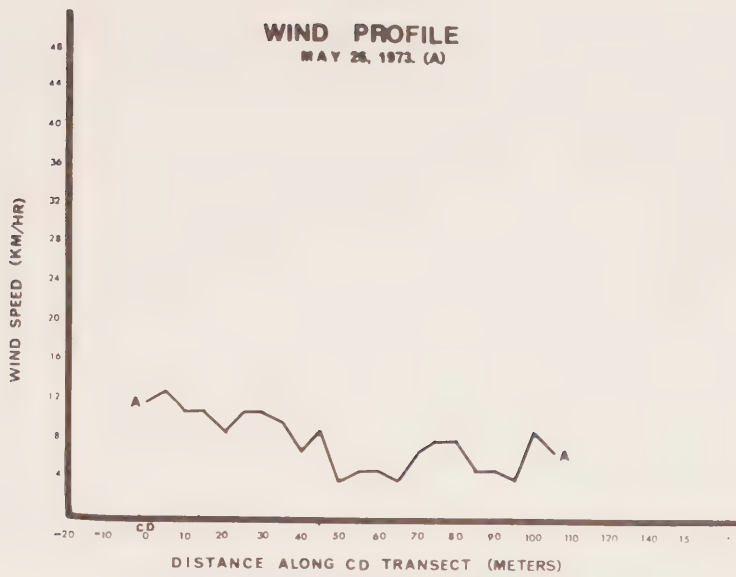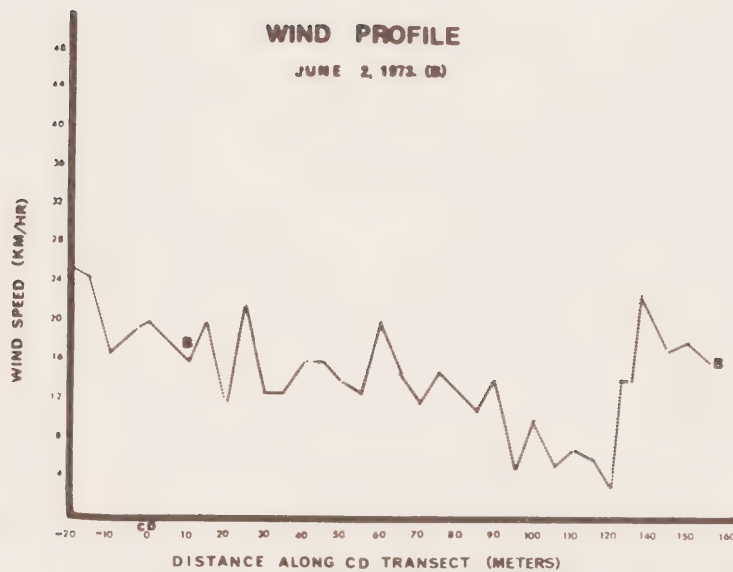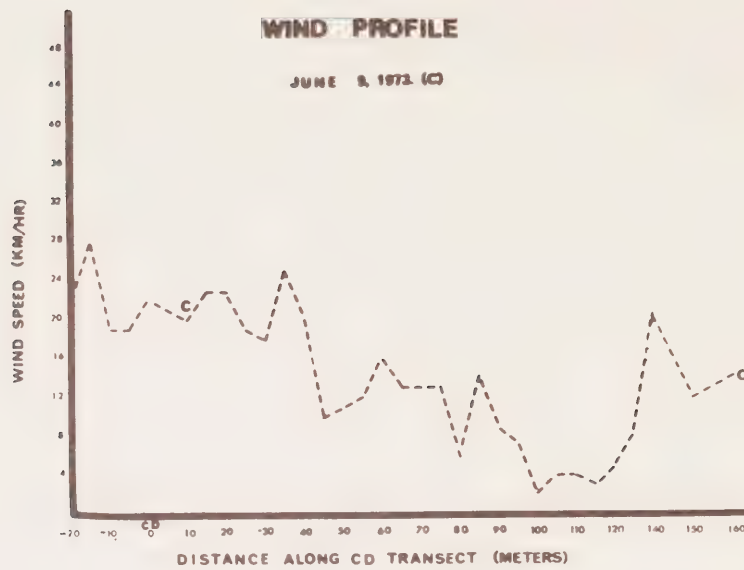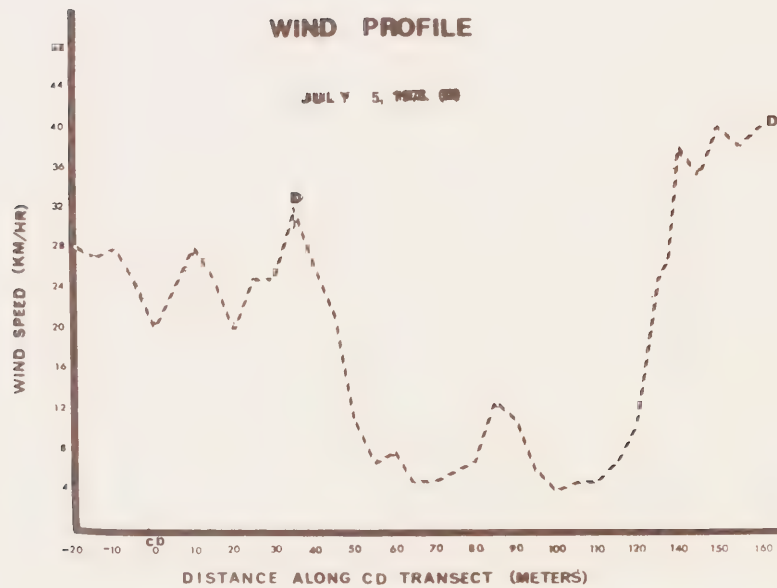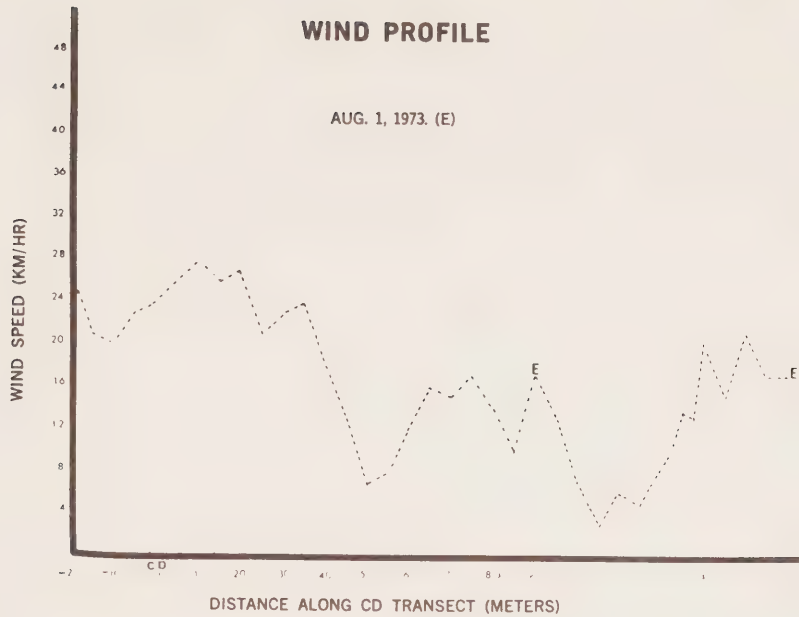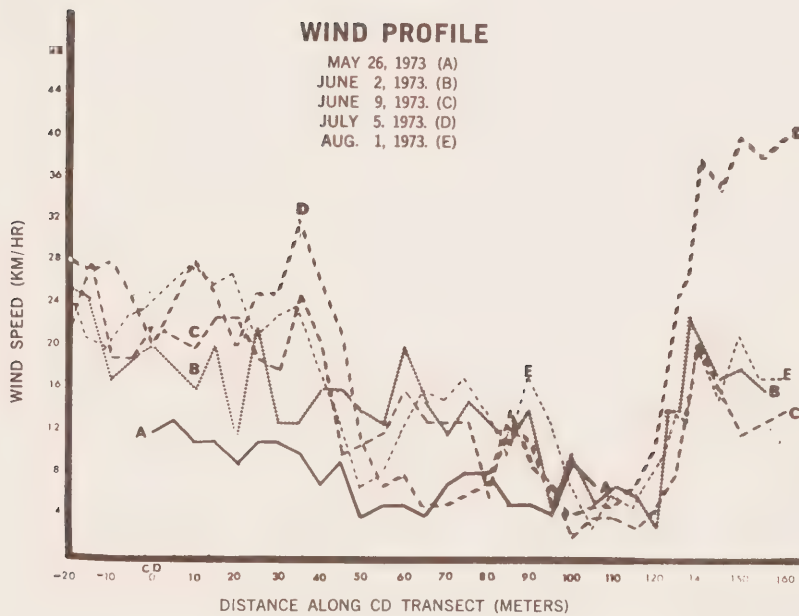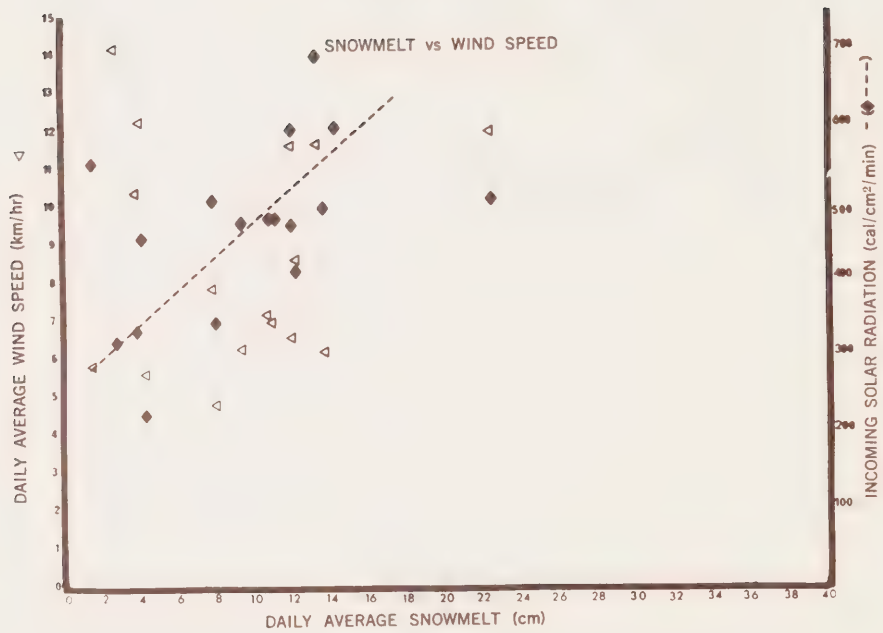
From May 18 to June 2, the snow depth thinned an average of
of 80 cm. Though underlying topography had only just begun to
be exposed, the actual snowbed itself was at a greater angle
(slope of 20 to 25°) to the slopes above (slope of 10°). Snow
started at CD45, meaning that from CD40-45, the upper band of
shrub willows had melted out, with a drop in elevation of at least
50 cm. Graph 1B shows a noticable drop in wind speed in this
area. CD45-120 at this time were snow covered, with CD90 at the
face of the drift and CD95 half way down the drift. CD100-115,
in the flat creek region had snow depths of 53, 90, 139 and 265 cm
respectively at this time. The edge of the snow with the NW facing
wall reached CD120, leaving CD125-140 above the snowbed and CD140-155
on the snow-free,flat hummock area above. There was a noticeable
decrease in wind speed across the snowbed, with the largest drop in
the region of the creek gulley. Speed rapidly picked up again along
the NW facing wall and hummock areas above. During the wind storm of
June 2, predominately from the NW, the wind on the NE facing slope on the
other side of Ridge 1 was 25 km/hr, on the top of Ridge 1, 23 km/hr,
and on the general slope above the snowbed averaged 13 to 15 km/hr.
The rapid decrease in wind speed once the wind entered the snowbed
area should mean that the wind would have a decreased effectiveness
in removing water vapour from above the snow compared to earlier in
the season. Further measurements done as the snow continued to melt
back closer to the underlying topography show that the wind was
increasingly affected by the steeper angles of the snowbed. By June 9,
the immediate drop in wind speed, upon passing into the snowbed area
at CD40 is even more apparent than June 2 (see Graph 1C). The snow,
by this time, had dropped a further 44.5 cm since June 2, though the
border was still at CD45. Further changes had occurred on the lower
slopes, with the snow border having retreated to CD115, leaving CD120-
140 on a snowfree NW facing slope. The snowbed at this time was at
a 25° angle, compared to 10° for the slopes above. As can be seen
from Graph 1C, the wind did pick up again slightly across the snowbed,

but dropped again going over the lip of the drift, and remained
low across the flat creek gulley. It immediately increased
in speed again going up the NW facing slope and over the
hummock area to the south. Even in this condition of higher
wind speeds (20 to 25 km/hr from the NW), the actual wind passing
over the snow surface was a half or less of the wind over exposed
areas.

By July 5, the snow had retreated to CD65-85 with a
considerable drop in volume. The angle with the slope above (now
the slope of the upper meadow SE facing sidehill with a slope
of 20°) was 20°. With this drop in snow, the upper willows (CD40)
and upper meadow (CD45-60) were completely exposed, as well as
the areas from CD90-160. The wind, from the NW, averaged 33 km/hr
with gusts over 50 km/hr on the slopes above the snowbed. As
Graph 1D shows, there was an immediate drop in wind speed past the
upper willows, with the speed on the upper side (CD50) at 11 km/hr.
The wind speed remained very low (5 to 7 km/hr) down the SE facing
slope, picking up slightly in the lower meadow (13 km/hr maximum),
but dropping again in the lower willows (4 to 5 km/hr.) Across
the entire extent of the remaining snowpatch, the wind remained
at speeds less than half that for the tundra above. Its effect
on the snowbed was most likely minimal, though the drying out of
upper tundra areas was readily apparent.

Table 2 (Appendix) shows how the effectiveness of the wind
over the snowbed decreased as the snow melted back, both horizontally
and volumetrically. It also shows most major wind storms throughout
the summer coming from a northwesterly direction (27 out of 41 days
where the average wind speed was greater than 10 km/hr on top of
Ridge 1). Even during winds from a southerly direction, this drop of
wind speed across the snowbed was apparent (see Table 2, June 11, June
13 and June 23). These values can be compared to data from earlier
in the season (see Table 2, May 21, May 28 and June 2). The decline in
speed is less than 50% over the snowbed while the snow was of
considerable volume.

The changing correlation of wind and melt rate was not shown in melt rate data. The effect of high wind speeds tended to be minimal when they coincided with periods of low temperature, low solar radiation, and high relative humidity (Table 6, Appendix). During May and June, high winds did occur on sunny days, but the air temperature on these days was low. As seen in Graph 1G and Table 1, there is no readily apparent correlation between total wind run or daily average wind speed and daily average snow melt or total snow melt. As Graph 1G shows, solar radiation seemed to be a more determining factor in snow melt. During the time period June 22-25, the wind speed was high (average 14 km/hr) but the incoming radiation was low (340 cal/cm^2/day), along with the melt rate (2.7 cm daily average). In contrast, during the period June 15-21, with a high average wind speed (14 km/hr) and a high average incoming radiation (600 cal/cm^2/day), the melt rate was high (14.3 cm daily average). Of course, the process was accelerated by ambient temperature, albedo, and snow density. During the period May 18-22, radiation was high (560 cal/cm^2/day), wind was moderate (6 km/hr), but temperature was low (3.6°C average), albedo was high (60%) and density was low (0.54 gm/cm^3). The resultant daily average snow melt was 1.4 cm.

Rain

Rain can affect the melt rate of snow by providing an energy input in the form of unfrozen water into the snow system, forming ice layers in the snowpack and increasing the snow density. As seen by Table 1 and Graph 2A, periods of heavy rainfall did not correspond to periods of high melt rates. Days with large amounts of precipitation usually corresponded to days of high relative humidity, low temperature and low solar input. The actual energy input of rain was not significant in melting the snow, but the rain augmented the snowpack water equivalent. This water was stored for later release during snowmelt, especially during days of significant incoming solar radiation. Days of high solar radiation, as Graph 2A shows, tended

GRAPH 2A

SNOWMELT vs RAINFALL

- 146 -
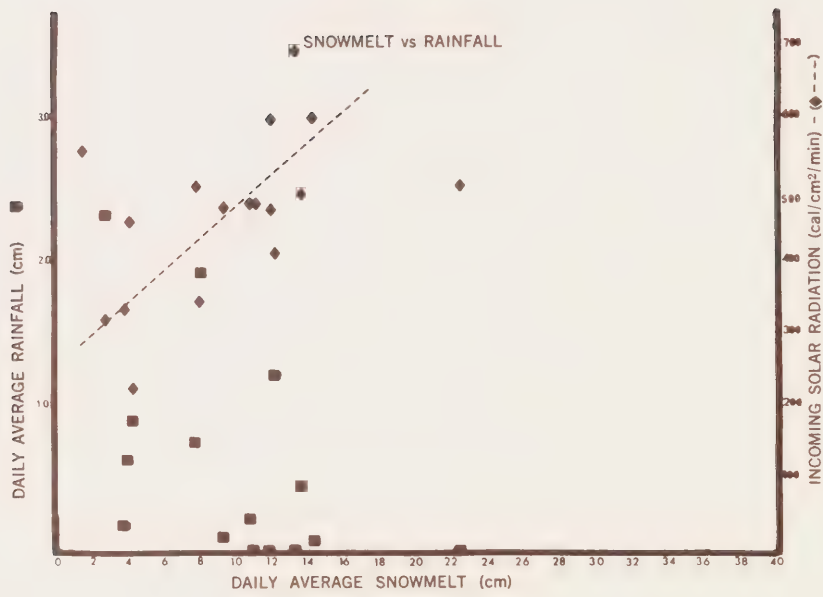
to correspond to days of lowest total rainfall. The direct
relationship between amount of total rainfall and daily average
melt rate appears to be a reverse one, because of the factors
outlined above. One important effect of rainfall, though, is the
movement of runoff waters from upslope areas, under the snowbed,
next to the frozen ground, creating air spaces between the snow
and ground which allow movement of warmer air under the snowpack.
Some of the spaces created are as deep as 10 cm in localized areas.

As Table 2 shows, there was no observable gradient of
rainfall between the upper snowbed (CD30) and the lower snowbed
(CD110).

Density

Densities listed in Table 1 are averages of snowpit
profiles. Actual surface densities, in areas with 10 to 15 cm of
snow/ice left, were recorded as high as 0.90 gm/cm^3. Snow on
top of ice layers next to the ground (this type of ice layer
was usually 5 to 15 cm thick) was very wet, its density averaging
0.80. As Table 1 shows, there was an overall increase in density
throughout the summer, due mainly to physical settling of the
ripened snow pack.

Albedo

Albedo, the percentage reflection of incoming short wave
radiation, decreased over the summer (see Table 1), corresponding
to the increasing daily average melt rate shown on Graph 4A. This
decrease in albedo was due to the melting out of plant debris and
soil particles that had been deposited in the snowpack along with
the snow during the winter. The snow changed from white (albedo of
70%), with most of the incoming light being reflected at the start
of the melt season, to blackish in appearance (albedo 24%) by July.

Graphs 3A to 3G show this change in albedo over the season.

Graph 3A, the May 26, 1973 albedo profile, shows the contrast between the high albedo of snow covered areas early in the melt season and the low albedos of adjacent tundra areas with little or no snow cover. From CD0-35, the snow was from 0 to 25 cm deep, with a 10 cm thick ice layer under the snow and patches of exposed vegetation. CD15 was covered with yellowish ice, CD20 contained clear ice in a depression, CD30 was a mossy area free of snow, and CD35 was covered with greyish ice. The average albedo for this area of shallow snow and ice was 21%, meaning that at least 75% of the incoming short wave radiation was absorbed. The resultant rapid melt of snow is manifested by the fact that all these points were free of snow by May 29, yet the May 19 snow depths had ranged from 8 to 33 cm (see Table 4) and the air temperatures during this period were relatively low (see Table 6). An early input of solar radiation into upper tundra areas is indicated.

In contrast, the average albedo of the snowbed May 26 was 59% (CD40-125), with values as high as 70%. Lower albedos (53 to 51%) were recorded in the creek gulley (CD95-100) where accumulated debris was scattered over the snow surface. Around shrub willows protruding through the snow in this area, the albedo was 50%.

By June 10, the snow extended from CD50-115. CD110 contained very muddy snow due to runoff by the adjacent creek. CD105 was a locally exposed patch of mossy wet ground (albedo 37%). Melted tundra areas of the S-facing slope had a fairly uniform albedo of 24 to 27%, averaging 23%. The snow, in contrast, still had a high average albedo of 46%, while the average albedo of the NW-facing slope and south hummock areas was 24%. Exposed areas near the snowbed were absorbing about 25% more of the incoming short wave radiation than the snow surface, which was still reflecting about half of the incoming light.

This distribution of albedos changed little by June 13, when the snow, from CD50-95 had an average albedo of 44% and adjacent areas kept within the same albedo value ranges that they had June 10.

GRAPH 3A

ALBEDO PROFILE
MAY 26, 1973. (A)

DISTANCE ALONG CD TRANSECT (METERS)

GRAPH 3B

ALBEDO PROFILE
JUNE 10, 1973. (B)

DISTANCE ALONG CD TRANSECT (METERS)

- 149 -

GRAPH 3C

ALBEDO PROFILE

JUNE 13, 1973. (C)

ALBEDO (PERCENTAGE)

DISTANCE ALONG CD TRANSECT (METERS)

GRAPH 3D

ALBEDO PROFILE

JUNE 29, 1973. (D)

ALBEDO (PERCENTAGE)

DISTANCE ALONG CD TRANSECT (METERS)

ALBEDO PROFILE

JULY 4, 1973. (E)

DISTANCE ALONG CD TRANSECT (METERS)

ALBEDO PROFILE

AUG. 1, 1973. (F)

DISTANCE ALONG CD TRANSECT (METERS)

GRAPH 3G

ALBEDO PROFILE

MAY 26, 1973. (A)
JUNE 10, 1973. (B)
JUNE 13, 1973. (C)
JUNE 29, 1973. (D)
JULY 4, 1973. (E)
AUG. 1, 1973. F)

ALBEDO (PERCENTAGE)

DISTANCE ALONG CD TRANSECT (METERS)

By June 29, though, the snow, from CD60-90, had decreased in albedo to 27%, an albedo almost equal to the average albedos for the NW facing slope and adjacent tundra areas (26%) and the now exposed lower meadow and willows (21% average). The snow now was reflecting only about one-quarter of the incoming radiation.

The July 4 profile, the last profile done while snow remained (see Graph 3E), showed that the snow had kept its 27% average albedo. Debris accumulating on the snow surface coloured the snow blackish in appearance. Readings taken July 8 on the last remaining patch of snow gave values between 19.5 and 25% albedo.

The decrease in albedo during the summer, with the corresponding increase in absorption of incoming solar radiation, is one of the several factors which accelerates the daily average melt rate over the summer (see Graph 4A).

Ambient Air Temperature

As Graph 4B shows, there seems to be a definite correlation between an increase in air temperature and an increase in daily average snow melt. Low temperature can override high incoming solar radiation, such as the period May 22-28, when the solar input was high (556 cal/cm^2/day), but the ambient average air temperature was low (3.6°C) and the melt rate was low (1.4 cm/day). Warmer air temperatures, not always corresponding to locally high incoming solar radiation (see Table 6), accelerate melt rates by the transfer of sensible heat to the snow surface. As explained before, though, the combined influence of wind, albedo and snow density also have an effect here.

GRAPH 4A

DAILY AVERAGE SNOWMELT — 1973

GRAPH 4B

SNOWMELT vs AIR TEMPERATURE

DAILY AVERAGE TEMPERATURE (°C)

INCOMING SOLAR RADIATION (cal/cm²/min) - (●---)

DAILY AVERAGE SNOW MELT (cm)

GRAPH 4C

SNOWMELT vs RELATIVE HUMIDITY

RELATIVE HUMIDITY (percent) - (◄·····)

INCOMING SOLAR RADIATION (cal/cm²/min) - (●---)
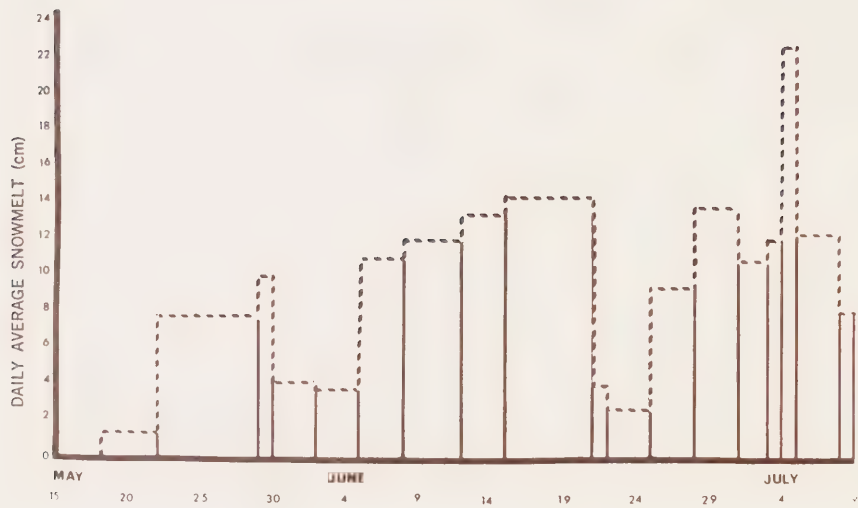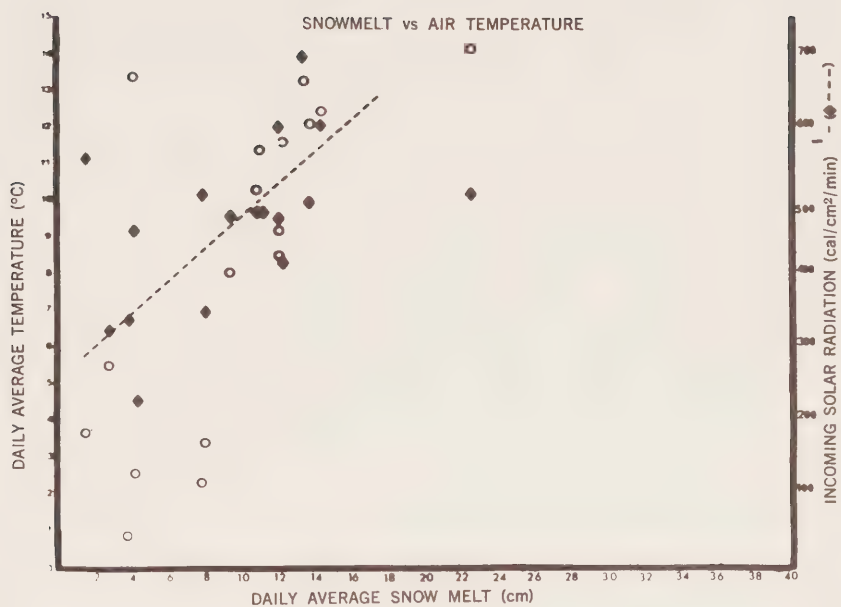
DAILY AVERAGE SNOWMELT (cm)
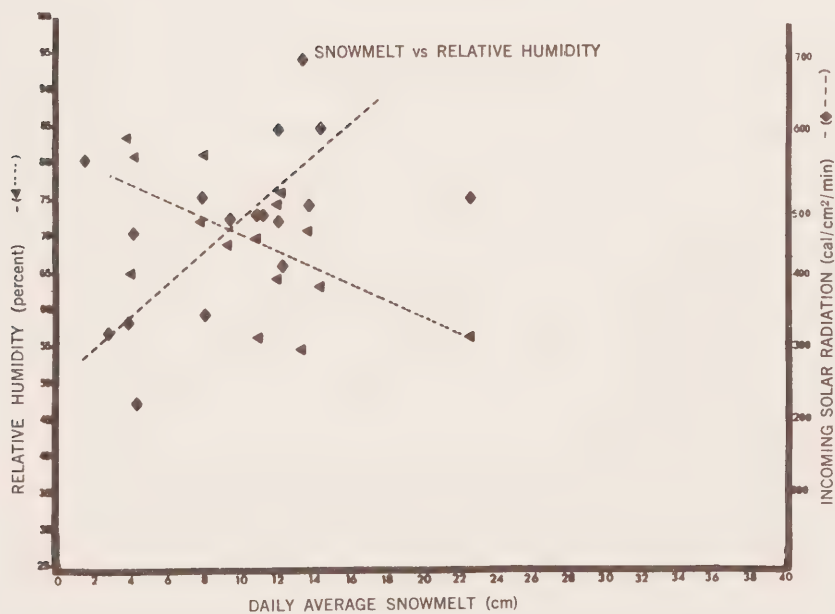
Relative Humidity

As can be expected, Graph 4C shows a trend towards increased daily average snow melt as daily average relative humidity decreases. A decrease in water vapour over the snowbed meant an increase in the gradient of water vapour between the air next to the surface of the snow (this air tends to be saturated with water vapour) and the air a few centimeters above. This gradient produces an upward flux of water vapour. The rate of sublimation over a snowpack and the rate of evaporation of melt waters are increased as ambient relative humidity decreases. Another obvious factor producing the relationship between relative humidity and melt rate is the tendency of days of lower solar input to be days of high relative humidity and low snow melt and vice versa (see Tables 1 and 6).

Creek and Spring Runoff

Pictures D1 and D2 show the sudden start in the spring flow of the creek at the base of Snowbed *1 the night of May 25, 1973. Water first flowed over the surface of the snow in the creek gulley and eroded away enough snow to form a trench one to three meters deep through the snowpack. This gulley continued to increase in width until such time as the surrounding snow melted away and/or the creek had worked its way under the snow to its natural bed. Erosion of the snow by the creek cut the snowbed into two unequal pieces on the north and south sides of the creek, and opened up caverns up to 60 cm high under the snow. Exposure of the sides of the gulley and holes under the snow to the ambient air and to sunlight most likely increased the snow melt rates in these areas.

Water from snowmelt on surrounding hillsides early in the season flowed in drainage pathways or, during periods of particularly vigorous melt, over the tundra vegetation and under the snowbed, wearing drainage channels between the snow and the ground. This, as for

the creek, created passageways (up to 10 cm high) for warmer air
to move under the snowpack. The significance of the air movement
probably wasn't too great, as usually the bottom of the snow formed
a dense ice layer, preventing upward movement of air. In many spots,
also, the snow was frozen right to the ground, with an ice layer 5
to 25 cm thick (density of 0.67 to 0.73 gm/cm^3).

Incoming Short Wave Radiation

As Graph 4B and Table 1 show, periods of high daily average
incoming short wave radiation tended to correspond to periods of
high daily average snow melt. Radiation values in excess of 700 cal/
cm^2/day were not reached during the melt period due to the local
weather of the region which had many days of fog or high percentage
cloud cover (see Table 6).

Local variations in incoming short wave radiation, can be
seen in Graphs 5A to 5F. Values were obtained with the Mk-6 Sol-A-
Meter, sensitive to the range of 0.35 to 1.15 microns.

Graph 5A, the May 26 profile, was drawn from data obtained on
a clear day from 1 to 2 pm, and shows higher incoming short wave
values for the slope of the snowbed (slope angle 10 to 20°) than for
the snowpatch area, CD0-35, with a 3 to 5° slope angle. This increased
solar input for CD40-105 did not increase the melt rate of this area
over CD0-35 because of the difference in albedo (see Table 1 and Graph 3A).

The June 10 profile, Graph 5B, shows a significant difference in
incoming solar radiation around solar noon for the NW-facing slope
(CD120-140) compared to the remainder of the snowbed. This lower
input of energy contributed to the observed slowness of snow border
retreat along the N facing slope.

The July 4 profile, Graph 5D, again shows this decrease in
radiation reaching the NW facing slope. Both the July 4 and August 1
(see Graph 5E) profiles indicate that the radiation hitting the steep

GRAPH 5A
INCOMING SOLAR RADIATION
MAY 26, 1973. (A)

INCOMING SHORT WAVE RADIATION (cal/cm²/min)

DISTANCE ALONG CD TRANSECT (METERS)

GRAPH 5B
INCOMING SOLAR RADIATION
JUNE 10, 1973. (B)

INCOMING SHORT WAVE RADIATION (cal/cm²/min)

DISTANCE ALONG CD TRANSECT (METERS)

- 158 -
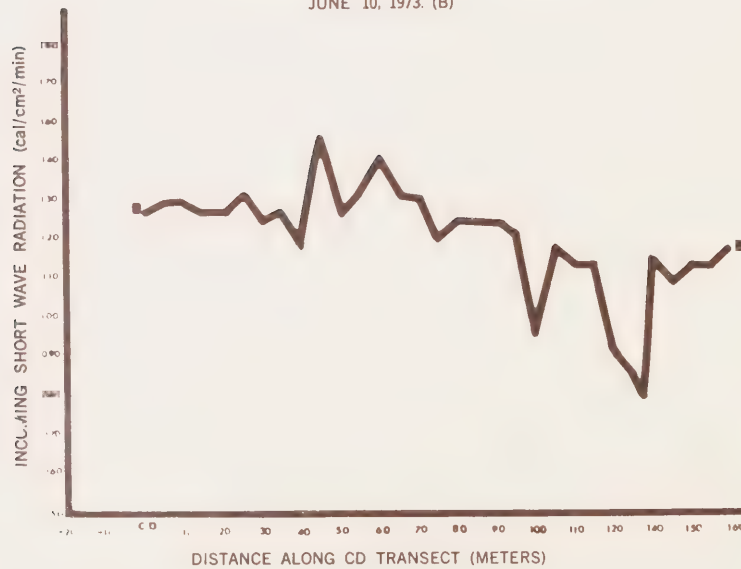
GRAPH 5C

INCOMING SOLAR RADIATION

JUNE 13, 1973. (C)
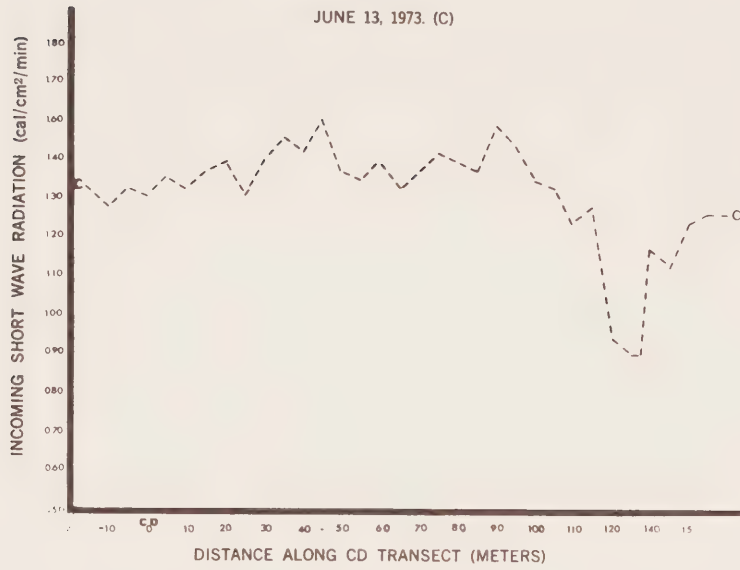
GRAPH 5D

INCOMING SOLAR RADIATION

JULY 4, 1973. (D)

- 159 -
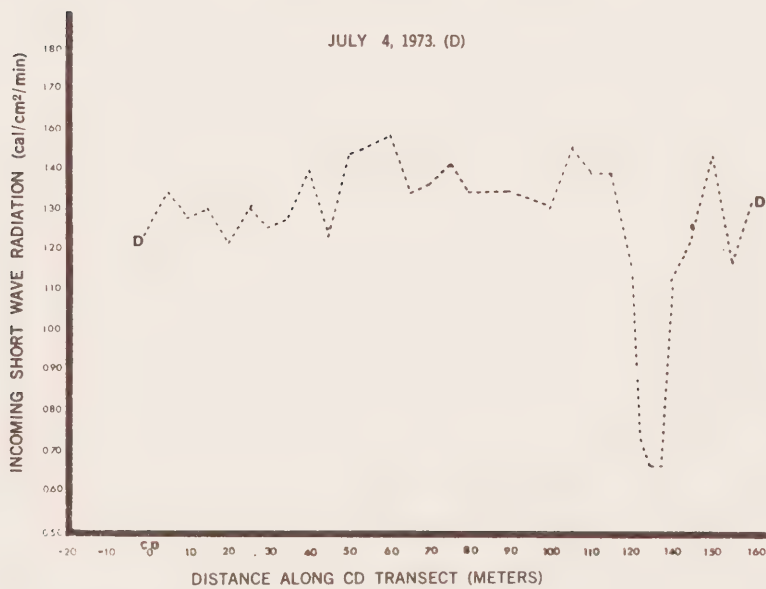
GRAPH 5E
INCOMING SOLAR RADIATION

AUG. 1, 1973. (E)

INCOMING SHORT WAVE RADIATION (cal/cm²/min)

DISTANCE ALONG CD TRANSECT (METERS)

GRAPH 5F
INCOMING SOLAR RADIATION

MAY 26, 1973. (A)
JUNE 10, 1973. (B)
JUNE 13, 1973. (C)
JULY 4, 1973. (D)
AUG. 1, 1973. (E)

INCOMING SHORT WAVE RADIATION (cal/cm²/min)

DISTANCE ALONG CD TRANSECT (METERS)

- 160 -
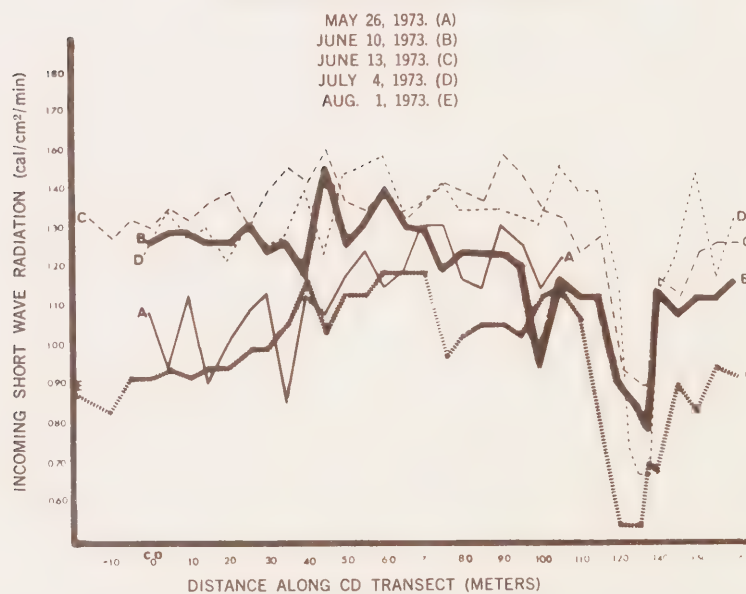
SE-facing slope of the snowbed is higher that that striking the flatter tundra areas adjacent to the snowbed (higher around solar noon, the time of highest intensities of incoming radiation). This implies that as the snow decreases in volume and increases in slope, the amount of radiation reaching it should be higher than while it was at a lesser angle. This might be another factor affecting the increase in daily average melt rate shown on Graph 4A.

Daily Average Melt Rate

In conclusion, though the melt rates varied locally depending upon albedo, snow density, solar input, wind and runoff patterns, the actual melt rates were remarkably consistent across the snowbed (see Table 1). The greatest variations occurred at CD100-115, on the flat creek area, where the snow, from the beginning of the melt season and throughout the summer, had a lower albedo than the rest of the snowbed.

Of all the factors considered, it appears that incoming short wave radiation, ambient air temperature, ambient relative humidity, and decreasing albedo had the most obvious effects on the snow melt rate. Graph 4A indicates that the actual daily average melt rate had a tendency to increase through the summer, probably due to changes in albedo, air temperature, and incoming short wave radiation.

Ground Temperature Regimes and Active Layer Development

Active Layer Development

The effect of the snowbed on active layer development is readily apparent on Graphs 6A and 6B and Table 3. Beyond CD0 and CD115, in tundra and lobe areas, active layer development ranged from 20 to 60 cm in hummock areas and hollows between solifluction features and to 75 cm on the bare mud and rock surfaces of some of the lobes or frost boils. Snow cover did exist in the hollows but did not usually exist over winter for the lobe tops, the upper three-quarters of the NW-facing slope,

GRAPH 6A

ACTIVE LAYER DEPTH vs SNOW DEPTH "A"

DISTANCE ALONG CD TRANSECT (METERS)

GRAPH 6B

ACTIVE LAYER DEPTH vs SNOW DEPTH "B"

SNOW DEPTH — CM
18 MAY 1973
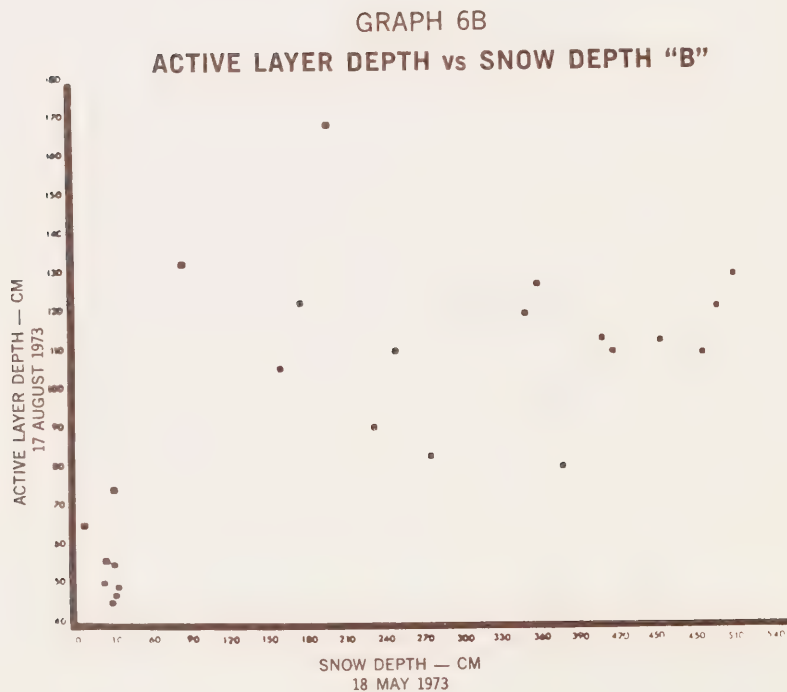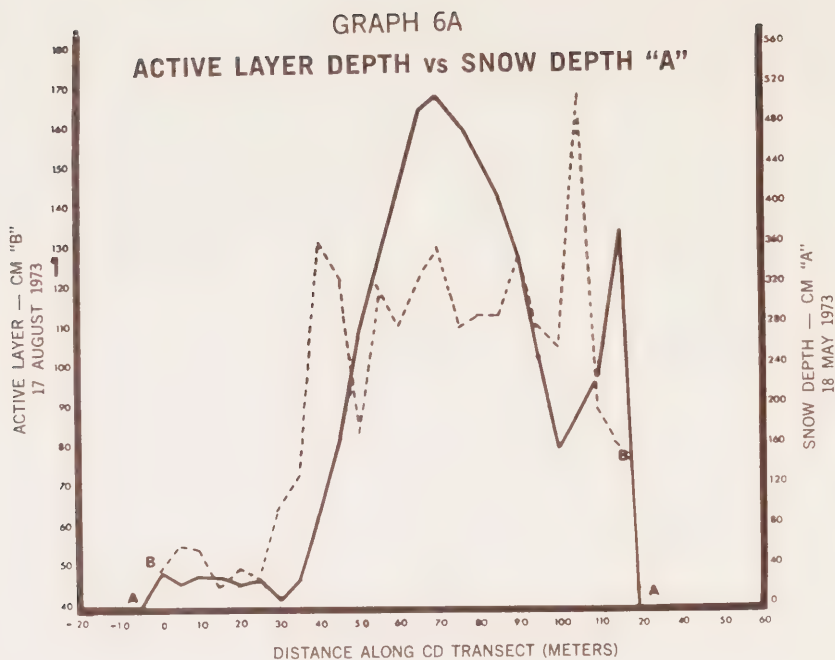
and the tops of most hummocks and tussocks in the region south
of the snowbed. True active layer depths were not obtained for the
NW-facing slope due to the presence of bedrock at or near the
surface. In the area of CD0 to CD25, where winter snow cover ranged
from 24 to 33 cm, active layer development was between 45 to 56 cm.
CD30 and CD35, which had 8 and 30 cm of snow respectively, had
significantly deeper active layer development (65 and 74 cm) than
CD0-25. The border of deep snow was at CD40. There appears to be
a perimeter effect by the snowbed on the area within 10 meters of
the deeper snow. From CD40 through to CD105, the May depth of snow
ranged from 84 to 509 cm, yet active layer development seems consistent
between 110 and 130 cm. Discrepancies exist in rocky areas (CD50, 110
and 115) where the true active layer depth was difficult to obtain,
and in the area near the creek (CD105) where active layer development
was comparatively very deep (168 cm). Data from soil pits dug to
permafrost, listed in Table 3, can be used for comparison. The
shallower depths obtained with soil pits for the upper willows is most
likely a localized effect, since other active layer profiles gave depths
of 98 to 100 cm for upper willow sites.

The consistency in active layer development in the snowbed
(see Graphs 6A and 6B) is difficult to explain as the drainage, water
regime, ground temperature regimes, incoming short wave radiation,
albedo, vegetation cover and snow depth vary considerably across the
snowbed. One possible explanation is that the presence of snow depths
greater than one meter gives enough of a uniformity in insulation from
winter cold that the annual temperature regime of the entire snowbed
area is relatively consistent and that the other factors modifying active
layer development are either cancelling each other out or of lesser
importance.

Ground Temperature Regimes

Ground temperature regimes, though an expression of regional
climatic conditions, are affected on a microscale by: local topography
(slope exposure to incoming radiation and drainage); time, depth and
duration of snow cover; water regime; plant cover; and type of soil.

The snowbed studied was divided into nine major areas, as outlined
earlier and the above mentioned factors are outlined for each
area in this section and in Table 4. Temperature regimes for
the 1973 season with corresponding data for September and November
1972 are shown in Table 4B. Since the soil temperature meters
were non-recording, gaps in Graphs 7A to 7I and 8A to 8F, including
June 18-20, July 12-21 and July 25-27 resulted when the author was
at other field locations.

Upper Lobe Area

Located above Snowbed *1 on the southerly facing slope of
Ridge 1, this area had 0 to 15 cm snow cover in the winter (except
for hollows between the solifluction features). On May 14, 1973,
snow cover was lacking over those probes used for upper lobe area
temperature determinations.   The top 5 cm at this time showed
quick freezing and thawing, even this early in the season, but at
50 cm, the ground temperature was $-3^{o}C$. November data suggests
that this area is even colder during most of the winter.

Throughout the summer, surface temperature fluctuations
were limited to the upper 10 cm of the soil, but these variations
were rapid and over a wide range of temperatures. These fluctuations
were most likely due to the reduced plant cover of the area - bare
frost boils interspaced with low lichen cover and a very rocky,well-
drained soil with reduced organic content. Heat penetration below
30 cm was slow, with soil at 50 cm depth remaining within $2^{o}C$.

Upper Birch Area

The upper birch band, located at the top edge of the snowbed
and having a thin snow cover, was also an area of rapid surface
temperature fluctuations but lower temperatures at depth. Once free
of a snow cover, this area had maximum temperatures recorded at
the 5 cm depth as high as 15 to $20^{o}C$. Some of the fluctuations
later in the summer penetrated as far as 10 cm. This moderation
in surface temperatures in most likely due to the cover

- 164 -

of birch shrub and leaf litter.   The shrub
cover, along with the shallow snow cover during the winter, are
two of the main factors which produce a cold temperature regime
in this area. The soil below 30 cm remained below 0°C until
July 11, and the soil at 50 cm (-2.7° on May 18,) did not ex-
ceed 1°C until after July 24. It fell below 1°C again on
August 16. Interestingly enough, the average albedo of the
surface under the birch shrub was 18.6%, a low albedo not reflected
by heat penetration deeper into the soil.

Upper Willows Area

Not exposed until the first week in June, this area had
a 100% cover of willows up to $1\frac{1}{2}$ meters high, with 5 to 10 cm of leaf
litter. Usually the first area of the snowbed to accumulate snow
(up to 1 meter in summer snow storms), by May, 1973, the snow cover
averaged 2.25 meters thick. The insulating qualities of this snow
are shown in the temperatures of the first 10 cm of the soil on May 19
(5 cm: -0.1°C, 10 cm: -0.3°C). Even at a depth of 50 cm, the
temperature was 1°C warmer than the birch or upper lobe areas at
the same depth. Once   free of snow, the upper willows also
showed temperature fluctuations in the top 10 cm, not penetrating
to 30 cm, but sometimes exceeding a range of 20°C. At 50 cm,
the soil did not reach 1°C until July 9 and never went above 5°C.
This area, though somewhat warmer than the birch or upper lobe
localities, also had a relatively cold temperature regime.

Upper Meadow Area

Covered with over a meter of snow in November, 1972, and 4.5
meters in May, 1973, this area showed a considerably warmer temper-
ature regime than the upper willows. Though the data from September,
1972 showed the upper willows with warmer temperatures than the
meadow, by May, 1973, this situation had reversed. The major factor
here is most likely the greater snow cover, even as early as November,
over the upper meadow, as both areas are well drained.

Temperatures for the upper meadow area at 50 cm never fell below -1°C and were above 1°C by the end of June. Surface heat penetrations seldom went below 10 cm but the general temperatures at 30 to 50 cm for most of July and August fell in the 5 to 10°C range. Summer factors - a low ground cover of 5 to 10 cm high willows with an average albedo of 26.3% also contributed to the relatively warm annual temperature regime of the upper meadow, where temperatures, even to a depth of 50 cm, remained close to the freezing point throughout the winter.

Upper Late Melt Area

Readings in this area did not start until July 1, due to the burial of wires and supporting pole under 5 meters of snow at the beginning of the season.

Temperatures on July 1, to a depth of 50 cm, were at freezing point. Whether these warm temperatures are due to an early snow cover of 160 cm by November and a deep winter snow cover of at least 5 meters, or due to melt waters and warm air passing under the snowbed during the melt period, raising the soil temperatures to a freezing point by July 1, is difficult to say, though the former seems the better explanation. Once melted out, this well drained area of chiefly bare mud and rock showed rapid, deep temperature fluctuations even to a depth of 50 cm. Once exposed from snow, the soil at 50 cm rapidly reached a temperature range between 5 and 15°C. This area showed the warmest temperature regime recorded for the snowbed.

Lower Late Melt Area

Lower late melt localities, on the lower, flatter slopes of the snowbed and usually saturated with water, had less snow cover than the upper late melt area throughout the entire winter. Not as warm as the upper late melt area, heat penetrations were not as deep or as high in temperature as the upper late melt, probably due to the shallower snow cover and the moderating effect of the water present in the lower late melt section. The 1°C mark was not passed at the 50 cm depth until July 10, but temperatures at this depth did remain in the 5 to 10°C range for at least part of the summer.

Lower Meadow Area

The lower wet meadow, with 1.2 meters of snow in May, 1973, showed a considerably colder temperature regime than the upper meadow area, exposed two weeks later but having 4.5 meters of snow in May. Situated at the lower side of the snowbed, the lower meadow tended to be saturated all summer with runoff water from the snow. Upper surface temperature fluctuations, once the snow cover had melted off, seldom reached below 10 cm. Surface temperatures tended to be cooler than the late melt areas and upper meadow area, probably due to the presence of standing water over much of the season. At depth in the soil, temperatures were much colder than the late melt areas or upper meadow, with the temperature at 30 cm being below $1^{o}C$ until June 28, and below $1^{o}C$ at 50 cm until July 7. The thinner snow cover over the winter, compared to the other three areas, allowed penetration of colder temperatures into the ground in this area.

In the later part of the summer, the lower meadow maintained a relatively warm temperature regime, with the daily average temperature at 50 cm, from August 1 to 17, at $4.3^{o}C$, compared to 7.8^{o} for the upper late melt, 4.9^{o} for the upper meadow, and 5.2^{o} for the lower late melt area.

Lower Salix Cham. Area

Though comparable in vegetation to the upper meadow area, this site was sometimes saturated with runoff water, being on the lower side of the snowbed. For most of the summer, because it was on slightly raised ground, the site was better drained that adjacent lower meadow areas. Covered with 1 meter of snow by November, 1972 and 2 meters by May, 1973, the lower Salix Cham. area had temperatures around $-1^{o}C$ on June 1 at all depths, compared to temperatures around freezing for the upper meadow. $1^{o}C$ was not totally reached at 50 cm until July 4, compared to June 28 for the upper meadow. Daily temperature fluctuations seldom went below 5 cm, and only occasionally reached 10 cm in depth. The surface temperature range was lower over

the summer for this area than the upper meadow, and the August 1-17, 50 cm average of $3.4^{o}C$ is again lower than that of the upper meadow ($4.9^{o}C$). The moderating effect on the lower Salix Cham.area is probably saturation of the ground with runoff water throughout much of the summer, compared to the well drained conditions of the upper meadow.

Lower Willows Area

The lower willow area, in spite of a snow cover of only 1.6 meters in May, had a warmer temperature regime than the upper willow site, which had a May snow cover of 2.25 meters. Temperatures in the lower willows were not below $-1^{o}C$ at 50 cm throughout the winter, and exceeded $1^{o}C$ June 28. Good cover, provided by the shrub willows, kept surface fluctuations in temperature usually below $20^{o}C$. Most fluctuations scarcely reached 5 cm in depth, and rarely reached 10 cm. The temperature regime at 50 cm was warmer than that of the upper willows – the August 1 to 17 average was $4.4^{o}C$ compared to $3.2^{o}C$ for the upper willows. Differences may be due to the presence of the creek within 10 meters of the lower willows and the passage of runoff water through or near this area throughout the melt season, or perhaps the influence of colder tundra areas above the snowbed upon the soil temperature regime of the upper willows.

Soil Temperatures at 50 cm

Soil temperatures at 50 cm depth do not generally show the rapid temperature fluctuations found in the surface 10 cm of ground, but tend to reflect the overall heat balance of an area. The magnitude of temperature penetration to greater depths, such as to 50 cm, has a direct relationship to the development of the active layer in a site. Graphs 7A to 7F show the temperature regimes, at 50 cm, of the major areas considered. It is apparent from the graphs that the areas above the snowbed or at the periphery are much colder at 50 cm

GRAPH 7A

SOIL TEMPERATURES — 50 CM

UPPER WILLOW   B
UPPER LOBE   C
HUMMOCK AREA   E
BIRCH   F
LOWER WILLOWS I
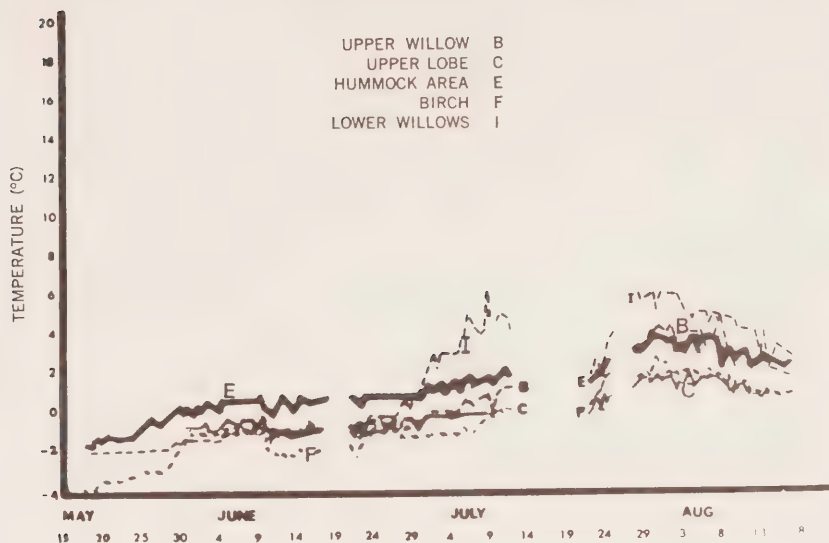
GRAPH 7B

SOIL TEMPERATURES — 50 CM

UPPER LOBE   C
HUMMOCK AREA   E
LATE MELT   G
LATE MELT — LOWER   H
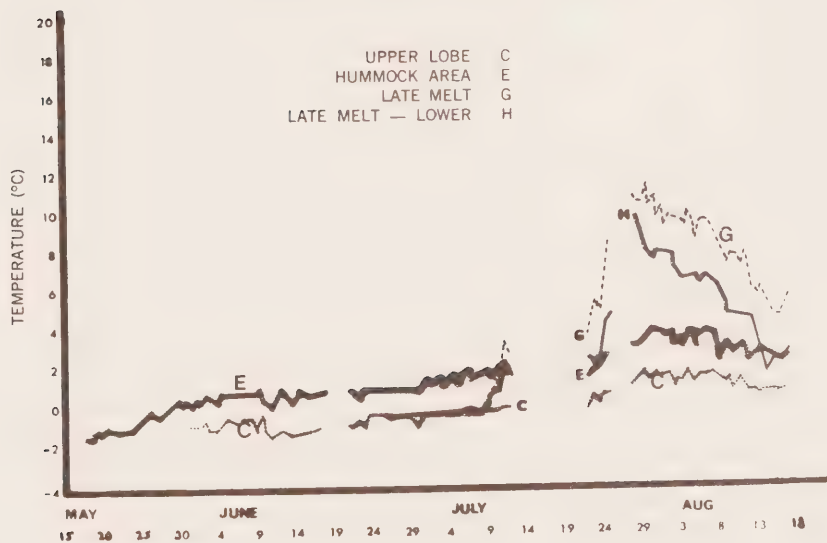
GRAPH 7C
SOIL TEMPERATURES — 50 CM

S. CHAM. LOWER   A

UPPER MEADOW   D

LOWER MEADOW   J
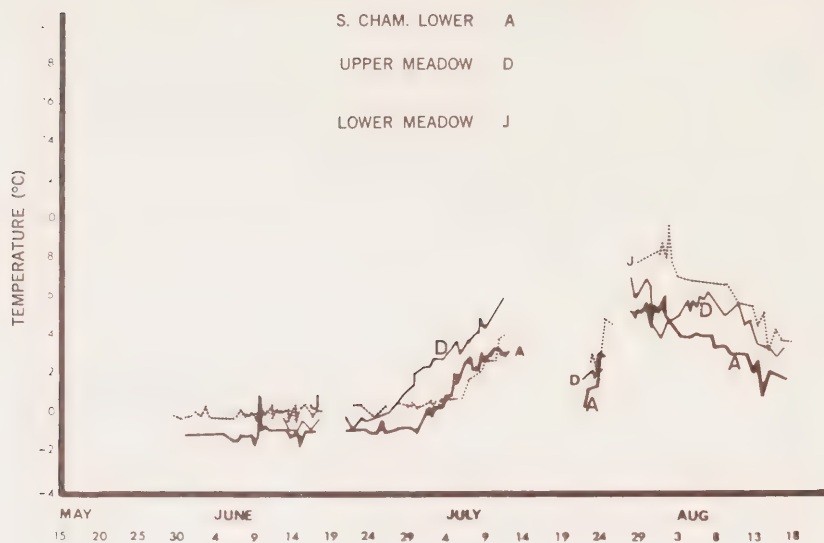
GRAPH 7D
SOIL TEMPERATURES — 50 CM

S. CHAM. LOWER   A

LATE MELT — LOWER   H
LOWER WILLOWS   I
LOWER MEADOW   J
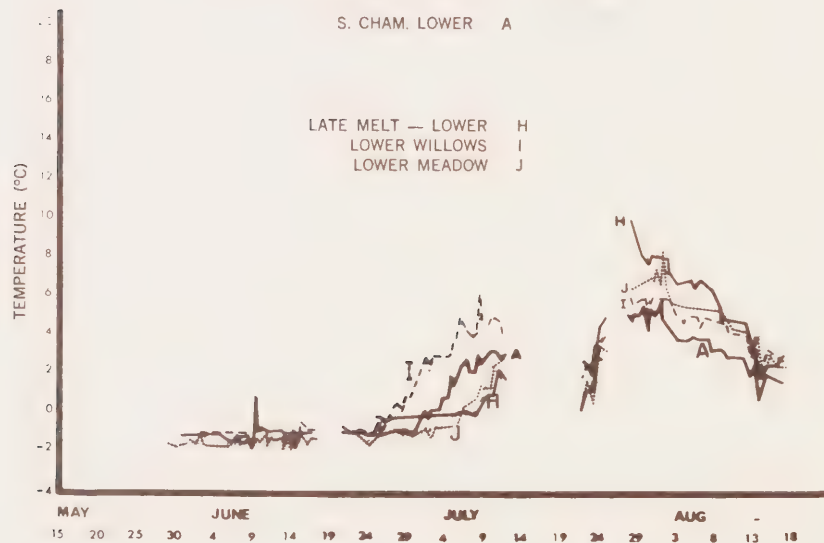
GRAPH 7E

SOIL TEMPERATURES — 50 CM
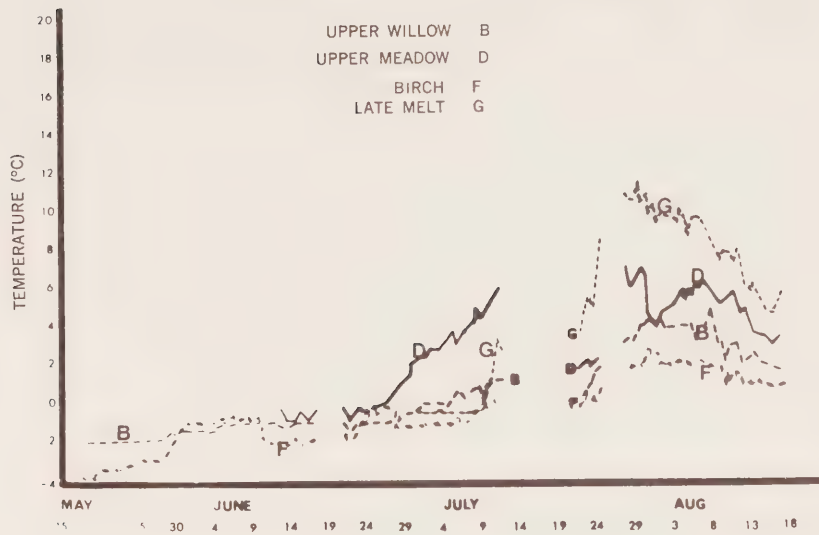
GRAPH 7F

SOIL TEMPERATURES — 50 CM
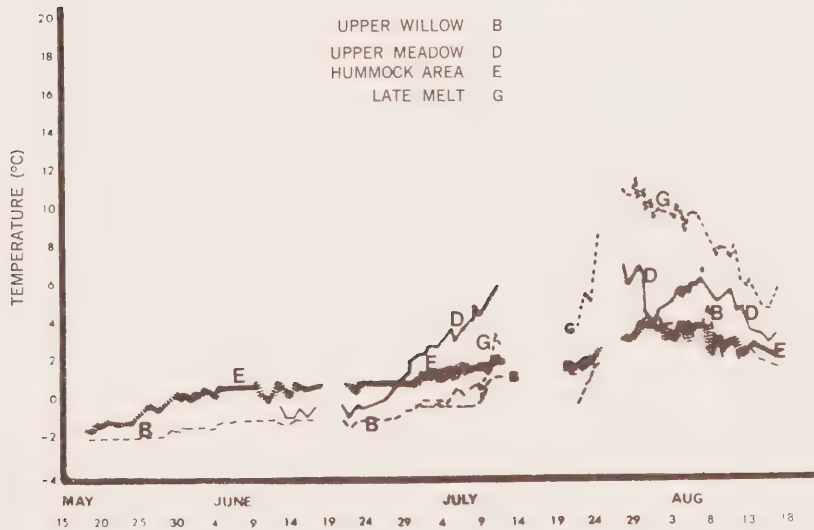
than the areas within the snowbed (i.e. the birch, upper lobe and hummock areas were colder than any snowbed sites). Within the snowbed, the upper willows were colder than the lower willows, yet the upper meadow was warmer than the lower Salix Cham. site. The upper meadow appeared to cool off faster than the wet lower meadow (Graph 7C), while the upper and lower late melt areas, once exposed, had the warmest temperature regimes at 50 cm of all the locations. Factors determining these results have been discussed in the previous sections. One can conclude, though, that vegetation cover (which provides insulation from incoming solar radiation), water regime, and nearness to tundra areas, have the greatest effects on soil temperatures, at depth, within any one area.

Ice Content and Stability of Underlying Soils

Ice content of soils found in snowbed areas below the active layer depth was not determined, as a drill was not available for probing into the permafrost. Due to the presence of either bedrock near the surface and/or the rockiness of most soils within the region, soil augers were ineffective in core drilling so that the structure and water contents of soils were examined by digging pits to the level of permafrost.

The soils within and around Snowbed *1 showed many signs of instability or of factors leading to unstable situations. Many snowbeds similar to Snowbed *1, form along creek gulleys or gentler slopes. In the rugged topography of the Richardson Mountains, these gulleys and gentle slopes represent potential paths for movement of ground vehicles or potential areas for gas pipeline construction. Such areas of deep snow accumulation represent a hazard to any such activities. To begin with, the wet soils created by snowbed runoff, the deep active layer depths, and the soil temperatures near 0°C throughout the winter, combine to create a potential for disturbance by vehicular activity.

The steep banks and runoff waters associated with most snowbeds give them and adjacent areas a natural tendency for unstable soils.

Picture E1 shows a mud slide which occurred on June 1, 1973, on
the steep NW-facing bank next to the snowbed. Even more dramatic
in 1973 was the collapse, to a depth of two meters, of ground four
meters from the natural bed of the creek at the bottom of Snowbed *1.
During spring runoff the creek cut an underground channel through the
lower willows, emerging 20 meters downstream through a large hole
about three meters from the natural creek bed, and cutting a new
channel across to its normal gulley. This underground channel, which
was not used in 1971 or 1972, suggests the presence of a large ice
lens which was rapidly eroded by the pressures of spring runoff.

The presence of springs which suddenly emerge halfway down
the slope or at the bottom of snowbeds was common. These under-
ground water drainage passageways suggest also a movement of water
along weak areas in the permafrost.

In summary, many of the snowbeds of the Canoe Lake area
represent areas of wet, unstable soils throughout the summer, and
areas of slow freezeup and high water content soils in the winter.
Danger of damage to peripheral areas near deep snow accumulations is
suggested by the deeper active layer depths here than at sites
further away.   Both the willow and birch bands, upper meadow
and especially lower meadow areas could be damaged by removal of
snow. This would expose the plants to colder winter temperatures
than normally experienced under the insulation of snow and to wind
abrasion and damage. Compaction of snow could lead to breakage of
shrubs, an increased melt period, and increased conductivity of cold
into the snow (Sellers, 1965).

Snowbeds of other Arctic regions also represent potentially
unstable areas. Picture E2 shows snowbeds found in the Shingle
Point, Yukon area along the Arctic coast. Fresh mud slides and old
mud slide scars are common about the snowbeds, as well as large cracks
and sliding pieces of vegetation (see Picture E2).

Estimation of the Energy Flux Over Snowbed

Values of wet and dry bulb temperatures were taken at the center of the snowpack during the melt season in June to determine estimates of the energy fluxes over the melting snow. On June 13, from 11:00 to 17:00 hours, values of wind, albedo, incoming short wave radiation, and wet and dry bulb temperatures were taken hourly. The average density of the surface snow was also determined. Table 5 outlines the values and estimates obtained.

The net energy balance over a snow pack can be determined by the equation $R_n = R_s\downarrow - r_s R_s\downarrow + R_L\downarrow - R_L\uparrow - e_L \sigma T_s^4$

where R_n = net radiation

$R_s\downarrow$ = incoming short wave radiation

r_s = short wave albedo

$R_L\downarrow$ = incoming long wave radiation

$R_L\uparrow$ = reflected long wave radiation

$e_L \sigma T_s^4$ = Stefan-Boltzman equation – the emmittance of heat from a body of surface temperature T_s

T_s = 0°C or 273°K for snow

e_L = emissivity = 0.90 for old snow

June 13 = clear day, without cloud cover.

Incoming short wave radiation between 0.35 and 1.15 microns was obtained with the Sol-A-Meter MK6. Incoming long wave radiation was estimated as 1% of the energy value of $R_s\downarrow$ (Sellers, 1965). Most likely this is an underestimate and values presented here represent a minimal range.

Using the energy balance equation R_n – G = LE + H

where G = flow of heat downwards into the snow

LE = latent heat flux

H = convective heat flux

estimates of the energy balance over the snowpack were obtained (Rouse & Kershaw, 1971). G was determined with thermistors placed

at 5 and 10 cm depth in the snow, and with the equation

$$G = -\lambda \frac{\Delta T}{\Delta z}$$

λ = thermal conductivity = cp^2 (Geiger, 1966)

p = snow density = 0.499688 gms/cm^3

c = constant= 0.0066 cal/cm/sec/degree

ΔT = change in temperature

Δz = 5 cm change in depth

R_n - G, then, was a measurable value. Using the Bowen Ratio
method where $B = \frac{H}{LE} = \frac{-pc_p K_p \frac{\Delta T}{L \Delta z}}{-pL K_w \frac{\Delta q}{\Delta z}} = \frac{c_p}{L} \frac{\Delta T}{\Delta q}$

c_p = heat capacity of the air at constant pressure

L = latent heat of vaporization

ΔT = gradient of temperatures

Δq = gradient of specific humidity

q = 0.622 $\frac{e}{P_a}$

e = water vapour pressure (millibars), determined
from wet and dry bulb temperatures by the method
outlined in Smithsonian Tables, 1971.

P_a = atmospheric pressure = 1010 millibars

Both temperature and water vapour gradients were measured by sets of
wet and dry bulb thermometers placed at 150 and 50 cm above the snow.

As can be seen by the results, difficulties with air inversions
over the snowbed and water vapour condensation on the surface of the
snow (a downward flux of water vapour), were encountered on this and
other days when attempts were made to measure energy flux values.
According to the literature (Geiger, 1966; Munn, 1966) work done over
glaciers, especially the Blue Glacier in the United States and the
Fedchenko Glacier studied by Kazansky, has shown that condensation over
snow surface is a common phenomenon and latent heat released in this
process is used to melt snow. The results obtained at Snowbed *1 suggest

- 175 -

a large input of energy from water vapour condensation and cooling of the air, into the snowbed system and into melting the snow, not evaporating water or heating the air above the snowbed. Further data analysis and study is required, though, before any definite conclusions can be reached.

CONCLUSIONS

During examination of the physical characteristics of snowbeds in the northern Richardson Mountains, N.W.T., formation of snowbeds was found to be mainly an expression of prevailing wind (NW) and local topography, with the sudden decrease in wind speed when passing over a steep drop in topography, leading to drift formation, especially on slopes facing south to east. Melt rate of the snow appeared to be most influenced by ambient air temperature, relative humidity, albedo and incoming solar radiation, though other factors such as wind, rain, density and creek runoff had some influence. The daily average melt rate was found to increase over the summer.

Active layer development was influenced by the presence of snow cover greater than one meter, but active layer depths for areas with snow from one to five meters deep were remarkably consistent. Ground temperature regimes, on the other hand, more expressed the depth of snow cover and the water regime of each area. Important factors affecting ground temperature were found to be plant cover, drainage, depth of snow cover, time of snow cover and duration of snow cover.

Slopes within and near the snowbeds showed signs of natural instability manifested by slides, underground springs, and slumpage of ground in wetter sites. Snowbed soils, with temperatures near freezing all winter and high moisture regimes during the summer, could be more easily damaged by human activity than adjacent tundra areas.

ACKNOWLEDGEMENTS

REFERENCES

Canadian Dept. of the Environment, Atmospheric Environment Service, 1973. CANADIAN WEATHER REVIEW, Vol. II, No. 6.

Geiger, R., 1966. THE CLIMATE NEAR THE GROUND. Harvard University Press.

Hulten, E., 1968. FLORA OF ALASKA AND NEIGHBOURING TERRITORIES. Stanford University Press.

Lambert, J.D.H., 1968. THE ECOLOGY AND SUCCESSIONAL TRENDS OF TUNDRA PLANT COMMUNITIES IN THE LOW ARCTIC SUBALPINE ZONE OF THE RICHARDSON AND BRITISH MOUNTAINS OF THE CANADIAN WESTERN ARCTIC. Unpublished Ph.D. Thesis, University of British Columbia.

Rouse, W.R. & K.A. Kershaw, 1971. THE EFFECTS OF BURNING ON THE HEAT AND WATER REGIMES OF LICHEN-DOMINATED SUBARCTIC SURFACES. Arctic and Alpine Research. Vol. 3, No. 4, pp. 291-304.

Sellers, W.D., 1965. PHYSICAL CLIMATOLOGY. University of Chicago Press.

Smithsonian Meteorological Tables, 6th Edition, 1971, editor R.J. List.

Munn, R.E., 1966. DESCRIPTIVE MICROMETEOROLOGY. Academic Press.

APPENDIX - 1

LIST OF TABLES

Table 1   Ablation Rates Snowbed *1

Table 2   Wind and Rain Records 1973

Table 3   Active Layer Development

Table 4A   Snow Depths, Snowbed *1, 1973

Table 4B   Ground Temperatures, Snowbed *1, 1973

Table 5   Bowen Ratio Values, Snowbed *1, 1973

Table 6   Weather Records, 1973, Snowbed *1

Table 7   Some Plant Species Associated with Snowbeds

SNOWBED*1, 1973

AVERAGES OF DAILY MAXIMUM AND DAILY AVERAGE TEMPERATURES (°C)

LOCATION	Depth (cm)	1972 Sept.15-19 Daily	Max.	1972 Nov.24 Daily	Max.	1973 1st Record Day Daily	Max.	1973 May 15-31 Daily	Max.	1973 June 1-17 Daily	Max.	1973 June 21-30 Daily	Max.	1973 July 1-11, 22-24, 28-31 Daily	Max.	1973 Aug. 1-17 Daily	Max.	1973 Total Average May-Aug. Daily	Max.
Upper Lobe (1st rec. May 18)	Surface																		
	5			-7.0		7.7	7.7	8.5	10.4	9.6	13.2	10.6	14.0	19.0	22.7	12.5	14.4	12.4	15.3
	10	0.3	0.4	-6.2		-0.1	-0.1	1.0	1.5	2.9	4.2	3.5	4.2	8.9	8.0	5.7	6.8	4.2	5.2
	30	0.3	0.4	-5.0		-1.7	-1.7	-1.2	-1.1	0.2	0.3	0.9	1.0	2.8	3.0	3.4	3.5	1.4	1.5
	50	0.1	0.5	-4.0		-2.8	-2.8	-2.0	-1.9	-0.8	-0.2	0	0	0.8	0.9	1.8	1.9	0.1	0.2
Upper Birch (May 18)	Surface																		
	5	0.4	0.5	-		-1.5	-1.5	-2	-1	4.4	5.3	4.5	5.2	8.8	10.7	9.0	10.4	5.7	6.7
	10	0.6	0.7	-		-0.6	-0.6	-2	-2	1.0	1.7	2.3	2.7	5.7	6.4	5.8	6.5	3.1	3.7
	30	0.3	0.4	-		-2.2	-2.2	-1.6	-1.6	-0.7	-0.5	-0.2	-0.2	0.8	0.9	2.5	2.6	0.3	0.3
	50	-0.2	-0.1	-		-2.7	-2.7	-2.8	-2.8	-1.3	-1.3	-1.8	-1.7	0.2	0.3	1.6	1.7	-0.6	-0.6
Upper Willows (May 19)	Surface																		
	5	0.4	0.6	-		-0.1	-0.1	0	0	6.7	9.3	6.1	7.1	12.0	13.5	11.7	15.1	7.8	9.7
	10	0.8	0.9	-		-0.3	-0.3	0	0.1	1.3	2.1	2.5	3.0	6.5	10.2	6.5	7.3	3.7	5.0
	30	0.8	0.8	-		-1.1	-1.1	-0.8	-0.7	-0.3	-0.2	0.1	0.2	3.4	3.5	4.7	4.8	1.7	1.8
	50	0.8	0.8	-		-1.9	-1.9	-1.8	-1.7	-1.1	-1.0	-0.9	-0.8	1.3	1.4	3.2	3.3	0.4	0.5
Upper Meadow (June 13)	Surface	0	0.2	-		-0.2	-0.2	-				12.3	16.8	15.9	18.9	9.3	11.4	11.3	14.0
	5	0.1	0.3	-		-0.2	-0.2	-		-0.3		6.1	7.0	9.5	10.5	7.2	8.0	7.1	7.9
	15	0.1	0.1	-		0	0	-		-0.1	-0.1	4.0	4.7	7.0	7.7	6.3	6.7	5.4	6.0
	30	0.5	0.6	-		0	0	-		-0.1		2.6	2.6	6.1	6.4	6.4	6.5	4.9	5.1
	50	0.2	0.2	-		-0.2	-0.2	-		-0.5	-0.4	0.3	0.3	4.1	4.2	4.9	4.9	3.1	3.2
Upper Late Melt (July 1)	Surface	0.6	1.1	-		0	0	-		-		-		10.9	13.4	12.8	13.9	11.8	13.6
	5	0.3	0.6	-		0	0	-		-		-		9.8	12.3	12.3	13.9	11.0	12.9
	15	0	0.3	-		0	0	-		-		-		7.4	8.6	9.6	10.7	8.4	9.6
	30	0.9	1.0	-		0	0	-		-		-		5.3	6.1	9.1	9.6	7.2	7.8
	50	0.5	0.5	-		0	0.1	-		-		-		3.4	3.9	7.8	7.9	5.5	5.7
Lower Late Melt (June 25)	Surface	0	0.1	-0.8		-0.2	-0	-		-		0	0.1	10.2	12.4	9.4	10.9	8.4	10.0
	5	0.3	0.5	-0.2		-0.2	-0.2	-		-		0.1	0.1	5.0	5.7	6.8	8.0	5.0	5.9
	10	-0.7	-0.1	-1.5		-1.0	-1.0	-		-		-1.1	-1.1	3.2	3.8	5.2	6.0	3.4	4.0
	30	0	0.2	-0.9		-0.3	-0.0	-		-		-0.7	-0.6	3.1	3.4	5.4	5.6	3.5	3.7
	50	0.1	0.1	0		-0.1	-0.0	-		-		-0.3	-0.2	2.6	2.9	5.2	5.3	3.3	3.4
Lower Meadow (May 29)	Surface	0.7	1.1	-0.5		-0.5	-0.5	-0.7	-0.6	5.8	7.3	7.8	10.3	13.2	16.1	7.2	8.7	8.2	10.2
	5	0.1	0.2	-0.8		-0.9	-0.9	-0.9	-0.9	0.1	0.6	2.9	4.1	8.9	10.5	6.5	7.4	4.6	5.6
	10	0.7	0.8	0		-0.3	-0.3	-0.3	-0.3	0	0.2	2.7	3.6	8.2	9.3	6.9	7.2	4.4	5.1
	30	0.2	0.3	0		-1.4	-1.4	-1.4	-1.4	-1.4	-1.3	-0.9	-0.8	4.2	4.7	4.8	4.9	1.8	2.0
	50	0.1	0.2	0		-1.5	-1.5	-1.5	-1.5	-1.4	-1.3	-1.1	-1.1	2.0	2.1	4.3	4.5	1.1	1.2
Lower Salix Cham. (June 1)	Surface	0.3	0.6	-0.9		-0.9	-0.9	-		1.6	2.3	10.1	13.4	14.8	17.4	7.5	8.9	8.4	10.3
	5	0.1	0.1	-0.3		-0.5	-0.5	-		0.6	0.9	4.3	5.8	9.1	10.3	6.3	6.9	5.2	6.1
	10	0.5	0.6	0		-0.9	-0.8	-		-0.3	0.3	3.6	4.9	8.6	10.2	6.1	6.6	4.7	5.6
	30	0.4	0.5	0.1		-0.9	-0.8	-		-0.5	-0.3	0.5	0.7	5.3	5.6	5.0	5.0	2.8	3.0
	50	0.2	0.2	0.1		-1.0	-1.0	-		-0.9	-0.8	0	0.1	2.6	2.8	3.4	3.4	1.4	1.6
Lower Willows (June 3)	Surface	0	0.1	-		-0.7	-0.7	-		3.4	4.2	9.4	12.9	12.3	14.2	7.1	8.1	8.1	9.8
	5	0.1	0.1	-		-0.6	-0.6	-		0.6	1.3	5.9	7.6	9.1	10.2	5.7	8.1	5.5	6.4
	10	0.6	0.7	-		-0.2	-0.2	-		-0.2	-0.1	4.7	5.6	8.3	8.9	6.1	6.3	5.1	5.5
	30	0.2	0.3	-		-0.3	-0.3	-		-0.2	-0.2	1.3	1.4	6.0	6.4	5.4	5.5	3.5	3.6
	50	0.9	0.9	-		-0.9	-0.9	-		-0.8	-0.8	-0.1	0	4.3	4.6	4.4	4.5	2.3	2.4

TABLE 2   WIND AND RAIN RECORDS, 1973

DATE	RAIN (cm)				WIND km/hr			
	UPPER	LOWER	RAIN	SNOW	TOP OF RIDGE I	UPPER	LOWER	DIRECTION
May 17						6.53	5.46	NW-NE
18						4.69	4.63	E
19					2.32	3. 24	2.49	E
20					3.38	2. 78	2.64	SE
21					15.20	13.78	11.48	NE-NW
22	0.140	0.118		X	5.12	4.99	4.08	NW-NE
23	0	0			4.97	4.37	3.46	NE
24	0.584	0.561	X		8.33	6.52	4.79	SW-NW
25	0.103	0.103	X		10.88	9.28	7.51	NW
26	0	0			9.46	8.50	6.71	WNW-SE
27	0.379	0.355	X		15.93	12.72	8.08	NNW-NW
28	0.268	0.291	X		11.09	8.98	6.15	SE-NW
29	0.756	0.726	X		6.17	4.82	2.88	NW
30	0.158	0.022	X		7.02	5.11	3.97	SE-E
31	0.932	0.829	X	X	7.52	5.84	3.43	NW
June 1	0.002	0.006	X		9.54	5.86	4.81	NW
2	0.001	0.001	X		20.65	16.90	9.98	NW
3	0.150	0.103	X		11.40	9.23	5.85	NW
4	0.085	0.070	X		5.43	5.06	4.18	NW-SE
5	0	0			8.03	6.76	6.73	SE
6	0.001	0.001	X		5.63	5.37	4.93	NW-NE
7	0	0			11.42	9.16	6.60	NE-NW
8	0	0			25.92	20.60	11.93	NW
9	0	0			7.51	6.56	5.02	NW-NE
10	0	0			6.73	6.69	6.52	ESE
11	0	0			16.13	12.78	8.65	SE-NE
12	0	0			15.49	13.55	7.76	NW
13	0	0			10.24	7.69	3.41	SE
14	0	0			19.56	13.73	5.78	NW-SE
15	0.001	0.001	X		32.39	26.34	7.63	NW
16	0.001	0.001	X		8.31	7.24	3.21	SE-NE
17								
18	0.205	0.207	X		12.24	9.25	3.49	NW
19								
20								
21	0.253	0.284	X		17.89	12.51	4.15	SE-NE
22	1.776	2.305	X	X	16.73	11.86	3.89	NW
23	0.916	0.829	X	X	28.59	19.58	6.86	NW
24	0.109	0.103	X	X	6.99	5.38	2.00	NW-SE
25	0.007	0.004	X		8.51	6.04	3.39	NW-SE
26	0.134	0.137	X		8.71	6.02	2.71	NW-SE
27	0.004	0.001	X		8.73	6.71	3.64	NE-SE
28	0.568	0.561	X		6.89	5.23	2.24	NE-SE
29	0	0			9.12	6.50	3.20	NE
30	0	0			10.46	6.88	3.64	NE
July 1	0.182	0.190	X		12.92	7.98	3.20	SE-NE
2	0	0			8.54	6.34	2.48	NW
3	0.001	0.001	X		7.23	6.60	3.63	SE
4	0	0			16.62	11.99	4.58	NE-SW
5	0.316	0.312	X		16.26	12.57	3.80	NW
6	0.158	0.205	X		6.51	5.77	2.05	SE
7	1.003	1.003	X		9.54	7.46	2.15	SE-NW

TABLE 2 (Continued)

8	0.063	0.055	X		5.79	4.77	1.77	SE
9	0.032	0.032	X		7.00	5.22	1.73	NW-NE
10	0	0			17.24	12.53	3.91	SE-NW
11-21	6.623	6.584	X	X	12.81	11.37	*2.91 blown over	
22	0.639	0.647	X		9.77	7.34	1.14	SE-NW
23	0	0			8.10	7.44	2.00	SE-NE
24-27	0	0			15.69	12.31	3.37	SW
28	0.884	0.876	X		11.9	8.96	2.45	SE
29	0.691	0.711	X		12.79	9.49	2.98	W-NW
30	0	0			27.01	20.27	5.84	W-NW
31	0	0			11.66	9.56	3.04	SE
Aug. 1	0	0			23.99	17.70	4.71	W-NW
2	0	0			9.45	8.71	2.82	WNW-SE
3	0.339	0.355	X		14.02	8.08	3 12	SE-NE
4	0	0			9.24	6.93	2.13	NW
5	0.055	0.071	X		13.25	8.44	2.22	SE
6	0.038	0.049	X		30.53	20.82	6.17	NE-NW
7	0.860	0.695	X		24.93	19.12	5.70	W-NW
8	0.006	0.006	X		10.17	6.82	1.88	NW
9	0.001	0.001	X		28.42	24.36	7.38	W
10	0.071	0.071	X		20.37	16.02	4.05	WNW
11	0.031	0.033	X		15.46	10.14	3.13	SW
12	0.987	1.026	X		17.28	9.09	3.14	SE-NW
13	0.024	0.032	X	X	20.39	14.06	4.21	NW
14	0.008	0.016	X	X	20.23	14.17	3.96	NW
15	0.001	0.016	X		8.55	5.95	2.47	NW
16	0	0			13.92	10.27	2.68	SE
17	0.?	0.?	X	X				SE-WNW

Total
May-Aug.

16	20.647cm	21.116cm			Run=28021km	22047km	9218km
					Time= 2158hr	2230hr	2204hr
					Aver.= 12.98 km/hr	9.83 km/hr	4.18 km/hr

TABLE 3   ACTIVE LAYER DEVELOPMENT

LOCATION CD LINE	DEPTH OF SNOW (cm)			TIME OF EXPOSURE 1973	ACTIVE LAYER DEPTH (cm), 1973							SOIL PITS
	SEPT. 18 1972	NOV. 24 1972	MAY 18 1973		MAY 29	JUNE 15	JULY 1	JULY 11	JULY 27	AUG 17	AVERAGE	
Upper 0	15	25	33	May 29	6	16	21	30	41	49		Lobe-75
Lobe 5	"	"	24	May 29	8	17	26	44	48	56		75
And 10	"	"	31	May 29	7	17	23	40	45	55		60
Heath 15	"	"	31	May 29	7	16	25	36	39	45	50	Heath 50
20	"	"	24	May 29	9	17	35	36	42	50		55
25	"	"	32	May 29	8	19	23	33	43	47		45
Transition 30	15	25	8	May 29	13	22	40	58	63	65	70	70 Birch
35	"	"	30	May 29	7	17	33	50	74	74		
Upper Willows 40	70	50	84	June 5		36	57	68	92	132	127	60
45	120	97	174	June 12		32	72	72	118	122		75
Upper Meadow 50	120		276	June 21			45	62	82	83		120
55	120		348	June 25			44	73	118	120	115	120
60			417	July 1			20	67	110	110		115
Upper Late 65	10 - 20	160	496	July 8				46	82	122	126	
Melt 70			509	July 22					95	130		
Lower Late 75	10 - 20		485	July 11				5	82	110		
Melt 80			452	July 11				18	84	113	112	
85			408	July 8				23	86	113		
Lower Meadow 90	10 - 20		358	July 1			15	30	97	127		100
95		63	249	July 21			38	68	107	110	119	100
Lower Willows 100	10 - 20	74	159	June 12		28	63	75	105	105		110
105		101	196	June 12		42	112	145	165	168	137	
Creek Area 110			234	June 15		7	44	55	90	90	85	
115			378	June 21			54	54	80	80		

TABLE 1 ABLATION RATES - SNOWBED*1

Time Period 1973	WIND Total Run (km)	WIND Average Speed (km/hr)	RAIN Total (cm)	RAIN Daily Average (cm)	Average Albedo (%)	DENSITY Average (grams/cm³)	DENSITY Surface	AVERAGE TEMPERATURE °C	AVERAGE RELATIVE HUMIDITY	RADIATION Total	RADIATION Daily Average	CD45 Total	CD45 Aver-age	CD55 Total	CD55 Aver-age	CD65 Total	CD65 Aver-age	CD75 Total	CD75 Aver-age	CD85 Total	CD85 Aver-age	CD95 Total	CD95 Aver-age	CD105 Total	CD105 Aver-age	CD115 Total	CD115 Aver-age
May 18-22	582	5.9				0.54	0.54	3.6	74.4	2224	556	6.0	1.2	4.5	0.8	5.5	1.1	5.5	1.4	7.0	1.4	7.5	1.5	4.5	0.9	5.0	1.0
May 22-29	1322	7.9	1.5	0.2	59	0.60	0.59	2.3	72.4	3568	510	61.0	8.7	57.0	8.1	56.5	8.1	54.5	7.8	55.0	7.9	55.5	7.9	56.5	8.1	57.0	8.1
May 29-30	114	4.8	0.8	0.8				3.3	82.8	297	297	3.9	3.9	6.3	6.3	5.5	5.5	8.0	8.0	13.0	13.0	15.5	15.5	5.5	5.5	9.0	9.0
May 30- 2	402	5.6	1.1	0.4		0.58	0.56	2.5	82.1	683	228	22.9	7.6	17.3	5.8	13.5	4.5	12.5	4.2	10.0	3.3	11.0	3.7	18.5	6.2	11.0	3.7
June 2 - 5	751	10.4	0.2	0.1		0.55	0.55	0.8	83.6	1014	338	18.0	6.0	15.0	5.0	12.0	4.0	11.5	3.8	12.0	4.0	14.0	4.7	19.5	6.5	13.0	4.3
June 5 - 8	501	6.9	tr	0		0.60	0.59	11.4	56.4	1500	483	7+	2.3+	38.0	12.7	29.0	9.7	33.0	11.0	29.0	9.7	32.0	10.7	34.0	11.3	32.0	10.7
June 8-12	1121	11.6	0	0	46	0.61	0.62	9.2	64.7	2393	598	27+	6.8+	57.0	14.3	51.0	12.8	48.0	12.0	48.0	12.0	50.0	12.5	56.0	14.0	63.0	15.8
June 12-15	845	11.7	0	0	44	0.59	0.59	13.3	54.8	2095	698	--	--	39.0	13.0	42.0	14.0	40.0	13.3	42.0	14.0	41.0	13.7			61.0	20.3
June 15-21	1744	14.2	0.2	0.03		0.61	0.61	12.4	63.7	3630	605			100.	16.7	83.0	13.8	86.0	14.3	80.0	13.3	--	--			102.	17.0
June 21-22	239	12.5	0.3	0.3				13.4	65.4	458	458			--	--	0	0	4.0	4.0	6.0	6.0					--	--
June 22-25	871	14.2	2.8	0.9		0.61	0.59	5.4	79.1	969	323					7.0	2.3	8.0	8.0	7.0	2.3						
June 25-28	451	6.3	0.1	0.05				8.0	69.2	1442	481					27.0	9.0	28.0	9.3	26.0	8.7						
June 28- 1	448	6.2	0.6	0.2	27	0.62	0.59	12.1	71.3	1491	497					43.0	14.3	41.0	13.7	38.0	12.7						
July 1 - 3	355	7.2	0.2	0.09				10.3	70.1	974	487					21.0	10.5	21.5	10.8	21.5	10.8						
July 3 - 4	155	6.6	tr	tr	27	0.66	0.66	8.4	74.9	474	474					11.0	11.0	12.0	12.0	10+	10+						
July 4 - 5	272	12.0	0	0				14.1	56.8	512	512					22.5	22.5	22.5	22.5	--	--						
July 5 - 8	626	8.6	1.5	0.5		0.62	0.62	11.6	76.5	1246	415					--	--	36.5	12.2								
July 8 - 9	109	4.8	0.06	0.1	23	0.67	0.67	13.0	80.6	401	401							8+	8+								

SNOW MELT RATE (cm) - 1973

- 184 -

TABLE 4A   SNOW DEPTHS   SNOWBED*1, 1973

LOCATION	D Depth (cm)	DEPTH OF SNOW (cm)			FIRST RECORDED DAY 1973	DATE OF EXPOSURE FROM SNOW 1973	WATER REGIME
		Sept.19 1972	Nov. 24 1972	May 18 1973			
Upper Lobe	Surface 5 10 30 50	0	15	0	0	May 18	?	Well drained. Upper slopes above snowbed.
Upper Birch	Surface 5 10 30 50	30-60	25	20 0 0 0 0	20 0 0 0 0	May 18	May 26 ? ? ? ?	Well drained. Upper edge of snowbed.
Upper Willows	Surface 5 10 30 50	120	75	225	225	May 19	June 5	Well drained. Upper edge of snowbed.
Upper Meadow	Surface 5 15 30 50	10-20 up to 150 cm if in drift area	132	450	98	June 13	June 21	Well drained after exposure. Upper slope of snowbed.
Upper Late Melt	Surface 5 15 30 50	10-20	160	513	50-100	July 1	July 7	Well drained after exposure. Upper slope of snowbed.
Lower Late Melt	Surface 5 10 30 50	10-20	–	345	88	June 25	July 5	Mostly saturated. Lower slope of snowbed.
Lower Meadow	Surface 5 10 30 50	10-20	63	118	57	May 29	June 7	Mostly saturated. Lower slope of snowbed.
Lower Calix	Surface 5 10 30 50	10-20	103	204	138	June 1	June 14	Sometimes saturated. Lower slope of snowbed.
Lower Willows	Surface 5 10 30 50	10-20	74	160	87	June 3	June 13	Sometimes saturated. Lower slope of snowbed.

TABLE 5 - BOWEN RATIO VALUES, SNOWBED*1, 1973

TIME	WIND (km/hr) SPEED	WIND DIREC-TION	ALBEDO (%)	SHORT WAVE RADIATION INCOMING-$R_s\downarrow$ BTU/HR/FT2	CAL/CM2/MIN	NET CAL/CM2/MIN	LONG WAVE RADIATION INCOMING CAL/CM2/MIN	NET CAL/CM2/MIN	NET RADIATION CAL/CM2/MIN
11:00	0-3	NE	39	260	1.1758	0.7172	0.03015	0.0270	0.7443
12:00	3.6	SE	38	275	1.2436	0.7710	0.03273	0.0295	0.80048
13:00	6.8	SE	37	290	1.3114	0.8262	0.03544	0.0319	0.85809
14:00	0-4	SE	37	310	1.4019	0.8832	0.03789	0.0341	0.91728
15:00	0-4	SE	38	295	1.3340	0.8271	0.03511	0.0316	0.85870
16:00	0	-	39	260	1.1758	0.7172	0.03015	0.0271	0.74434
17:00	4-11	SE	44	215	0.9723	0.5447	0.02210	0.0199	0.56459

TIME	FLUX INTO SNOW (G) ΔT for G	G CAL/CM2/MIN	R_n-G	DRY BULB (t)(°C) 150cm	50cm	ΔT	WET BULB (t')(°C) 150cm	50cm	t-t'	ADJACENT VEGETATED AREA (CD30) T(°C)	RH(%)
11:00		($\times 10^{-3}$)		13.5	15.9	-2.4	11.5	10.5	2.0 / 5.4	12.2 / 12.2	45 / 45
12:00				14.0	14.8	-0.8	11.5	11.0	2.5 / 3.8	13.3 / 15.6	45 / 45
13:00	0	0	0.858	13.5	14.0	-0.5	11.5	10.5	2.0 / 3.5	15.6 / 15.6	44 / 45
14:00	+0.2	+3.95503	0.913	14.8	15.3	-0.5	13.1	11.0	1.7 / 4.3	15.6 / 15.6	44 / 44
15:00	+0.6	+11.86510	0.847	15.3	14.0	+1.3	13.5	11.0	1.8 / 3.0	15.6 / 16.1	43 / 40
16:00	+1.1	+21.17527	0.723	17.5	17.0	+0.5	15.3	14.0	2.2 / 3.0	16.7 / 17.2	37 / 37
17:00	+1.4	+27.76852	0.537	15.9	14.8	+1.1	13.5	12.0	2.4	16.7	33

TIME	WATER VAPOUR PRESSURE (e) millibars 150 cm	50 cm	SPECIFIC HUMIDITY GM/KGM 150 cm	50 cm	Δq	BOWEN RATIO $\frac{H}{LE}$	LE cal/cm2/min	H cal/cm2/min
11:00	12.211	9.086	7.520	5.596	1.9245	-0.507		
12:00	11.873	10.554	7.312	6.500	0.8127	-0.396		
13:00	12.211	10.354	7.520	6.377	1.1436	-0.178	-0.729	+0.296
14:00	13.417	10.216	8.570	6.292	2.2788	-0.088	-0.839	+0.074
15:00	14.248	11.094	8.774	6.832	1.9424	+0.272	-0.666	-0.181
16:00	15.084	13.945	9.782	8.588	1.1939	+0.168	-0.619	-0.104
17:00	13.841	12.129	8.524	7.469	1.0546	+0.424	-0.377	-0.160

TABLE 6   WEATHER RECORDS, 1973

SNO..B'D*1

DAY 1973	SUN	RAIN	SNOW	FOG	TEMPERATURE (°C) * MORE THAN ONE VALUE			RELATIVE HUMIDITY (%)			WIND (km/hr)		RAIN (cm)	SHORT WAVE RADIATION (cal/cm²)
					AVERAGE	MAXIMUM	MINIMUM	AVERAGE	MAXIMUM	MINIMUM	AVERAGE	DIRECTION		
May 14	X											SE		
15	X			X								NNW		
16	X	X	X	X								NNW		
17	X		X	X	-5.2	-2.8	-7.2				6.5	NW-E		
18	X				-4.6	1.7	-8.9				4.7	E		409.7
19	X				0	4.4	-4.4	65	82	60	2.5	SE		669.7
20	X				-0.2	1.7	-1.1*	76	84	62	2.6	SE		559.9
21	X		X	X	-2.5	0	-3.9*	82	97	73	13.8	NE-NW		628.8
22			X	X	-3.4	1.7*	-4.4*	88	94	79	5.0	NW-NE	0.14	460.8
23	X			X	-1.9	0	-5.6*	85	94*	75*	4.4	NE	0.0	538.3
24	X			X	0.4	2.2*	-2.2*	82	92*	67*	6.5	SW-NW	0.58	507.5
25	X	X		X	1.0	6.1*	-1.1*	86	93	53	9.3	NW	0.10	289.7
26	X				7.1	12.2*	3.3*	38	48	21	8.5	NW	0	673.5
27	X	X			6.4	11.1	0	64	93	40*	12.7	NNW	0.38	466.3
28	X	X			6.6	11.7	0.6*	66	91*	36*	9.0	NW	0.27	629.3
29	X	X			3.3	6.1	1.1*	83	92*	70*	4.8	NW	0.76	308.6
30			X		X	2.8	3.9*	1.7*	79	91*	65	5.1	SE	0.16	252.3
31			X		2.6	3.3*	1.7*	82	93*	54	5.8	NW	0.93	125.6
June 1	X			X	2.1	3.3*	0	86	92*	78*	5.9	NW	0.02	297.4
2	X	X		X	0.3	1.7*	-1.1*	84	92*	72	16.9	NW	tr	456.5
3			X		X	-1.1	0	-1.1*	89	92	84	9.2	NW	0.15	157.1
4	X	X		X	3.1	7.2	-0.6*	78	90*	58	5.1	NW	0.09	373.2
5	X				11.2	13.6*	4.7	44	67	31	6.8	SE	0	535.9
6	X	X			12.4	16.4*	8.6	56	72	47	4.9	NW	tr	433.7
7	X				10.4	12.8*	6.7*	70	84	56	9.2	NE	0	489.1
8	X				7.6	11.1*	3.3*	73	91*	52	20.6	NW	0	501.3
9	X				6.4	8.9*	3.3*	75	93*	61*	6.6	NW	0	489.6
10	X			X	9.2	15.0*	1.7*	62	88	28*	6.5	ESE	0	706.8
11	X				13.6	16.7	10.0	49	64	37*	12.8	SE	0	681.2
12	X				10.9	13.3*	7.2*	63	89	49*	13.5	NW	0	719.2
13	X				13.0	17.8*	6.1	54	79	40*	7.7	SE	0	706.0
14	X				16.0	17.8	10.6	47	70	31*	13.7	NW	0	691.3
15	X	X		X	7.9	10.0*	3.3	80	94	68*	26.3	NW	tr	622.5
16	X	X		X	9.5	13.3*	2.2	63	98	50*	7.2	SE	tr	613.0
17	X	X			13.4	15.6*	10.0*	60	84	37*		NW	0	
18	X	X			14.7	17.8*	12.2	59	89	41*	9.3		0.21	601.3
19	X	X			14.5	17.2*	11.1	60	92	43*				
20	X	X			14.8	18.3	9.4	60	84	47				
21	X	X			13.4	16.1	8.9*	65	87*	53	12.5	SE	0.23	462.7
22			X	X	X	8.6	14.4*	6.1	80	97*	60	11.9	NW	1.78	229.1
23			X	X	X	3.7	7.8	2.2*	85	92	79	19.6	NW	0.92	302.0
24	X	X	X		3.9	6.1	2.2*	72	80	57	5.4	NW	0.11	437.0
25	X	X		X	5.9	7.8	4.4*	71	87	59*	6.0	NW	0.01	370.4
26	X	X		X	8.6	12.2	5.6*	69	89	42	6.0	NW	0.13	426.6
27	X	X		X	9.4	12.8	5.6*	68	93	47*	6.7	NE	0.01	656.5
28	X	X			10.9	15.6	7.2*	72	91	49	5.2	NE	0.57	387.2
29	X				12.7	14.4*	10.6*	72	93	54	6.5	NE	0	543.6
30	X			X	12.6	15.6*	8.9*	70	96	49	6.9	NE	0	554.7
July 1	X	X		X	10.8	13.3	7.8	77	93	59	8.0	SE	0.18	358.2

– 187 –

Month	Day														
	2	X				9.7	12.2*	6.7*	64	93	41	6.3	NW	0	631.5
	3	X	X		X	8.4	12.8*	5.0	75	92	59*	6.6	SE	tr	442.0
	4	X				14.1	18.9*	6.7	57	87*	35	12.0	NE	0	527.0
	5	X	X		X	10.1	15.6	7.2*	75	95*	53	12.6	NW	0.	379.9
	6	X	X		X	9.9	14.4	5.6*	80	94	60	5.3	SE	0.16	529.9
	7	X	X		X	14.7	16.1	11.1	75	90	53	7.5	SE	1.00	360.1
	8	X	X		X	13.0	16.1	10.0	81	95	58	4.8	SE	0.06	403.4
	9	X	X		X	11.9	15.0	8.9*	68	92*	32	5.2	NW	0.03	452.0
	10	X				15.7	21.7	9.4	46	72	30*	12.5	SE	0	627.2
	11	X	X		X	12.7	16.7	10.0	78	96	49		NE		140.1
	12					6.7	9.4	6.1*	85	91*	78*				596.0
	13					6.9	7.8	6.1*	88	90*	83*				
	14					11.1	14.4	6.7	76	90*	63				
	15					13.9	16.7	9.4	50	89	37*				
	16					8.6	9.4	8.3	87	91*	68	11.4		5.62	648.9
	17					10.1	13.3	8.3	64	91*	41				
	18					6.0	10.0	4.4*	85	91*	79*				
	19					9.8	14.4	5.6*	62	89*	77*				
	20					6.4	11.1	2.2*	71	89	43				
	21					5.2	8.9	2.8*	72	90	46				
	22	X	X			8.9	12.8	3.9*	78	92*	59	7.3	SE	0.64	349.1
	23	X				14.5	19.4	9.4*	65	92*	46	7.4	SE	0	526.7
	24	X				21.1	25.6	14.4	48	82	30		SW	0	373.5
	25	X				22.8	26.7	18.3*	49	65*	32*			0	503.7
	26	X	X			23.9	26.7	18.9*	48	60*	35*	12.3		0	547.5
	27	X				19.9	21.7	14.4*	50	80*	42			0	560.8
	28	X	X			18.1	22.8	13.3*	69	92	45 -	9.0	SE	0.88	527.0
	29	X	X		X	18.1	23.3	14.4	65	94*	49*	9.5	SE	0.69	411.8
	30	X				19.5	18.9	12.8*	61	96*	43*	20.3	NW	0	471.1
	31	X				14.1	15.6	11.7	70	84	53	9.6	SE	0	493.3
Aug.	1	X				15.1	18.3	10.0*	52	80	36*	17.8	NW	0	571.9
	2	X				15.2	19.4	8.9	48	72	29*	8.7	SE	0	530.8
	3	X	X			16.7	18.3	12.2*	62	78	53*	8.1	SE	0.34	454.3
	4				X	12.9	15.6	12.2*	79	92*	66*	6.9	NW	0	236.9
	5	X			X	13.2	18.9*	7.2*	60	96*	49	8.4	SE	0.07	458.4
	6	X	X			15.9	17.8	13.3	58	90	40	20.8	NW	0.05	508.6
	7	X			X	13.5	16.7*	8.9*	64	93	45	19.1	NW	0.69	329.0
	8		X		X	8.1	8.9*	7.2*	89	94*	82*	6.8	NW	0.01	173.2
	9	X	X			12.2	15.0	7.8*	64	94*	42*	24.4	W	tr	344.8
	10	X	X			12.3	15.0	11.1*	62	92	53	16.0	WNW	0.07	294.7
	11	X	X			9.7	11.1*	7.2*	72	92*	54	10.1	SW	0.03	393.3
	12		X		X	7.1	7.8	6.1*	92	95*	83	9.1	NW	1.03	128.0
	13	X	X	X	X	4.8	7.8	7.9*	82	92*	60	14.1	NW	0.03	273.9
	14	X	X	X	X	3.2	5.0*	1.1*	78	92	60	14.2	NW	0.02	275.2
	15		X			3.6	6.7*	1.1*	69	90*	49*	6.0	NW	0.02	405.6
	16		X			6.9	12.2*	0.0*	60	94	36*	10.3	SE	0	428.5
	17	X	X	X		10.6	15.0	5.6*	44	62	34*	-	WNW	-	399.9
	18		X		X	11.1	11.7*	10.0	55	95*	54*	-	NW	-	-
	19		X		X								NNE		

TABLE 7   SOME PLANT SPECIES ASSOCIATED WITH SNOWBEDS

(Key: Hulten, 1968)

Achillea borealis Bong.
Aconitum delphinifolium DC. subsp. delphinifolium
Anemone narcissiflora L. subsp. interior Hult.
Anemone Richardsonii Hook.
Antennaria monocephala DC. subsp. monocephala
Arctagrostis latifolia (R.Br.) Griseb. var. latifolia
Arctostaphylos alpina (L.) Sprong. (snowpatch or tundra)
Arnica Lessingii Greene subsp. Lessingii
Artemesia artica Less. subsp. arctica
Artemesia Tilesii Ledeb. subsp. Tilesii
Betula glandulosa Michx.
Calamagrostis canadensis (Michx.) Beauv. subsp. canadensis
Carex aquatilus Wahlenb. subsp. aquatilus
Carex lachenalii Schkuhr.
Carex podocarpa C.B. Clarke
Cassiope tetragona (L.) D. Don subsp. tetragona (snowpatch)
Castilleja Raupii Pennell.
Dodocatheon frigidum Cham. & Schlecht.
Empetrum nigrum L. subsp. hermaphroditum (Lange) Böcher
(snowbed, snowpatch and tundra)
Epilobium angustifolium L. subsp. angustifolium
Equisetum arvense L. (snowbed, snowpatch and tundra)
Eriophorum angustifolium Honck. subsp. subarcticum (Vassiljev) Hult.
Eriophorum Scheuchzerii Hoppe var. tenuifolium Ohwi(snowpatch and snowbed)
Festuca altaica Trin.
Ledum palustre L. subsp. decumbens (Ait.) Hult. (snowbed, snowpatch and
     tundra)
Loiseleuria procumbens (L.) Desv. (snowbed, snowpatch and tundra)
Lupinus arcticus S. Wats. (snowpatch and tundra)
Luzula confusa Lindeb.
Myosotis alpestris F.W. Schmidt subsp. asiatica Vestergi
Oxyria digyna (L.) Hill
Parnassia Kotzebuei Cham. & Schlecht.
Pedicularis Kanei Durand subsp. Kanei (snowpatch or tundra)
Pedicularis sudetica Willd. subsp. interior Hult.
Petasites frigidus (L.) Franch.
Poa arctica R. Br. subsp. arctica
Polemonium acutiflorum Willd.
Polygonum bistorta L. subsp. plumosum (Small) Hult.
Polygonum viviparum L.
Ranunculus nivalis L.
Ranunculus pygmaeus Wahlenb. subsp. pygmaeus
Ranunculus Turneri Greene
Rubes chamaemorus L. (snowpatch or tundra)
Rumex arcticus Trautv.
Salix Chamissonis Anderss.
Salix polaris Wahlenb. subsp. pseudopolaris (Flod.) Hult.

Salix pulchra Cham.
Salix reticulata L. subsp. reticulata (snowpatch and tundra)
Saussaurea angustifolia (Willd.) DC (snowpatch and tundra)
Saxifraga punctata L. subsp. Nelsoniana (D. Don) Hult.
Senecio lugens Richards.
Spiraea Beauverdiana Schneid.
Stellaria longipes Goldie
Taraxacum alaskanum Rydb.
Trisetum spicatum (L.) Richter subsp. spicatum
Vaccinium uliginosum L. subsp. alpinum (Bigel.) Hult. (snowbed,
    snowpatch and tundra)
Vaccinium vitis-idaea L. subsp. minus (Lodd.) Hult. (snowbed,
    snowpatch and tundra)
Valeriana capitata Pall. (snowpatch and tundra)
Viola epipsila Ledeb. subsp. repens (Turcz.) Becker

* Not all these species are confined to snowbeds only.

APPENDIX - 2

PICTURES

PICTURE FA1 - CANOE LAKE AREA - June 7, 1973 - SW OF SKYLINE RIDGE

PICTURE FA2 - CANOE LAKE - July 11, 1973 - LICHEN RIDGE

PICTURE F1 – SHINGLE POINT – July 17, 1973 – SNOWBEDS ALONG COAST

PICTURE F2 – SHINGLE POINT – July 19, 1973 – SNOWBEDS ALONG COAST

PICTURE F3 – SHINGLE POINT – July 18, 1973 – SNOWBED NEAR WALKING RIVER

PICTURE F4 – SHINGLE POINT – July 19, 1973 – SNOWBED NEAR BLOW RIVER

PICTURE A1 – SNOWBED *1
July 28, 1973

KEY (applying also to Pictures A2, A3 and A4)

B – Upper Birch
C – Upper Willows
D – Upper Meadow
E – Upper Late Melt Area
F – Lower Late Melt Area
G – Lower Meadow
H – Lower Salix Cham. area
I – Lower Willows
x – 5 foot, 5 inch high field assistant
y – 270 cm high pole

PICTURE A2 - SNOWBED *1, August 13, 1973. CD PROFILE LINE.

PICTURE A3 - SNOWBED *1, July 28, 1973

PICTURE A4 - SNOWBED *1, July 28, 1973
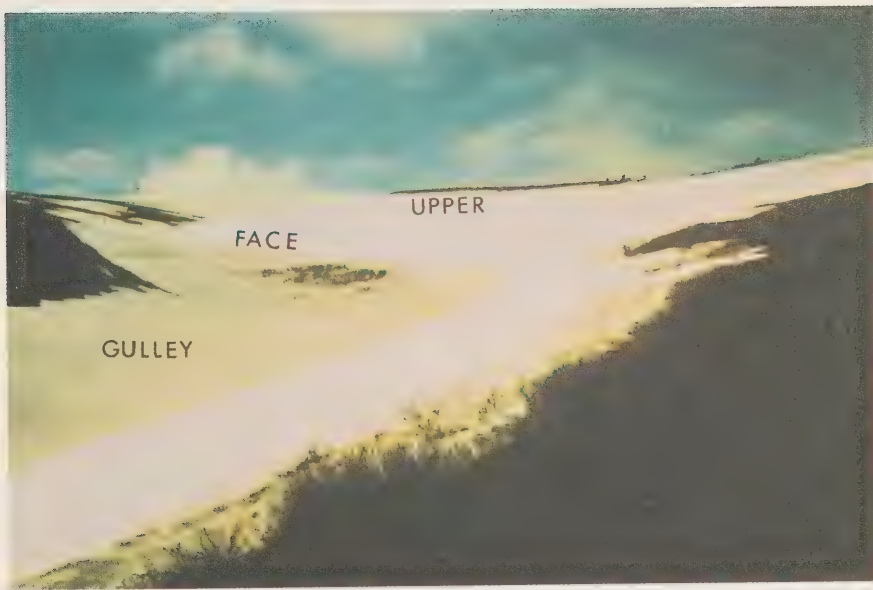
PICTURE C1 - SNOWBED *1, May 24, 1973
FEATURES OF THE DRIFT FORMING SNOWBED *1

PICTURE D1 - SNOWBED *1, May 30, 1973
CREEK ERODING BOTTOM SLOPE OF SNOWBED

PICTURE D2 - SNOWBED *1, June 21, 1973
GULLEY CUT THROUGH SNOWBED BY CREEK
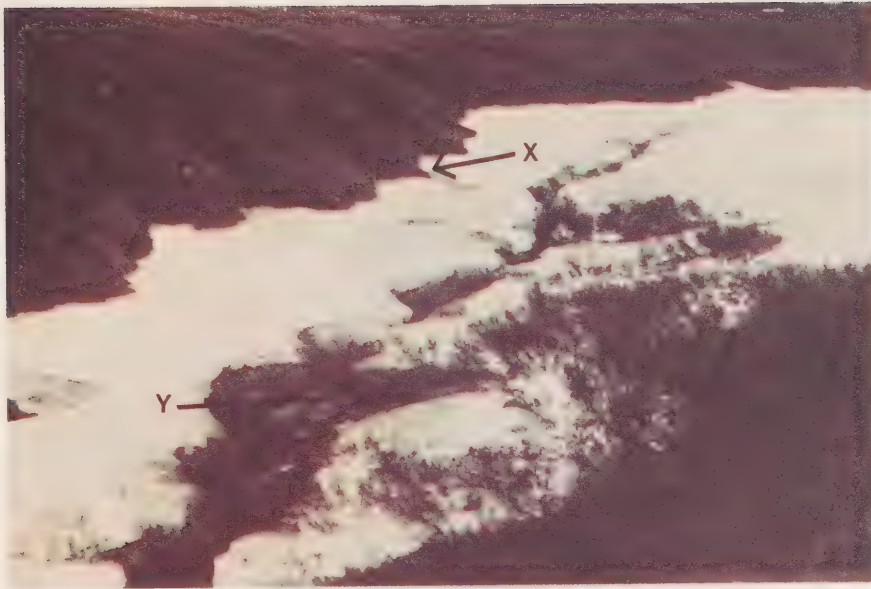
PICTURE E1 - SNOWBED *1, June 6, 1973
Minor mud slide (x), NW facing bank of Snowbed *1
Exit of underground stream (y)

PICTURE E2 - SHINGLE POINT, YUKON, July 19, 1973
Unstable areas associated with late snowbeds
Cracks in ground and sliding blocks of vegetation (x)

Progress of Hydrologic Studies at
Boot Creek and Peter Lake Watersheds,
N.W.T., during 1973

by

J.C. Anderson and D.K. Mackay

Glaciology Division
Water Resources Branch
Department of the Enviroment

under the

Environmental-Social Program
Northern Pipleines

CONTENT

LIST OF TABLES

LIST OF FIGURES

ABSTRACT

        Two small drainage basins in the Mackenzie Delta
region, N.W.T. are under study to obtain hydrologic data needed
for assessment of pipeline and highway designs, and to determine
water supply conditions. Each basin is instrumented during the
summer field season to measure precipitation, runoff and latent
evaporation. Results for 1973 are presented, and comparisons with
former year's findings are made. Precipitation is observed to be
light, the annual normal for Inuvik being 285 mm. Maximum runoff
typically occurs during the spring snowmelt period. A peak discharge
of 0.22 $m^3/s/km^2$ was recorded at one of the basins in 1973. Direct
runoff following summer storms is minimal, less than 5% of precipitation.
Potential evapotranspiration for each basin for the period June to
September is estimated at 225 to 275 mm. Water balance calculations
for one of the basins have revealed a storage depletion of up to 115 mm
of water, for the period October 1, 1972 to September 30, 1973.

PROGRESS OF HYDROLOGIC STUDIES AT BOOT CREEK AND PETER LAKE WATERSHEDS
N.W.T., DURING 1973

J.C. Anderson and D.K. MacKay

INTRODUCTION

Hydrologic studies have been in progress at Boot Creek basin since 1967, and at Peter Lake basin since 1970. Figure 1 shows the location of these basins in the Mackenzie Delta region. Progress during the 1973 field season is discussed in this report. Preliminary results obtained from former years' data, as well as a general description of the basins, are to be found in an earlier report (Anderson and MacKay, 1973).

In 1973, the instrument networks were established basically as they had been in 1972. In addition, a second rain gauge was installed in a pit at the north end of Peter Lake, in order to perform an experiment on rain gauge catch efficiency. Also, the atmometer network was expanded slightly, and the 250 cm^3 atmometers were replaced with 500 cm^3 instruments, to overcome the difficulty of reservoirs running dry between instrument readings. Analysis of data collected in 1973 at the two basins has improved our knowlege of water budget components in the Delta region.

PRECIPITATION

Annual precipitation is light in the Delta region, and decreases northward toward the coast of the Beaufort Sea. Rain is the dominant form of precipitation from June through September. Snow predominates for the

remainder of the year. Annual precipitation normals for Inuvik and Tuktoyaktuk are listed in Table 1.

During the summer field season, precipitation is measured at each basin in two locations, using M.S.C. tipping bucket rain gauges. Precipitation data collected by the Atmospheric Environment Service (AES) at Inuvik airport, 6 km south of Boot Creek basin, are used to supplement the records of the latter basin. Monthly precipitation totals obtained at Boot Creek have been in good agreement with those recorded at the airport in recent years (Anderson and MacKay, 1973, p. 48).

No AES weather observing stations are located close enough to Peter Lake to be of any use in extrapolating records for that basin. However, the summer data that are available for Peter Lake suggest that precipitation during that season is normally slightly less there than at Boot Creek (Table 2).

It is noteworthy that monthly precipitation can vary considerably about the mean (Table 2). For example, in 1971, only 14% of the mean May and 35% of the mean June precipitation fell at Inuvik. The following October, 230% of the normal monthly precipitation occurred. In 1973 at Inuvik, 4 months were above normal in precipitation, 8 were below normal, and the year itself was below normal by 20%.

RUNOFF

Peak runoff for the year at Boot Creek and Peter Lake watersheds occurs in the spring, with the melting of the snow pack. The pack normally reaches its maximum water equivalent in early May, following a winter snow accumulation period which can last as long as seven months.

Snowmelt runoff occurs in late May and early June, over a period of two to four weeks. Permafrost and seasonal frost beneath the snowpack act as a barrier to infiltration of the melt water, and a large percentage of the snowmelt contributes directly to runoff.

The 1973 snowmelt flood at Boot Creek peaked on May 27, at a measured flow of 6.9 m^3/s (245 cfs) or 0.22 m^3/s/km^2 (20 cfs/mi^2) (Figure 2). As discharge was not being recorded continuously at the time, the maximum flow could have been still greater. The peak flood came in response to inputs of rain and heat. On May 25, 6 mm of rain fell at Inuvik. The 26th was the warmest day of the month, the maximum temperature being 22°C (71°F).

Other studies on basins of about the same areal extent as Boot Creek (31 km^2), particularly those in the high arctic, have revealed the spring snowmelt flood to be the major event of the year. At Weir River basin (area 29.4 km^2), on Ellesmere Island, the 1973 maximum unit area discharge was 0.17 m^3/s/km^2 (Ambler, 1974). At the Mecham River basin (area 78 km^2), on Cornwallis Island, a maximum unit area discharge in 1970 of 0.34 m^3/s/km^2 was recorded during the spring runoff (McCann, Howarth and Cogley, 1972, p. 69).

On May 1, 1973, the snowpack water equivalent at the Inuvik airport snow course was 140 mm. By June 10, Boot Creek basin was almost completely free of snow, and the flood had receded to 1 m^3/s (35 cfs). Neglecting all water storage sources except the snow pack, and adding to that the 44 mm of precipitation which occurred from May 1 until June 10, there were approximately 185 mm of water available for runoff, evapotranspiration and change in storage, during the snowmelt period. Through June 10, 155 mm of runoff were measured, or 85% of the "available"

water. This high percentage is consistent with findings in other arctic watersheds underlain by permafrost (for example, Brown, Dingman and Lewellan, 1968, p. 13: concerning a small watershed on the Alaskan coastal plain).

No measurements of peak snowmelt runoff at Peter Lake are available to date. However, the hydrographs illustrate that spring snowmelt produces the most significant runoff of the year (Figure 4). Maximum recorded discharge at the basin is 2.4 m^3/s (84 cfs), or 0.05 m^3/s/km^2 (4.7 cfs/mi^2) on June 12, 1973, during the snowmelt flood recession.

A secondary maximum of runoff commonly occurs at these basins in August (Figures 2, 3, 4). Runoff increases noticeably following storms of a magnitude that bring little or no runoff response in June and July. Compare, for example, the marked increase in runoff following the storms of August 8 and 22, 1973 at Boot Creek basin, with the lack of response to the storm of July 13, 1973 (Figure 2). In the month of August, there is normally a trend toward cooler and wetter weather in the Delta region, with a consequent decline in the rate of evapotranspiration. It is hypothesized that the increased runoff in August is primarily due to a rise in base flow. This is thought to result from a greater availability of soil moisture, which itself is a response to the decline in the rate of evapotranspiration.

Elsewhere (Anderson and MacKay, 1973, p. 54), mention has been made of the meager response of these basins to storms, in the form of direct runoff. Ratios of direct runoff to precipitation are typically 0.05 or less. Analysis of midsummer storms is continuing. Plots of the logarithm of discharge versus time for storms at Boot Creek yield a recession limb with a change in slope, the change likely reflecting a

shift from base flow plus interflow (direct runoff negligible) to base flow only. These recessions can be defined mathematically as follows:

$$Q_t = Q_o K^{-t} \qquad (1)$$

$$Q_t = Q_o \exp(-t/t^*). \qquad (2)$$

Q_t is the discharge at time t, Q_o is the discharge at time $t = o$, K is the recession constant, and t^* is a decay constant. For the interflow plus base flow portion of the recession, K has varied from 1.26 to 1.48, and t^* from 61 to 105 hours, or 2.0 to 3.4 hr/km^2 for midsummer Boot Creek storms. For the ensuing base flow recession, K has been 1.05 to 1.10, and t^*, 247 to 497 hours, or 8.0 to 16 hr/km^2. At Glenn Creek, Alaska (basin area of 1.8 km^2), t^* was observed to be of the same order of magnitude, varying between 10.9 and 42.4 hr/km^2 (Dingman, 1973, p. 449).

EVAPOTRANSPIRATION

"Latent evaporation" is measured with 500 cm^3 black porous disc atmometers, in order to determine the "drying ability of the meteorological environment" (Robertson and Holmes, 1958, p. 399). Analysis of atmometer data from several stations across Canada has revealed the relationship:

$$PE = 0.086(LE)$$

where PE is the potential evapotranspiration (mm) and LE is the latent evaporation (cm^3) (Roberston and Holmes, 1958, p. 406). Using this conversion factor, the potential evapotranspiration near Cynthia Lake in Boot Creek basin for the period June 19 to September 21, 1973 was 186 mm. Near the south end of Peter Lake, the potential evapotranspiration from

June 12 until September 23 totalled 238 mm. For the period June 1 to
September 30, respective totals for the two basins were likely in the
neighbourhood of 225 and 275 mm.

No class A evaporation pan data are available for Inuvik for
comparison. However, estimates of mean small lake evaporation have been
made for Canada (Ferguson, O'Neill and Cork, 1970), and at Inuvik, the
total for June to September inclusive is 175 mm. These estimates are
thought to provide a "useful index of potential evapotranspiration"
(Ferguson, O'Neill and Cork, p. 1631). Note that the mean small lake
evaporation is only in fair agreement with the 1973 atmometer data.

THE WATER BALANCE

For the 12-month period October 1, 1972, to September 30, 1973,
an estimate of the water balance at Boot Creek has been derived.
Precipitation at the basin, as supplemented by data from Inuvik airport,
totalled 285 mm. (equal to the mean for 1961-70 for Inuvik). Runoff,
from the beginning of snowmelt in May, 1973 until September 21 amounted
to 210 mm. Runoff was not measured in October, 1972, prior to freeze-up,
or in late September, 1973, but the total for those missing periods would
have been small by comparison, as runoff is of low magnitude late in the
fall.

If the assumption of zero storage change is made for the 12-month
interval, then actual evapotranspiration is at most 75 mm. This is
probably too small a value. Snow sublimation could be at least 40 mm
for the winter of 1972-73, and evapotranspiration for the summer of 1973
might be 150 mm or more (letter dated March 5, 1974 from G. R. Holecek, Hydro-
logy Branch, Department of Environment, Alberta, 10040 - 104 Street, Edmonton). On

this basis, the total runoff, snow sublimation and evapotranspiration would be at least 400 mm. Assuming the precipitation total to be correct, a storage depletion of the order of 115 mm would have to have occurred at Boot Creek basin.

It is possible, however, that the precipitation total may be inaccurate. Precipitation gauge deficiencies that cause undermeasurement are known to occur, particularly when high winds accompany the precipitation, and especially if the precipitation is in the form of snow. (See, for example, Rodda, 1971). The more important gauge deficiencies, turbulence and eddies caused by the gauge itself, can be overcome by putting the receptacle into a conical pit, in such a manner that the top of the instrument is at the same level as the ground surface. A comparison between the precipitation catch of a tipping bucket rain gauge located in a pit, and the catch of an identical gauge located on level ground nearby, was made at Peter Lake in the summer of 1973. The experiment revealed that over a 3-month period, the pit gauge caught 15% more rain-fall than its counterpart. It is conceivable that undermeasurement of precipitation of the same order of magnitude could be occurring at Inuvik the year round, especially when it is realized that more than half of the annual precipitation normally falls as snow there. On the assumption of a 15% error in measurement, precipitation at Boot Creek basin for the year October 1, 1972, to September 30, 1973 would be 328 mm, and storage depletion would then be 72 mm.

CONCLUSIONS

Precipitation in the vicinity of Inuvik is normally light, averaging about 285 mm annually. In 1973, the total was 20% below normal.

Peak runoff of 6.9 m³/s occurred during the snowmelt runoff period in 1973 at Boot Creek. This was by far the greatest runoff of the year. A secondary maximum occurred in August, as base flow increased. Direct runoff response to midsummer storms continued to be minimal, constituting less than 5% of precipitation for major storms. Long recessions with large decay constants were noted for those storms.

Potential evapotranspiration for the period June to September, 1973 has been estimated at 225 to 275 mm for the basins studied. Water balance calculations for Boot Creek basin revealed a storage depletion of as much as 115 mm for the period October 1, 1972 to September 30, 1973. However, if precipitation was being undermeasured, this depletion would be considerably less.

IMPLICATIONS FOR PIPELINE AND HIGHWAY DEVELOPMENT

Exploration for oil and gas in the Mackenzie Delta region is continuing. If sufficient reserves are found, pipelines may be constructed to transport those commodities to southern markets. Construction has already begun on the Mackenzie and Dempster highways in the Delta region.

In building these roads and pipelines, it is important that a proper assessment of the magnitude of hydrologic events be made. This is particularly so in the case of river crossings. Inadequate planning may result in spring wash-outs or winter icings, which would jeopardize the continuity of the transportation system. Analysis of data collected at Boot Creek and Peter Lake watersheds should prove of great value in predicting the magnitude of hydrologic events to be expected in the eastern portion of the Mackenzie Delta region. For example, the peak flow data collected during the 1973 snowmelt period are extremely useful for the planning of the size of culverts to be used along the local highways.

PLANS FOR FUTURE WORK

In addition to the program of data collection and analysis already underway, other projects are being planned. The spring snowmelt runoff peak has been identified as the most significant event of the annual hydrograph in the Mackenzie Delta region, and attention is to be focussed upon that event. Instrumentation has been installed in Boot Creek basin to study the ground and snowpack temperature regimes during snowmelt. Time and manpower permitting, measurement of the snowmelt flood will be extended to some larger drainage basins crossed by the Mackenzie Highway near Inuvik, in order to compare unit area discharges for drainage basins of various sizes.

A comparison of pit and regular tipping bucket rain gauges is to be continued at Peter Lake, and a similar experiment could be set up in Boot Creek basin. Representative values of gauge catch deficiency need to be established for these basins, in order to obtain better estimates of basin precipitation.

Soil temperature regimes are to be monitored on a gravel spit in Peter Lake, and on north- and south-facing slopes at Boot Creek basin. Readings of water temperature at the discharge measurement location in each basin will also be taken.

ACKNOWLEDGEMENT

REFERENCES

Ambler, D.C., 1974. "Runoff from a small arctic watershed". Presented at the Workshop Seminar on Permafrost-Hydrology and Geophysics, held in Calgary, Alberta, February 26-28, 1974.

Anderson, J.C., and D.K. MacKay, 1973. "Preliminary results from Boot Creek and Peter Lake watersheds, Mackenzie Delta region, N.W.T." pp. 33-70 in MacKay, D.K. et al, Hydrologic Aspects of Northern Pipeline Development, Environmental-Social Committee, Northern Pipelines, Report No. 73-3.

Brown, J., S.L. Dingman and R.I. Lewellan, 1968. "Hydrology of a drainage basin on the Alaskan coastal plain". CRREL Research Report 240, Hanover, N.H., 18 pp.

Dingman, S.L., 1973. "Effects of permafrost on stream flow character-istics in the discontinuous permafrost zone of central Alaska". pp. 447-453 in, Permafrost - Second International Conference (North American Contribution), National Academy of Sciences, Washington, D.C.

Ferguson, H.L., A.D.J. O'Neill and H.F. Cork, 1970. "Mean evaporation over Canada." Water Resources Research, Vol. 6, No. 6, pp. 1618-1633.

Holecek, G.R., 1974. Personal Communication.

McCann, S.B., P.J. Howarth and J.G. Cogley, 1972. "Fluvial processes in a periglacial environment." Transactions of the Institute of British Geographers, No. 55 pp. 66-82.

Robertson, G.W. and R.M. Holmes, 1958. "A new concept of the measurement of evaporation for climatic purposes". Int. Assoc. of Sci. Hyd., General Assembly of Toronto, 1957, Pub. No. 43, Vol. III, pp. 399-406.

Rodda, J.C., 1971. "The precipitation measurement paradox - the instrument accuracy problem." World Meterological Organization, WMO/IHD Report No. 16.

Table 1   Annual precipitation normals for Inuvik and Tuktoyaktuk,
for the period 1961-70.

	Inuvik (mm)	Tuktoyaktuk (mm)
Total precipitation	285	137
Rain	123	80
Snow (water equivalent)	162	57
Snow (depth when newly fallen)	1840	570

Table 2   Monthly precipitation totals for Boot Creek basin and Peter Lake
basin (where available)*

	Inuvik Airport Normals 1961-70 (mm)	Boot Creek and, in parenthesis, Peter Lake (mm)		
		1970	1971	1972	1973
JAN	19	7	10	14	24
FEB	13	9	14	12	4
MAR	15	9	7	15	10
APR	15	10	9	28	9
MAY	21	15	3	15	36
JUN	23	27	8	44	28
JUL	40	28	27(25)	12	42(34)
AUG	54	59	40	36(33)	33(32)
SEP	19	39	19	37	4
OCT	32	43	74	39	20
NOV	15	15	19	21	14
DEC	21	18	14	36	6
ANNUAL	285	281	244	309	230

*Boot Creek data supplemented by Inuvik airport data
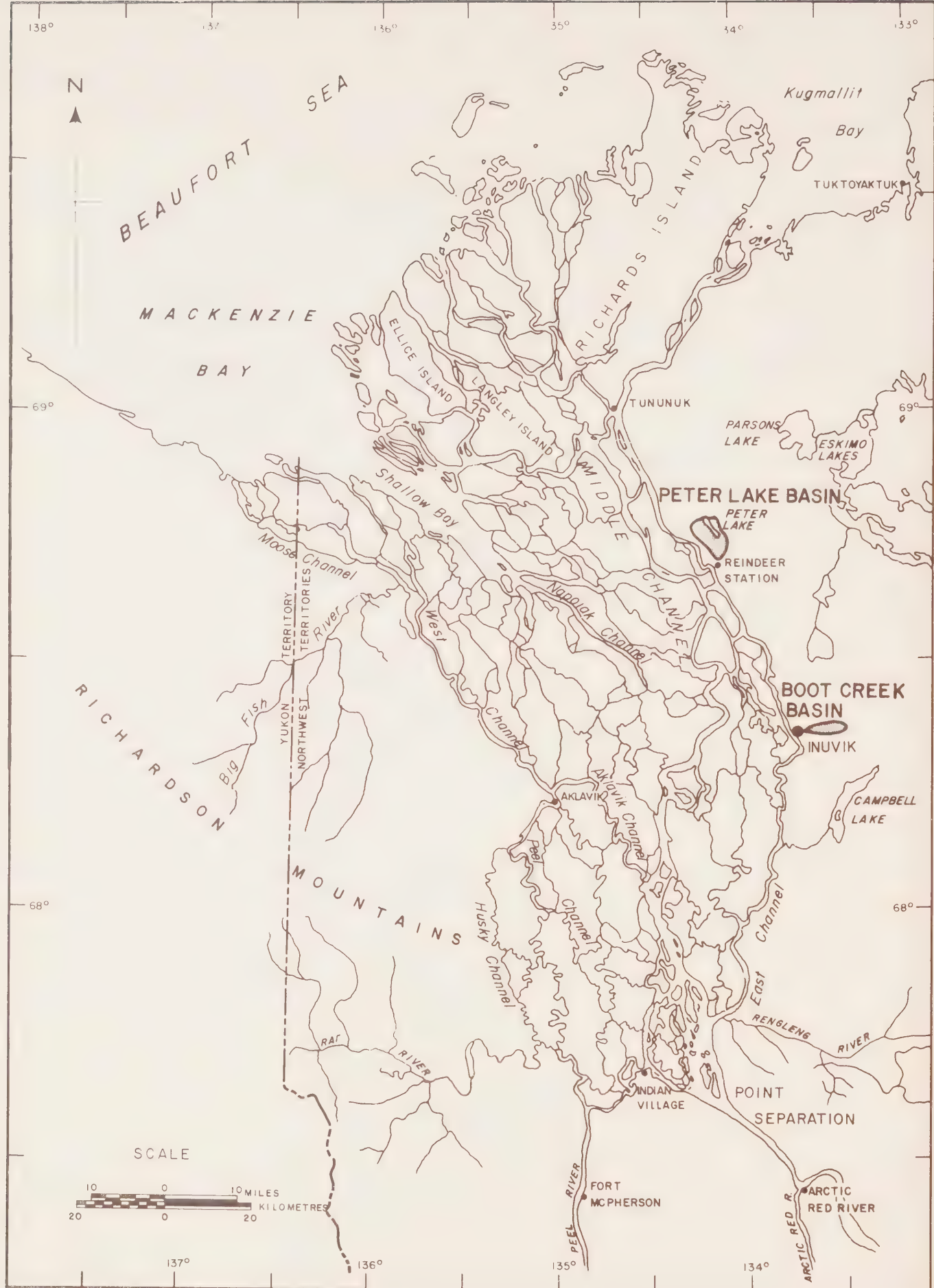
Figure 1. Location of Boot Creek and Peter Lake basins, N.W.T.
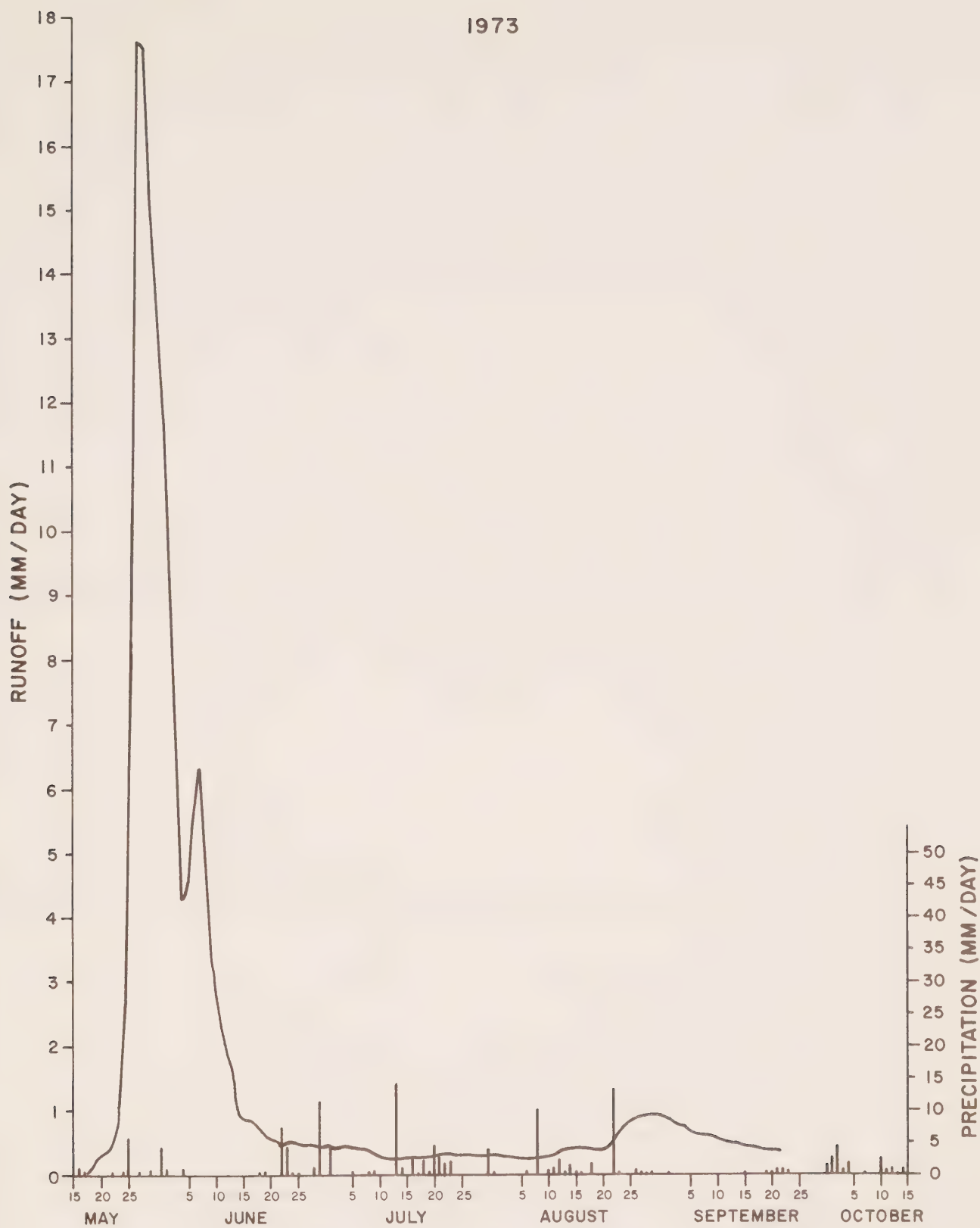
Figure 2. Runoff and precipitation at Boot Creek basin, 1973.
(Precipitation data supplemented by Inuvik airport data).
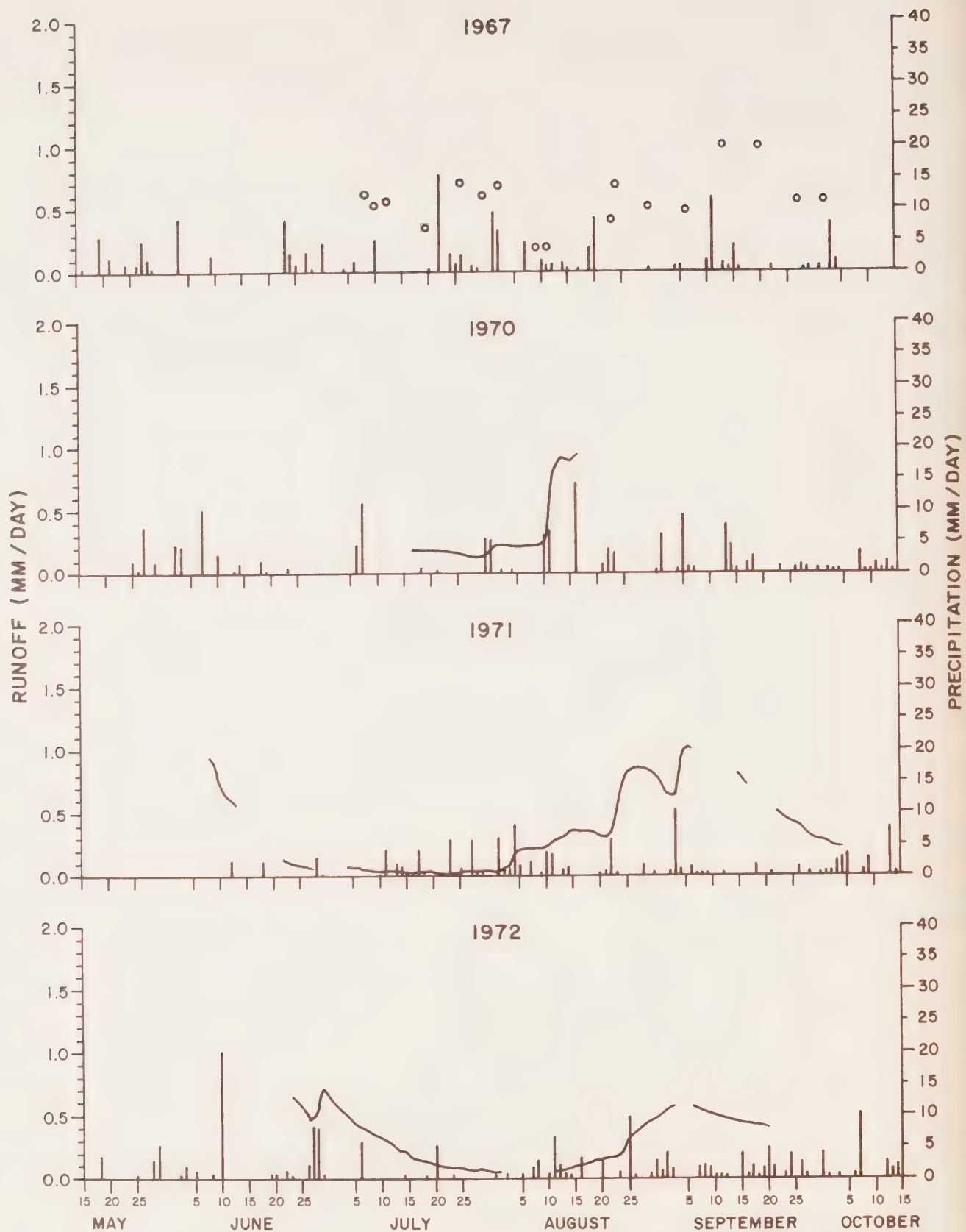
Figure 3. Runoff and precipitation at Book Creek basin, 1967, 1970, 1971, 1972. (Precipitation data supplemented by Inuvik airport data).
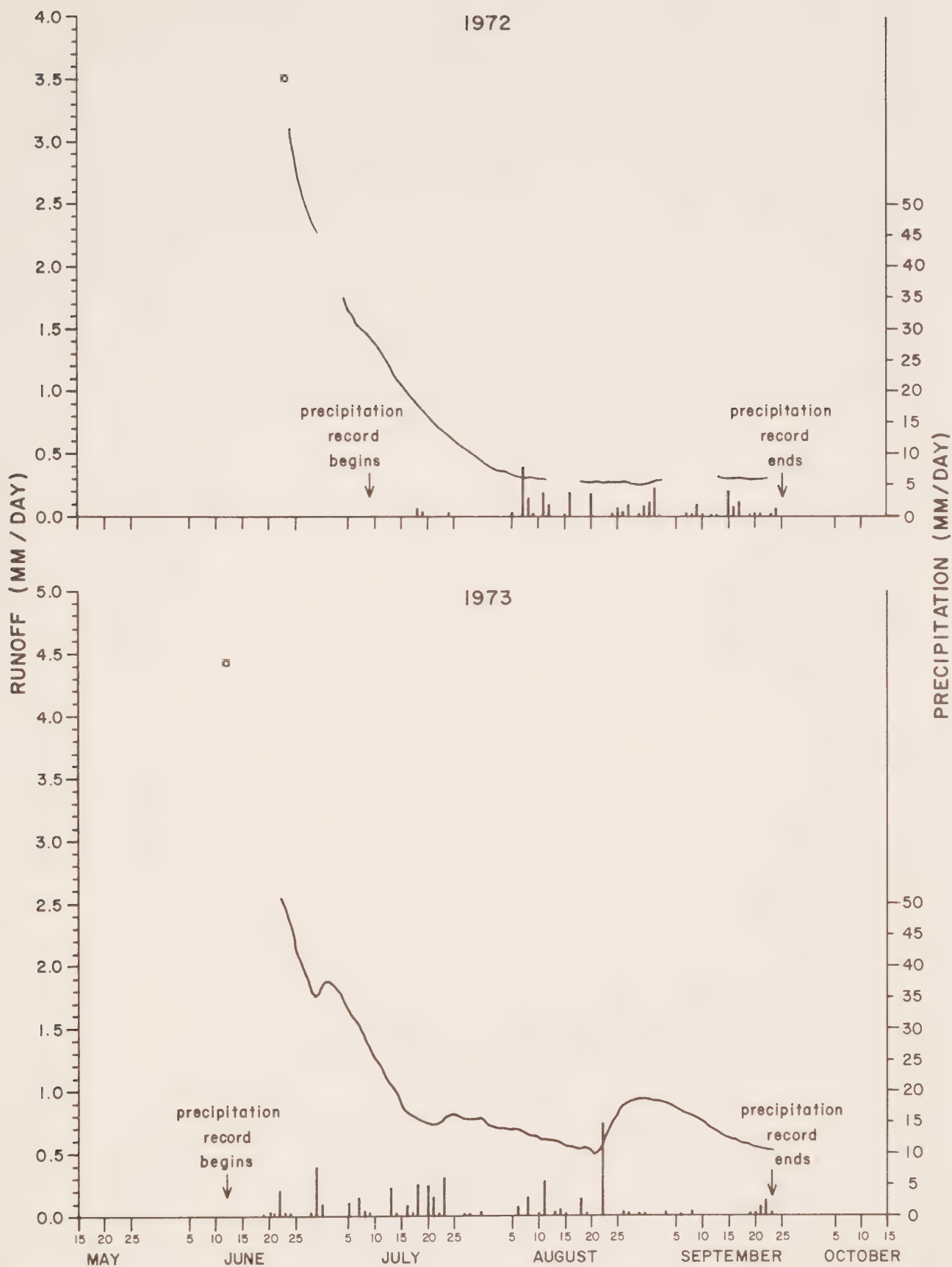
Figure 4. Runoff and precipitation at Peter Lake basin, 1972, 1973. (Circles designate runoff data estimated from a single discharge measurement).

Progress Report On

Winter Distribution Of Flow In

The Mackenzie Delta, N.W.T.

By

J.C. Anderson and R.J. Anderson

CONTENTS

LIST OF FIGURES

LIST OF TABLES

APPENDICES

ABSTRACT

A hydrometric study is in progress in the Mackenzie
Delta, N.W.T., to determine the discharge and seasonal distri-
bution of flow through the delta, hydraulic geometry relation-
ships in delta channels, water and ice levels, ice thicknesses,
and the causes of delta flooding. A network of 28 stations to
measure discharge has been established in the delta region.
Results of the flow distribution program for three successive
winters are presented. At the time of measurement (March), the
Middle Channel carried most of the inflow to the delta. More
than 80% remained in the Middle Channel as far downstream as a
site west of Inuvik, and more than 55% at a site west of Reindeer
Station. Below the latter section, flow was dispersed, into major
distributaries branching away from the Middle Channel. Delta
discharge (expressed as a percentage of total inflow to the
delta) entered the Arctic Ocean via the following routes:
Shallow Bay -- 33 to 62%; Mackenzie Bay, east of Shallow Bay --
4 to 28%; Kugmallit Bay -- 25 to 35%. Ice thicknesses, obtained
during the winter flow program, have varied from 0.7 to 1.6 m
for individual cross sections. Mean ice thickness at all sites
has been 1.0 to 1.2 m.

PROGRESS REPORT ON
WINTER DISTRIBUTION OF FLOW IN
THE MACKENZIE DELTA, N.W.T.

by

J.C. ANDERSON and R.J. ANDERSON

INTRODUCTION

In co-operation with Water Survey of Canada, a hydrometric
study is being conducted in the Mackenzie Delta, N.W.T., to determine:

(1) the discharge and seasonal distribution of flow
     through the delta;

(2) the hydraulic geometry equations which pertain to flow
     during the open water season;

(3) variations in water levels, ice levels, and ice thicknesses
     on major delta channels;

(4) the causes of flooding in the delta.

Since publication of a preliminary report (Anderson and
MacKay, 1973), research has been focused on the winter (March) dis-
tribution of flow. Results of this program to date are presented
in this report.

THE FLOW MEASUREMENT NETWORK

The network of discharge measuring stations is shown in
Figure 1, and a list of station names appears as Appendix I.
Table 1 outlines the format used to estimate flow at various
sections across the delta.

The amount of water which enters the Mackenzie Delta in winter is considered to be the sum of contributions from the Peel, Arctic Red and Mackenzie Rivers. Discharge from smaller streams such as the Rat and Rengleng Rivers is assumed negligible during the winter season. Section U-U (Figure 1) represents delta inflow.

Within the delta, discharge measurements are made on the main channels crossing various sections of the delta. Totals for the cross-sections V-V, W-W, and X-X + Y-Y are calculated as a check on the conservation of flow. Several smaller channels are omitted from the measurement program. Flow, if any, contributed by them across a section is estimated by subtracting measured output along the next downstream section from input above the section in question.

Neglecting time lags, the flow across sections U-U, V-V, W-W and X-X + Y-Y at any one time should be approximately equal during the winter season, owing to the relatively static flow condition of the input rivers. However, the length of the measurement program (usually about two weeks) introduces a time lag. Also, the severity of winter weather conditions can reduce the accuracy of discharge measurements made in winter over those taken during the summer. For these reasons, some discrepancies in flow can be expected to occur.

THE MARCH FLOW DISTRIBUTION

Three winters' data are now available for comparison. A full data listing is provided as Appendix II. Discharge data

for the three years are compared in Tables 2 and 3.

Flow into Delta - Section U-U

At the time of measurement, inflow to the delta was higher by 61% in 1973 and 27% in 1974 than in 1972. This flow variation is dependent upon conditions upstream in the Mackenzie basin, and no attempt is made here to explain it. As would be expected, the Mackenzie River is the largest by far of the three measured contributing sources, supplying between 97.0 and 98.4% of total flow.

Flow at Station A

Station A is on a delta channel that links the Peel Channel with a branch of the Mackenzie, near Point Separation. Reversals of flow are known to occur along this waterway. Discharge rates obtained by actual measurement at A are listed in Table 2. In 1972, no flow was recorded, but an overflow of water onto the ice surface occurred, suggesting a pressure build-up behind an ice blockage in the channel. If flow at A is calculated using the method of Table 1, negative values result (1973: -41 m^3/s; 1974: -32 m^3/s). This implies an inflow from the Mackenzie to the Peel Channel.

Flow in Middle Channel at V_1

Discharge at this location in the Middle Channel is assumed to be equal to that not measured elsewhere along V-V. With only minor possible exception, this is true. Note that between 96.0 and 97.5% of total inflow remains in the Middle Channel as

far as V_1, at the time of measurement (Table 2).

Flow Across Section V-V

Very favourable results are observed in a comparison of flow across V-V with that across U-U. Over the three seasons, the maximum deviation at Section V-V from total inflow is only 0.4%.

Flow at W_1

This represents the discharge which remains unmeasured across that portion of Section W-W lying westward of Y-Y. To obtain it, outflow along the West Channel (station 11) is subtracted from inflow of the Peel, Pokiak and Aklavik Channels (stations 9, 10 and 12). The 1974 estimate, calculated as above, was -48.5 m^3/s. This result is assumed due to measurement error, and flow at W_1 in 1974 has been set at 0 m^3/s.

Flow Across Section W-W

Discharge to the east of Y-Y across Section W-W is all accounted for in measurements, and flow across W-W follows as noted in Table 1. Comparison of total discharge between Sections V-V and W-W shows a loss of water in 1972 and 1973 of 15% and 8%, and a gain in 1974 of 5%.

Flow at X_1

This is the residual of discharge not measured across Section X-X. It accounted for 3% of total inflow in 1973, and 4% in 1974.

Flow Across Section X-X

Discharge along this section enters Shallow Bay from the west and south. The quantity has varied between 2 and 6% of total inflow.

Flow at Y_1

This represents unmeasured flow across Y-Y. In 1972 and 1974, it was 4 and 5% of total inflow, respectively. In 1973, when inflow was greatest, the corresponding value for Y_1 was 26%. The smaller channels crossing Y-Y were obviously playing a more important role in flow distribution in 1973. Lower ice thicknesses (to be mentioned later) were probably an important cause of this occurrence, in addition to greater inflow.

Flow Across Section Y-Y

The Middle Channel is by far the major contributor of flow across this section. More than 80% of total inflow has been measured each year at station 18, and more than 55% at station 20.

Summation of flow across Sections X-X and Y-Y represents a complete flow section across the delta. Discharge at this point in the delta was found to be less than total inflow in 1972 and 1973, but more in 1974.

Flow at Z_1

All main channels crossing ZZ are accounted for with

the exception of one (Z_1). In 1973, when flow Y_1 was significant, Z_1 was only 3% of total inflow. In 1972 and 1974, the reverse situation existed, with Z_1 accounting for 19% and 27% of the total inflow.

Flow Across Section Z-Z

Most of the water crossing this section is supplied by the Middle Channel; flow in the East Channel at and above station 21 is minor by comparison. Near Tununuk, the flow is distributed westward into Shallow Bay via Reindeer Channel, northwestward into Mackenzie Bay, and northeastward via the East Channel into Kugmallit Bay.

Kugmallit Bay has received between 25 and 35% of total delta inflow during the periods of investigation in March. Discharge into Mackenzie Bay, eastward of Ellice Island, has accounted for 20, 4 and 28% of the total inflow in three successive years. The remainder has entered Mackenzie Bay via Shallow Bay. Percentages of total inflow to the latter are: 1972 - 33%; 1973 - 62%; 1974 - 43%.

ICE COVER

Ice Thickness

Ice thickness data obtained in conjunction with discharge measurements are listed in Table 4. As would be expected, thickest ice occurs at the more northerly stations. A major reason for this is that the snowfall and snow cover decrease northward toward the arctic coast. Snowfall normals for Ft. McPherson, Inuvik and

Tuktoyaktuk illustrate this (Table 5). A heavy snow cover insulates
the ice below it from extremely low air temperatures, and consequently
ice accretion takes place at a slower rate.

Other important parameters that affect ice depth include
channel width and the orientation of channels with respect to
prevailing winds. Narrow channels are better protected from the
wind by the proximity of their banks. This reduces the amount of
snow redistribution, and a thick snow cover can develop. Such
is the case at channel Sections 4 and 5 in the south end of the
delta, and at Sections 17 and 19 near Inuvik, among others. Wider
channels, where they are oriented parallel to the prevailing wind,
can be swept clean of snow along some sections. Broad stretches
of snow-free ice were observed on the East Channel below Reindeer
Depot and on the West Channel below Aklavik, in 1974.

Ice was generally thicker in 1972 and 1974 than in 1973.
Temperatures were only slightly below normal through the winter
prior to March 1972 (Table 5), but snowfall was less than normal
at Ft. McPherson. At Inuvik, a snowfall anomaly of 118 cm
occurred in October, 1971. Much of it fell before the ice formed
on delta channels. Thus, the October snowfall did not affect ice
accretion later in the winter. Snowfall was close to normal
for the remainder of the winter at Inuvik.

The winter of 1972-1973 was above normal temperature-wise
in the delta region, and above normal for snowfall at Inuvik and
Tuktoyaktuk. As a result, ice was thinner, the mean depth being

0.2 m less than for the previous winter.

Ice thicknesses in 1974 were similar to those of March, 1972. This was apparently a result of low snowfall during previous months. Ft. McPherson, in particular, received only 42% of its normal fall for the period September to February.

Other Ice Properties

Overflows of water onto the ice surface, which happened in March, 1972, and which were caused by blockage or restriction of flow due to ice, did not occur in the next two seasons. No slush or frazil ice was found beneath the ice cover in the delta, and no polynas were observed.

Rough ice was encountered on some larger channels. These were the last to freeze over in the fall, and they became the resting place for broken ice from upstream. Greatest difficulty with rough ice was encountered on the Middle Channel. Near Horseshoe Bend (site C), ice protruded at all angles to heights of two and three feet, and sometimes more.

CONCLUSIONS

Based upon 3 years of March flow data, the following conclusions are made:

(1) Flow entering the delta in March can vary considerably in magnitude. This is dependent upon upstream conditions. The Mackenzie River is the most important source, contributing 97.0 to 98.4% of total flow.

(2) The Middle Channel of the delta carries most of the
     winter flow. More than 80% of total inflow has been
     recorded as far downstream as station 18, each year.
     At station 20, near Reindeer Station, percentages
     of total inflow for the years 1972, 1973 and 1974
     were 78, 57 and 91, respectively.

(3) A small amount of water appears to be entering the
     Peel Channel from the Middle Channel near Point
     Separation. This was recorded in two of the three
     years, as was flow down the East Channel at stations
     B and 16.

(4) Outflow to the Arctic Ocean from the Mackenzie Delta
     is distributed in the following manner (expressed as
     percent of total inflow): Shallow Bay -- 33 to 62%;
     Mackenzie Bay east of Ellice Island to Richards Island
     Bay -- 25 to 35%.

(5) Ice thickness in the delta has varied between 0.7 and
     1.6 m. Mean ice depth at all sites has been between
     1.0 and 1.2 m.

(6) Overflows of water onto the ice are not common during
     drilling in March.

(7) No slush or frazil ice has been encountered beneath the
     ice cover. Rough ice is to be expected on the larger
     channels, especially the Middle Channel.

ACKNOWLEDGMENT

REFERENCES

Anderson, R.J. and D.K. MacKay, 1973. "Preliminary study of the seasonal distribution of flow in the Mackenzie Delta, Northwest Territories." pp. 71-109 in MacKay, D.K. et al, Hydrologic Aspects of Northern Pipeline Development, Environmental-Social Committee, Northern Pipelines. Information Canada, Cat. No. R27-172.

Burns, B.M., 1973. "The climate of the Mackenzie Valley - Beaufort Sea". Climatological Studies No. 24, Atmospheric Environment Service, Environment Canada, Ottawa. 227pp.

Figure 1. Discharge measurement stations and cross-sectional analysis of flow distribution, Mackenzie Delta.

Table 1. Distribution of flow in the Mackenzie Delta, by sections (refer to Figure 1).

Section		Stations
Flow into Delta - Section U-U	=	$1 + 2 + 3$
Flow at Station A	=	$1 - 4 - 5 - 6$
Flow in Middle Channel at V_1	=	$A + 2 + 3 - B$
Flow across Section V-V	=	$4 + 5 + 6 + V_1 + B$
Flow at W_1	=	$9 + 10 + 12 - 11$
Flow across Section W-W	=	$11 + W_1 + 16 + 17 + 18$
Flow at X_1	=	$11 - 13 - 14 - 15$
Flow across Section X-X	=	$W_1 + 13 + 14 + 15 + X_1$
Flow at Y_1	=	$16 + 17 + 18 - 19 - 20 - 21$
Flow across Section Y-Y	=	$19 + Y_1 + 20 + 21$
Flow at Z_1	=	$20 + 21 - 22 - 23 - 24 - 25$
Flow across Section Z-Z	=	$23 + 24 + 25 + Z_1$

Table 2. March distribution of flow in the Mackenzie Delta.

	Discharge (m^3/s)		
	1972	1973	1974
Flow into Delta - Section U-U	2360	3800	3000
Flow at Station A	0	29.7 (toward Peel)	14.9 (toward Peel)
Flow in Middle Channel at V_1	2300	3646	2905
Flow across Section V-V	2350	3811	3012
Flow at W_1	15.9	78.2	0
Flow across Section W-W	2000	3510	3150
Flow at X_1	unknown	108	112
Flow across Section X-X	49.4	193	182
Flow at Y_1	104.8	990	148
Flow across Section Y-Y	1950	3320	2970
Flow at Z_1	441	125	813
Flow across Section Z-Z	1840	2220	2780

Table 3. Percentage of total inflow at Delta stations in March.

Station	1972	1973	1974	Station	1972	1973	1974
1	2.7	1.4	1.8	16	0.0	0.1	0.2
2	0.4	0.2	0.3	17	0.0	0.6	0.0
3	97.0	98.4	97.9	18	82.6	86.7	99.0
4	-	0.0	0.0	19	0.0	1.9	1.2
5	-	0.0	0.0	20	77.7	57.3	90.5
6	2.3	2.5	2.9	21	0.4	2.0	2.7
9	0.4	2.3	2.5	22	0.3	0.8	0.5
10	0.0	0.02	0.04	23	25.9	28.6	30.0
11	1.3	3.0	6.1	24	32.1	25.6	34.5
12	1.6	2.7	1.9	25	1.2	1.1	1.0
13	0.0	0.0	0.2	A	0.0	0.8	0.5
14	0.3	0.2	0.1	B	0.0	1.8	0.7
15	1.2	0.0	2.1	C	81.4	86.7	100.8

Table 4. March ice thickness data, Mackenzie Delta, N.W.T.

Area	Station	Mean Ice Thickness (m)		
		1972	1973	1974
south (Ft. McPherson)	1	1.0	0.9	1.1
	2	0.7	0.7	0.7
	3	1.1	1.2	1.5
	4	–	0.9	1.1
	5	–	0.9	1.1
	6	0.8	0.8	1.2
	A	0.9	0.9	1.1
	all	0.9	0.9	1.1
west central (Aklavik)	9	1.4	0.9	1.3
	10	1.5	0.8	1.0
	11	1.5	1.1	1.4
	12	1.2	0.7	1.3
	13	1.1	0.8	1.2
	14	1.4	0.9	1.5
	15	1.1	0.9	1.4
	all	1.3	0.9	1.3
east central (Inuvik)	16	1.2	0.9	1.5
	17	1.0	0.7	0.9
	18	1.3	1.0	1.4
	19	1.1	0.8	0.9
	B	1.0	1.0	1.0
	C	1.4	1.1	1.3
	all	1.2	0.9	1.2
north (Reindeer Depot; Tununuk)	20	1.2	1.0	1.2
	21	1.4	1.0	1.3
	22	1.2	1.1	1.3
	23	1.5	1.1	1.5
	24	1.6	1.5	1.5
	25	1.5	1.4	1.6
	all	1.4	1.2	1.4
all		1.2	1.0	1.2

Location	Month	Mean Temperature (°C)				Snowfall (cm)			
		Normal	1971-72	1972-73	1973-74	Normal	1971-72	1972-73	1973-74
Ft. McPherson	Sept.	3.5	4.7	1.2	6.7	12	4	26	0
	Oct.	-7.0	-7.7	-4.7	-7.3	46	35	15	18
	Nov.	-20.3	-21.8	-19.9	-22.3	36	14	41	9
	Dec.	-26.9	-27.5e	-22.9	-25.6	26	19	19	6
	Jan.	-29.4	-28.0	-25.3	-25.7	21	10	22	19
	Feb.	-27.9	-29.4	-25.9	-33.1	20	7	13	15
	Sept.-Feb.	-13.0	-18.3e	-16.3	-17.9	161	89	136	67
Inuvik	Sept.	2.7	3.6	0.3	5.8	11	6	29	T
	Oct.	-7.2	-8.5	-6.9	-7.4	35	118	41	19
	Nov.	-20.6	-21.4	-21.2	-21.1	19	30	28	18
	Dec.	-27.1	-28.4	-22.7	-24.0	22	21	42	7
	Jan.	-29.3	-28.9	-26.4	-25.8	22	20	31	37
	Feb.	-29.4	-30.4	-26.2	-33.7	12	16	7	7
	Sept.-Feb.	-18.5	-19.0	-17.2	-17.7	121	211	178	88
Tuktoyaktuk	Sept.	2.3	3.4	0.6	5.9	4	T	11	3
	Oct.	-6.9	-7.2	-6.3	-7.3	12	29	6	13
	Nov.	-19.3	-21.3	-20.1	-17.4	5	7	13	4
	Dec.	-25.2	-28.9	-21.9	-21.7	8	2	14	5
	Jan.	-27.2	-28.7	-25.6	-24.5	5	5	9	13
	Feb.	-29.2	-30.4	-27.7	-32.6	5	5	4	4
	Sept.-Feb.	-17.6	-18.9	-16.8	-16.3	39	48	57	42

e = data estimated

(Source for temperature and snowfall normals: Burns, 1973)

Appendix I   Station Locations, Mackenzie Delta, N.W.T.

1.   Peel River above Fort McPherson   - gauging station

2.   Arctic Red River at Martin House   - gauging station

3.   Mackenzie River above Arctic Red River - gauging station

4.   Husky Channel

5.   Phillips Channel

6.   Peel Channel

7.   Kalinek Channel

8.   East Channel (Mackenzie River)

9.   Peel Channel above Aklavik

10. Pokiak Channel above Aklavik

11. West Channel (Mackenzie River) below Aklavik Channel

12. Aklavik Channel above Schooner Channel

13. Nikoluk Channel

14. Leland Channel

15. Hvatum Channel

16. East Channel (Mackenzie River) at Inuvik - gauging station

17. Kalinek Channel - N.W. of Inuvik

18. Middle Channel (Mackenzie River) above Napoiak Channel

19. Napoiak Channel

20. Middle Channel (Mackenzie River) west of Williams Island

21. East Channel (Mackenzie River) below Williams Island

22. Marcus Channel

Appendix I Continued

23. Reindeer Channel

24. East Channel (Mackenzie River) below Tununuk Point

25. Channel to west of, and below Tununuk Point

A. Channel below Indian Village

B. East Channel (Mackenzie River) above Kalinek Channel

C. Middle Channel (Mackenzie River) above Horseshoe Bend

Appendix II.   Streamflow data, Mackenzie Delta, March, 1972.

Location	Area "A" (m2)	Width "W" (m)	Mean Depth "D" (m)	Discharge "Q" (m3/s)	Mean Velocity "v" (m/s)	Stage (m)	Mean Ice Depth (m)	Date Day/mo./yr.
1	506	262	1.93	62.8	0.12	-	1.0	10/03/72
2	159	137	1.16	8.48	0.05	-	0.7	2/03/72
3	7590	655	11.6	2290	0.30	-	1.1	21/03/72
4	data unavailable							
5	data unavailable							
6	404	149	2.71	53.0	0.13	20.17	0.8	23/03/72
9	1440	256	5.62	8.80	0.01	-	1.4	14/03/72
10	19.1	27.4	0.70	OVERFLOW 0	0	-	1.5	14/03/72
11	985	762	1.29	31.2	0.03	24.71	1.5	15/03/72
12	856	215	3.98	38.3	0.04	-	1.2	15/03/72
13	462	94.5	4.88	0	0	25.96	1.1	15/03/72
14	196	130	1.51	5.87	0.03	25.89	1.4	14/03/72
15	586	216	2.71	27.7	0.05	26.48	1.1	14/03/72
16	328	137	2.39	0	0	25.65	1.2	16/03/72
17	752	328	2.30	0	0	-	1.0	22/03/72
18	14900	1110	13.4	1950	0.13	-	1.3	22/03/72

Appendix II. Streamflow data, Mackenzie Delta, March, 1972 (cont'd)

Location	Area "A" (m^2)	Width "W" (m)	Mean Depth "D" (m)	Discharge "Q" (m^3/s)	Mean Velocity "V" (m/s)	Stage (m)	Mean ice Depth (m)	Date Day/mo./yr.
19	540	189	2.86	0	0	–	1.1	22/03/72
20	15600	610	25.5	1830	0.12	–	1.2	20/03/72
21	959	468	2.05	10.4	0.01	–	1.4	20/03/72
22	234	151	1.55	7.65	0.03	–	1.2	20/03/72
23	8650	506	17.1	612	0.07	–	1.5	17/03/72
24	4260	840	5.08	757	0.18	–	1.6	17/03/72
25	459	140	3.27	OVERFLOW 27.9	0.06	–	1.5	17/03/72
A	347	268	1.29	OVERFLOW 0	0	20.97	0.9 snow	23/03/72
B	1130	244	4.65	0	0	–	1.0	30/03/72
C	12200	1160	10.5	1920	0.16	–	1.4	6/04/72

Appendix II. Streamflow data, Mackenzie Delta, March, 1973.

Location	Area "A" (m^2)	Width "W" (m)	Mean Depth "D" (m)	Discharge "D" (m^3/s)	Mean Velocity "V" (m/s)	Stage (m)	Mean Ice Depth (m)	Date Day/mo./yr.
1	511	262	1.95	53.8	0.11	3.40	0.9	14/03/73
2	198	131	1.51	8.70	0.04	1.74	0.7	14/03/73
3	10300	1030	9.98	3740	0.36	-	1.2	2/04/73
4	16.6	19.8	0.84	0	0	-	0.9	23/03/73
5	15.1	42.7	0.35	0	0	-	0.9	23/03/73
6	577	152	3.79	95.1	0.16	20.50	0.8	21/03/73
9	1520	268	5.67	88.1	0.06	-	0.9	26/03/73
10	81.1	45.7	1.77	0.76	0.01	-	0.8	26/03/73
11	1900	488	3.90	114	0.06	-	1.1	26/03/73
12	847	206	4.12	104	0.12	-	0.7	26/03/73
13	453	96.0	4.72	0	0	26.00	0.8	21/03/73
14	207	122	1.70	6.12	0.03	25.96	0.9	21/03/73
15	595	218	2.73	0	0	-	0.9	26/03/73
16	390	145	2.69	2.92	0.01	25.49	0.9	19/03/73
17	686	396	1.73	21.5	0.03	-	0.7	29/03/73

Appendix II.   Streamflow data, Mackenzie Delta, March, 1973.   (cont'd)

Location	Area "A" (m²)	Width "W" (m)	Mean Depth "D" (m)	Discharge "Q" (m³/s)	Mean Velocity "V" (m/s)	Stage (m)	Mean Ice Depth (m)	Date Day/mo./yr.
18	15300	945	16.2	3290	0.21	–	1.0	23/03/73
19	531	172	3.08	73.6	0.14	–	0.8	22/03/73
20	17700	579	30.6	2180	0.12	–	1.0	27/03/73
21	1030	411	2.50	74.9	0.07	–	1.0	22/03/73
22	341	128	2.67	28.7	0.08	–	1.1	27/03/73
23	8180	546	15.0	1090	0.13	–	1.1	27/03/73
24	3550	841	4.22	972	0.27	–	1.5	20/03/73
25	435	126	3.44	39.8	0.09	–	1.4	20/03/73
A	375	277	1.35	29.7	0.08	20.41	0.9	21/03/73
B	1050	241	4.35	69.5	0.07	–	1.0	28/03/73
C	13200	838	15.7	3290	0.25	–	1.1	28/03/73

Appendix II.   Streamflow data, Mackenzie Delta, March, 1974.

Location	Area "A" (m^2)	Width "W" (m)	Mean Depth "D" (m)	Discharge "Q" (m^3/s)	Mean Velocity "V" (m/s)	Stage (m)	Mean Ice Depth (m)	Date Day/mo./yr.
1	533	244	2.18	54.3	0.10	3.72	1.1	14/03/74
2	157	134	1.17	7.43	0.05	1.61	0.7	11/03/74
3	8670	1010	8.62	2930	0.34	2.21	1.5	16/03/74
4	5.02	16.8	0.30	0	0	–	1.1	13/03/74
5	45.1	30.5	1.48	0	0	–	1.1	13/03/74
6	485	171	2.84	86.3	0.18	–	1.2	14/03/74
9	1290	229	5.63	74.8	0.06	–	1.3	18/03/74
10	54.3	45.7	1.19	1.20	0.02	–	1.0	18/03/74
11	2420	396	6.10	182	0.08	–	1.4	18/03/74
12	1060	165	6.43	57.4	0.05	–	1.3	19/03/74
13	177	107	1.66	4.84	0.03	–	1.2	18/03/74
14	226	130	1.75	1.66	0.01	–	1.5	18/03/74
15	599	219	2.73	63.6	0.11	–	1.4	18/03/74
16	324	130	2.50	6.81	0.02	25.44	1.5	12/03/74
17	705	335	2.10	0	0	–	0.9	15/03/74

Appendix II. Streamflow data, Mackenzie Delta, March, 1974. (Cont'd)

Location	Area "A" (m²)	Width "W" (m)	Mean Depth "D" (m)	Discharge "Q" (m³/s)	Mean Velocity "V" (m/s)	Stage (m)	Mean Ice Depth (m)	Date Day/mo./yr.
18	15000	898	16.7	2970	0.20	–	1.4	19/03/74
19	459	241	1.91	35.6	0.08	–	0.9	19/03/74
20	19100	622	30.7	2710	0.14	–	1.2	15/03/74
21	942	625	1.51	79.7	0.08	–	1.3	13/03/74
22	250	168	1.49	14.0	0.06	–	1.3	15/03/74
23	7770	472	16.5	899	0.12	–	1.5	15/03/74
24	3790	831	4.56	1030	0.27	–	1.5	13/03/74
25	398	122	3.27	30.5	0.08	–	1.6	13/03/74
A	374	259	1.45	14.9	0.04	–	1.1	14/03/74
B	499	244	2.05	20.9	0.04	–	1.0	17/03/74
C	12500	1160	10.8	3020	0.24	–	1.3	23/03/74

PROGRESS REPORT ON

GEOMORPHIC AND CLIMATIC STUDIES IN THE MACKENZIE DELTA AREA

AIDED BY DENDROCHRONOLOGY

BY

W.E.S. HENOCH

During the month of August 1973, a field party consisting of
W.E.S. Henoch, M. L. Parker (Western Forest Products Laboratory,
Vancouver, B.C.) and D. Outhet (graduate student, University of
Alberta) visited the Mackenzie River Delta to study some aspects
of geomorphic processes and climate in the region. Extensive tree
sampling was carried out during the field season, particularly in
the vicinity of Point Separation where sections of buried tree stumps
were collected to study:

    (a)   growth of adventitious roots and the rate of sedimentation;

    (b)   age of the holocene deposits in the Delta near Point
           Separation; and

    (c)   minimum age of a buried tree stump pierced by an ice wedge.

In addition, three pingo-like humps were located between drained channels
on the Peel River floodplain near a site known as Indian Village. There,
preliminary work was carried out as follows:

    (a)   five vegetation zones were recognized and mapped.

    (b)   flood levels were surveyed;

    (c)   the depth of active layer across the humps was surveyed
           by probing at one metre intervals;

    (d)   the active layer depth was also probed under a windthrow.
           Tree samples were taken to determine the age of the windthrow
           and the rate of degradation of the permafrost under it; and

    (e)   tree samples were collected in order to study the relation
           between tree rings and permafrost-soil conditions.

Two new tree ring chronologies were built under Parker's supervision
in the Western Forest Products Laborary from the samples collected in 1972.

These chronologies of ring width and density in the Inuvik and
Fort Simpson areas were compared with recipitation, temperature
and river discharge records for the growing months from May to
September. Some highly significant correlations were obtained.
Analytical work is in progress and the results will be reported
in the near future.

HYDROLOGIC STUDIES AT "TWISTY CREEK"
IN THE
MACKENZIE MOUNTAINS, N.W.T.

- 1973 Progress Report -

by

J.N. Jasper

Glaciology Division
Water Resources Branch
Department of the Environment

under the

Environment-Social Program
Northern Pipelines

CONTENTS

ABSTRACT

In 1973, hydrologic data collection was continued in the Twisty
Creek watershed. This small sub-arctic upland basin in the Mackenzie
Mountains was chosen to examine the relationships among precipitation,
runoff and sediment yield. Runoff from a heavy rainstorm on July 6th
resulted in a new peak flow of 16.99 m^3/s or 2.45 m^3/s/km^2. The percentage
of runoff to precipitation was found to average 91 per cent over the field
season with a resulting low evapotranspiration component. About 80 per cent
of total sediment yield occurred during peak flood events. Such results
should be of value in developing design criteria for highway and pipeline
crossing of rivers and streams.

HYDROLOGIC STUDIES AT "TWISTY CREEK"
IN THE
MACKENZIE MOUNTAINS, N.W.T.

- 1973 Progress Report -

By

J.N. Jasper

"TWISTY CREEK" WATERSHED STUDY

"Twisty Creek" is a small sub-tributary of the Arctic
Red River and is located in the foothills of the Mackenzie Mountains,
N.W.T. at latitude $65^{\circ}23'$ N and longitude $131^{\circ}16'$W (Figure 1).
The study was initiated in 1972 to understand the hydrologic response
characteristics for small drainage basins in the area (Sellars, 1973).
This location was selected with the intention of filling a gap in the
present network of meteorological stations as well as for the size,
accessibility and representativeness of the watershed. In addition,
the Mackenzie Mountains have been identified as the source area for
major floods in the MacKenzie River tributaries on the west side of
the Mackenzie Valley (Mackay, Fogarasi, and Spitzer, 1973).

The specific objectives are to collect and publish relevant
data, and derive the relationships among precipitation, runoff, and
erosion for a small upland watershed. Results are presented for 1972 and
1973 and may be of use in determining design criteria for river crossing
structures in watersheds with similar physiographic and precipitation
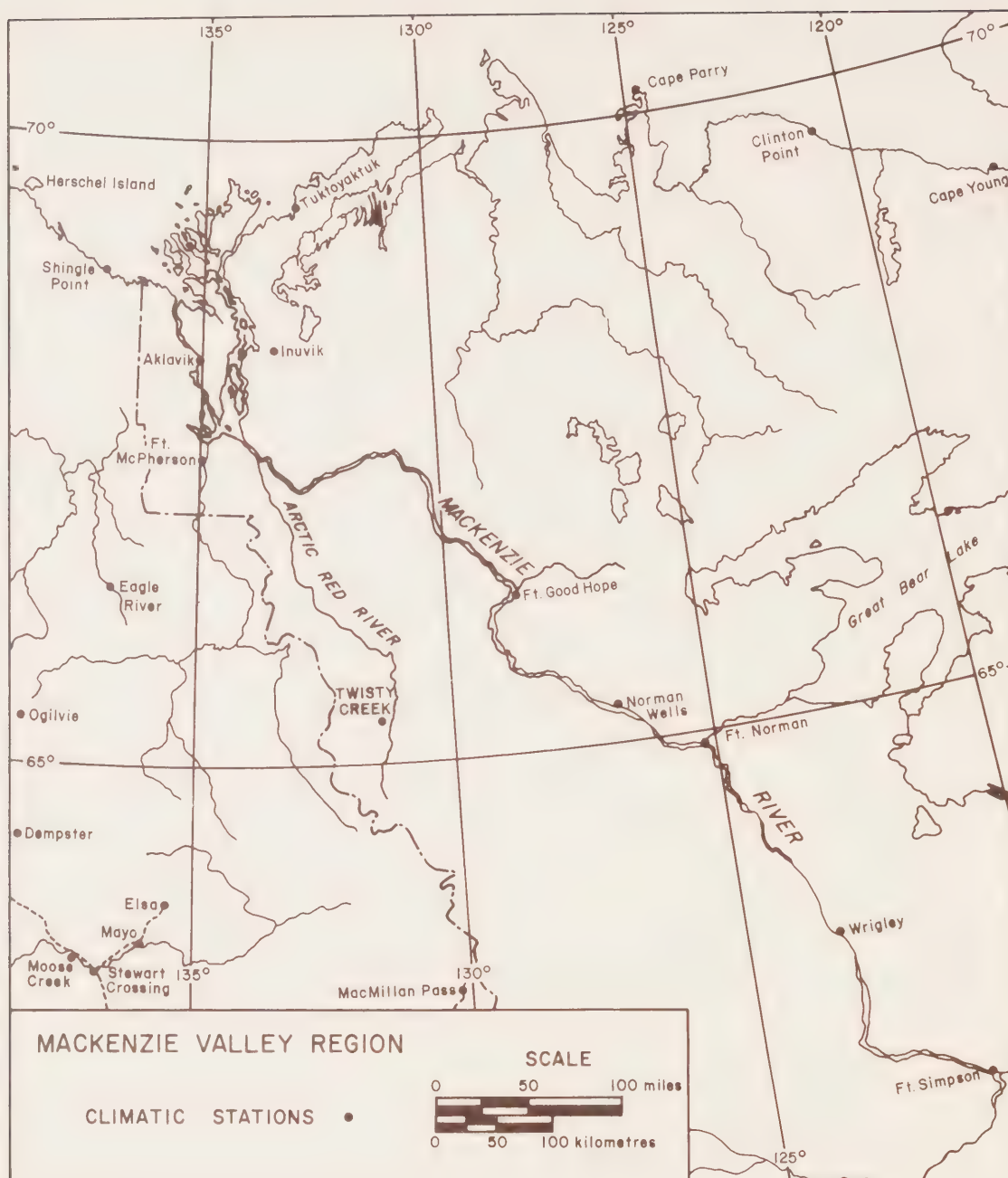characteristics.

Figure 1.   Mackenzie Valley region showing the location of Twisty Creek
            and other meteorologic stations.

METHODS OF DATA COLLECTION

As in 1972, six M.S.C. pattern tipping bucket rain gauges and three Lambrecht model 252C thermohygrographs in Stevenson screens were utilized to record units of 1/100 of an inch of rainfall, air temperature and humidity. A continuous record of stream stage was kept using a Stevens type F water level recorder at the main discharge station. Stream velocities were measured with an Ott current meter and rating curves developed from 12 measurements in 1972 and 32 in 1973.

Dissolved load in the stream has been estimated from water chemistry analyses of stream waters, which were tested for pH, calcium and total hardness, and alkalinity. Dissolved loads were roughly calculated as the sum of the latter two, with the assumption that the major proportion of dissolved solids are of this composition.

A U.S. DH-48 suspended sediment sampler was used to collect depth integrated suspended sediment samples at the main stream gauging site. Bed load moving in the stream at this site was sampled with a ½-inch mesh basket-type sampler. Discharge-sediment rating curves have been developed from 191 water chemistry analyses and 60 suspended sediment samples taken during the two field seasons. The 12 bed load measurements from 1973 have been utilized to give a preliminary rating curve for bed load.

The records obtained are for the period July 2 - August 25, 1972 and June 29 - September 5, 1973. The 1973 network was basically the same as that established in 1972, however the rain gauge at site R1 was moved to R7 and a standard gauge substituted at R1 (Figure 2). Water level recorder W2 was moved to site W3 to allow development of a unit hydrograph for a smaller unit basin. However problems with stilling well intakes at both W2 and W3 have resulted in discontinuous records which have not been analyzed.

A ground control survey carried out in 1973 has resulted in the drafting of a 1:10,000 scale contour map from 1972 aerial photographs. Drainage area of the basin above the main stream gauging site is 6.94km^2, 6 percent greater than the original estimate of 6.55km^2, which was measured from an enlargement of the available 1:250,000 NTS coverage (Figure 2).

RESULTS AND DISCUSSION

Precipitation and Runoff

Tables 1 and 2 are summaries of precipitation, runoff, and sediment yields compiled on a daily basis. From these records the average precipitation over the catchment for the periods of record has been computed to be 234mm in 1972 and 367mm in 1973. Total runoff was 162mm or 69% of precipitation in 1972, 332mm or 91% in 1973. Both ratios are high and indicate small evapotranspiration losses, as would be expected from a watershed with less than 20% vegetation cover. As well, the soil in the basin is
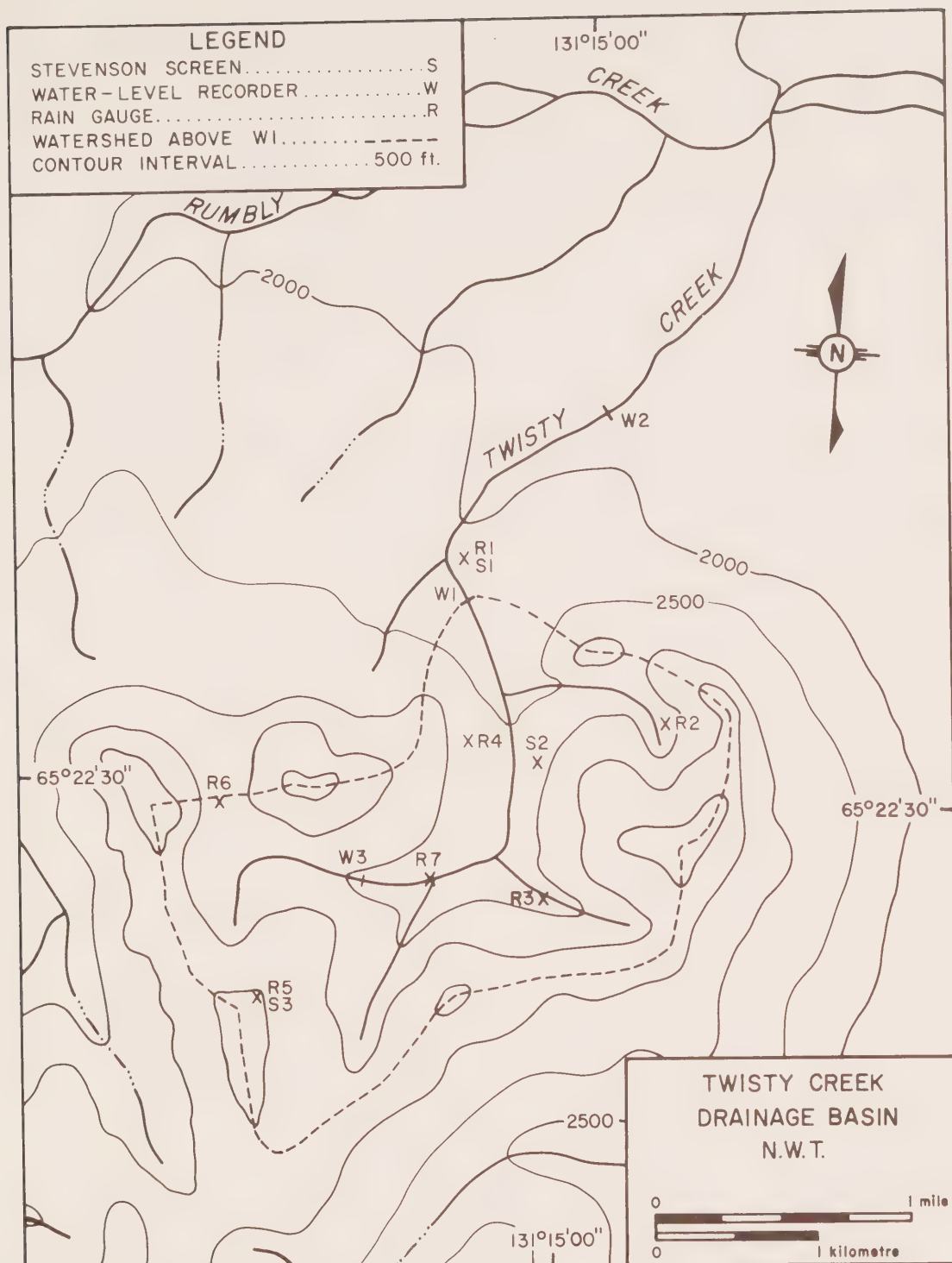
Figure 2. Location of instruments in "Twisty Creek" drainage basin

quite shallow except for a narrow strip immediately adjacent to the main channel.

Base flow separation has been carried out for both years' data from observations on the response of groundwater flow to short intense rainfalls, as well as long duration light intensity events. Figure 3 gives several examples from 1973. A short duration high intensity rainstorm typically produces a direct runoff peak, which occurs as rainfall ceases. Groundwater flow begins to increase 6 to 8h later and produces a second peak some 12-15h after rainfall has stopped. Sellars (1973, p. 527) has presented similar evidence for 1972. Long duration or light intensity storms produce a similar rise in groundwater, usually without the direct runoff peak. These response characteristics of groundwater flow, and the linear recession curves of groundwater flow obtained from semi-logarithmic plots of the streamflow data, have allowed a physically based graphical separation of direct runoff and baseflow.

Further analysis of the ratio of runoff to precipitation has shown that the high value of 91% for 1973 can be largely explained in terms of the rapid runoff which follows high intensity storms. The most impressive example is for the maximum flood experienced over the 2 years of record, when 57.78mm of rain (44.68mm in a 2h period) produced a peak discharge of $16.99m^3$/sec on 6 July 1973 (Figure 4). At the time, baseflow was very low ($0.023m^3$/sec)

STORM RUNOFF

$$RATIO = \frac{DIRECT\ RUNOFF + INTERFLOW}{PRECIPITATION}$$
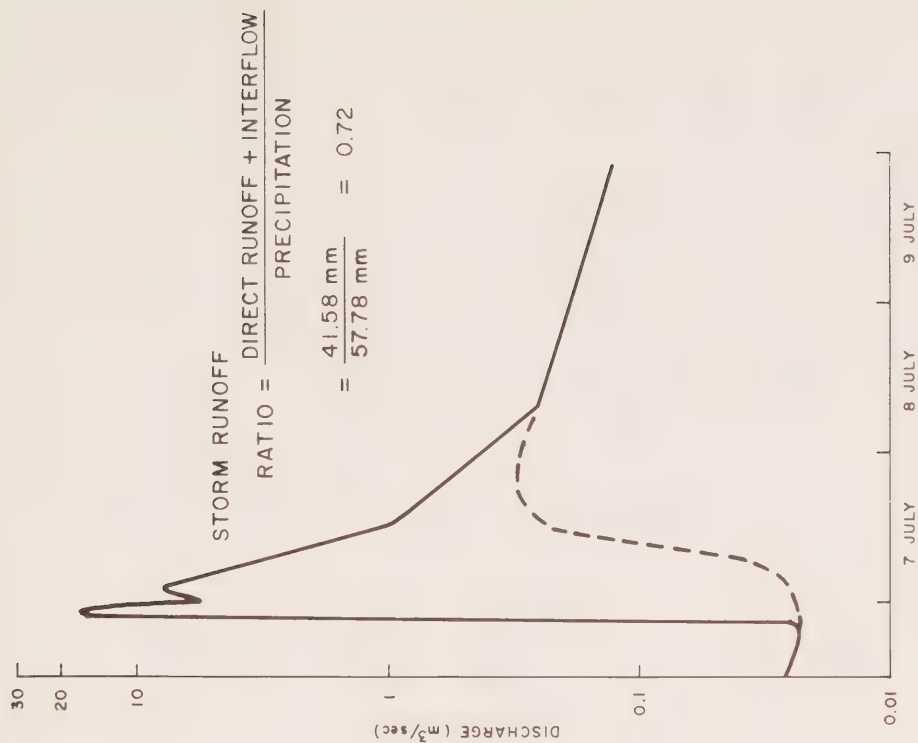
$$= \frac{41.58\ mm}{57.78\ mm} = 0.72$$

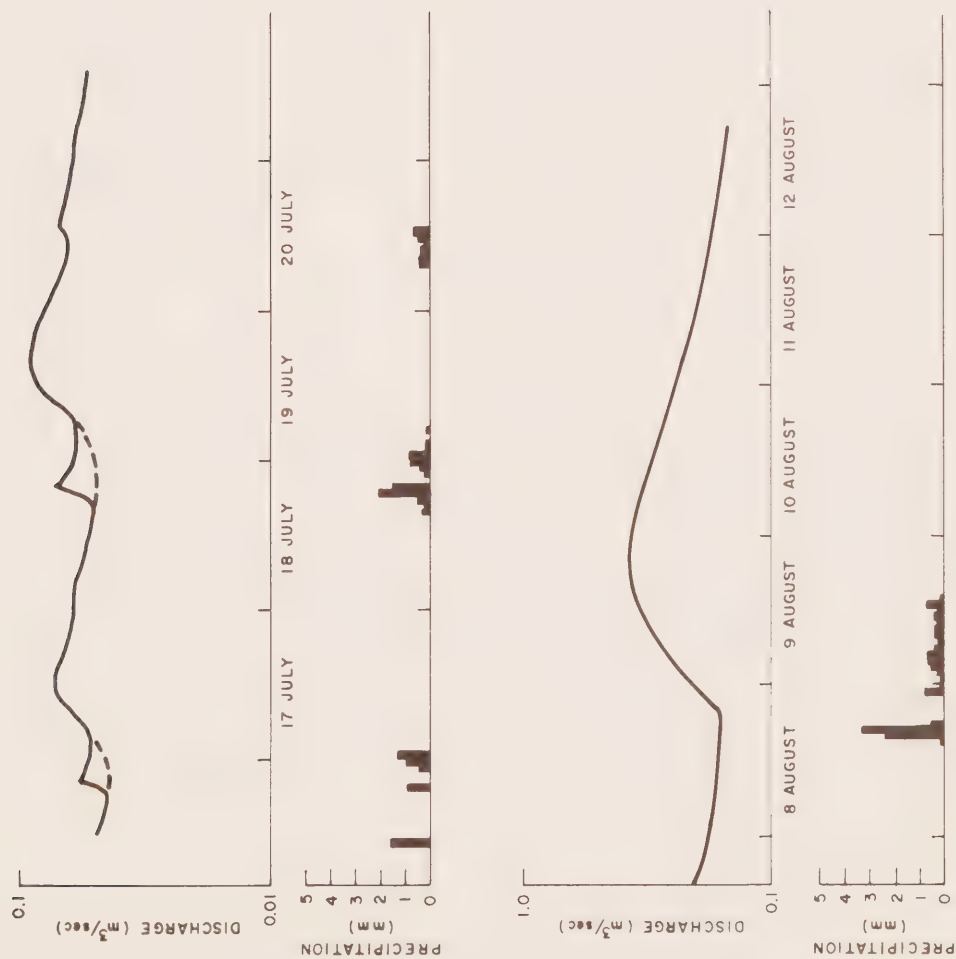Figure 4. Hydrograph separation for 6 July, 1973 flood

Figure 3. Response of groundwater flow to rainfall during 1973 field season

due to a lengthy dry period; thus the major proportion of runoff in the several days afterwards was largely a result of this storm. The hydrograph separation technique described above, results in a prediction of 41.58mm for direct runoff and interflow, which corresponds to a direct runoff ratio of 0.72. A second major rainfall of 60.19mm on 4 August 1973 produced a peak discharge of 8.14m^3/sec and 36.53mm of direct runoff + interflow.

If these two events had not occurred the runoff-precipitation ratio for 1973 decreases to 0.70, which is comparable to the 1972 value of 0.69. Therefore the ratio of 0.91 no longer seems as unrealistic as it first appeared. The estimates of total direct runoff + interflow based on hydrograph separation for the two field seasons are 51mm in 1972 and 120mm in 1973, which correspond to 31.6 and 36.2% of total streamflow, 21.8 and 32.9% of precipitation.

Sediment Yield

The results of the water chemistry analyses are presented in Figure 5, with regression lines fitted by eye. Although fewer data are available for 1973, the pattern of changing dissolved solids concentration under different flow conditions noted during 1972 (Jasper, 1973, p. 654) is repeated. Transition from one rating curve to the next coincided with changes in flow conditions, often resulting from major floods, and is attributed to the
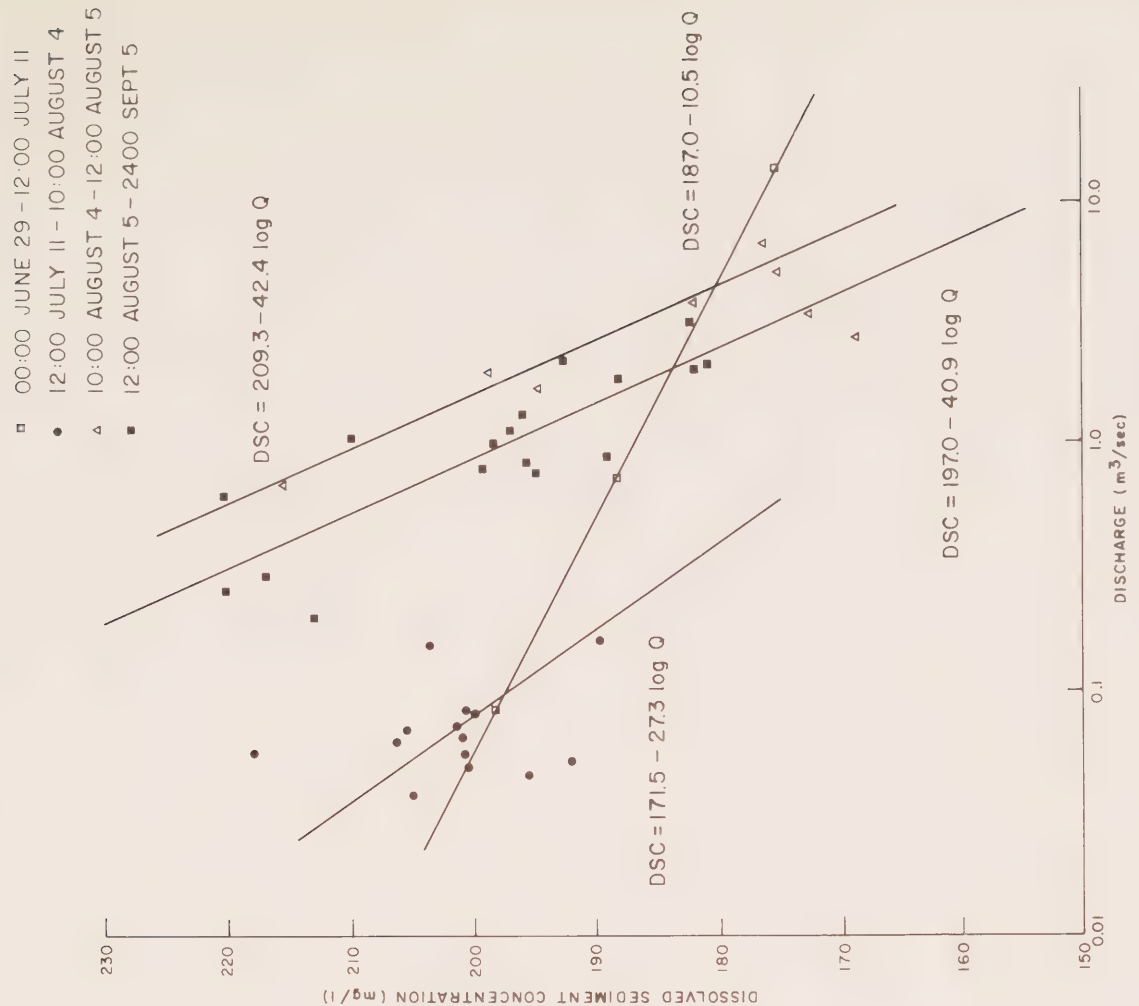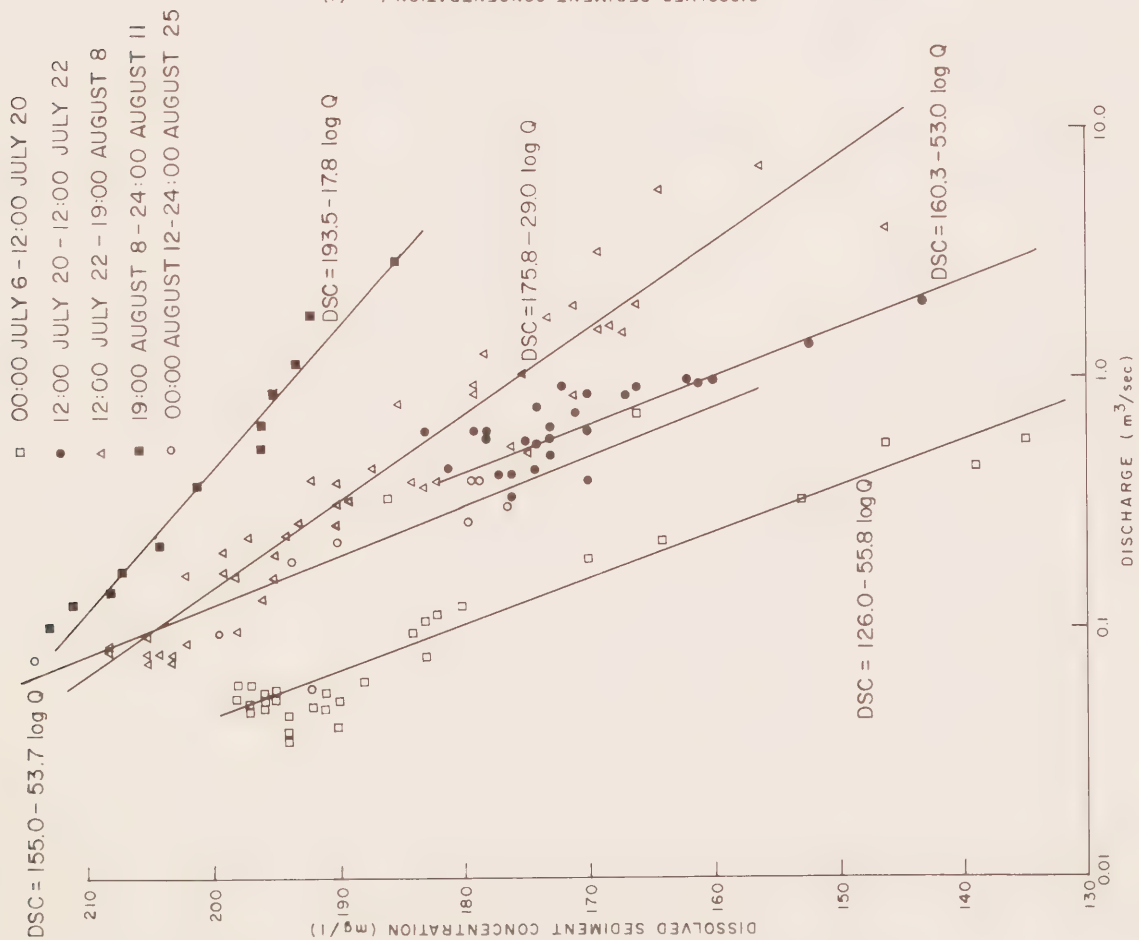
Figure 5. Dissolved load rating curves for 1972, 1973

- 271 -

relative contribution of groundwater flow to runoff.

Suspended sediment data (Figure 6) show good consistency between the two field seasons. As 1973 was a much wetter year (see Tables 1 and 2), with an estimated 367mm of rain compared to 234mm in 1972, a greater proportion of samples are for higher discharges than in 1972. Also the 1973 suspended sediment concentrations are higher for similar discharges, possibly due to higher moisture conditions prevalent during the 1973 field season. Simple regression between discharge and suspended sediment yields a correlation coefficient of 0.88. It is hoped that the 77% of variance in suspended sediment concentration explained by variation of discharge may be increased, perhaps by representing moisture conditions through an antecedent precipitation index.

The 12 bed load samples have been analyzed and total yields calculated for the stream cross-section. The results have been interpreted in a somewhat arbitrary manner for the following reasons. Firstly, it has been assumed that the traps were 100% efficient. This is of course not in agreement with the laboratory tests of Gibbs and Neill (1973) and others too numerous to mention. Moreover, the flow conditions were so turbulent during sampling that the traps had little effect on movement of bed load. In addition, a least squares fit to all 12 data points gives an estimated yiel rate of 1,080,000kg/sec at the peak runoff rate of $16.99m^3$/sec on 6 July 1973. As the runoff rate corresponds to 17,000 kg/sec of water, this estimated

Figure 7.   Bed load rating curves

$Y \, BED = 0.053 \, Q^{3.488} (Q > 3.5 \; m^3/sec)$

$Y \, BED = 3.51 \times 10^{-4} \, Q^{7.712}$

DISCHARGE (m^3/sec)

TOTAL BED LOAD YIELD (kg/sec)

Figure 5.   Suspended sediment rating curve

$SSC = 0.0948 \, Q^{2.187}$

● 1972 DATA
○ 1973 DATA

DISCHARGE (m^3/sec)

SUSPENDED SEDIMENT CONCENTRATION (gm/L)

- 273 -
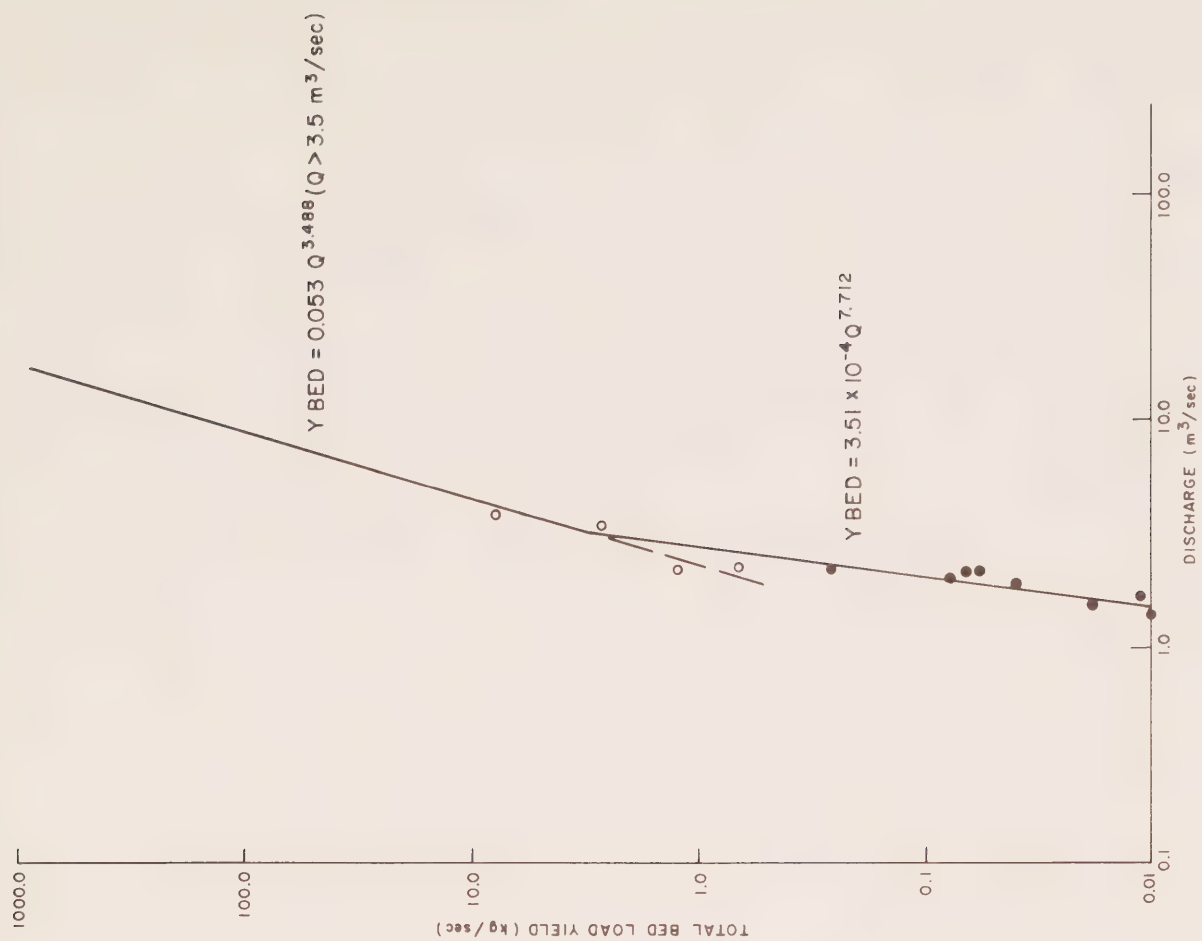
value is unrealistic. Alternatively, separate regression lines were fitted to all data points as well as to the 4 highest points. The resulting correlation coefficients were 0.91 and 0.95 respectively. The upper line (Figure 7) estimates a more realistic transport rate of 1,030 kg/sec at 16.99 m^3/sec and has been used when discharges exceed 3.5 m^3/sec.

Computed sediment yields for 1972 are as follows: bed load - 0.51 million kg; suspended load - 0.56 million kg; dissolved load - 0.22 million kg; for a total loss of 1.29 million kg of material. The values for 1973 are: bed load - 4.87 million kg; suspended load - 4.57 million kg; dissolved load - 0.45 million kg; for a total loss of 9.86 million kg. Assuming an average rock density of 2.71, these totals correspond to basin erosion rates of 0.0069 cm/yr for 1972 and 0.0524 cm/yr for 1973. Both values are within an order of magnitude of the estimated range of 0.0399 - 0.0998 cm/yr quoted for high mountain areas by McPherson (1971, p. 232). In addition McPherson obtained a value of 0.0495 cm/yr of erosion for Two O'Clock Creek, Rocky Mountains.

The significance of the two major floods of 1973 and one in 1972 may be appreciated when one considers that 4.59 million kg bed load and 3.10 million kg suspended load were transported past the gauging station in a total of 16 h in 1973. Almost all bed load

movement and 0.51 million kg of suspended load occurred during an 8 h period in 1972. Daily values of dissolved material transported varied over a smaller range due to the decrease of dissolved solid concentrations with increasing streamflow. Thus approximately 80 percent of total erosion occurred in time intervals accounting for 0.6% of the 1972 field season and 0.8% in 1973.

In addition to the problems of bank erosion and channel shifting due to a highly mobile bed during peak floods, care must also be taken to provide protection for structures in the stream channel and to ensure passage of high bed load. As an example, a concrete and boulder weir constructed at the mainstream gauging site in late June 1973 was largely destroyed during the July 6 flood by boulders being swept along the bed and into the upper face of the weir. The weir was reconstructed after the flood subsided but continued to be slowly worn away as the rest of the field season passed. It is recommended that special care be taken in the design of structures crossing streams with similar bed load movement patterns. The size of bed material, channel slopes, watershed relief, etc., are obvious reference indicators.

CONCLUSIONS AND RECOMMENDATIONS

Although two summers of data do not warrant the drawing of definite conclusions, several hydrologic and sediment movement characteristics have been observed which are thought to be valid for similar watersheds in the region. The observations and

and tentative conclusions are as follows:

1. Mean rainfall was 4.25mm/day in 1972 and 4.65mm/day in 1973.

2. Mean total runoff was 2.95mm/day in 1972 and 4.20mm/day in 1973.

3. Major floods result from heavy rainstorms produced orographically by systems approaching from the NW, N and NE (Sellars, 1973).

4. Runoff of excess water is rapid, with lag time from centroid of the mass of effective rainfall to centre of area of the unit hydrograph computed to be 2.5h (Sellars, 1973).

5. Groundwater flow, as estimated from a physically-based graphical separation technique, accounts for 60-70 percent of total runoff. Groundwater responds more slowly to rainfall, beginning to rise 6-8h after rainfall begins and peaking about 12-15h after rain ceases.

6. The peak discharge of $16.99m^3/sec$ ($2.45m^3/sec/km^2$ or 229 cfs/mi^2) is thought to be the highest since at least June 1972 and possibly for several years previous, due to lack of similar evidence of recent major bank and gully erosion at the commencement of the study.

7. As much as 80% of total sediment yield may occur during the peak flood event(s) in a year. Extremely high rates

of bed load movement (i.e. 1030kg/sec or 141kg/km^2 on 6 July 1973) can be destructive to improperly designed structures in the stream channel. Consideration for passage of high bed load should be incorporated into their design.

8. Peak at-a-station and basin averaged rainfall for several durations, based on the available data, are presented below. The 25-year return period regional intensity-frequency curves for the area have been described by Northwest Hydraulic Consultants Ltd. (1972) and are given for reference. It should be noted that the latter are obtained from records at Yellowknife, Whitehorse, Fort McPherson, Inuvik, and Aklavik, all of which are located at low elevations.

Duration	Mackenzie Region 25-Year Return Period mm	At-a-Station Precipitation mm	Watershed Averaged Precipitation mm
15min	5.08	18.29	13.72
30	8.89	34.54	24.64
60	10.16	56.13	38.61
2hr		69.08	44.66
6		81.28	57.78
24	50.80	81.28	60.19

Gibbs, C.J. and C.R. Neill, 1973. Laboratory testing of model VUV
    bed-load sampler. Research Council of Alberta, Pub. No.
    REH/73/2. 16 p.

Jasper, J.N., 1973. "Suspended sediment and dissolved material in
    Twisty Creek, a small subarctic watershed" in, Hydrologic
    aspects of Northern pipeline development, MacKay, D.K. et al.,
    Report No. 73-3, Task Force on Northern Oil Development, Ottawa,
    pp. 645-664.

MacKay, D.K., S. Fogarasi, and M. Spitzer, 1973. "Documentation of an
    extreme summer storm in the Mackenzie Mountains, N.W.T." in,
    Hydrologic aspects of Northern pipeline development, MacKay, D.K.
    et al., Report No. 73-3, Task Force on Northern Oil Development,
    Ottawa, pp. 191-222.

McPherson, H.J., 1971. "Dissolved, suspended and bed load movement
    patterns in Two O'Clock Creek, Rocky Mountains, Canada, summer,
    1969". Journal of Hydrology, Vol. 12, pp. 221-233.

Northwest Hydraulic Consultants Ltd., 1972. Mackenzie/Dempster highway
    hydrology study, Inuvik to N.W.T. - Yukon border. Government of
    Canada, Department of Public Works, Edmonton, Alberta. 26 p.

Sellars, C.D., 1973. "Hydrologic processes in a sub-arctic upland watershed" in, Hydrologic aspects of Northern pipeline development, MacKay, D.K., et al., Report No. 73-3, Task Force on Northern Oil Development, Ottawa, pp. 513-555.

TABLE 1. DAILY RAINFALL, RUNOFF AND SEDIMENT YIELDS FOR 1972 FIELD SEASON

Theissen Polygon Weight → Date	Rainfall mm 1 — 0.027	2 — 0.180	3 — 0.256	4 — 0.173	5 — 0.251	6 — 0.114	Runoff mm	Mean Disch. m^3/s	Sediment Yield Dissolved kg	Suspended kg	Bed Load kg	Peak Disch. m^3/s	Peak Sed. Rates Dissolved kg/s	Suspended kg/s	Bed Load kg/s
July 2	0	0.25	3.05	1.52	2.29	0.25	1.19	0.10	1,510	5.10	0	0.13	0.02		
3	0	0	0	0	0	0	1.11	0.09	1,420	3.96	0				
4	0	0	0	0	0	0	0.77	0.06	1,040	1.18	0				
5	0	0	0	0	0	0	0.61	0.05	847	0.56	0				
6	0.25	0.51	1.52	0.51	0.76	1.78	0.59	0.05	815	0.49	0				
7	2.79	2.79	3.05	2.54	1.27	3.81	0.69	0.06	941	0.85	0	0.06			
8	0	0	0	0	0	0	0.65	0.05	896	0.70	0				
9	0	0	0	0	0	0	0.52	0.04	735	0.34	0				
10	0	0	0	0	0	0	0.48	0.04	679	0.25	0				
11	0	0	0	0	0	0	0.48	0.04	679	0.25	0				
12	0	0	0	0	0	0	0.47	0.04	667	0.24	0				
13	0	0	0	0	0	0	0.48	0.04	679	0.25	0				
14	2.03	1.27	0.51	2.54	0.51	0.25	0.46	0.04	661	0.23	0	0.04			
15	3.56	4.06	4.83	4.06	3.30	6.35	0.47	0.04	640	0.25	0	0.05			
16	0	0	0	0	0	0	0.60	0.04	857	0.53	0	0.05			
17	2.54	2.29	5.08	5.08	3.81	17.02	0.62	0.05	851	0.57	0	0.05			
18	4.83	7.87	11.68	7.37	10.16	8.64	1.43	0.12	1,640	135.00	0	0.81	0.11	0.05	
19	0	0.51	0.51	0.25	0	0.51	1.75	0.14	1,840	20.40	0				
20	14.99	17.27	19.81	16.00	18.54	16.26	7.41	0.60	7,810	7,640.00	551	2.23	0.24	1.23	0.
21	8.38	10.16	15.75	6.35	10.41	11.94	6.68	0.54	7,760	1,580.00	1	1.04	0.17	0.11	
22	7.11	8.89	18.80	13.21	25.15	16.00	13.75	1.10	16,400	20,800.00	1,320	2.23	0.37	1.23	0.
23	3.81	4.57	7.37	5.33	5.84	9.91	6.89	0.55	8,740	1,550.00	0	0.60	0.13	0.02	
24	0.25	0.25	0.76	0.25	0.51	1.02	4.80	0.39	6,230	505.00	0				
25	0	0	1.02	0.51	0.51	0.51	2.30	0.19	3,150	40.80	0				
26	0	0	0	0.51	0.25	0.76	1.47	0.12	2,060	9.33	0				
27	0	1.02	1.02	0	0.25	1.02	1.09	0.09	1,510	3.61	0				
28	12.45	12.70	12.70	12.19	10.67	12.19	1.43	0.12	1,980	39.20	0	0.39			
29	0.25	0	0.76	0.51	2.03	1.02	2.95	0.24	3,960	111.00	0				
30	0	0	0	0	0	0	1.57	0.13	2,110	11.60	0				
31	1.52	1.02	0.51	1.02	0.51	3.30	1.10	0.09	1,640	3.63	0				
Aug. 1	13.97	16.26	22.61	14.73	13.46	21.84	3.51	0.28	4,260	720.0	1				
2	5.84	7.62	12.95	8.13	8.64	10.92	8.87	0.71	11,400	6,070.00	107	1.70	0.29	0.51	0
3	0	0.25	0	0	0.51	1.02	5.98	0.48	7,440	1,240.00	0	0.86	0.15	0.06	
4	0	0	0	0	0	0	2.37	0.19	3,310	48.10	0				
5	0	0	0	0	0	0	1.45	0.12	2,140	9.07	0				
6	12.95	15.24	14.99	14.99	14.73	13.72	1.23	0.10	1,740	8.83	0				
7	2.29	9.91	14.73	5.84	12.45	8.38	4.85	0.39	6,280	767.00	0.493×10^6	0.88	0.16	0.06	
8	23.11	23.62	33.78	24.64	32.00	32.77	18.85	1.51	23,600	0.492×10^6	13,700	9.15	1.61	110.00	119
9	1.27	2.03	2.29	1.78	1.27	1.78	11.29	0.91	15,100	26,900.00	0				
10	0	0	0	0	0	0	3.34	0.27	4,720	153.00	0				
11	0	0	0	0	0	0	2.04	0.16	2,950	26.70	0				
12	2.79	11.18	5.33	11.18	7.62	9.91	1.80	0.15	2,490	17.50	0				
13	5.84	12.19	1.94	13.97	8.64	12.19	3.70	0.30	4,690	202.00	0	0.38	0.07		
14	0.51	0.25	0.25	0.25	0	0.25	3.19	0.26	4,130	113.00	0				
15	0	0	0	0	0	0	2.26	0.18	3,060	36.40	0				
16	2.29	1.78	5.08	1.52	8.13	4.32	1.76	0.14	2,450	16.30	0				
17	21.08	18.54	16.51	19.81	17.27	23.88	2.53	0.20	3,270	217.00	0	0.58	0.10	0.02	
18	10.41	10.67	8.38	9.65	5.33	9.40	5.98	0.48	7,130	892.00	0	0.59	0.11	0.02	
19	0	0	0	0	0	0	3.16	0.25	4,100	110.00	0				
20	0	0	0	0	0	0	2.34	0.19	3,150	41.00	0				
21	0	0	0	0	0	0	1.82	0.15	2,530	18.30	0				
22	0	0	0	0	0	0	1.46	0.12	1,990	9.01	0				
23	0	0.51	0	0	0	0	1.23	0.10	1,360	5.22	0				
24	3.56	4.06	2.79	3.05	3.81	2.54	1.05	0.08	1,030	3.14	0				
25	0	0	0	0	0	0	0.91	0.07	924	1.98	0				
TOTALS	170.68	209.55	260.34	209.29	230.63	267.72	161.76	0.24	206,000	562,000	506,000				

Theissen Polygon Weight → Date	Rainfall mm 1 0.027	2 0.180	3 0.203	4 0.148	5 0.196	6 0.084	7 0.164	Runoff mm	Mean Disch. m³/s	Sediment Yield Dissolved kg	Suspended kg	Bed Load kg	Peak Disch. m³/s	Peak Sediment Yield Rates Dissolved kg/s	Suspended kg/s	Bed Load kg/s
June 29	0	0	0	0	0	0	0	3.44	0.28	4,600	147.00	0				
30	0	0	0	0	1.52	2.03	1.02	2.28	0.18	3,080	39.20	0				
July 1	0	0	0	0	0	0	0	1.53	0.12	2,090	11.10	0				
2	1.78	2.03	1.78	1.78	0.76	0	1.02	1.00	0.08	1,370	2.81	0				
3	0	0	0	0	0	0	0	0.71	0.06	991	0.95	0				
4	0	0	0	0	0	0	0	0.55	0.04	763	0.40	0				
5	0	0	0	0	0	0	0	0.42	0.03	594	0.17	0				
6	49.02	54.36	44.20	75.69	34.80	49.53	50.29	14.23	1.14	17,500	2.26x10⁶	2.78x10⁶	16.99	2.96	790.00	1030.00
7	6.10	7.62	6.35	5.84	5.84	2.29	6.10	29.73	2.39	37,300	0.821x10⁶	0.79x10⁶	7.93	1.41	69.60	72.10
8	0	0	0	0	0	0	0	3.10	0.25	4,160	126.00	0				
9	0	0	0	0	0	0	0	1.92	0.15	2,610	22.50	0				
10	0.51	0	0	0	0	0.25	0	1.28	0.10	1,750	6.26	0				
11	6.10	16.76	14.99	6.60	10.41	5.33	7.11	3.24	0.26	4,120	526.00	0	0.82	0.14	0.51	
12	3.94	1.52	2.29	0	10.67	0.51	2.03	2.62	0.21	3,450	69.00	0				
13	0	0ᵉ	0	0	0	0	0	1.39	0.11	1,900	9.30	0				
14	2.79	2.29ᵉ	2.03	2.54	3.05	3.05	3.30	0.75	0.06	1,070	1.12	0				
15	0.25	0.51ᵉ	0.25	1.02	1.02	1.02	0.51	0.59	0.05	845	0.50	0				
16	8.51	4.57ᵉ	4.32	4.57	4.57	4.06	4.57	0.58	0.05	839	0.49	0	0.06			
17	0	0	1.27	1.52	1.78	1.52	0.51	0.76	0.06	1,080	1.18	0	0.07			
18	9.02	7.62	6.35	7.37	4.83	7.37	5.84	0.69	0.06	988	0.86	0	0.07			
19	0	1.02	1.27	0.76	1.78	2.54	1.27	0.95	0.08	1,330	5.19	0	0.09			
20	3.15	2.79	2.03	3.05	1.78	4.32	2.03	0.81	0.07	1,150	1.49	0				
21	2.54	2.54	2.29	3.05	2.03	3.56	2.03	0.64	0.05	924	0.66	0				
22	11.18	10.16	8.89	10.67	9.14	9.14	8.64	3.16	0.25	4,100	141.00	0	0.34	0.06		
23	0	0	0ᵉ	0	0	0ᵉ	0	2.62	0.21	3,450	63.50	0				
24	0	0	0ᵉ	0	0	0ᵉ	0	1.58	0.13	2,140	12.20	0				
25	0	0	0ᵉ	0	0	0ᵉ	0	1.08	0.09	1,500	3.44	0				
26	0	0	0ᵉ	0	0	0ᵉ	0	0.86	0.07	1,210	1.64	0				
27	0	0	0ᵉ	0	0	0ᵉ	0	0.69	0.06	982	0.82	0				
28	0	0	0ᵉ	0	0.25	0ᵉ	0	0.64	0.05	923	0.66	0				
29	2.21	5.84	4.82ᵉ	2.79	10.41	8.00ᵉ	5.33	0.60	0.05	857	0.51	0				
30	0	0	0	0	0.25	0ᵉ	0	0.56	0.05	809	0.42	0				
31	1.57	1.27	1.27ᵉ	1.52	1.27	1.27ᵉ	1.52	0.66	0.05	938	0.70	0				
Aug. 1	0	0	0	0	0	0ᵉ	0	0.68	0.06	972	0.78	0				
2	1.02	0.51	0.76	0.76	1.78	1.02ᵉ	0.25	0.59	0.05	848	0.50	0				
3	0.25	0.25	0.25	0.25	0	0ᵉ	0.51	0.45	0.04	655	0.21	0				
4	61.72	53.09	64.26	56.64	66.04	65.00ᵉ	55.63	31.45	2.53	39,200	1.08x10⁶	1.07x10⁶	8.14	1.39	75.60	79.00
5	0	0	0	0	0	0.25	0.25	9.91	0.80	14,300	8,750.00	271				
6	0	0.25	0.76	0.25	0.51	0.25	0.76	3.50	0.28	5,330	153.00	0				
7	2.03	1.78	2.03	3.56	2.54	3.30	1.78	2.59	0.21	4,040	56.40	0				
8	9.32	8.00ᵉ	7.87	9.14	7.11	9.91	7.37	2.11	0.17	3,340	29.20	0				
9	5.59	5.59ᵉ	5.33	5.84	6.86	5.33	5.59	3.87	0.31	5,850	215.00	0	0.36	0.08		
10	0	0ᵉ	0	0.25	0	0.25	0	3.64	0.29	5,520	170.00	0				
11	0	0ᵉ	0	0	0	0	0	2.47	0.20	3,870	49.00	0				
* 12	23.47	19.56	19.05	22.35	14.73	16.76	20.07	4.01	0.32	5,860	1,410.00	0	0.97	0.19	0.09	
* 13	12.73	13.21	17.02	11.68	1.78	7.37	16.76	11.68	0.94	16,000	7,130.00	20.3	1.13	0.22	0.14	
* 14	14.99	13.72	17.02	7.87	0	17.00ᵉ	17.53	7.32	0.59	10,600	1,690.00	0				
* 15	0	1.78	0.51	1.52	1.52	0ᵉ	0	4.48	0.36	8,240	347.00	0				
16	0	0	0	0	10.67	0ᵉ	0	3.36	0.27	5,130	129.00	0				
17	0	0	0	0	0	0ᵉ	0	3.85	0.31	5,810	197.00	0				
18	12.19	10.67	10.67	12.96	9.91	13.00ᵉ	13.72	12.55	1.03	17,000	45,800.00	27,000	3.77		5.62	4.77
19	17.78	19.56	17.53	17.78	15.74	17.00ᵉ	16.76	31.00	2.49	38,500	0.268x10⁶	0.197x10⁶	4.44	0.76	11.00	9.57
20	8.64	8.38	8.38	9.14	9.40	9.40ᵉ	9.40	12.84	1.03	17,500	9,640.00	53.4				
21	0	0	0	0	12.95	7.00ᵉ	0	6.19	0.50	8,970	1,070.00	0				
22	2.92	2.79	3.30	3.56	23.37	15.00ᵉ	3.56	3.37	0.27	5,150	134.00	0				
23	26.67	29.46	31.50	32.00	27.18	32.00ᵉ	24.64	12.09	0.97	16,300	15,800.00	615	1.95	0.36	0.80	0.06
24	1.78	1.27	1.27	1.52	1.27	1.27ᵉ	1.02	12.39	1.00	16,900	11,200.00	168				
25	16.69	15.49	14.48	14.73	13.21	17.00ᵉ	17.53	7.59	0.61	10,800	2,420.00	5	1.04	0.20	0.11	
26	24.84	24.13	23.37	26.42	21.59	24.00ᵉ	22.10	14.85	1.20	20,000	16,600.00	282	1.59	0.30	0.41	0.01
27	2.03	1.52	7.62	4.06	6.86	6.00ᵉ	5.08	10.87	0.87	15,000	7,220.00	66				
28	5.08	5.59ᵉ	6.10	4.83	3.05	5.00ᵉ	4.32	9.04	0.73	12,700	3,280.00	0	0.92	0.18	0.07	
29	1.27	1.27ᵉ	0.76	1.52	1.52	1.52ᵉ	1.27	4.93	0.40	7,290	463.00	0				
30	1.37	0.76ᵉ	0.51ᵉ	0.25	0.76	0.25	1.27	3.25	0.26	4,980	118.00	0				
31	0ᵉ	0ᵉ	0ᵉ	0	1.02	1.27	0	2.33	0.19	3,670	40.40	0				
Sept. 1	0	0ᵉ	0	0	0	0	0	1.88	0.15	3,000	20.10	0				
2	3.56	2.03ᵉ	1.78	2.29	0.76	0.25	2.29	1.51	0.12	2,460	10.10	0				
3	0	0ᵉ	0	0	0	0	0.25	1.19	0.10	1,970	4.72	0				
4	0	0ᵉ	0	0	0	0	0	0.91	0.07	1,540	2.02	0				
5	0	0ᵉ	0	0	0	0	0	0.67	0.05	1,160	0.77	0				
TOTALS	364.61	330.95	359.13	379.94	367.53	141.71	352.83	331.98	0.38	452,000	4,570,000	4,870,000				
Estimated Totals		360.00ᵉ	365.00ᵉ			382.00ᵉ										

e   missing data, values estimated

* snow

PROGRESS REPORT ON A STUDY

OF OIL POLLUTION IN ICE COVERED RIVERS

Benjamin E. Keevil and René O. Ramseier

Glaciology Division
Water Resources Branch
Department of the Environment

under the

Environmental-Social Program
Northern Pipelines

CONTENTS

ABSTRACT

This study examines the behavior of oil under ice.
Cold room experiments are carried out to determine the physical
properties of crude oil in ice-covered water bodies.

Comparisons are made with observations taken under
field conditions.

PROGRESS REPORT ON A STUDY
OF OIL POLLUTION IN ICE-COVERED RIVERS

by

Benjamin E. Keevil and René O. Ramseier

INTRODUCTION

The discovery of oil in commercial quantities in northern
Canada could lead to the construction of oil pipelines to southern
markets. Such pipelines would cross many rivers and streams that
are subject to ice conditions of varying seasonal length. Any
river crossing is hazardous from the oil pollution standpoint and
a pipeline break at such a location could cause a great amount of
environmental damage. Problems associated with containment and
clean-up could also be intensified by a spill at a river crossing
site, particularly if ice conditions prevailed at the time of
the event.

Oil spills can be large such as those caused by a major
pipeline fracture or they can be small and insidious such as those
developing through pinholes of about 1 cm diameter in the pipe.
The behavior of oil spilled on and under ice at particular stages
of river ice cover development is not well understood. This study
attempts to define the behavior of oil under ice and its interactions
with an ice-covered river.

To date, laboratory experiments to determine the behavior
of oil under ice conditions have mainly been carried out in small
0.3 m square tanks of 0.6 m depths topped by a cold plate connected
to a refrigeration unit. In this study, a larger tank measuring
1.5 m in diameter and 0.7 m in depth was set up in a cold room.
Although this technique does not duplicate spill conditions in a
natural ice-covered water body, it nevertheless provides considerable
insight into the behavior of crude oil under ice. In addition,
a comparison of the experimental results with those of real spills
adds to the understanding of these events. The objectives of the
study are, therefore, to: (1) carry out cold room experiments
to determine the physical properties of crude oil under ice
conditions; (2) correlate the behavior of crude oil in cold room
tests with accidental spills in the field; and (3) write a scenario
on the behavior and fate of spilled crude oil in an ice-covered
river.

METHOD AND INSTRUMENTS

A circular aluminum basin, 1.5 m diameter and 0.7 m
deep is installed in a cold room capable of maintaining the air

temperature at   -15 ± 3°C. The cold room is equipped with a fan
to ensure uniform air flow and heat transfer in the basin. A
pressure relief overflow pipe releases and measures the volume of
water displaced by the growing ice sheet. Heating tapes are glued
to the outside of the tank and are covered with 10 cm of polystyrene
insulation. The heating tapes are connected to variacs set at very
low power to cancel out the bottom and side heat losses. This
combination of heating tapes and insulation allows one-dimensional
freezing in the basin and effectively simulates the growth of
natural ice. A schematic diagram is shown in Figure 1.

        The ice thickness is measured with ice-thickness gauges
(Syrinkov, 1963). The gauge is a small steel cylinder suspended
by a wire under the ice. To measure the thickness ,the cylinder
is raised to the ice-water interface and the distance from the
ice-air interface measured and subtracted from the total wire length.
The oil injection system is a 25-litre plastic tank with a gravity
fed electric pump. The system is portable and can easily be carried
into the cold room and connected to the oil injection pipe.

        An air-ice-water thermistor probe is used to obtain
temperature profiles with a relative accuracy of ± 0.2°C. The probe
contains 19precision thermistors (YSI No. 44033) mounted in a PVC rod
at a separation of 1 cm in the ice and 5 cm in the air and water. Each
thermistor, solder joint and wire is waterproofed with epoxy to ensure
that no water can leak into the system. A multi-conductor plug is
installed at the top of the probe for connection of the bridge circuit.
A rotary.switch enables each thermistor to be switched into the bridge,
balanced and the resistance recorded.

        The typical test procedure is as follows. At a cold
room temperature of -15°C the basin is filled with water to a
height of 60 cm. Two days later, a primary ice layer begins to
form. Its growth is predominantly in the horizontal plane forming
a very thin ice layer. The secondary ice grows parallel to the heat
flow, perpendicular to the water surface and reaches the desired
(6 to 8 cm) thickness in three days time. The temperature gradient
in the ice (about 0.5°C/cm) is linear. Norman Wells crude oil
(5 litres at 20°C) is pumped for about 70 seconds through a 1.3 cm
pipe and released 30 cm below the ice-water interface in the center of
the basin. A plastic grid (2 cm reference lines) and clock are placed
on top of the clear ice and the oil behavior is photographed through
the ice. Clear ice is obtained in the cold room due to one-dimensional
heat flow in the basin. After the oil is injected the ice continues to
grow and "sandwiches" the oil between ice layers. The mechanism of oil
entrapment is shown in Figure 2.

The following variables are kept constant for each test:

        oil type (Norman Wells crude, pour point -51°C)
        oil injection temperature ($+20^{\circ}$C)
        cold room temperature (-15°C)
        force and injection rate of oil pump ($0.4 \, kg/cm^2$;
          70 cc/sec)
        ice roughness (smooth)

PHYSICAL PROPERTIES OF NORMAN WELLS CRUDE OIL

The most significant properties of crude oil for the under-ice experiments are "pour point" and specific gravity. Pour point is the temperature below which the oil does not flow freely. Norman Wells crude oil has a pour point of -51°C. As all temperatures under the ice are above 0°C and the pipeline oil temperature is about 60°C, the crude oil will not freeze or become semi-solid. The specific gravity of Norman Wells crude (0.8) is less than water or fresh-water ice and as evaporation, aging and emulsification are negligible in still water under ice, crude oil will tend to flow over rather than under the ice. However, a natural ice cover floats with its ice surface above the water level thus preventing oil from spreading over the ice.

OIL BEHAVIOR UNDER ICE

The circular basin tests are designed to investigate the basic behavior of crude oil under fresh-water ice. Observations of oil particle formation, oil layer thickness, spreading rate under ice, sandwich mechanism and effect of a circular current have been made.

Particles

The most significant observation (Figure 5) of the behavior of hot crude oil released under ice is the separation of the oil into hundreds of small globs or particles 0.1 to 2.0 cm in diameter. When released from the injection pipe, the oil acts much in the same way as water falling from a tap and is separated into particles by surface tension. The crude oil particles are less dense than water and will rise to the water surface. However, the ice sheet is a boundary and the particles are flattened on the under-ice surface by reason of their buoyancy. While at the ice-water interface the smaller particles coalesce to form larger particles. This coalescing continues until several minutes later an oil layer has formed.

Oil Layer Thickness

The oil at the ice-water interface forms a layer about 1.0 cm thick under smooth planar ice.

Spreading Rate

The spreading rate of oil under ice is affected by the oil injection rate, properties, partitioning, separation into particles and the ice roughness. In the circular basin tests the oil injection rate, properties and ice roughness were constant, however, the separation into particles and partitioning cannot be controlled. As a result the spreading mechanism is complicated and there is no simple equation to predict spreading rate. The graph (Figure 3) shows the oil spreading radially at a rate of about 1.0 cm/s. The contrast between oil spreading on and under ice is shown in Figure 4.

Sandwich Mechanism

The mechanism by which an oil layer becomes sandwiched between fresh-water ice layers has been established. Ice grows around the oil layer and the oil is incorporated as a lense into the ice-oil-ice sheet. Even with a slow growth rate (0.5 cm/day) the oil is not pushed ahead by the growing ice-water interface. During one test 5.0 litre of oil was sandwiched between two 10 cm ice layers. A small hole was drilled down to the oil layer and about 1.0 litre of oil rose up the hole and spread on top of the ice. This indicates that sandwiched oil is pressurized within an ice cover which could be caused by cooling and subsequent contracting of the ice surrounding the oil layer. Future experiments will examine this mechanism further as it has practical application for clean-up of oil under ice.

Circular Current

To study the effect of a circular current on the behavior of oil under ice an electric outboard motor was mounted on the side of the basin and a circular oil boom installed to prevent the oil from rising up the tank walls and spreading over the ice surface. The outboard motor was turned on when the basin was filled with water and left running for the duration of the test. A detailed velocity profile across the basin was not obtained, however, a small current meter indicated an average velocity of about 0.1 m/s. The oil when released rose to the ice-water inter-face and circled around the center of the basin (Figure 6). Globs of oil broke up and coalesced due to the rotating motion. The

oil did not adhere to the smooth under-ice surface. The
partitioning effect, where the lighter and heavier fractions of
oil separate, was observed. During one circular current test
freezing of slush ice produced a very rough and uneven ice-water
interface. Most of the oil after injection collected in holes
and pockets and one day later all the oil was sandwiched by the
growing ice (2.0 cm/day).

OIL BEHAVIOR REPORTED IN ACCIDENTAL SPILLS

To compare the cold room behavior of crude oil with oil
behavior at accidental spills a summary of oil spills in rivers
is being prepared. Unfortunately accurate field observations of
oil spills in rivers are rare and it is difficult to find useful
reports. Most reports just mention that spilled oil disperses
rapidly in fast flowing waters. During 1972 and 1973 there have
been about 20 reported oil spills in rivers but only a few in
ice-covered rivers.

TABLE 1. SUMMARY OF OIL SPILLS IN RIVERS - JAN. 1972 - AUG. 1973

CAUSE	NO. OF INCIDENTS	GALLONS OF SPILLED OIL AT EACH INCIDENT		
Pipelines	3	20,000	52,000	250,000*
Storage Tanks	2	800*	13,000	
Tank Trucks	2	1,000	7,000	
Tests	1	270		
Others	2	900	1,500	
Unknown	4		Minor	

* Oil spill in ice-covered river

The only major reported spill in an ice-covered river
occurred in Sweden. In February 1972, an estimated 250,000 gallons
of diesel oil was spilled under the frozen river Ume. (Jerbo,
1973). The oil spread underneath the ice at the ice-water inter-
face and collected in the hollow surfaces beneath the ice. When
the oil was sandwiched, the thickness was estimated to be about
0.5 cm (personal communication, Jerbo). In the initial stages of the
oil spill 100,000 gallons were contained by the ice and did not move
more than 7 km downstream.

CIRCULAR BASIN FOR OIL
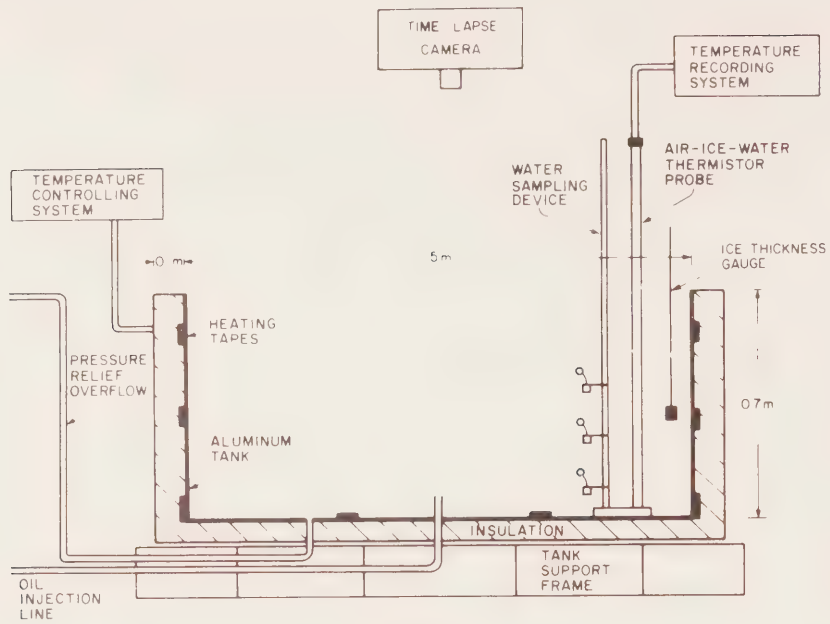
FIGURE I

ENTRAPMENT OF OIL UNDER ICE
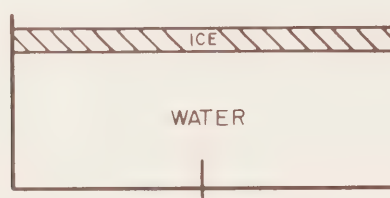
(A) INITIAL ICE LAYER
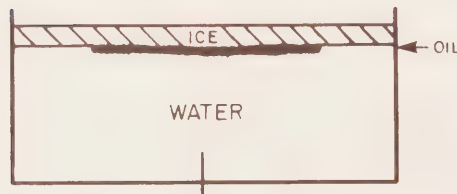
(B) OIL INJECTED UNDER
THE ICE
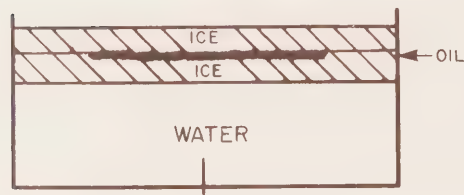
(C) OIL "SANDWICHED"
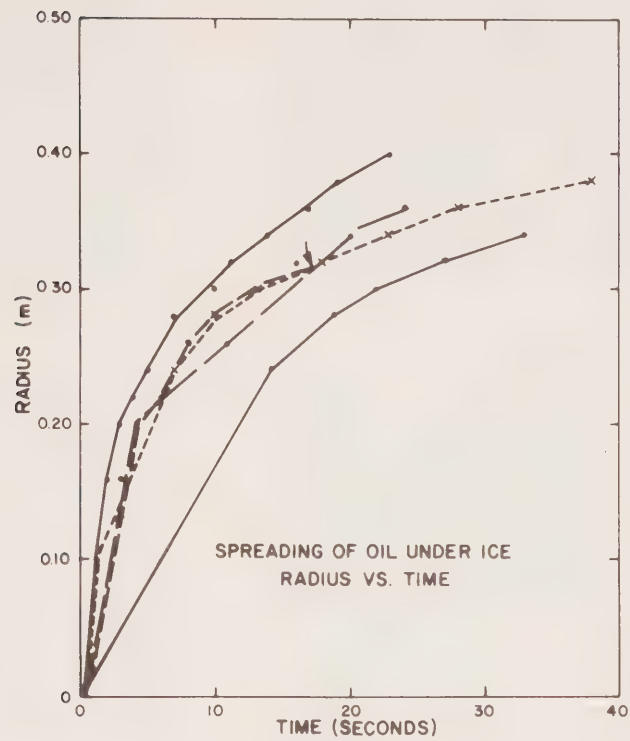BETWEEN ICE LAYERS

FIGURE 2

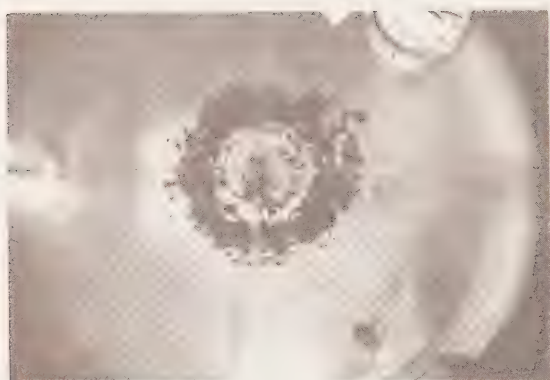# SPREADING OF OIL UNDER ICE

SPREADING OF OIL UNDER ICE
RADIUS VS. TIME

FIGURE 3

OIL ON AND UNDER ICE

FIGURE 4

FIGURE 5
OIL SPREADING UNDER ICE
NO CURRENT
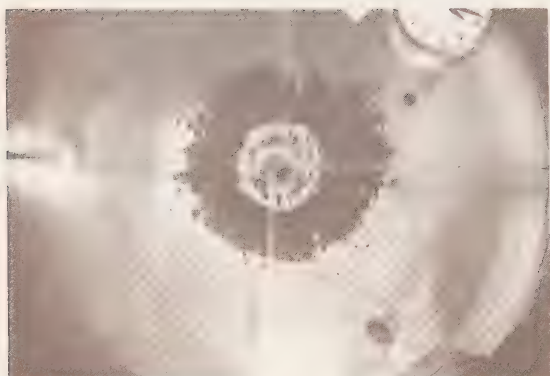
FIGURE 6
OIL SPREADING UNDER ICE
CIRCULAR CURRENT

5 - 1

note: grid spacing
2.0 cm.

6 - 1

5 - 2

6 - 2

5 - 3

6 - 3

5 - 4
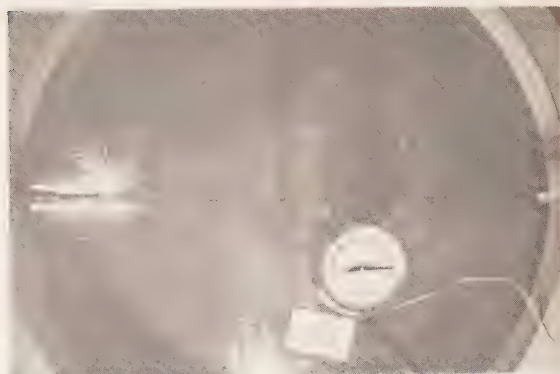
6 - 4

Two conclusions can be drawn from this summary of oil spills in rivers. First, oil spilled in ice free rivers is quickly dispersed and emulsified downstream. Second, oil spilled in ice-covered rivers quickly disappears from sight under the ice and many spills are not reported.

SUMMARY OF PROJECT PROGRESS

Cold room experiments designed to simulate an under-ice pipeline leak demonstrated the basic behavior of crude oil under ice. The following observations were made:

(1) That crude oil when released under the ice separates into small globs or particles 0.1 to 2.0 cm in diameter.

(2) The particles coalesce at the ice-water interface and form an oil layer about 1.0 cm thick under smooth fresh-water ice.

(3) In still water the oil layer is not pushed ahead of the growing ice-water interface but becomes sandwiched by the growth of the ice around the oil.

(4) In moving water the oil can be sandwiched in pockets and holes at the ice-water interface providing the current is less than 0.1 m/s.

Observations at accidental oil spills have confirmed the basic behavior of oil under ice.

PLANS FOR FUTURE WORK

Future cold room experiments will determine the insulating effect of a sandwiched oil layer on heat transfer through an ice sheet. The circular basin will be divided in two halves with polystyrene, one-half will have oil under ice and the other will be a control.

Data on the fate and behavior of spilled oil at accidental oil spills will be collected. Arrangements have been made with Environment Protection Service to notify us of any oil spills in ice-covered rivers. Sampling equipment to measure oil layer thickness and to sample for oil in water under ice is being developed.

This combination of cold room experiments and accidental oil spill documentation will provide enough data to write a scenario on the behavior and fate of spilled crude oil in an ice-covered river.

BIBLIOGRAPHY

1. Barber, T., 1971. <u>Oil spills in ice. Some clean-up options</u>, Arctic 23:285.

2. Chen, E.C., 1973. <u>Arctic Winter Oil Spill Test</u>, Inland Waters Directorate, Department of the Environment, Technical Bulletin No. 68, Canada.

3. Frank, R.J., 1969. <u>Oil Pollution Control on the Buffalo River</u>, Proceedings of the Joint Conference on Prevention and Control of Oil Spills, Washington, D.C.

4. Gleaser, J.L. and Vance, G.P., 1971. <u>A Study of the Behavior of Oil Spills in the Arctic</u>, AD717142 National Technical Information Service, Springfield, Virginia.

5. Jerbo, Alan, 1973. <u>Two types of Oil spills in Swedish Inland Waters</u>, Proceedings of Joint Conference on Prevention and Control of Oil Spills, Washington, D.C.

6. Johannessen, O.M., 1970. <u>Note on some vertical profiles below ice floes in the Gulf of St. Lawrence and near the North Pole</u>. J. Geophys. Res. 75:2857.

7. Lewis, E.L., 1970. <u>Experiments on freezing oil-sea water combinations</u>, Frozen Sea Research Group. Unpublished Report.

8. McMinn, T.J. and Golden, P., 1973. <u>Behavioral Characteristics and Clean-up Techniques of North Slope Crude Oil in an Arctic Winter Environment</u>, Proceedings of Joint Conference on Prevention and Control of Oil Spills. Washington, D.C., March, p. 263.

9. Operation Oil, 1970. <u>Clean-up of the Arrow oil spill in Chedabucto Bay</u>, Report to the Minister of Transport.

10. Ramseier, R.O., 1973. <u>Possible Fate of Oil in the Arctic Basin</u>, First World Congress on Water Resources, Chicago.

11. Ramseier, R.O., 1971. <u>Oil Pollution in Ice-Infested Waters</u>, Proceedings International Symposium on Identification and Measurement of Environmental Pollutants, June 14-17, Ottawa, p. 271.

12. Ramseier, R.O., 1973. Gantscheff, G.S. and L. Colby. <u>Oil spill at Deception Bay, Hudson Strait</u>. Department of the Environment, Ottawa. (in press).

13. Syrinkov, P.I., 1963. "Means of Measuring the Thickness of Ice Without Making Holes in the Ice, "Sbornik "Za Ratsionalizatsiyu v Gidrologii", (Handbook "Toward Rationalization in Hydrology"), Leningrad.

14. Wolfe, L.S. and Hoult, D.P., 1973. <u>Effects of Oil Under Ice</u>, Department of Mechanical Engineering, Massachusetts Institute of Technology.

PROGRESS REPORT ON BANK EROSION STUDIES
IN THE MACKENZIE RIVER DELTA, N.W.T.

by

David N. Outhet

TABLES

FIGURES

ABSTRACT

Analysis of time lapse photography in the field and from the air, along with other data collected in the field, indicates that in the southern Mackenzie River Delta, the shape of an eroding bank is positively correlated with the erosion process and the rate and character of erosion. The primary factors of current velocity, channel orientation to the wind, and ice content of the bank sediment act along with several minor factors to cause the differences in shapes. There are five different easily-distinguished bank shapes in the study area each with its own maximum and minimum erosion rates and manner of erosion. This information allows the prediction of eroding bank behaviour and the production of a map showing the behaviour category into which each bank fits. This map may be used in the planning of construction in the area to avoid rapidly eroding banks such as those that may erode up to 30 m/yr.

PROGRESS REPORT ON BANK EROSION STUDIES
IN THE MACKENZIE RIVER DELTA, N.W.T.*

by

DAVID N. OUTHET

Introduction

Human activities in the Mackenzie River Delta have increased markedly over the last few years due to the search for oil and gas. Construction of wharves, buildings, drilling platforms and storage tanks has occurred or is contemplated at a number of sites within the delta. The choice of these sites is important because delta flooding is common, bank erosion is variable and permafrost is present. This study examines the bank erosion problem and its relation to current velocity, wind, break-up associated current velocities, permafrost and other parameters.

Bank erosion can be examined in a number of ways. Air photographs taken over a large interval of years can provide information from which estimates of erosion rates can be made. Prediction of bank behaviour may also be possible if the effects on channel geometry caused by changes in flow, suspended sediment, break-up and other physical factors are known. A third clue to estimation and prediction of bank stability lies in the analysis of ages of successional vegetation on point bars and slip-off slopes situated cross-channel from retreating cut banks. A fourth approach (used in this study) is to examine the processes of erosion at specific delta sites and relate them to the character, shape and evolution of the channel banks.

Area and Site Selection

A study area in the upper delta south of 68°N (Figure 1), was chosen for several reasons:

1. The apex of the delta is the site of highest fluvial energy and therefore the site of highest banks and highest erosion rates.
2. Extensive field reconnaissance during 1971 and 1972 showed that a wide range of eroding bank types exist on all sizes of channels with a variety of orientations.

---

* This report is a summary of a thesis submitted by the author for partial fulfillment of an M.Sc. degree at the University of Alberta under the title of: Bank Erosion in the Southern Mackenzie River Delta, N.W.T., Canada, 85 pages.

3. Most of the channels are deep enough for navigation by
   boats with a 1 m draft through the summer period until
   freeze-up.
4. The study area is easily accessible from Inuvik.
5. No previous studies of erosion have been done in the
   study area.

The locations of specific study sites are shown in Figure 2. These
sites are characteristic of the varying erosional behaviour seen along the
channels that form the upper delta complex. Several small reversing channels
and one large one, a section of Peel Channel above and below Indian Village
(Figure 2), are included as are channel segments with large ice wedges (Plate 1)
and ones with ice-rich sediments (Plate 2). The levees of the area are
approximately 10 m above average late summer low water (Mackay, , 1963). The
details of the 15 sites chosen for intensive study are as follows:

Site A - an overhanging bank with a deep thermo-erosional niche
         (hereafter referred to as a niche), located on a NW oriented
         reach; ice layers visible in the thawing bank face; high
         current velocities near the bank levee; surface covered by
         a mature white spruce forest; large stumps with well
         developed adventitious rooting* in the bank material.

Site B - an overhanging bank with a shallow niche; a former
         point bar deposit; no visible ice in the bank; very
         high current velocities with boils and eddies; a
         reversing flow during break-up.

Site C - a concave bank similar to Site A , with a different
         orientation; ice layers visible in the bank.

Site D - situated on a concave bank of the reversing part of
         Peel River; bank appearance similar to that of Site C.

Site E - typical of an eroding island with a willow-alder plant
         association; low ice-content sediment; very little
         vegetation mat overhang; current fairly strong; NW
         orientation of the channel reach.

---

* White spruce can send out lateral roots into new additions of alluvium
  enabling it to survive the associated upward movement of the permafrost
  surface occurring in such environments.

Site F - very similar to E although on a convex bank;
        erosion is by current coming out of the channel
        running past Indian Village; orientation
        similar to E but shorter fetch in a NNW Direction.

Site G - on a convex bank eroded by current from the Peel
        River entering the Peel Channel; bank much lower
        than others (4 m instead of 8 m); erosion of a
        former slip-off slope.

Site H - on a short concave bank backed by a levee of the
        Middle Channel; this site has been cleared of
        trees by man.

Site I - similar to site C; a concave bank of the Peel River.

Site J - a short concave section in a convex bank being eroded
        by current from the Peel River.

Site K - a concave levee of the East Channel; chosen as repre-
        sentative for this particular size of channel.

Site L - representative of many eroding levees with beaches
        along the Middle Channel; a NNW orientation with long
        open-water fetch and active wave erosion.

Site M - similar to L except for a larger beach and some ice-
        rafted pebbles; no measurable current velocity at
        sites L and M when chosen.

Site N - chosen as representative of eroding levees along
        channels the size of Peel Channel; on a concave
        bank, with some vegetation on slopes.

Site O - similar to site N, although bank material more bonded
        by roots and driftwood.

Only banks which appeared to be actively eroding were chosen for
continued observation. Choices were made in August, 1972. Field work
and air photo interpretation were carried out over the following year.

Many banks in the area are relatively stable and did not warrant
observation. Prograding point bars with temporary strandline erosion*
(Plate 3) were omitted as were highly vegetated banks (Plate 4) and
banks with sufficient vegetation (Plate 5) to minimize annual erosion.

*Strandline erosion here refers to fluvial erosion at the water line
along a channel. A succession of eroded strandlines can develop with
a drop in water levels.

Methods and Data Collection

As mentioned previously, one method of determining bank erosion and retreat is to examine air photographs. Photos for the area taken in the years 1950, 1962, 1965, 1971 and 1972 were examined and estimates of bank retreat were made for the 23-year period of aerial photo coverage.

Data collection in the field involved the establishment of control points at all sites in August, 1972. These points were either on trees or consisted of stakes placed sufficiently deep in the ground that frost-heaving would not significantly affect horizontal control. The distance from the control point to the bank edge was measured as in Figure 3.

Stereo photos (Plate 6) were taken of the banks at the time of measurement. This provided a scaled visual record of: 1) the distance of the bank face to the horizontal control point; 2) the height of the bank above water level; 3) the shape of the bank; and 4) the extent of roots and driftwood incorporated in the sediment. Measurements were made every 2 weeks in 1973, covering the period from spring ice clearance through to the end of August.

A number of factors considered important in bank erosion were measured during the field program. Current velocity measurements (Table 1) were made every two weeks 5 m out from the water's edge and 1 m below the water surface. Windspeed and direction were monitored continuously with a Lambrecht Woelfle type recorder located at the junction of the Middle and East channels (Figure 2). The results are presented in the form of a wind rose for the period of measurement in 1973 (Figure 4). The open-water fetch, measured in a NNW direction to coincide with the prevailing wind, is shown in Table 2 and is later used in multivariate analysis of the erosion problem. Wind blowing upstream over a long open-water fetch produces larger waves than a wind of the same velocity blowing downstream.

Sediment samples taken at a minimum of 3 points along the bank profile were tested for moisture content, liquid limit and, in some cases, for particle size distribution. Averaged results for moisture content and liquid limit are recorded in Table 3 and particle size distribution ranges are shown in Figure 5.

Erosional Processes

The visible effects of erosional processes were examined and recorded at each bank site. Sloughing occurs at many bank faces. Sloughing is the falling away of small blocks (several cm^3) from the vertical face of a bank. The size of these blocks, where they accumulated, and the type of surface left on the bank face were noted.

Soil flow occurs at bank faces with ice-rich sediment. Thawing releases water from segregated ice layers which saturates surrounding thawed sediment layers causing an unstable condition. The movement, appearance, and location of flows were noted.

Wave action undercuts some banks at the waterline and builds beaches of loosened material through swash and backwash. The extent and location of beaches developed by this process was noted along with the approximate heights of waves producing them.

Depths and locations of thermo-erosional niches were noted although penetration of the larger niches (more than 3 m) was only estimated due to the hazardous situation at such locations. As the niche develops, the weight of the overhanging block of soil increases the tension in the bank along a vertical line from the apex of the niche to the top of the bank. Eventually, the tension exceeds the tensile strength of the sediment, failure occurs, and the block falls into the channel. Notes were made on the size of such blocks, the dimensions and location of tension cracks, and the nature of features such as ice wedges which provide zones of weakness.

A number of other erosional factors have been considered. Roots are important for the bonding of bank materials as indicated, for example, in Plate 7. Surface bank temperatures and water temperatures can be significant as frozen silt is harder to erode by fluvial action than unfrozen silt. Although break-up current velocities may be high, water temperatures close to freezing allow only loose material to be eroded. The action of ice alone in the delta channel break-up can sometimes be important, but its erosional effects are often attenuated by a near shore ice wreckage barrier. Plate 8 demonstrates the protection afforded banks by near-shore ice. Mackenzie River ice also enters the delta and, with high water conditions, is swept onto beaches, banks and levees with apparent minor erosional degradation (plates 9, 10 and 11). Another factor, the surface vegetational mat retards thaw of bank materials and reduces erosion.

Results and Conclusions

Banks at research sites were categorized according to profiles or "shapes" and placed into 5 classes. Idealized profiles considered representative of each class are shown in Figures 6, 7 and 8. Although the procedure is arbitrary for banks which are borderline cases, the groupings are realistic on the basis of initial field examination in August 1972. Plates 12 to 18 illustrate banks in the various classes.

Figures 9 to 12 show the amount of 1973 linear erosion from the date of one measurement to the next. The initial measure of bank recession on June 7th, 1973 indicates the total amount from the date of selection in August 1972. These non-cumulative graphs show that much of this erosion for some banks (shapes 3, 4 and 5) took place during the 1973 break-up (Table 5). Other banks (shapes 1 and 2) eroded mostly during the two weeks after break-up.

Mean rates of bank retreat determined from inspection of aerial photographs are listed in Table 4. The August 1973 position of many lengths of bank were plotted on old photos and mean yearly rates determined by measurement of differences. One example of air photo use is given in Plate 19.

The association of a number of physical factors likely to be important in bank recession was tested statistically using correlation and regression techniques. The dependent variable was linear erosion taken every 2 weeks or over the year. The independent variables were current, open water fetch and sediment ice content. All variables were tested in various combinations. The variables, in general terms, are presented in Table 5 for each site. The results of the statistical tests are shown in Tables 6 and 7. It appears from the multiple regression analysis that high near-shore current velocities are associated with actively eroding banks. This suggests that delta and river channels in permafrost environments shift as elsewhere with erosion occurring on the outside or cut bank side of meanders where currents are highest. Large scale sloughing, however, is somewhat greater than in more temperate delta environments due to the development of thermo-erosional niches and to structural weaknesses associated with ice wedges and other forms of ground ice. Banks along channels with favourable orientation for wave production (a long open-water fetch for upstream winds) will have erosion accelerated by wave action. Wave erosion is also significant in affecting the appearance of banks to produce beaches or strandline erosion.

Bank shapes may evolve from one to another due to the primary factor of near-shore current velocities mentioned above. Hydraulic geometry changes caused by new bars, scouring beneath ice jams or changes in channel discharge may change near-shore current velocities. A higher velocity will lower the number of the shape and vice versa. For example, deposition of a new bar may be associated with higher near-shore current velocity resulting in a change from shape 3 to shape 2 or even shape 1. There is no evolution between shapes 4 and 5 as their distinction is caused by differences in the orientation and open-water fetch of a channel reach for upstream winds.

Bank sediments with high near-surface ice content are subject to slow attrition by melting and movement of flowing mud and, in addition, to rapid degradation by development of thermo-erosional niches at the waterline with subsequent large-scale sloughing. Banks made up of low-ice content sediments will be more susceptible to sloughing of materials rather than a flowage and are less likely to develop thermo-erosional niches.

Tables 4 and 5 indicate that, within the study area, banks classed according to shape experience the following rates of recession:

Shape 1:   5-30 m/yr
Shape 2:   10-15 m/yr
Shape 3:   5-10 m/yr
Shape 4:   0-5 m/yr
Shape 5:   0-5 m/yr

Table 5 also indicates the character of erosion associated with each of the above shapes. Catastrophic erosion (type 1) is caused by the undermining of a bank by a niche which may cause a block to fall. This may occur at both bank shapes 1 and 2 if niches are deep enough. Continuous removal of material by current and wave action (type 2) also happens at bank shapes 1 and 2 which have moderate to high current velocities all summer. Continuous removal is why these bank shapes have higher erosion rates than other shapes. A combination of erosion types 1 and 2 may produce the extremely high rate of 28 m/yr found at Site B. Intermittent removal of material (type 3) is caused by variations in channel discharge or variations in wind velocities and directions. Type 3 erosion is associated with bank shape 3. Because of soil flow, banks of shape 4 or 5 with ice-rich sediment will have continously-retreating bank faces all summer (type 4). Banks with low ice content sediment will have very slowly-

retreating bank faces all summer. Mass wasting by sloughing is much
slower than by soil flow. Both types 4 and 5 are characterized by
the removal of sediment during break-up when unconsolidated slough slope
material is carried away.

The application of these rates shapes, and behaviour to part of the
study area is demonstrated in Figure 13. Mapping of other delta areas could
prove of benefit to agencies concerned with development of logistic networks,
community services, oil and gas exploration and other activities. Further
data collection will enhance the basis for making recommendations relevant
to construction and development within the Mackenzie Delta.

Acknowledgements

BIBLIOGRAPHY

Abrahamsson, K.V. 1966. Arctic environmental changes.
Arctic Institute of North America, Research
Paper 39. 79 pp.

Abramov, R.V. 1957. Thaw-out niches. Priroda:
ezhemsiachyni: estestvennc nauchnyii zhurna;
Akademii nauk SSSR 46(7):112-113.

American Society For Testing Materials. 1960. Book of
standards, Part 4:151-161.

Anderson, R.J. and D.K. MacKay. 1973. Seasonal distri-
bution of flow in the Mackenzie Delta, N.W.T.
Pages 71-109 in Hydrologic aspects of northern
pipeline development. Environmental-Social
Committee on Northern Pipelines, Task Force on
Northern Oil Development, Report No. 73-3.
Information Canada, Cat. No. R27-172. 664 pp.

Annersten, L.J. 1966. Interaction between surface cover
and permafrost. Biul. Peryglacjalny 15:27-33.

Blench, T. 1966. Mobile-bed fluviology. T. Blench and
Assoc. Ltd., Edmonton. 300 pp.

Brown, R.J.E. 1956. Permafrost Investigations in the
Mackenzie Delta. Can. Geog. 7:21-26.

Brown, R.J.E. 1966. Influence of vegetation on permafrost.
Pages 20-25 in Permafrost: proceedings of an
international cconference. National Academy of
Sciences, Wash. D.C.

Chyurlia, J. 1973. Stability of river banks and slopes
along the Liard and Mackenzie River, N.W.T.
Pages 111-152 in Hydrologic aspects of northern
pipeline devlcpment. Environmental-Social
Ccmmittee on Northern Pipelines, Task Force on
Northern Oil Development, Report No. 73-3.
Information Canada, Cat. No. R27-172. 664 pp.

Cooper, R.H. and A.B, Hollingshead. 1973. River bank
erosion in regicns of permafrost. Unpubl.
paper presented at N.R.C. Ninth Canadian
Hydrology Symposium, University of Alberta,
Edmonton, May 8-9. 14 pp.

Gill, D. 1971. Vegetaticn and environment in the Mackenzie
River Delta: a study in subarctic ecology.
Unpubl. Ph.D. thesis, University of British
Columbia. 694 pp.

Gill, D.   1972a.   The point bar environment in the
          Mackenzie River Delta.   Can. Jour. Earth Sci.
          9(11):1382-93.

Gill, D.   1972b.   Modification of levee morphology by
          erosion in the Mackenzie River Delta.   Pages
          123-138 in R.J. Price and D.E. Sugden (eds.),
          Polar geomorphology.   I.B.G. Special Publ. No. 4.

Gill, D.   1973a.   Floristics of a plant succession sequence
          in the Mackenzie Delta, Northwest Territories.
          Polarforschung 43(1/2):55-65.

Gill, D.   1973b.   Native-induced secondary plant succession
          in the Mackenzie River Delta, Northwest Terri-
          tories, Canada.   Polar record 16(105):805-808.

Gill, D.   1973c.   Modification of northern alluvial habitats
          by river development.   Can. Geog. 17(2):138-153.

Gill, D.   1973d.   A spatial correlation between plant
          distribution and unfrozen ground within a region
          of discontinuous permafrost.   Pages 105-113 in
          Permafrost: the North American contribution to
          the Second International Conference, ISBN 0-309-
          02115-4, Nat. Acad. Sci., Wash. D.C.

Gill, D.   1973e.   Ecological modifications caused by the
          removal of tree and shrub canopies in the
          Mackenzie Delta.   Arctic 26(2):95-111.

Gusev, A.I.   1959.   On the methods of surveying the banks
          at the mouths of rivers of the polar basin.
          Nauchno-issledovatel'skii institut geologii
          Arktiki, Leningrad 107:127-132.

Henderson, F.M.   1966.   Open channel flow.   Macmillan
          Co., New York.   522 pp.

Henoch, W.E.S.   1960.   Fluvio-morphological features of the
          Peel and Lower Mackenzie Rivers.   Geog. Bull.
          15:31-45.

Jessop, A.M.   1970.   How to beat permafrost problems.
          Oilweek, Jan. 12.

Johnston, G.H., and R.J.E. Brown.   1964.   Some observations
          on permafrost distribution at a lake in the
          Mackenzie Delta, N.W.T., Canada.   Arctic 17(3):
          163-175.

Johnston, G.H. and R.J.E. Brown.   1965.   Stratigraphy of the
          Mackenzie River Delta, N.W.T., Canada.   Bull.
          Geol. Soc. Amer. 76:103-112.

Kaplina, T.N.   1959.   Some features of outwash shores
          composed of permanently frozen earth.   Doklady
          Okeanograficheskaia Komissiia, Moscow, Akademiia
          nauk SSSR 4:   113-117.

King, L.J.   1969.   Statistical analysis in geography.
          Prentice-Hall Inc., Englewood Cliffs, N.J.
          288 pp.

Kolb, C.R.   1963.   Sediments forming the bed and banks of
          the Lower Miss. River and their effect on river
          migration.   Sedimentology 2:227-234.

Lambe, T.W. and R.V. Whitman.   1969.   Soil mechanics.   John
          Wiley and Sons Inc., New York.   553 pp.

Leopold, I.B., M.G. Wolman, and J.P. Miller.   1964.   Fluvial
          processes in geomorphology.   W.H. Freeman and Co.,
          San Francisco.   522 pp.

Lewellen, R.J.   1972.   Studies on the fluvial environment,
          arctic coastal plain province, northern Alaska.
          Published by the author, P.O. Box 1068, Littleton,
          Col.   282 pp.

Lomachenkov, V.S.   1959.   The preparation of maps on the
          morphology and dynamics of the banks of low river
          terraces in an area of permafrost.   Nauchno-
          issledovatel'skii institut geologii Arktiki,
          Leningrad 107:127-132.

MacKay, D.K.   1965.   Break-up on the Mackenzie River and its
          delta, 1964.   Geog. Bull. 7:117-128.

MacKay, D.K.   1966.   Mackenzie River and Delta ice survey,
          1965.   Geog. Bull. 8:270-278.

MacKay, D.K.   1969.   The ice regime of the Mackenzie Delta,
          N.W.T.   Inland Waters Br., Ottawa, Reprint
          Series, No. 83:356-362.

MacKay, D.K. and J.R. Mackay.   1973.   Break-up and ice
          jamming of the Mackenzie River, N.W.T.   Pages
          223-232 in Hydrologic aspects of northern pipeline
          development.   Environmental-Social Committee on
          Northern Pipelines, Task Force on Northern Oil
          Development, Report No. 73-3.   Information Canada,
          Cat. No. R27-172. 664 pp.

Mackay, J.R.   1963.   The Mackenzie Delta area, N.W.T.
          Memoir 8, Geographical Br., Canada.   202 pp.

Mackay, J.R.   1967a.   The age of permafrost in the lower

Mackenzie Valley, N.W.T. A.A.A.G. 57(4):795.

Mackay, J.R. 1967b. Permafrost depths, Lower Mackenzie
        Valley, N.W.T. Arctic 20(1):21-26.

McCloy, J.M. 1969. Morphologic characteristics of the
        Blow River Delta, Yukon Territory, Canada. Ph.D.
        Thesis. Louisiana State University. 161 pp.
        University Microfilms, Ann Arbor, Mich.

McCloy, J.M. 1970. Hydrometeorological relationships and
        their effects on the levees of a small arctic
        delta. Geograf. Annaler 52A(3-4):223-240.

McRoberts, E.C. 1973. Stability of slopes in permafrost.
        Unpubl. Ph.D. thesis. University of Alberta,
        Edmonton.

Mollard, J.D. 1973. Airphoto interpretation of fluvial
        features. Ninth Canadian Hydrology Symposium,
        Univ. of Alberta, Edmonton, May 8-9. 38 pp.

Shirley, M.L., ed. 1966. Deltas. Houston Geological
        Society. 251 pp.

Smith, M.W. 1972. Observed and predicted ground
        temperatures, Mackenzie Delta, N.W.T. Pages 95-
        106 in D.E. Kerfoot (ed.), Mackenzie Delta mono-
        graph. 22nd Int. Geogr. Cong., Brock Univ., St.
        Catharines, Ont.

Smith, M.W. 1973. Factors affecting the distribution of
        permafrost, Mackenzie Delta, N.W.T. Unpubl. Ph.D.
        Thesis. Univ. of British Columbia. 186 pp.

Smith, M.W. and C.T. Hwang. 1973. Thermal disturbance due
        to channel shifting, Mackenzie Delta, N.W.T.,
        Canada. Pages 51-60 in Permafrost: The North
        American Contribution to the 2nd Int. conf.,
        ISBN 0-309-02115-4, Nat. Acad. Sci., Wash. D.C.

Stearns, S.R. 1966. Permafrost. Cold Regions Science and
        Engineering, Part1, Sect. A2, CRREL. 77 pp.

Terzaghi, K. and R. Peck. 1948. Soil mechanics in
        engineering pracitce. John Wiley and Sons, New
        York. 566 pp.

Turnbull, W.J., M. Krinitzsky, and F.F. Weaver. 1966.
        Bank erosion in soils of the Lower Miss. Valley.
        Proc. ASCE 92(SM4):121-136.

Walker, H.J. 1969. Some aspects of erosion and sedimenta-

tion in an arctic delta during breakup. Tech.
Report No. 90, Coastal Studies Inst., Office of
Naval Research, U.S. Govt. 11 pp.

Walker, H.J. and L. Arnborg. 1966. Permafrost and ice-
wedge effect on riverbank erosion. Pages 164-171
in Proc. Perm. Int. Conf., Nov. 11-15, Lafayette,
Ind. N.R.C. Pub. No. 1287:164-171.

Walker, H.J. and J.M. McCloy. 1969. Morphologic change in
two arctic deltas. Arctic Inst. of North America,
Final Report cf Grant No. DA-ARO-D-31-124-G832.
91 pp.

Walker, H.J. and H.M. Morgan. 1964. Unusual weather and
river bank erosion in the delta of the Colville
River, Alaska. Arctic 17(1):41-47.

Williams, J.R. 1952. Effect of wind-generated waves on
migration of the Yukon River in the Yukon Flats,
Alaska. Science 115(2283):519-520.

Williams, P.J. 1968. Ice distribution in permafrost
profiles. Can. Jour. Earth Sci. 5:1381-1386.

Wolman, M.G. 1959. Factors influencing erosion of a
cohesive river bank. Am. Jour. Sci. 257: 204-
216.

Table 1 CURRENT VELOCITIES (cm/sec)

Site	Shape	Velocities at the Termination of Break-up June 7 - 9 1973	Average Summer Velocities	Highest Recorded Velocities	Dates of Highest Recorded Velocities	Lowest Recorded Velocities	Dates of Lowest Recorded Velocities
A	1	----	15.4	32.4	June 22	0	July 18
B	1	33.5	45.0	77.5	Aug. 21	16.2	June 21
C	1	35.7	41.0	46.5	June 22	30.5	July 6
D	1	49.5	46.3	61.0	Aug. 2	34.0	July 6
E	2	----	38.1	50.5	June 20	0	Aug. 2
F	2	----	33.5	34.5	June 21	32.3	July 5
G	2	24.4	0	24.4	June 8	0	All summer
H	3	46.5	15.3	46.5	June 9	0	July 18
I	3	36.0	39.0	56.5	Aug. 18	28.0	June 21
J	3	49.5	23.6	61.0	Aug. 2	0	July 6
K	3	----	12.2	15.3	July 7	6.1	July 31
L	4	0	0	0		0	All summer
M	4	0	0	0		0	All summer
N	5	24.4	21.4	25.9	July 7	15.0	Aug. 17
O	5	----	22.2	25.6	July 7	19.8	Aug. 17

---- no measurement taken

0   velocity too slow to measure

Table 2   OPEN-WATER FETCH IN A NNW DIRECTION (337.5°)
FROM EACH BANK SITE IN KILOMETERS
(Measured from NTS Maps: 106M/9; 106M/10; 106M/16)

Site	A	B	C	D	E	F	G	H	I	J	K	L	M	N	O
Fetch km	0	0.4	0.4	0	7.0	0	0	10.3	0	0	0	5.8	5.6	0	0
Channel Orientation	NW-SE	NW-SE	NE-SW	NW-SE	NW-SE	NW-SE	E-W	N-S	E-W	N-S	NE-SW	N-S	N-S	NW-SE	NW-SE

Table 3   AVERAGE MOISTURE CONTENT AND LIQUID LIMIT FOR ALL
SAMPLES TAKEN FROM EACH BANK SITE

	Group 1: sites with segregated ice						Group 2: sites with no segregated ice								
Site	A	C	D	J	L	M	B	E	F	G	H	I	K	N	O
Moisture Content	53	60	73	38	43	54	33	30	35	28	29	42	26	40	26
Liquid Limit	27	39	37	26	31	38	27	23	25	26	28	35	25	40	27
Difference	26	21	36	12	12	16	6	7	10	2	1	7	1	0	-1

Table 4   EROSION RATES MEASURED FROM AIR PHOTOGRAPHS AT LOCATIONS
          CHECKED BY HELICOPTER SURVEY.   SHAPES DETERMINED BY BOAT
                                    SURVEY.

Bank Length Location	Erosion Rate m/yr.	Common Shapes
Upstream and downstream of Site A	9-11	1 and 2
" B	7	2 and 3
" C	8	1 and 3
" D	5-8	2 and 3
" E	6-8	2 and 3
" F	7	2 and 3
" G	9	3
" H	4-6	3 and 4
" I	4	3 and 5
" J	5	3
" K	1-3	5
" L	2-4	4
" M	1-2	4
" N	2	5
" O	1	5
East Channel-East Bank	1-2	4
Across from Site J	3	3 and 5
67°39'N 134°37'W	6	3

Table 5 BANK BEHAVIOR, SHAPES, AND EROSION FACTORS

Site	Shape	Meters of Annual Linear Erosion	Average Summer Current	Sediment Ice Factor	Wave Factor	Height (m) Above Water Level Aug. 16	% of Annual Erosion at Break-up	Current Pattern a	Character of Erosion b
A	1	25.0	moderate	high	moderate	7.0	61	1	1 and 2
B	1	28.0	high	low	moderate	5.5	13	1	1 and 2
C	1	6.2	high	high	low	6.5	16	1	2
D	1	6.5	high	high	moderate	7.5	15	1	2
E	2	12.6	high	low	high	8.5	48	1	1 and 2
F	2	11.8	high	low	moderate	8.5	9	1	1 and 2
G	2	13.8	low	low	low	3.7	76	2	3
H	3	7.0	moderate	low	high	7.5	43	1	3
I	3	7.5	high	low	low	7.0	47	1	3
J	3	7.0	moderate	high	moderate	6.5	36	1	3
K	3	4.7	moderate	low	low	5.0	45	1	3
L	4	2.6	low	high	high	6.0	54	2	4 or 5
M	4	2.5	low	high	high	6.5	52	2	4 or 5
N	5	2.5	moderate	low	moderate	6.0	80	1	4 or 5
O	5	1.0	moderate	low	moderate	6.0	50	1	4 or 5

Notes: a) Current Pattern
1. Measurable current all summer
2. Measurable for c. 2 weeks following break-up
b) Character of Erosion
1. catastrophic
2. continuous by current or wave
3. intermittent by current or wave
4. continuous but mainly at break-up
5. continuous but slow at low ice content sites

Table 6 MULTIPLE LINEAR REGRESSION ANALYSIS OBTAINED USING THE UNIVERSITY OF ALBERTA
PROGRAM *MLREGR ON IBM 360/67 COMPUTER

Variable Erosion Factor	Mean	Standard Deviation	Correlation x vs y	Regression Coefficient	Std. Error of Reg. Coef.	Std. Partial Reg. Coef.	T Value
Current (cm/sec)	24.10	14.3	0.31	7.36	5.53	0.44	1.33
Wave (fetch in km)	2.33	2.26	0.13	1.02	1.09	0.30	0.94
Ice (% weight)	11.01	10.17	0.12	-0.07	0.25	0.09	-0.29

Intercept	1.83
Multiple Correlation	0.40
Standard Error of Estimate	8.24
Total Degrees of Freedom	14
F Value	0.72

Table 7 LINEAR CORRELATION ANALYSIS OBTAINED USING THE UNIVERSITY OF ALBERTA PROGRAM *CORPLT ON IBM 360/67 COMPUTER

Variables Used	Correlation (R)	Student T	Degrees of Freedom	Probability Level of Significance	Relation
Annual (Erosion in m/yr)					
Fetch NNw direction vs erosion	0.63	2.31	8	5 %	positive
Av. Summer Current vs erosion	0.31	1.18	13	15 %	positive
M.C.— WL vs erosion	0.136	0.49	13		none
Moisture content vs erosion	-0.05	-0.19	13		none
Bi-Weekly (Erosion in m/day)					
M.C.— WL vs erosion	0.81	6.25	21	0.1%	positive
Moisture content vs erosion	0.76	5.36	21	0.1%	positive
Current vs erosion	0.57	3.25	22	1%	positive
Water level vs current	0.29	1.68	31	10%	positive
Wind Velocity vs erosion	-0.270	-1.61	33		none
Water Temp. vs erosion	-0.19	-1.26	41		none
Air Temp. vs erosion	-0.04	-0.28	41		none
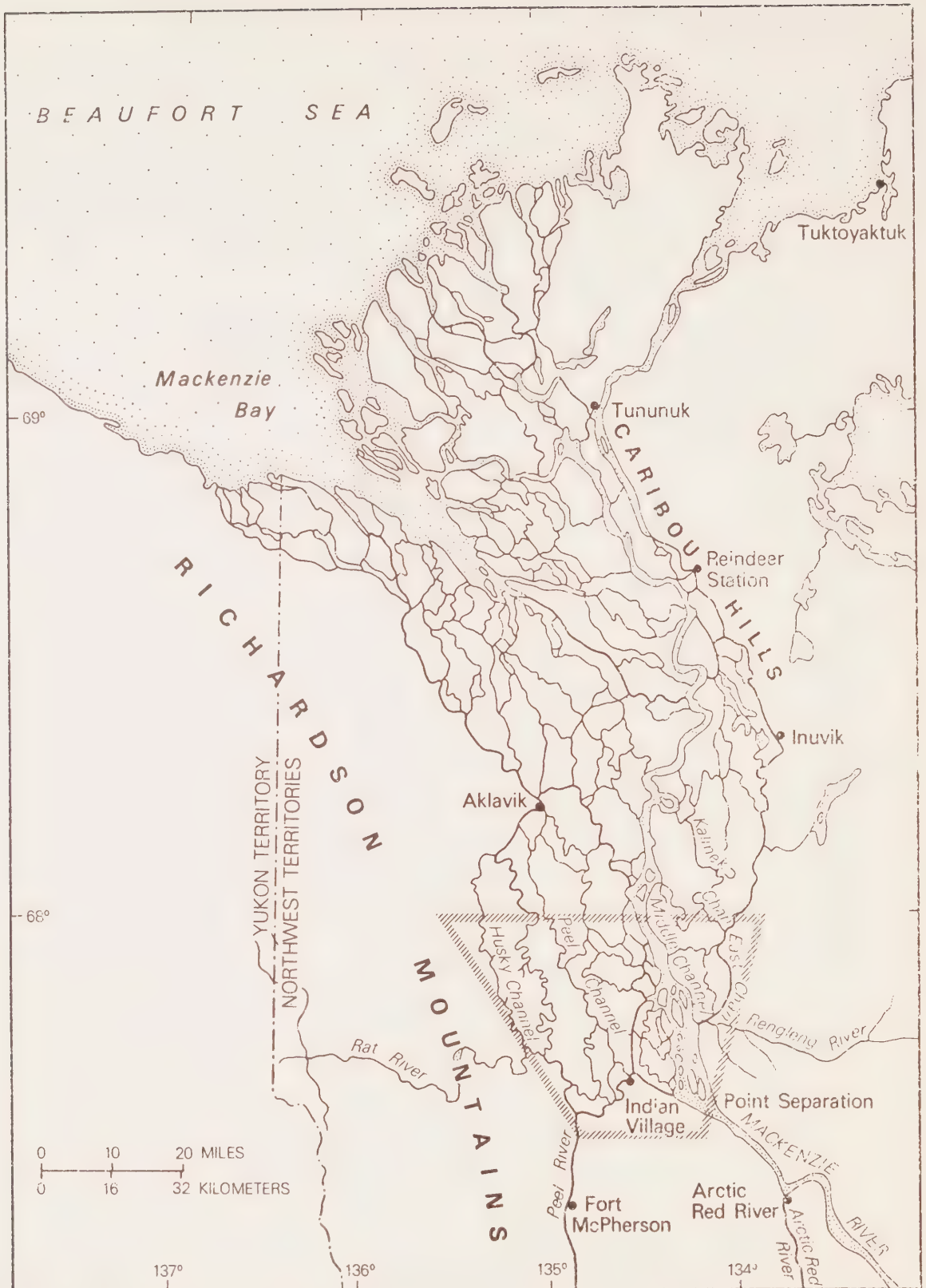
Figure 1   The Mackenzie Delta, N.W.T.. Outlined Location is the Study Area
in Which Erosion was Observed and Measured
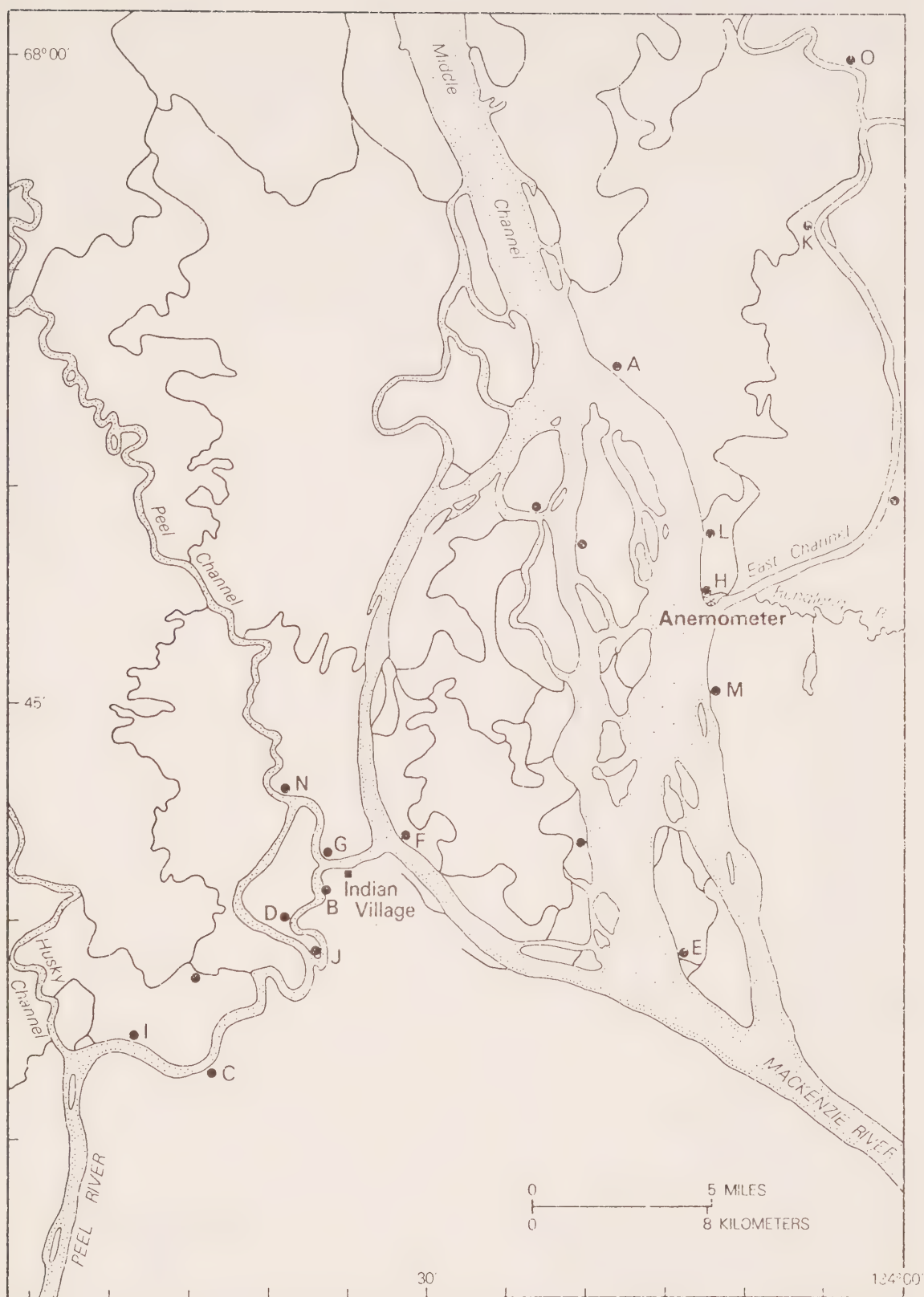
Figure 2   Bank Sites Established for the Observation and Measurement
of the Erosion in the Study Area. Lettered Sites are Described in Section 2.3
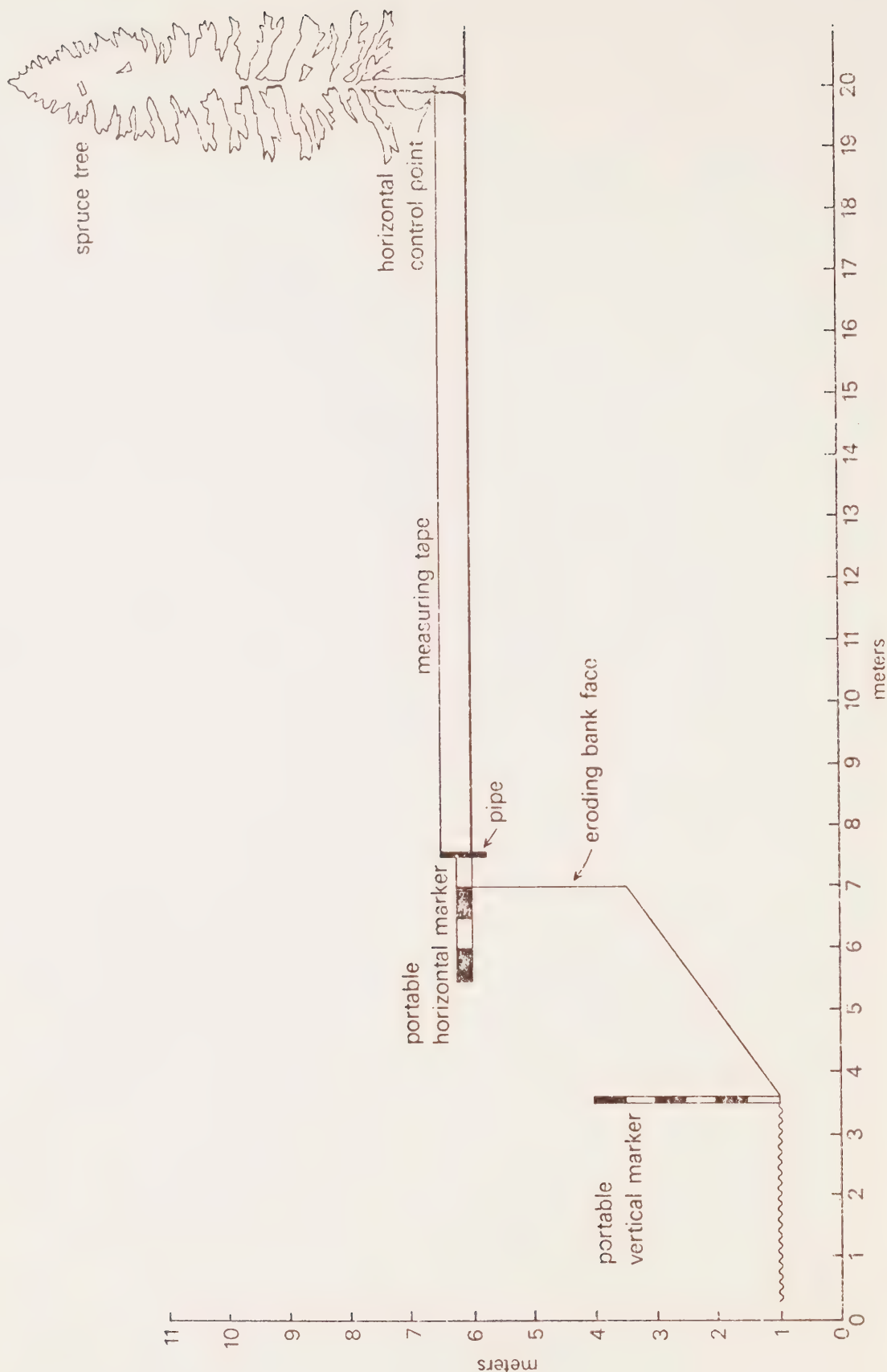
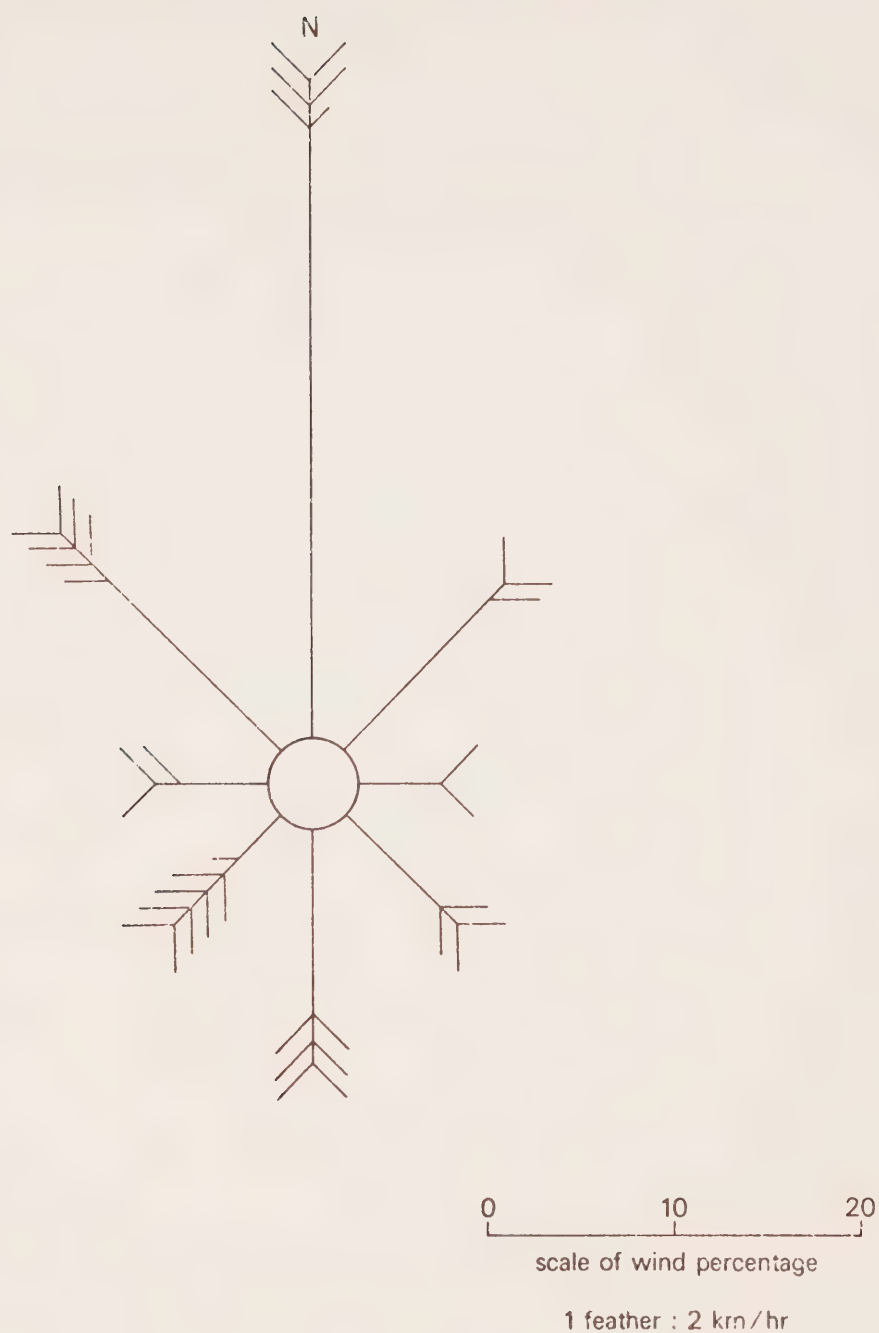Figure 3   Typical Bank Measurements and Scale Marker Placement Prior to the Taking of Stereo Photographs

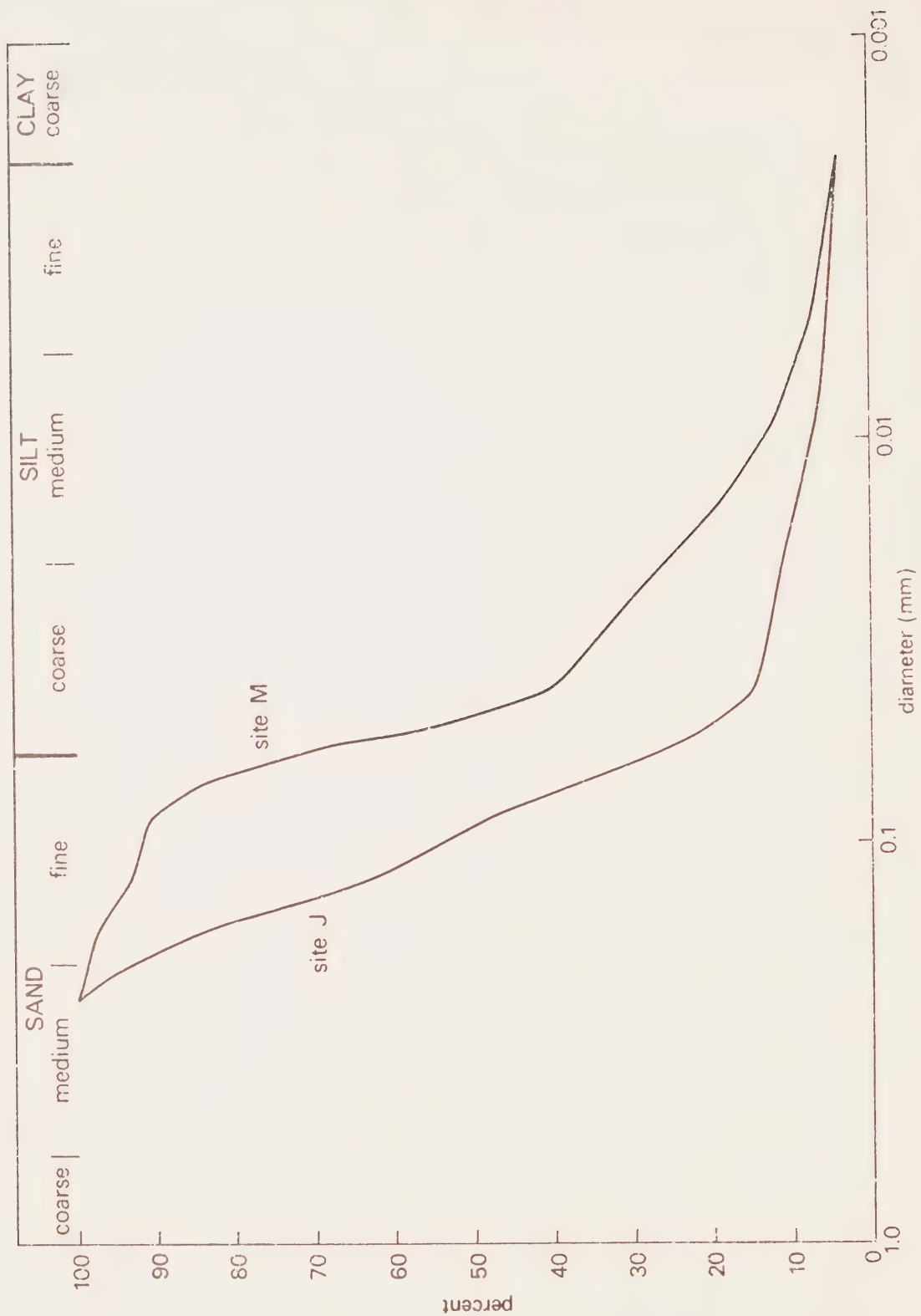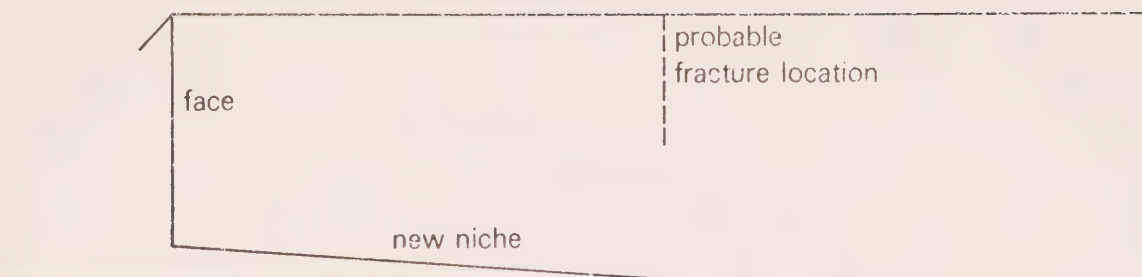Figure 4   Wind Rose for the Anemometer Location Shown in Figure 2,
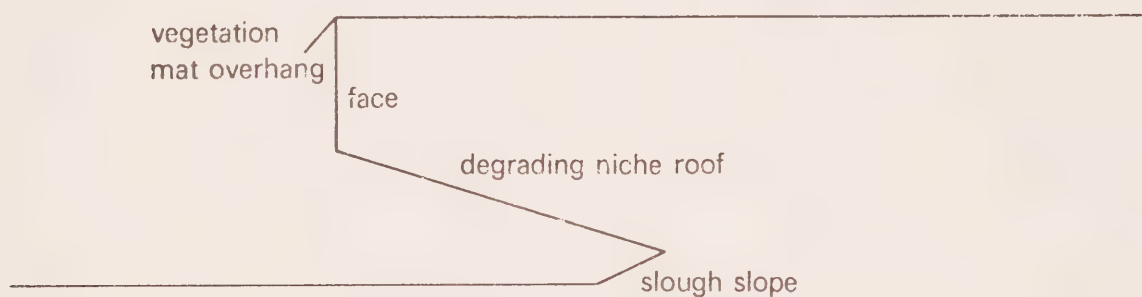June 7 to August 25, 1973

Figure 5 Particle Size Distribution Curves for the Largest and Smallest-sized Samples (M.I.T. Classification)

1   INITIAL NICHE DEVELOPMENT

face

probable
fracture location

new niche

2   DEGRADING NICHE

vegetation
mat overhang

face

degrading niche roof

slough slope

3   OVERHANGING BANK

face

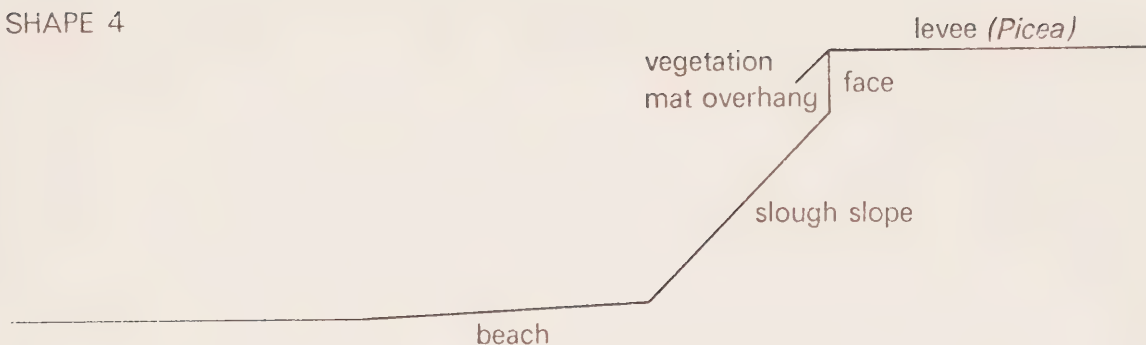degrading niche roof

slough slope
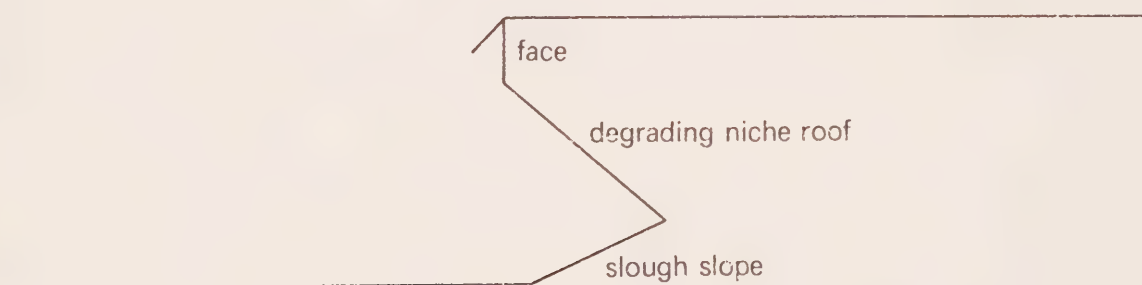
0   5   10   15 meters

Figure 6 Diagrammatic Side Views of Bank Shape Category 1, in 3 Stages
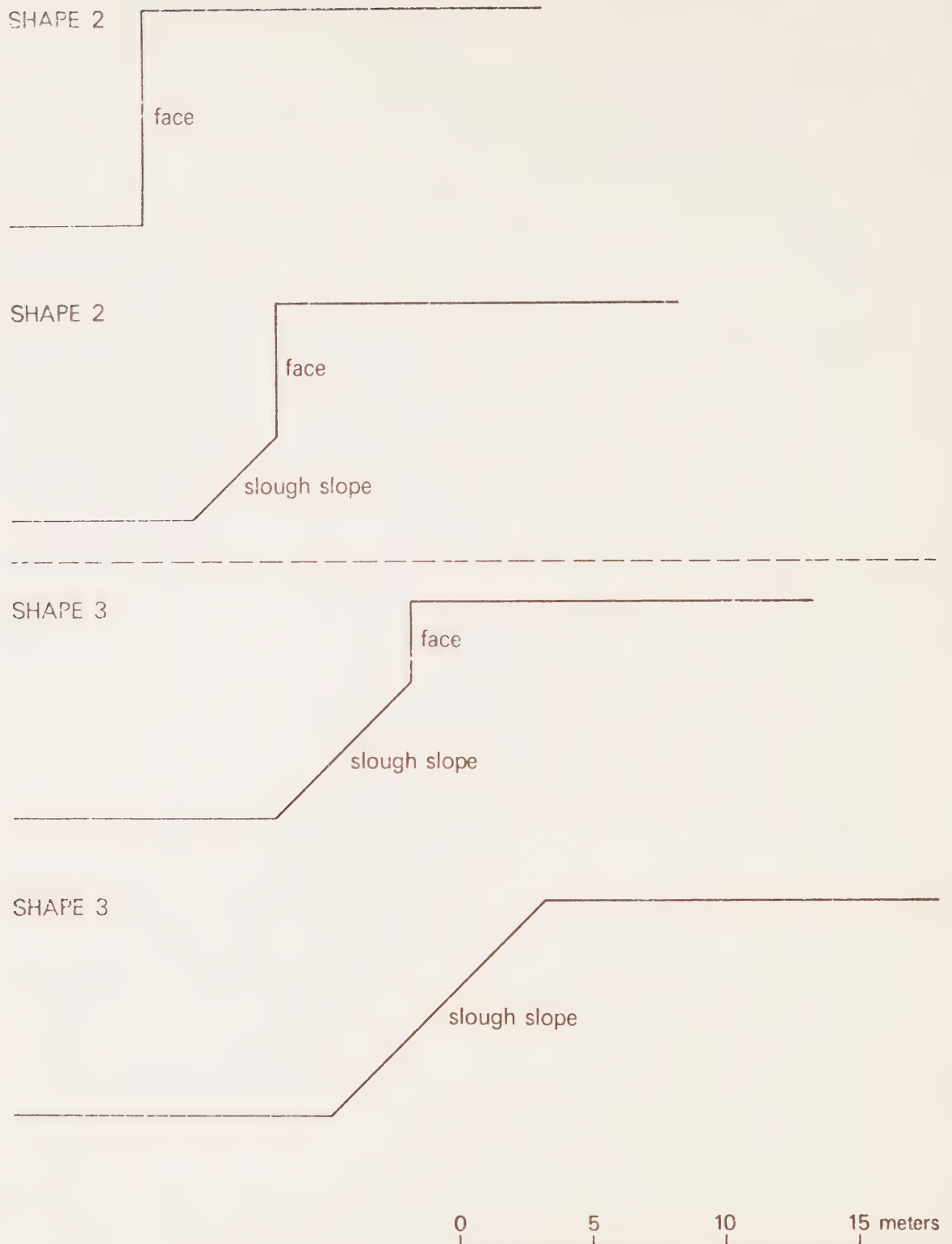
Figure 7 Diagrammatic Side Views of Bank Shape Categories 2 and 3

SHAPE 4

levee *(Picea)*

vegetation
mat overhang | face

slough slope

beach

SHAPE 5

levee *(Picea)*

vegetation
mat overhang | face

slough slope

strandline erosion
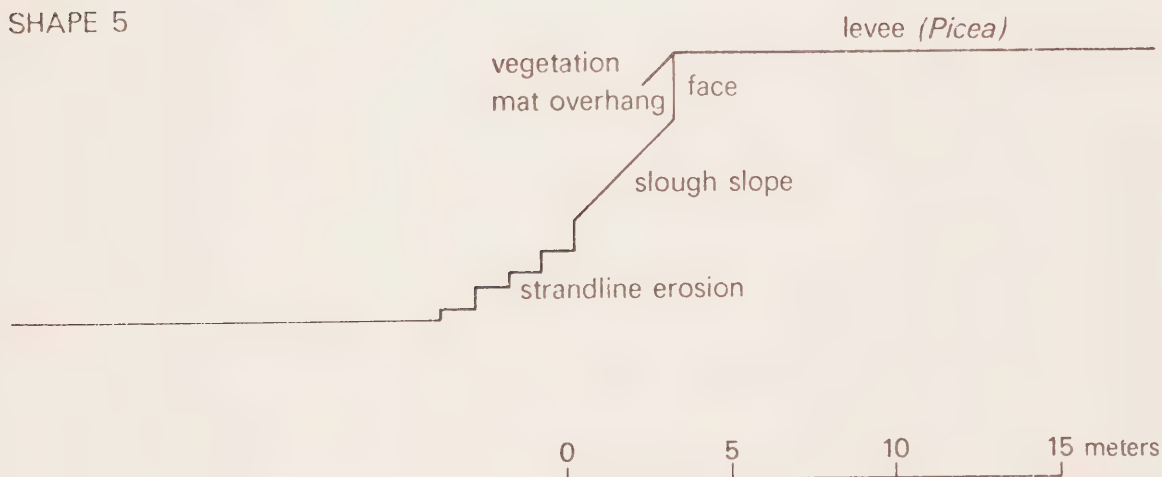
0   5   10   15 meters

Figure 8   Diagrammatic Side Views of Bank Shape Categories 4 and 5

Figure 9 Erosion with Time, 1973, for Sites with Shape 1   Total linear recession is shown from date of previous measurement to date of following one.
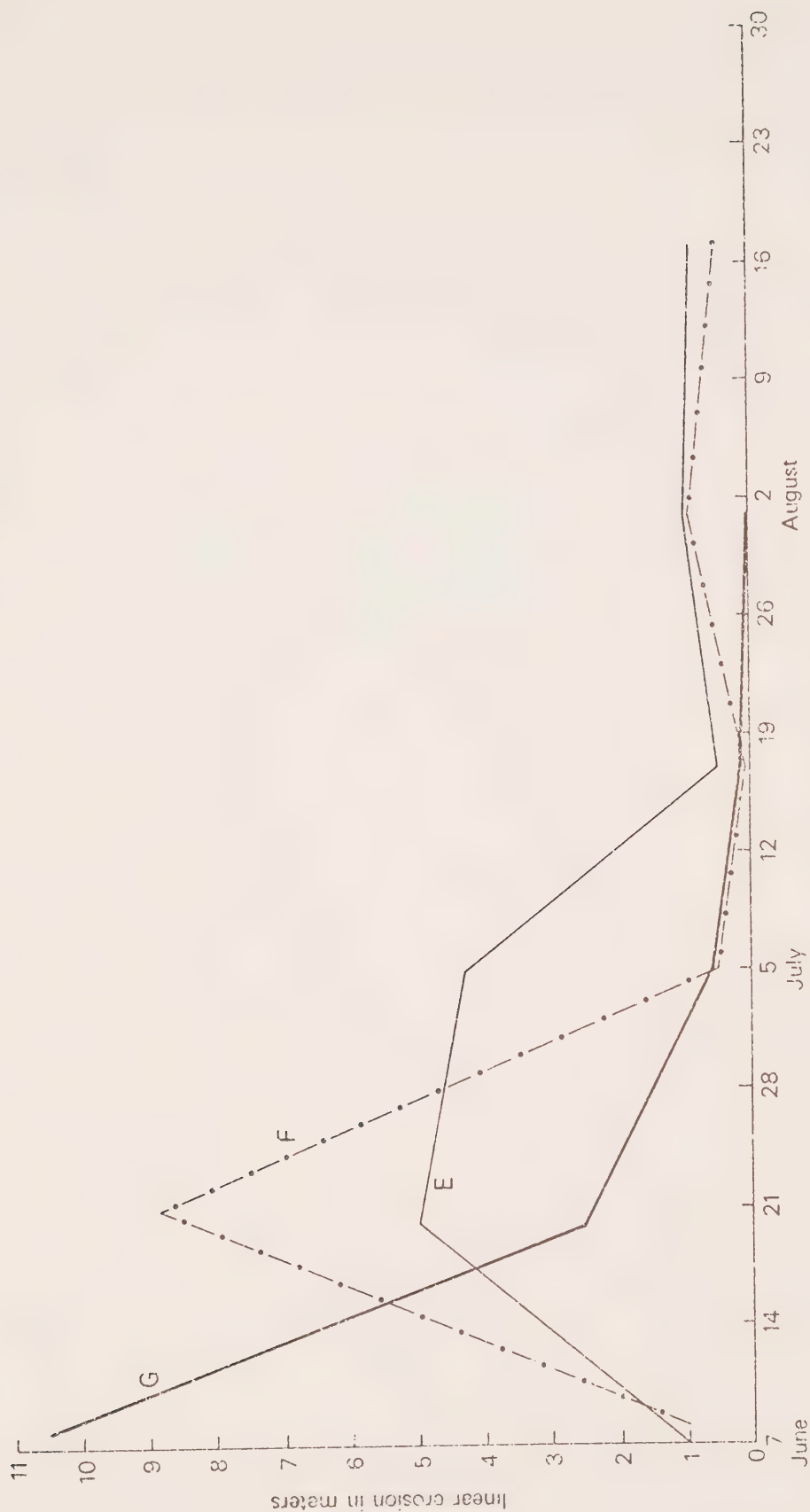
Figure 10 Erosion with Time, 1973, for Sites with Shape 2   Total linear recession is shown from date of previous measurement to date of following one.
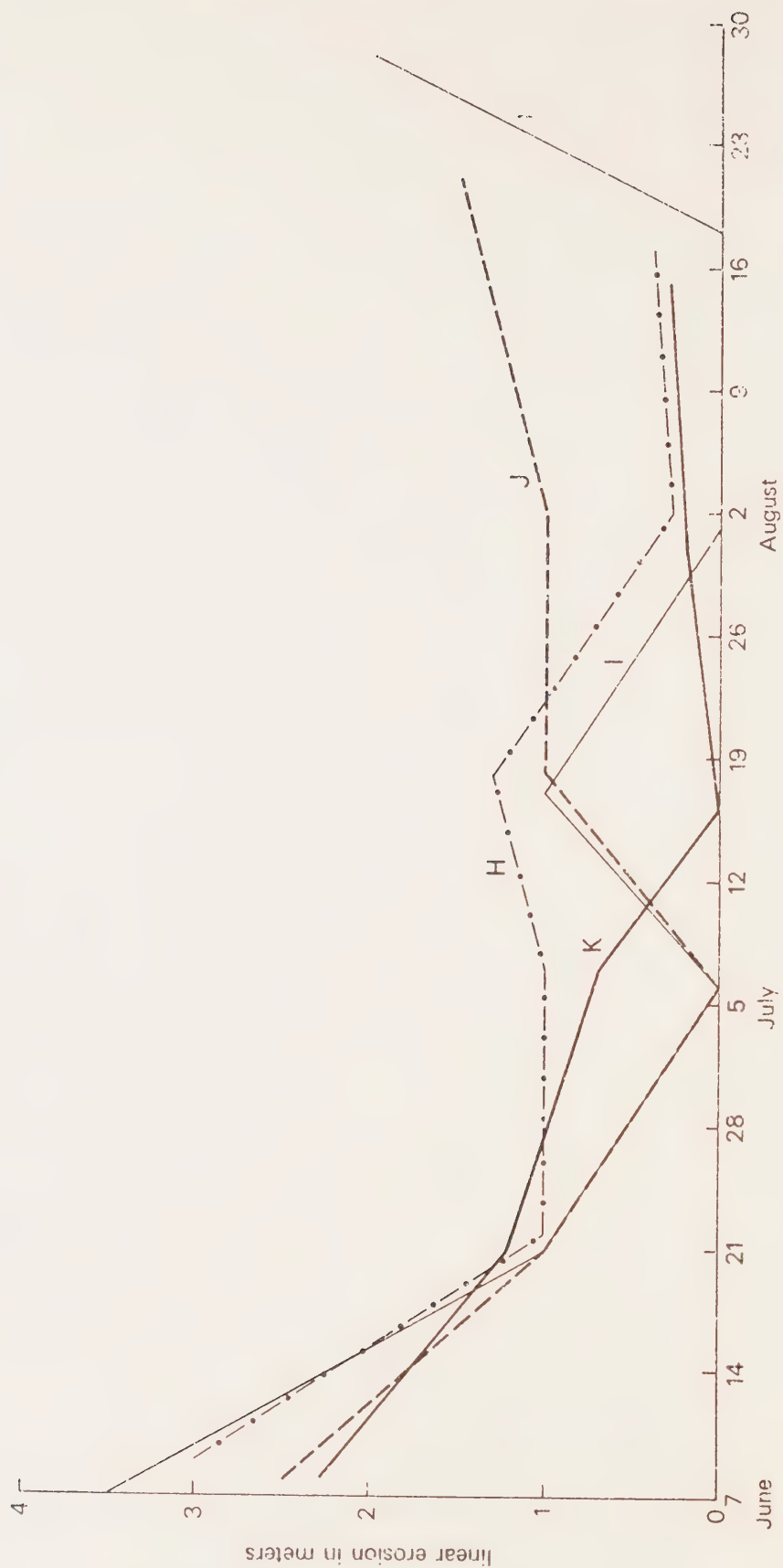
Figure 11 Erosion with Time, 1973, for Sites with Shape 3   Total linear recession is shown from date of previous measurement to date of following one.
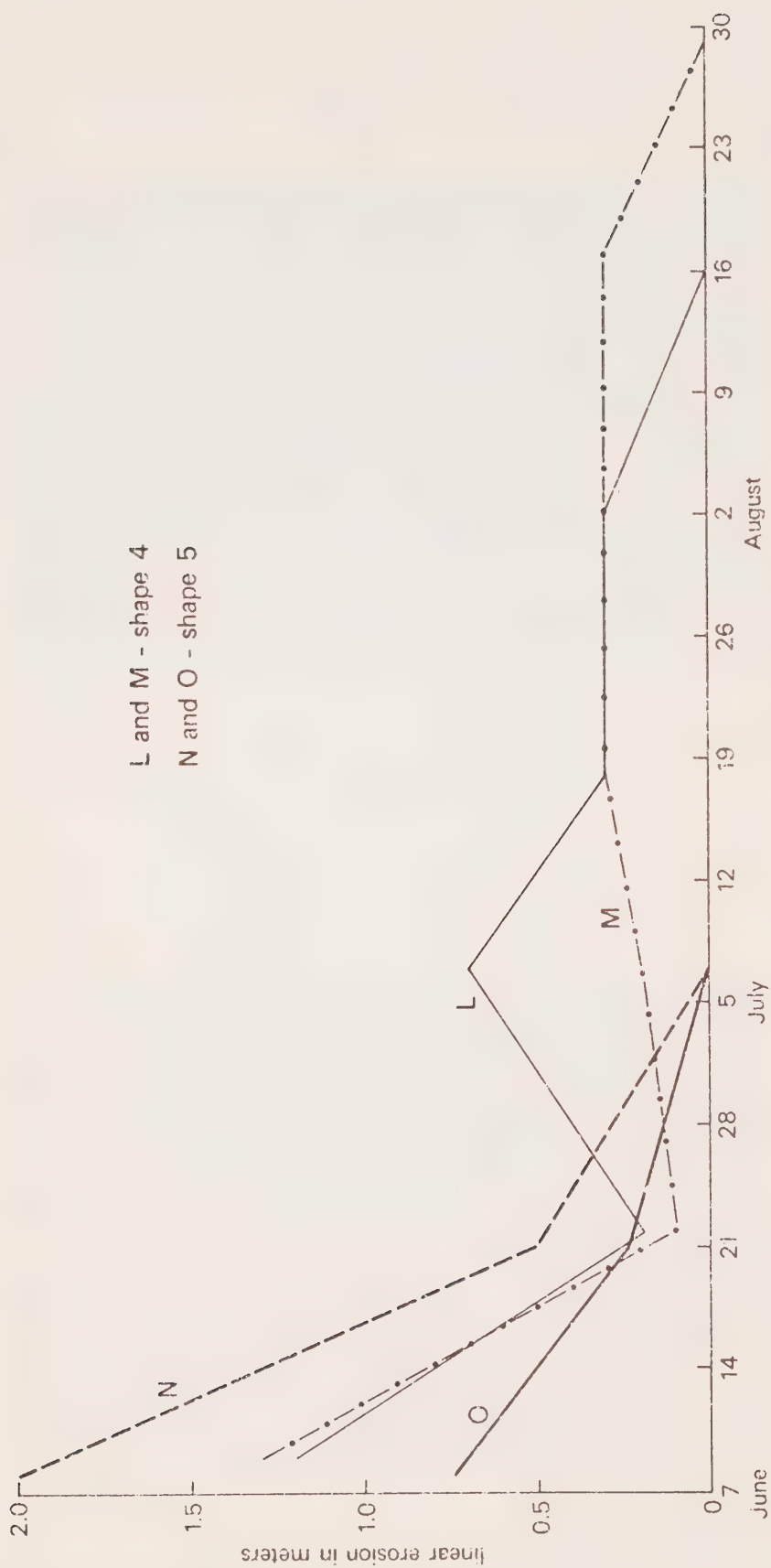
Figure 12 Erosion with Time, 1973, for Sites with Shape 4 or 5 Total linear recession is shown from date of previous measurement to date of following one.

Figure 13 Portion of the Study Area Showing Surveyed Bank Shape Categories

Plate 1   An ice wedge in a bank with ice-rich sediment.   Alluvium layers
have been upturned by its formation.

Plate 2   Taking a sample from a bank with ice-rich sediment.   Note the
wet appearance of the thawing sediment and ice layers.

Plate 3 A point-bar near Reindeer Station eroded by strandline erosion
(By permission, Don Gill).

Plate 4 A stable bank of a small channel.

Plate 5   A relatively stable bank of the Peel Channel.

Plate 6 A stereo pair taken at site G from which bank retreat was
         measured (see Figure 3). All scale markers have 0.5 m
         divisions.

Plate 7   Roots retarding the perturbation of a niche roof (center of
          photo).

Plate 8   Break - up.   Moving ice on the left is separated from bank - protecting stationary ice on the right by a shear line.

Plate 9   Massive Mackenzie River ice pushed onto a bank at the junction of East and Middle Channels.

Plate 10   Willow stems broken by the ice pushed up in Plate 16.

Plate 11   Ridges of alluvium formed by the ice shown in Plate 16.

Plate 12 A bank with shape 1, at stage 1, within a few days of initial niche development (June 8, 1973).

Plate 13 The same bank as in Plate 7, at stage 2, 13 days later (June 21, 1973).
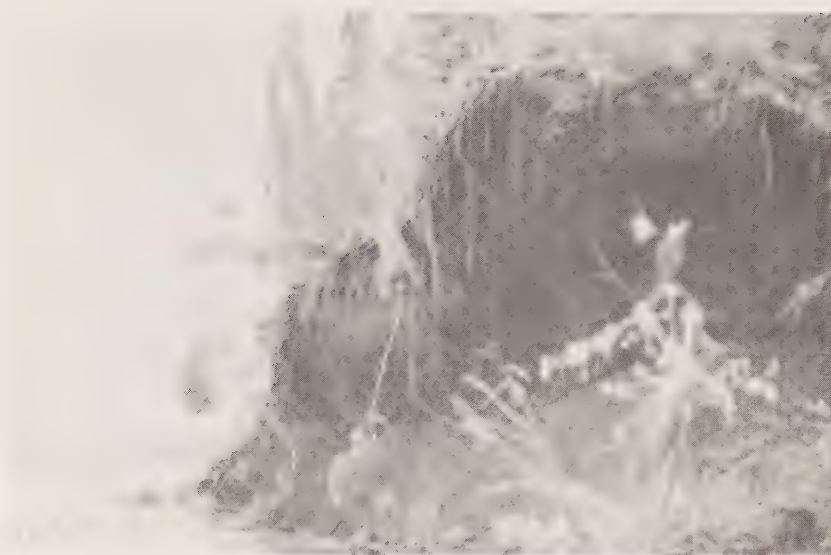
Plate 14 The same bank as in Plate 7, at stage 3, 40 days later
(July 18, 1973).

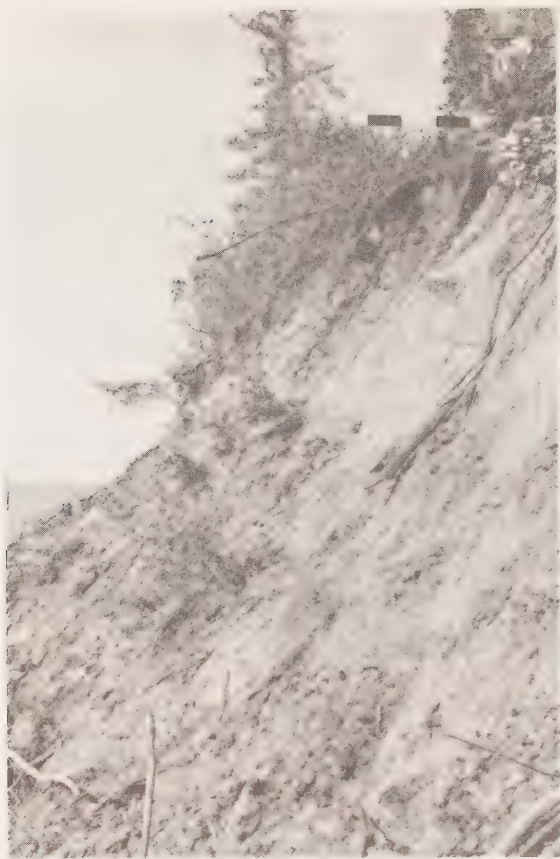Plate 15 A bank with shape 2 (site F).

Plate 16 A bank with shape 3 (site H).

Plate 17 A bank with shape 4 (site L).

Plate 18   A bank with shape 5 (site O).
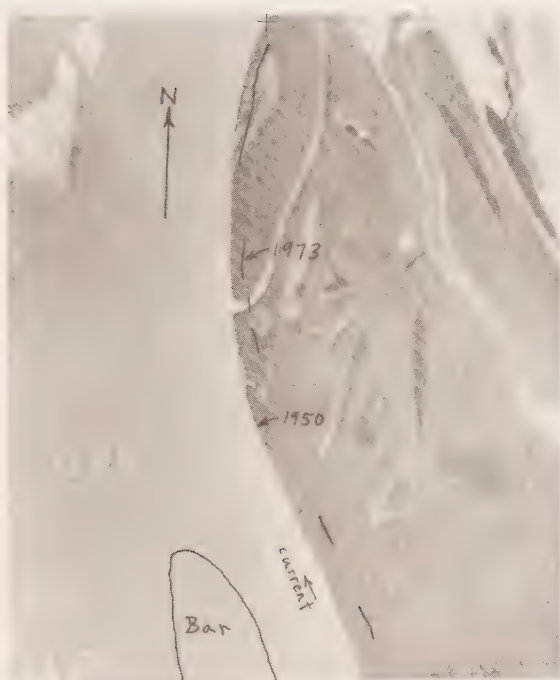
Plate 19   A part of Government
of Canada air photo
A12848-11 (1950, from
6,100 m altitude).
Erosion is approxi-
mately 8 m/yr at this
location (near site E)

A STUDY OF GEOMORPHIC AND HYDROLOGIC CHARACTERISTICS

OF MACKENZIE RIVER TRIBUTARY BASINS

by

T. Thakur and A.G.F. Lindeijer

Glaciology Division

Water Resources Branch

Department of the Environment

under the

Environmental - Social Program

Northern Pipelines

CONTENTS

Abstract

The geomorphic character of Mackenzie tributary watersheds
is described by a number of morphometric parameters measured
from available maps. Statistically determined hydrologic-
geomorphic relationships based on multiple - regression
analysis are used to estimate selected hydrologic characteris-
tics of ungauged basins. Mathematical procedures of factor
analysis are used in conjunction with regression analysis to
formulate new prediction relationships for mean 50-year and
100-year floods. On the basis of results obtained so far the
east side of the Mackenzie River seems to offer a safer route
for pipelines than the west side.

NOTATION

Morphology

AVE = Average elevation (ft)
 BF = Bifurcation ratio
CCM = Constant of channel mainenance (ft^2)
CLA = Latitude (degrees)
CLO = Longitude (degrees)
 CP = Basin perimeter (miles)
CSIN = Sinuosity
 DA = Drainage area ($miles^2$)
 DD = Drainage density ($miles/miles^2$)
  F = Stream frequency
  H = Basin relief (ft)
HCK = Hypsometric coefficient
HYI = Hypsometric integral
 LB = Basin length (miles)
MAE = Maximum elevation (ft)
MCL = Main channel length (miles)
MEE = Mean elevation (ft)
MIE = Minimum elevation (ft)
PAA = Percent area above average elevation
PAEI = Percent area at elevation 0-2000 ft
PAE2 = Percent area at elevation 2000-4000 ft
PAE3 = Percent area at elevation 4000-6000 ft
PAE4 = Percent area at elevation 6000 ft and over
 PF = Percent area of basin covered by forest
PGL = Percent area of basin covered by glacier
PLSW = Percent area of basin covered by lake and swamp
 RA = Area ratio
 RB = Weighted mean bifurcation ratio
 RC = Circulatory ratio
 RE = Elongation ratio
 RH = Relief ratio x 100
 RL = Length ratio
SLOP = Slope factor (ft/mile)

Hydrology

 MAF = Mean annual flow ($ft^3 s^{-1} miles^{-2}$)
MAFF = Mean annual flood with 50-yr. return period ($ft^3 s^{-1} miles^{-2}$)
MAFH = Mean annual flood with 100-yr. return period ($ft^3 s^{-1} miles^{-2}$)
   T = Mean flood with 2.33 - yr. return period ($ft^3 s^{-1} miles^{-2}$)

Introduction

Thakur and Lindeijer (1973) have discussed a method of describing the complete morphology of Mackenzie tributary watersheds. Morphometric characteristics of 54 Mackenzie tributary basins with a total drainage area of approximately 250,000 square miles have already been published.

Selected hydrologic characteristics related to mean peak flow conditions were estimated by flood frequency analysis (Dalrymple, 1960) from hydrologic records of 11 gauged basins. Statistical procedures of multiple regression analysis were used to develop relationships between hydrologic characteristics (dependent-variables) and morphometric characteristics (independent variables) of the basins. Criteria of error estimation and reliability were defined. The following equations express the relationships between hydrologic and geomorphic parameters:

$$MAF = 0.00007 \ (DA) + 0.00026 \ (MEE) - 0.9391 \ (RL) + 2.038 \qquad (1)$$

$$T = -7.504 \ (HCK) - 2.576 \ (RL) - 0.118 \ (SLOP) + 10.57 \qquad (2)$$

$$MAFF = 0.575 \ (CLO) + 15.45 \ (DD) - 9.58 \ (RL) - 55.21 \qquad (3)$$

$$MAFH = 0.620 \ (CLO) + 18.23 \ (DD) - 9.90 \ (RL) - 61.80 \qquad (4)$$

An alternative set of equations was developed for a few basins which did not fit the broad homogeneous geomorphic character of other basins in the group. Thus, for watersheds with drainage area (DA) greater than 10,000 square miles, mean annual flow (MAF) is estimated from the following equation:

$$MAF = 0.00048 \ (MEE) - 1.368 \ (RL) - 0.054 \ (HYI) + 4.78 \qquad (5)$$

For basins with a value of the hypsometric integral (HYI) greater than 0.5, the mean annual flood is estimated as:

$$T = 0.378 \ (CLO) - 0.0028 \ (MIE) - 4.774 \ (RL) - 72.543 \qquad (6)$$

For basins with longitude greater than 137.0 or less than 123.0 degrees, the mean 50-year and 100-year floods were estimated from the following equations:

$$\text{MAFF} = 0.00041 \ (\text{DA}) - 8.640 \ (\text{RL}) + 13.974 \ (\text{DD}) + 15.803 \qquad (7)$$

$$\text{MAFH} = 0.00045 \ (\text{DA}) - 8.777 \ (\text{RL}) + 16.642 \ (\text{DD}) + 14.888 \qquad (8)$$

Hydrologic characteristics of ungauged basins were then estimated by substituting morphometric variables in the established hydrologic-geomorphic relationships (equations 1 - 8.)

Morphometric Analysis

Following the general procedure outlined in our earlier report (Thakur and Lindeijer, 1973), morphometric characteristics of nine additional Mackenzie tributary watersheds were determined. The results are given in Table 1. Hypsometric curves of the basins under study are shown in Figures 1 - 5.

From the results it is apparent that watersheds on the eastern side of Mackenzie River in general have smaller drainage areas with lower mean elevations and gentler slopes than those on the western side. Consequently, the flood potential and erosional hazards to pipelines built on the eastern side of the Mackenzie River are of lesser magnitude.

Hydrologic Characteristics

Hydrologic characteristics of nine ungauged rivers were determined using the morphometric parameters in equations 1 - 8. Results obtained are shown in Table 2. Flood values are presented in cubic feet per second per square mile. The results compare favourably with those recorded in our earlier report.

Factor Analysis:

Factor analysis is a technique used to derive a smaller number of
independent factors from a larger number of inter-correlated variables.
From these factors, variables which are close to being independent in
the original set are identified and subsequently employed in the step-
wise multiple regression analysis to obtain hydrologic-geomorphic relation-
ships. Factor analysis is carried out utilizing the Factor Analysis Computer
program BMD 08M from the set of Biomedical computer programs of the Univer-
sity of California.

General Procedure

The analysis is carried out following the procedure suggested by T.V.A.
(1966). First, factor analysis with varimax rotation is performed on the
complete set of 30 morphometric variables as determined for the full sample
of 63 basins. The number of factors obtained depends upon the percentage
contribution made by each factor to the cumulative proportion of the total
variance explained by the analysis. If the percentage contribution by
inclusion of an additional factor is less than 1% of the total variance
explained, it is not included in the search for independent morphometric
variables.

In the identification of independent variables, only those with factor loadings
greater than 0.800 are selected. Thus, with screening by means of factor
analysis, the number of variables obtained is reduced to 18. These
variables are then used in multiple regression analysis to obtain hydrologic-
geomorphic relationships for gauged basins. For mean 50-year and 100-year
floods, the results obtained are shown in Table 3.

Four variables are used in each equation giving a high correlation coefficient
and a correspondly low standard error of estimate.
The final equations are,

$$MAFF = 1.21919 \ (CLO) + 0.00256 \ (MAE) - 0.64014 \ (PLSW) + 11.64312 \ (DD)$$
$$-171.26928 \qquad\qquad\qquad (9)$$
$$MAFH = 1.32268 \ (CLO) + 0.00283 \ (MAE) - 0.69055 \ (PLSW) + 14.01378 \ (DD)$$
$$-187.29584 \qquad\qquad\qquad (10)$$

Results

The foregoing equations could not be applied to all basins, especially
those with a centre of gravity located at 126 degrees longitude
or less and maximum elevation in the basin 5,000 feet or less. Most of
these basins are located on the eastern side of the Mackenzie River. On
the other hand, as our original sample of gauged basins from which
hydrologic-geomorphic relationships were obtained comes exclusively from
the western side of Mackenzie, the above two relationships probably yield
better results for basins on the western side of Mackenzie, because of
higher correlations and lower standard errors than equations based on
multiple regression analysis alone.

Values of 50-year and 100-year floods based on equations 9 and 10
are shown in Table 4. The results are only for basins on the western
side of Mackenzie. Table 5, shows the results of all basins so far
studied. These results are based on equations 3, 4, 7 and 8.

Conclusions

Using multiple regression procedures, flood characteristics of ungauged
Mackenzie tributary watersheds were estimated. On an equivalent area
basis, the flood magnitudes of east side Mackenzie tributaries appear
to be lower than those on the west side, making the eastern side of the
Mackenzie a safer route for pipelines.

Factor analysis was performed on morphometric data to screen inter-
correlated variables. The resulting variables, when used in stepwise
multiple regression analysis, yielded very stable statistical relation-
ships with four significant morphometric parameters. However, the
applicability of the equations is restricted to tributaries on the western
side of Mackenzie.

References:

Dalrymple, T. 1960. Flood Frequency Analysis. United States Geological
     Survey, Water Supply Paper 1543-A, 80 p.

Tennessee Valley Authority, 1966. Design of a hydrologic condition survey
     using Factor Analysis. International Association of Scientific
     Hydrology Bulletin, Annee 11, No. 2, pp 131-176.

Thakur, T.R. and Lindeijer, A.G.F., 1973. In, Hydrologic Aspects of
     Northern Pipeline Development. A series of 16 reports, for the
     Environmental-Social program, Northern pipelines, Information Canada,
     Cat. No. R27-172, pp. 571-644.

Table 1   Morphometric Data

SUBBASINS		DRAINAGE AREA (MILES²)	MAXIMUM ELEVATION (FT)	MINIMUM ELEVATION (FT)	AVERAGE ELEVATION (FT)	MEAN ELEVATION (FT)	LONGITUDE	LATITUDE	HYPSOMETRIC COEFFICIENT	HYPSOMETRIC INTEGRAL	% AREA AT ELEVATION 0-2000 FT	% AREA AT ELEVATION 2000-4000 FT	% AREA AT ELEVATION 4000-6000 FT
Blackwater at Mackenzie	10HC1	3157	1275	300	788	1237	122.5	63.9	-0.01	29.6	92.2	7.8	0.0
Ochre at Mackenzie	10HC2	445	1875	300	1088	1641	123.0	63.5	-0.02	26.0	80.8	19.2	0.0
Big Smith at Mackenzie	10HC3	367	4800	260	2530	1116	124.4	64.6	-0-02	22.1	96.4	3.6	0.0
Little Bear at Mackenzie	10KA1	877	6100	75	3088	1499	126.1	64.7	-0.14	30.2	72.8	24.2	3.0
Hanna at Mackenzie	10KA2	260	1400	75	738	522	128.0	65.7	+0.15	40.1	100.0	0.0	0.0
Oscar at Mackenzie	10KA3	306	2900	75	1488	974	127.0	65.5	-0.08	40.3	90.5	9.5	0.0
Ramparts at Mackenzie	10KD1	2908	6549	49	3299	535	130.8	66.0	+2.00	17.8	81.4	14.4	4.2
Hume at Mackenzie	10KD2	1254	4551	49	2300	656	129.5	65.7	+1.20	23.8	79.0	17.6	3.4
Donnelly at Mackenzie	10KD3	614	1600	98	849	1877	128.0	65.8	-0.26	31.9	57.4	36.5	5.2

Table 1 (continued)

SUBBASINS		STREAM FREQUENCY	85-10' SLOPE FACTOR	CONSTANT OF CHANNEL MAINTENANCE (FT)	MAIN CHANNEL LENGTH (MILES)	DIRECT DISTANCE FROM MOUTH TO HEAD (MILES)	SINUOSITY RATIO	STREAM ORDER	PERIMETER (MILES)	HYDROLOGIC DATA	TOPOGRAPHIC MAP SCALE
Blackwater at Mackenzie	10HC1	0.356	3.59	7135	154	108	1.43	6	410	NO	1:250,000
Ochre at Mackenzie	10HC2	0.447	20.61	5733	57	38	1.50	5	116	NO	
Big Smith at Mackenzie	10HC3	0.234	25.84	6947	67	36	1.86	4	124	NO	
Little Bear at Mackenzie	10KA1	0.328	22.67	5893	99	51	1.94	5	175	NO	
Hanna at Mackenzie	10KA2	0.658	7.66	5048	68	35	1.94	4	104	NO	
Oscar at Mackenzie	10KA3	0.523	15.50	5019	57	30	1.90	4	92	NO	
Ramparts at Mackenzie	10KD1	0.237	14.03	7233	260	126	2.06	6	315	NO	
Hume at Mackenzie	10KD2	0.411	14.45	5106	150	71	2.11	5	188	NO	
Donnelly at Mackenzie	10KD3	0.490	9.35	5483	84	55	1.53	5	160	NO	

Table 1 (continued)

SUBBASINS		% AREA AT 6000 FT ELEVATION AND OVER	% AREA ABOVE AVERAGE ELEVATION	% LAKE AND SWAMP	% FOREST	% GLACIER	CIRCULATION RATIO	ELONGATION RATIO	RELIEF RATIO X 100	WEIGHTED MEAN BIFURCATION RATIO	LENGTH RATIO	AREA RATIO	DRAINAGE DENSITY (Miles miles-2)
Blackwater at Mackenzie	10HC1	0.0	10.2	14.7	84.0	0.0	0.563	0.686	0.17	4.21	2.08	4.19	0.74?
Ochre at Mackenzie	10HC2	0.0	18.4	2.6	91.5	0.0	0.648	0.630	0.79	3.37	1.92	3.88	0.921
Big Smith at Mackenzie	10HC3	0.0	9.1	13.3	85.2	0.0	0.549	0.600	2.39	4.79	2.10	5.47	0.760
Little Bear at Mackenzie	10KA1	0.0	10.0	6.3	78.4	0.0	0.603	0.659	2.24	3.95	2.10	4.60	0.896
Hanna at Mackenzie	10KA2	0.0	52.6	9.8	87.9	0.0	0.546	0.512	0.72	5.25	2.13	7.43	1.046
Oscar at Mackenzie	10KA3	0.0	29.5	7.0	86.6	0.0	0.675	0.649	1.44	5.77	2.16	6.49	1.052
Ramparts at Mackenzie	10KD1	0.0	8.3	10.8	71.9	0.0	0.606	0.483	0.96	4.46	2.01	3.71	0.730
Hume at Mackenzie	10KD2	0.0	16.1	7.2	74.5	0.0	0.665	0.561	1.19	4.57	2.01	5.22	1.034
Donnelly at Mackenzie	10KD3	0.9	9.6	9.0	90.0	0.0	0.548	0.511	0.52	3.93	2.05	4.48	0.963

Table 2

Computed Hydrologic Characteristics*
(Multiple-regression analysis)

WATERSHED	NO.	AREA (MILES^2)	MAF	T	MAFF	MAFH
1. Blackwater at MacKenzie (E)	10HC1	3157	0.63	4.86	(3) 9.47	(4) 10.37
2. Ochre at MacKenzie (E)	10HC2	445	0.69	3.34	11.35	12.24
3. Big Smith at MacKenzie (E)	10HC3	367	0.48	2.26	7.99	8.39
4. Little Bear at MacKenzie	10KA1	877	0.52	3.54	11.02	11 93
5. Hanna at MacKenzie (E)	10KA2	260	0.20	3.05	14.14	15.53
6. Oscar at MacKenzie (E)	10KA3	306	0.28	3.86	13.36	14737
7. Ramparts at MacKenzie	10KD1	2908	0.50	(2) 11.30	12.00	12.71
8. Hume at MacKenzie	10KD2	1254	0.40	(2) 11.29	15.97	17.44
9. Donnelly at MacKenzie (E)	10KD3	614	0.64	6.14	13.63	14.82

(E) Indicates basins east of MacKenzie River.

(2,3,4) These values have been estimated from equation 5,6 and 7 respectively

* All runoff values are presented in cubic feet per second per square mile.

Table 3

Multiple-Regression Analysis – Significant Morphometric Variables
Presented in Order of entry into the multiple regression equations

Variables Estimating Mean 50 – Year Flood

$\overline{\text{MAFF}}$ = 10.27182, σ = 2.52895, % σ / $\overline{\text{MAFF}}$ = 24.62

	MAE	CLO	PLSW	DD
Correlation coefficient R	.6697	.7990	.8983	.9819
coefficient of Determination R^2	.4484	.6383	.8070	.9641
Stepwise increase in R^2	.4484	.1899	.1687	.1571
Level of Significance	5%	5%	1%	1%
Standard Error of Estimate (σ)	1.9798	1.7004	1.3279	.6188
% σ/$\overline{\text{MAFF}}$	19.27	16.55	12.93	6.02

Variables Estimating Mean 100 – Year Flood

$\overline{\text{MAFH}}$ = 11.20455, σ = 2.82729, % σ/ $\overline{\text{MAFH}}$ = 25.23

	MAE	CLO	PLSW	DD
Correlation coefficient R	.6764	.7994	.8878	.9850
Cofficient of Determination R^2	.4575	.6390	.7881	.9702
Stepwise increase in R^2	.4575	.1815	.1491	.1812
Level of Significance	5%	5%	1%	1%
Standard Error of Estimate (σ)	1.9798	1.7004	1.3279	.6188
% σ / $\overline{\text{MAFH}}$	19.59	16.95	13.88	5.62

Table 4

Computed Hydrologic Characteristics of watersheds on
the western side of Mackenzie based on Multi-regression
analysis after screening by Factor Analysis.

	WATERSHED	DA	MAFF	MAFH
1.	Liard at upper crossing	13675	10.66	11.59
2.	Frances Near Watson Lake	4952	11.73	12.76
3.	Dease at McDame	2710	11.88	12.82
4.	Blue at Dease	682	11.69	12.64
5.	Hyland near Lower post	3424	13.45	14.82
6.	Turnagain at gauging station	2519	10.86	11.78
7.	Kechika at Liard	8533	7.41	7.97
8.	Kechika above Boya Creek	4249	6.16	6.52
9.	Coal at Liard	3620	12.67	14.07
10.	Flat at S. Nahanni	3326	11.23	12.36
11.	S. Nahanni above Virginia Falls	5653	13.41	14.65
12.	Liard above Meister	3639	13.08	14.45
13.	Meister at Liard	805	9.55	10.22
14.	Rancheria at Liard	2021	9.15	9.81
15.	Dease at Liard	5754	5.99	6.29
16.	Turnagain at Kechika	2696	10.95	11.89
17.	Beaver at Liard	4184	9.25*	9.83*
18.	Root at Mackenzie	3835	8.86	9.71
19.	N. Nahanni at Mackenzie	2751	8.62	9.46
20.	Ram at N. Nahanni	1149	12.35*	13.31*
21	Tetcela at N. Nahanni	1509	15.27*	16.74*
22.	Keele at Mackenzie	10467	8.68	9.42
23.	Dahadinni at Mackenzie	1046	12.29*	13.44*
24	Johnson at Mackenzie	855	12.71*	13.72*
25.	Wrigley at Mackenzie	502	9.80*	10.71*
26.	Redstone at Mackenzie	6080	9.63	10.57
27.	Carcajou at Mackenzie	3527	9.46	10.30
28	Arctic Red at Mackenzie	8284	16.63	18.05
29.	Ontaratue at Mackenzie	2646	9.14	10.19
30.	Wind at Peel	3783	16.55	18.10
31.	Blackstone at Peel	1512	20.74	22.37
32.	Ogilvie at Peel	2791	18.97	20.34
33.	Hart at Peel	4672	15.54	16.59
34.	Peel above Canyon Creek	9709	17.79	19.10
35.	Snake at Peel	2931	15.94	17.55
36.	Bonnet Plume at Peel	3724	15.38	16.70
37.	Snake above Iron Creek	1071	12.42	13.38
38.	Peel at Mackenzie Delta	30404	12.313	13.424
39.	Blow at Arctic Ocean	1412	18.04	19.92
40.	Babbage at Arctic Oean	1756	17.92	19.55
41.	Firth at Arctic Ocean	2425	19.63	21.20
42.	Malcolm at Arctic Ocean	427	23.83	25.97
43.	Mountain at Mackenzie	5785	8.07	8.73*
44.	Little Bear at Mackenzie	877	11.02*	11.93*
45.	Ramparts at Mackenzie	2908	6.55	7.01
46.	Hume at Mackenzie	1254	5.70	6.40

*Values estimated using equations 3 and 4.

Table 5

Computed Hydrologic Characteristics of all Watersheds under Study
(multiple-regression analysis)

	WATERSHED	NO.	(AREA SQ. MILES)	MAFF	MAFH
1.	Liard above Meister	10AA1	3639	14.28	15.90
2.	Meister at Liard	10AA2	805	9.62	10.41
3.	Rancheria at Liard	10AA3	2021	12.08	12.97
4.	Francis near Watson Lake	10AB1	4952	10.72	11.73
5.	Liard at Upper Crossing	10AA001	13675	12.85	13.87
6.	Dease at McDame	10AC2	2710	12.50	13.43
7.	Blue At Dease	10AC4	682	9.74	10.57
8.	Dease at Liard	10AC3	5754	8.86	9.46
9.	Hyland near Lower Post	10AD1	3424	14.42	15.80
10.	Turnagain at Kechika	10BA1	2696	8.25	8.93
11.	Turnagain Gauging Station	10BA001	2519	8.61	9.41
12.	Kechika above Boya Creek	10BA002	4249	8.77	9.19
13.	Kechika at Liard	10BB001	8533	8.97	9.49
14.	Coal at Liard	10BC001	3620	11.84	13.27
15.	Beaver at Liard	10BD1	4184	9.25	9.83
16.	Flat at S. Nahanni	10EA003	3326	11.80	12.90
17.	S. Nahanni above Virginia Falls	10EB001	5653	12.72	13.75
18.	Root at MacKenzie	10GA1	3835	11.22	12.14
19.	Willow Lake River at MacKenzie (E)	10GB2	8179	[3]9.70	[4]10.59
20.	River Between Two Mountains at MacKenzie (E)	10GB1	1345	[3]9.17	[4]9.67
21.	N. Nahanni at MacKenzie	10GD1	2751	12.35	13.31
22.	Ram at N. Nahanni	10GD2	1149	15.27	16.74
23.	Tetcela at N. Nahanni	10GD3	1509	10.47	11.37
24.	Keele at MacKenzie	10HA1	10467	12.29	13.44
25.	Dahadinni at MacKenzie	10HB1	1046	12.71	13.72
26.	Johnson at MacKenzie	10HB2	855	9.80	10.71
27.	Wrigley at MacKenzie	10HB3	502	12.77	13.80
28.	Redstone at MacKenzie	10HB001	6080	14.19	15.07
29.	Carcajou at MacKenzie	10KB1	3527	11.71	12.71
30.	Arctic Red at MacKenzie	10LA1	8284	12.70	13.66
31.	Loon at MacKenzie (E)	10LB1	1168	9.19	12.91
32.	Tieda at MacKenzie (E)	10LB2	365	11.16	12.86
33.	Travaillant at MacKenzie (E)	10LB3	1124	12.60	13.74
34.	Ontaratue at MacKenzie	10LB4	2646	10.06	10.60
35.	Rabbit Hay at MacKenzie (E)	10LC1	139	10.87	11.61
36.	Pierre at MacKenzie (E)	10LC2	259	12.58	12.79
37.	Rengleng at MacKenzie (E)	10LC3	551	13.28	13.37
38.	Gull at MacKenzie (E)	10LC4	1662	18.81	20.35
39.	Hare Indian at MacKenzie (E)	10LD1	1383	10.12	10.76
40.	Blue Fish at Hare Indian (E)	10LD2	1580	11.34	11.99
41.	Wind at Peel	10MA1	3783	16.31	17.97
42.	Blackstone at Peel	10MA2	1512	[3]38.21	[4]9.00
43.	Ogilvie at Peel	10MA3	2791	[3]10.56	[4]11.34
44.	Hart at Peel	10MA4	4672	[3]7.84	[4]8.61
45.	Peel above Canyon Creek	10MA001	9707	16.20	17.31

WATERSHEDS	NO.	(AREA SQ. MILES)	MAFF	MAFH
6. Snake at Peel	10MB1	2931	15.30	17.01
7. Bonnet Plume at Peel	10MB2	3724	11.93	13.09
8. Snake above Iron Creek	10MBOO1	1071	11.94	12.94
9. Peel at MacKenzie Delta	10MC1	30404	[3]15.03	[4]16.26
0. Blow at Arctic Ocean	10MD1	1412	[3]18.18	[4]20.26
1. Babbage at Arctic Ocean	10MD2	1756	[3]14.97	[4]16.58
2. Firth at Arctic Ocean	10MD3	2425	[3]11.09	[4]12.26
3. Maclcolm at Arctic Ocean	10MD4	427	[3]12.54	13.91
4. Mountain at MacKenzie	10KC1	5785	12.58	[4]13.45
5. Blackwater at MacKenzie (E)	10HC1	3157	[3]9.47	[4]10.37
6. Ochre at MacKenzie (E)	10HC2	445	11.35	12.24
7. Big Smith at MacKenzie (E)	10HC3	367	7.99	8.39
8. Little Bear at MacKenzie	10KA1	877	11.02	11.93
9. Hanna at MacKenzie (E)	10KA2	260	14.14	15.53
0. Oscar at MacKenzie (E)	10KA3	306	13.36	14.74
1. Ramparts at MacKenzie	10KD1	2908	12.00	12.71
2. Hume at MacKenzie	10KD2	1254	15.97	17.44
3. Donnelly at MacKenzie (E)	10KD3	614	13.63	14.82

(E) Indicates basins east of MacKenzie River.

[3],[4] These values have been estimated by alternative equations 7 and 8 respectively.
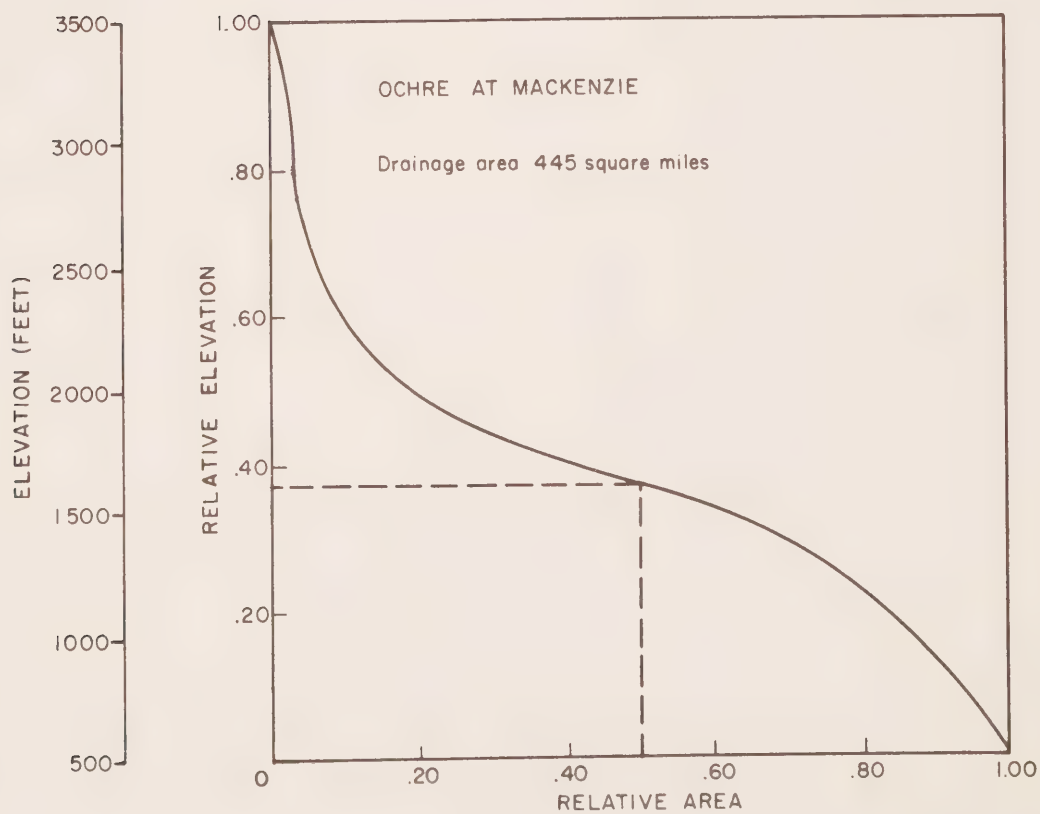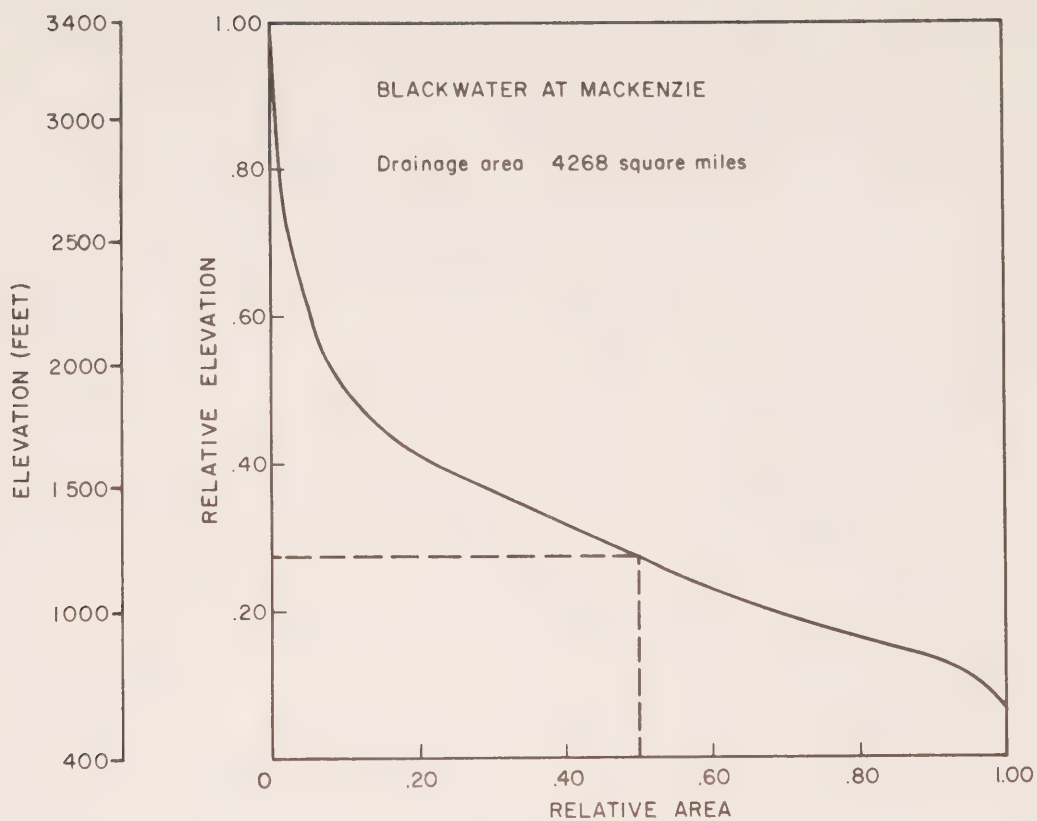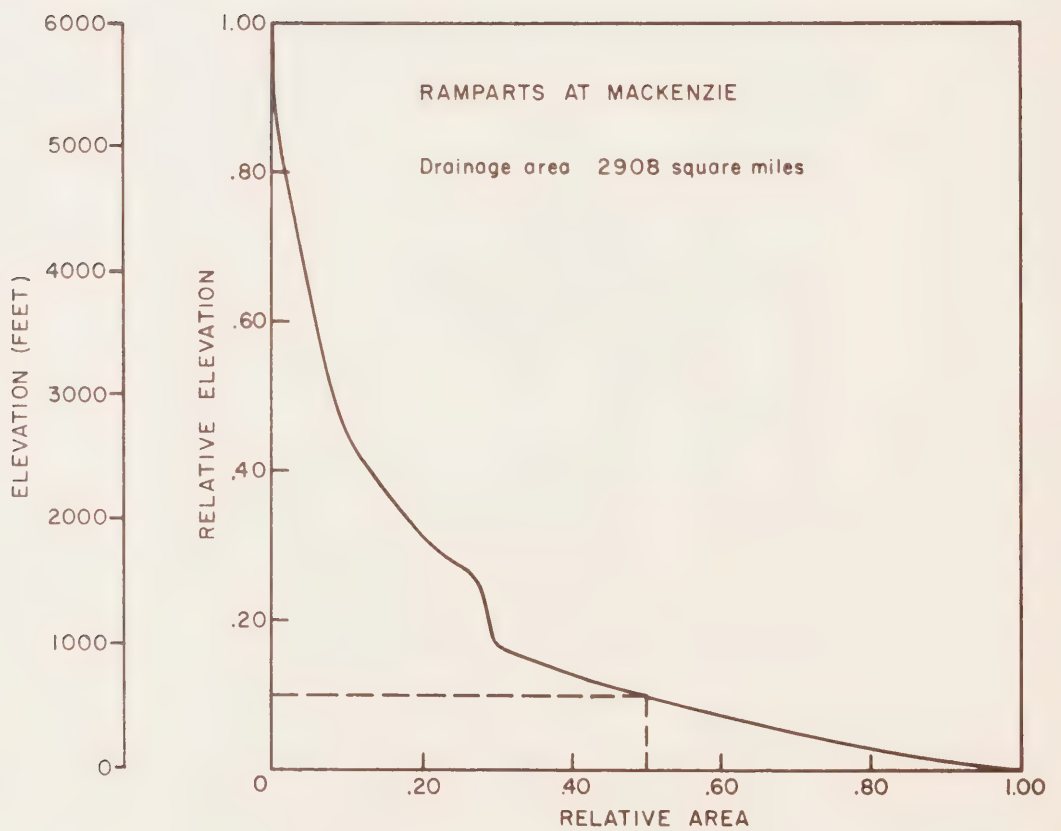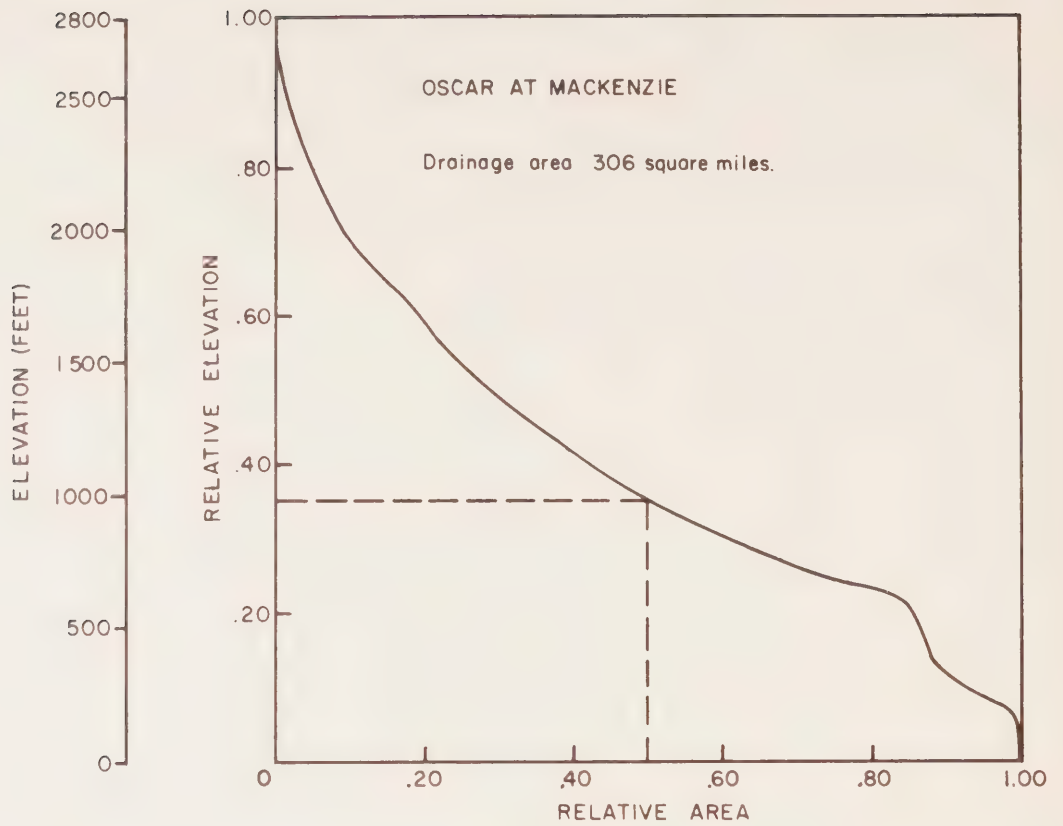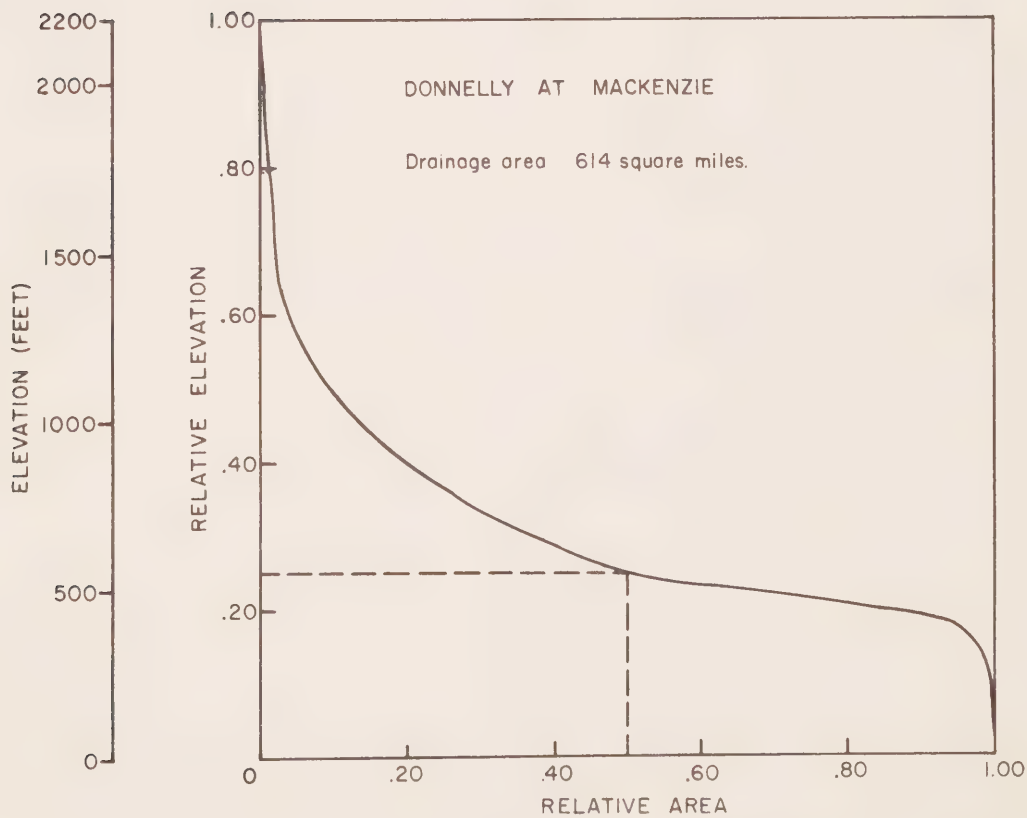
FIGURE 1. Hypsometric curve.

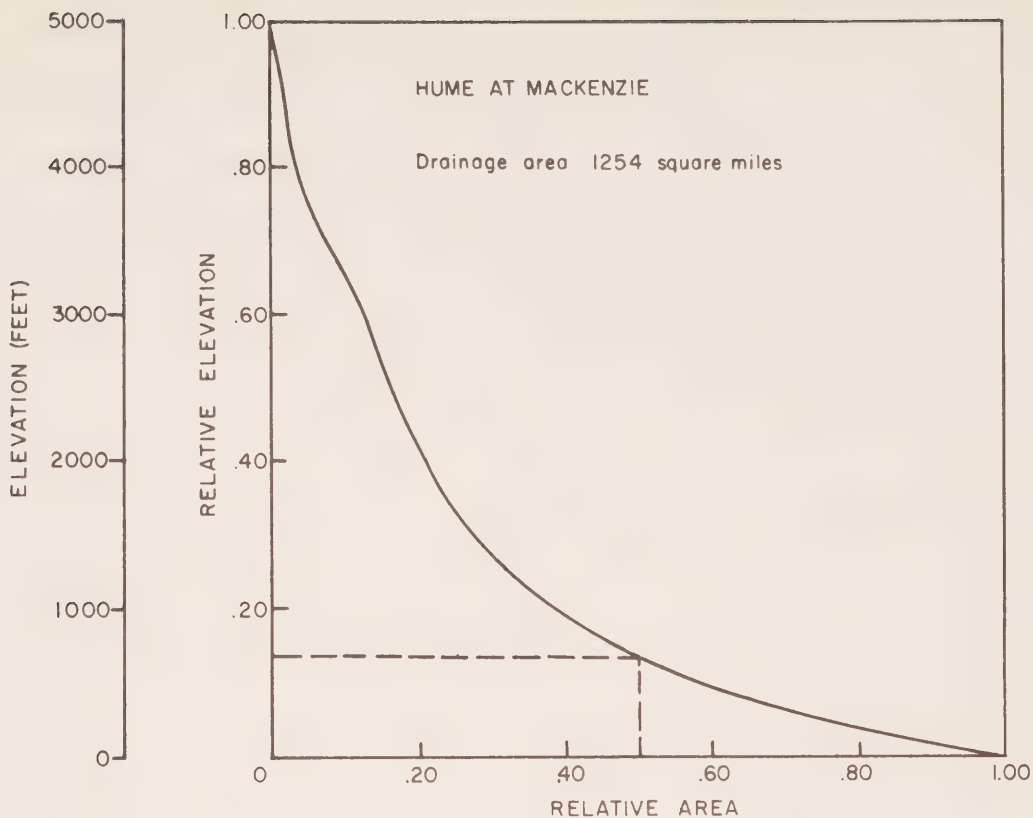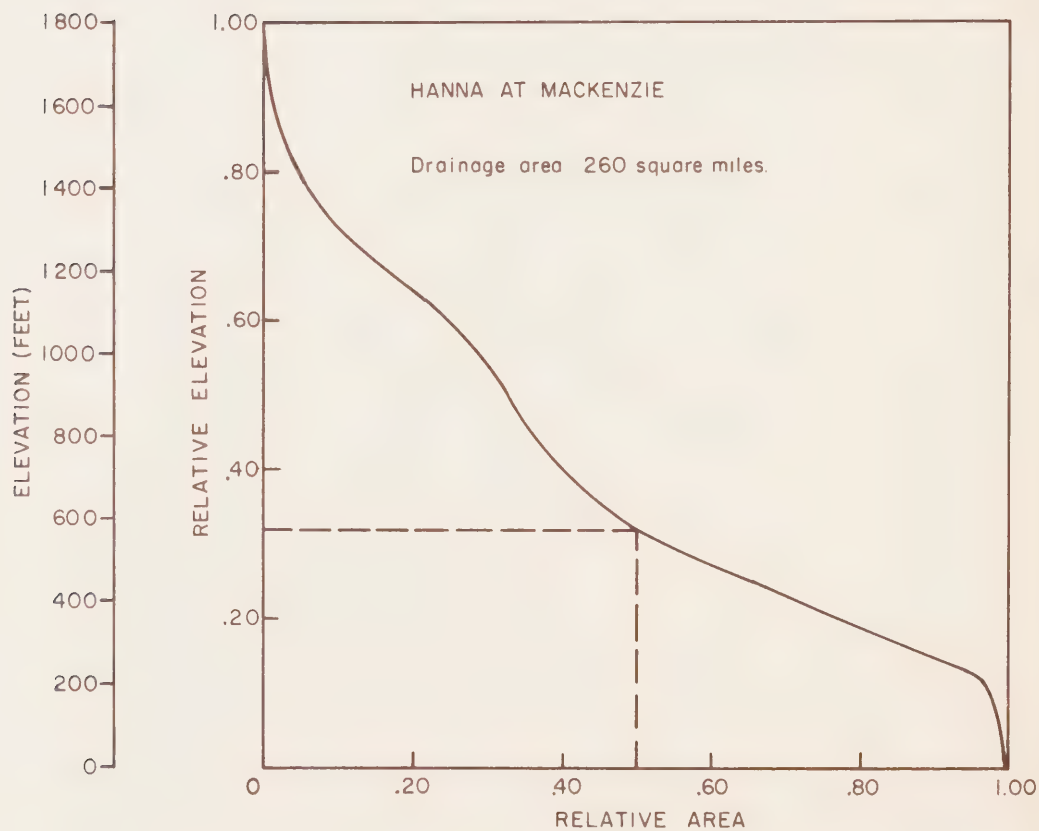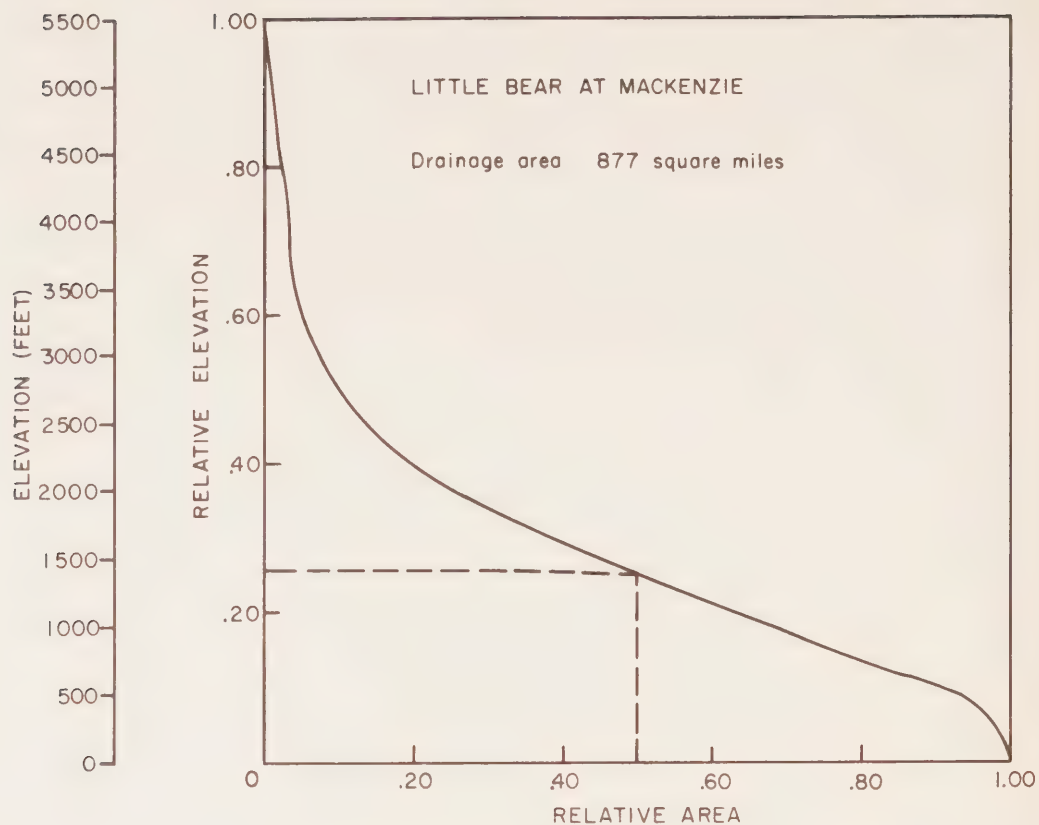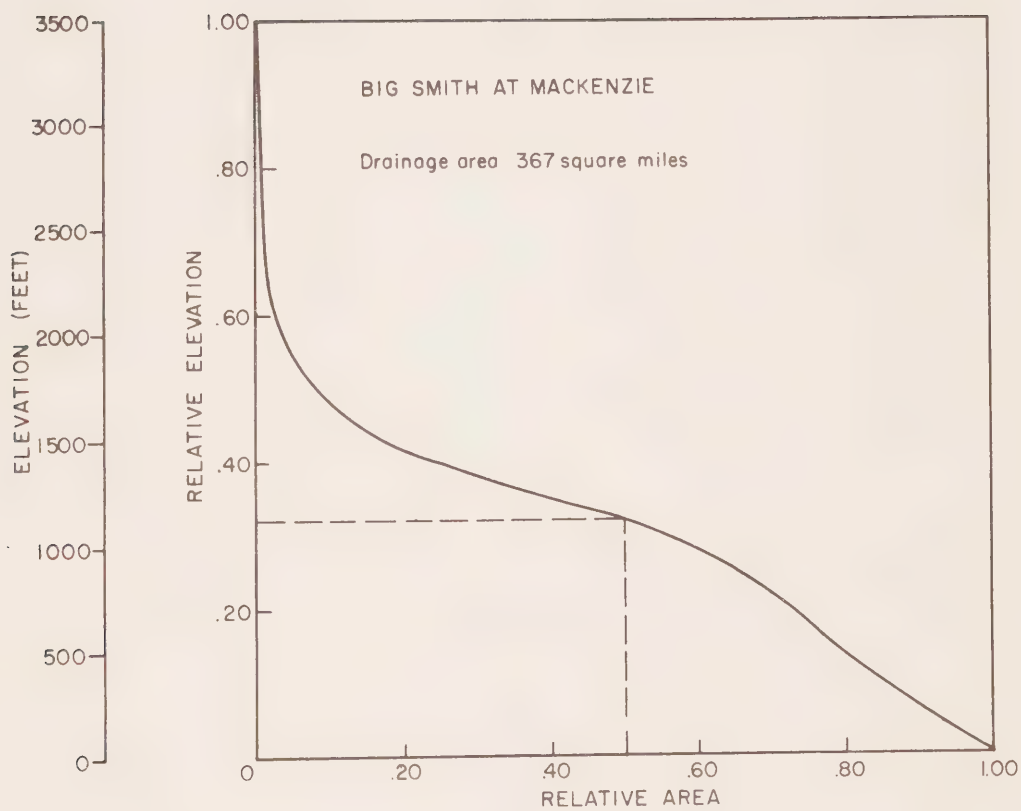FIGURE 2.   Hypsometric curve.

24711

FIGURE 3. Hypsometric curve.

- 367 -

FIGURE 4. Hypsometric curve.

FIGURE 5. Hypsometric curve.